UNIVERSITY OF CALGARY

A Study of the Therapeutic Value of the Mashkiki Bacteriophage: A lambda display and subunit vaccine system.

by

Bradley Scott Thomas

A THESIS

SUBMITTED TO THE FACULTY OF GRADUATE STUDIES

IN PARTIAL FULFILMENT OF THE REQUIREMENTS FOR THE

DEGREE OF DOCTOR OF PHILOSOPHY

Biochemistry and Molecular Biology

CALGARY, ALBERTA

September 2009

Your file Votre référence
ISBN: 978-0-494-54449-5
Our file Notre référence
ISBN: 978-0-494-54449-5

UNIVERSITY OF CALGARY

FACULTY OF GRADUATE STUDIES

The undersigned certify that they have read, and recommend to the Faculty of Graduate Studies for acceptance, a thesis entitled " A Study of the Therapeutic Value of the Mashkiki Bacteriophage: A lambda display and subunit vaccine system." submitted by Bradley Scott Thomas in partial fulfilment of the requirements of the degree of Doctor of Philosophy.

Supervisor, Dr. Derrick E. Rancourt,
Department of Biochemistry and Molecular Biology

Dr. Frank Jirik
Department of Biochemistry and Molecular Biology

Dr. Steve Robbins
Department of Biochemistry and Molecular Biology

Dr. Mike Surette
Department of Biochemistry and Molecular Biology

Dr. David Proud
Department of Physiology and Biophysics

External Examiner, Dr. Keith Fowke
University of Manitoba

Date

Abstract

The utility of bacteriophage lambda (λ) phage display, herein coined Mashkiki, has been investigated. Mashkiki phage displaying TAT proved ineffective for delivery of recombinant genetic cargos. However, Mashkiki phage did prove effective for antigen presentation to the immune system. As a subunit vaccine vector, λ was shown to be a potent stimulus for splenocytes, regardless of immunization. The pro-inflammatory nature of Mashkiki was associated with IFNγ production. This co-stimulatory signal produced cellular and humoral immunity against λ and antigen. Antigen was effectively presented with λ as either a displayed peptide or by genetic immunization.

The adjuvant activity of Mashkiki phage was examined and was found to be intriguing. A study to find the pattern recognition receptor responsible for λ adjuvant activity ensued. λ was found to cause TLR4 receptor ligation, therefore a vaccine trial was performed with Mashkiki phage in the TLR4 hypo-responsive mutant C3H/HeJ. The humoral immune response to λ was found to be TLR4-independent, as titers of λ recognizing antibodies were equivalent between C3H/HeJ mice and the TLR4 responsive mouse strain C3H/HeOuJ. Interestingly, the adjuvant activity for a λ displayed antigen was 1 $\log_{10}$ weaker in C3H/HeJ mice than *wt* C3H/HeOuJ.

In order to determine the involvement of TLR4 in adjuvant activity, downstream signalling pathways from TLR4 were assayed for activity after λ treatment. TLR4 ligation with λgfp10-TAT-GFP caused activation of the NF-κβ pathway in a TLR4-independent fashion, but lack of MyD88 attenuated activation. In contrast signalling through p38 was largely TLR4-dependent, but MyD88-independent. In the context of TLR signalling, MAPK signalling is therefore TRIF-dependent, and results in IP10 expression. On the other hand NF-κβ signalling was largely MyD88-dependent and signalling resulted in IFNγ and IL-6 expression. The cytokines produced from this response, which differ in timing and amplitude from LPS, the prototypical TLR4 ligand, are: IFNγ, IL-2, IL-6, IL-10, IL-13, IL17a, IP-10, and MIP-1α. The initiation of an adaptive immune response from λ is therefore multifaceted. The adjuvant activity of λ is not TLR4 restricted. It is postulated that λ will provide immune stimulation through TLR9, a NOD-like receptor, and complement

Acknowledgements

Dr. Derrick Rancourt, my academic mentor. Thank you for taking a chance on this kid from Mattawa. I've learned so much during this time. Our early discussions dreaming up projects were inspiring. You're an ideas man, a free thinker and a superb strategist. Thanks for letting me go where the science took us. You've given me the tools to become a scientist.

Dr. Steve Robbins, you're a lateral thinker. You've pushed me to learn more and helped me work out the signalling in this project. This work wouldn't be what it is without your support. Thank you for the dialogue over the years.

Dr. Frank Jirik, you helped mold this project from a technical thesis into a therapeutics based trial. It's been a fun journey. You've always got a challenging question for me and you push me intellectually.

Dr. Mike Surette, your support through all this work has been greatly appreciated. When the work or ideas were becoming to tangential you brought it all back to what was important. Thanks for the help.

Examining Committee Members: Dr. David Proud, and **Dr. Keith Fowke,** thank you for taking an interest in this work, and participating in my defense, especially given that it was in August.

Dr. Oliver Bathe, you helped guide me along the immunology. Thanks for always taking the time to have coffee and chat about results.

Dr. Ken Ito, you've been a great friend and teacher. Late nights working in the lab were always fun, we discussed ideas, pulled papers, and finished last minute cloning. I miss the early days of this project during the building phase. Your love of the craft is without

equal. I hope to be as skilled as you someday, or at least to pass on what I know to someone who might be.

Knut Woltjen, thanks for showing me the ropes when I first arrived.

Navneet Sharma, your a steady ship in a raging sea. Thanks for indoctrinating me into the world of biochemistry. Someday I might be as calm as you.

Eileen Ratner, you have a gift with people. When someone is having a bad day, or some experiments didn't work, or some doubt has crept into my mind, you know just what to say to bring things around. Thank you for your helpt in teaching me how to work with stem cells, but most of all thanks for being in my cheering section.

Sandi Nishikawa, thanks for making the lab fun. We've always had a good time 'on the other side'. The breath of this work would not be where it was without your help.

Shiying, we never got to work together enough, but your support and help with the ELISAs this past year was instrumental.

Members of the Rancourt lab past and present, you've all helped me immensely over the years.

Punkaj Tailor, you've been very helpful throughout the years. Thanks for listening.

Elizabeth Long, thank you for helping me rediscover immunology. The TLR signalling work would not be possible without you.

Christa Chatten, thank you for the help with all my FACS work. It was great to be able to work through the problems with you.

Dr. Mellissa Lafreniere and **Serge Laroque**, I always enjoyed science and loved the west, you showed me the way. I'll always be grateful for the summer of 1998. It was life changing.

The Calgary Thomas's, **Martin, Nancy, Libby, Ian**, and **Peter** many a great supper was shared at your table. Great food, great beer and wine, and great times have always been had. You've always opened your home to Steph and I and made us feel welcome. Of course you also provided with the necessary distractions. A football game here, a whitewater kayak there, or a rock climbing session was always great medicine. Your support and encouragement throughout the years has been greatly appreciated.

Isabel Thomas. My granny. Your stories of the family, past and present made me proud to be a Thomas. When a school subject was tough, I just had to remember someone in the family aced it, and if they could do it so could I. The encouragement this provided to a boy from Mattawa was immeasurable. You opened my eyes to the world with your travels, both real and literary. The Ottawa valley was a part of the world and a great place to grow. Your faith has been unending.

Nanna and Grandpa Pratt, you showed me the world beyond books, you kept me grounded, and helped me discover biology.

Greg Thomas, my brother. We discovered the world together. It's been an honour and a pleasure to walk the earth with you. Life's always more fun with good cheer. You're the best. Your hard work and success keeps me going. I'm proud of you little brother.

Carol and Gerry, my parents. Thank you for everything. You have done so much for me.

Dedication

To **Stephanie Minnema**, I don't have words for the all that you are to me. You believe in me, and you support me. It has been a great journey but I know the best is yet to come. Above anything else, I'm happy to have entered grad school to meet you.

I Love You.

Table of Contents

List of Tables

List of Figures and Illustrations

List of Symbols, Abbreviations and Units of Measure

Symbol	*Definition*
λ	Bacteriophage Lambda
aa	Amino acid
AAV	Adeno-associated virus
ACK	Ammonium calcium potassium lysis buffer
APC	Antigen presenting cell
ATP	Adenosine Triphosphate
BCR	B cell receptor
BMDM	Bone Marrow Derived Macrophages
BSA	Bovine Serum Albumin
CTL	Cytotoxic T Lymphocyte
CVF	Cobra Venom Factor
DC	Dendritic Cell
DNA	Deoxyribonucleic acid
ECM	Extracellular matrix
ES cell	Embryonic Stem cell
ESCs	Embryonic stem cells
ELISA	Enzyme-Linked Immunosorbent Assay
EP	Electroporation
EtBr	Ethidium Bromide
EtOH	Ethanol
EU	Endotoxin Unit
FACS	Fluorescent-activated cell sorting
FBS	Fetal Bovine Serum
HiB	Haemophilus influenza B
HSPG	Heparin sulphate proteoglycan
IFN	Interferon
Ig	Immunoglobulin
IM	Intramuscular

IP	Intra-peritoneal
IPTG	Isopropyl β-D-1-thiogalactopyranoside
IV	Intravenous
KLH	Keyhole Limpet Hemocyanin
KO	Knockout
LAL	Limulus Amebocyte Lysate
LB	Luria Broth
LBP	LPS binding protein an
LPS	Lipopolysaccharide
MCS	Multiple cloning site
MLN	Mesenteric lymph node
MPLA	Mono-phosphoryl Lipid A
NKT	Natural killer T cells
NLR	Nucleotide-binding and oligomerization domain (NOD)-like receptor
NTC	Non-template Control
PAMP	Pathogen associated molecular pattern
PBS	Phosphate Buffered Saline
PCR	Polymerase chain reaction
PEG	Polyethylene glycol
PFU	Plaque forming unit
PLN	Peripheral lymph node
Pp38	Phospho p38
PRR	Pattern recognition receptor
PTD	Protein Transduction Domain
QRT-PCR	Quantitative Real Time – Polymerase Chain Reaction
RBC	Red blood cell
RLR	Retinoic acid-inducible gene I (RIG-I)-like receptor
RLU	Relative Light Units

RNA	Ribonucleic acid
SA488	Streptavidin alexafluor488
SDS	Sodium Dodecyl Sulfate
SDS-PAGE	SDS-polyacrylamide gel electrophoresis
T4 PNK	T4 Polynucleotide Kinase
TAE	Tris acetate EDTA buffer
TB	Tuberculosis
Tc	cytotoxic T cell, $CD8^+$
T_{CM}	central memory T cell
T_{EM}	effector memory T cell
TC	Tissue Culture
TCR	T cell receptor
TF	Transcription factor
Th	T helper cells, $CD4^+$
Th1	T helper 1 cell, IFNγ secreting
Th2	T helper 2 cell, IL-4 secreting
Th17	T helper 17 cell, IL-17 secreting
TMB	3,3',5,5' Tetramethylbenzidine
TLR	*Toll*-Like Receptor
Tregs	regulatory T cells
wt	Wild-type
VLP	Virus like particle
v/v	volume/volume
w/v	weight/volume

Units of Measurement

sec.	second
min.	minute
hrs.	hours
µL	microlitre
mL	millilitre

L	litre
x g	times the force of gravity
nm	nanometre
µm	micrometre
mm	millimetre
cm	centimetre
m	metre
pg	picogram
ng	nanogram
µg	microgram
mg	milligram
g	gram
µM	micro molar
mM	milli molar
M	moles/L
bp	base pair
kbp	kilobase pair
kDa	kilo Dalton
Da	Dalton
EU/mL	endotoxin unit/mL

Epigraph

My strength lies solely in my tenacity.

~Louis Pasteur

Chapter One: **Introduction**

1.1 Historical Perspective – Bacteriophage

The first description of bacteriophage was made in 1896 by Hankin.[1,2] In Hankin's work, the analysis of certain rivers in India, several were described as having bacteriocidal action. In 1915 a further refinement of the bacteriocidal effect was presented by Frederick Twort, whereby he found a 'glassy transformation' on bacterial agar plates, but he never isolated the effect, or virus.[1,3,4] The recognized discoverer of bacteriophage is Felix d'Herelle, who in 1917 published a paper describing 'clear plaques' on bacterial agar plates.[1,5] d'Herelle would later write that he first observed the effect in 1910 while isolating locust killing coccobacillus in Mexico and later, 1915, in Tunisia, but he didn't understand the clear plaques nor did he know how to propagate them.[1] In his 1917 paper, d'Herelle was successful at isolating the molecule away from bacteria, as he found it smaller than filters that removed bacteria, and the activity was specific for dysenteric bacilli. Furthermore, it was indefinitely transmissible in serial dilution.[1,5] From these results d'Herelle successfully deduced the effect or medium responsible was a virus as described in 1892 by Ivanowska, or in 1898 byBeijerinck.[6]

Without visual proof of bacteriophage, d'Herelles work was divisive as this era was defined by intensive debates on the nature of viruses. It proved very effective against many diseases, due to its bacterial 'eating' ability, but skeptics believed the anti-bacterial activity could be an enzyme, or a chemical 'ferment' from the body in response to bacteria.[1,7] d'Herelle persisted in his assertion of a living microbe. He correctly deduced that as it was a filtrate, it could be a virus, and as it was replicative, it was not an enzyme as proposed by skeptics.[1,8]

During the 1920s to the 1940s bacteriophage therapy, or more commonly known as phage therapy, became *de rigueur* for many in the golden age of bacteriology.[7] A frenzy of research was undertaken on bacteriophage, as interest in phage therapy was spurred along by the popular media. The best example of cultural interest in bacteriophage was the 1925 novel 'Arrowsmith', which based a character on d'Herelle, and described phage therapy. The novelist, Sinclair Lewis,entered the limelight and

secured his place in American literary history by winning a Nobel prize in literature for the novel in 1930.[4]

Society and the popular media were understandably excited about a new medical breakthrough, as the pharmacopeia of the time was limited. Early 20th century medicine consisted primarily of opium for pain, willow bark as an analgesic, cinchona bark which contained quinine to treat malaria, the herb digitalis for heart disease, and a limited number of vaccines which included Jenner's smallpox vaccine and Pasteur's Rabies vaccine.[6] The only known 'antibiotic' was the arsenic based *salvarsan*, which was used to treat syphilis but had serious side effects for patients.[6] Many common remedies of the time involved mercury, strychnine, and cocaine. Given the context of the era, phage therapy was a major advancement and expanded the limited repertoire of medicines.

Felix d'Herelle's original paper described the utility of bacteriophage in *Shigella dysenteriaeia*. Rabbits infected with dysentery alone died after 5 days, whereas those infected with dysentery and bacteriophage lytic for *Shigella dysenteriaeia* survived.[5] The first large scale phage therapy was against an outbreak of chicken typhus in 1919.[7,9] d'Herelle was asked to investigate the disease in the Champagne region. At the beginning of the outbreak, no chicken was found that survived the disease, but eventually a surviving hen was found. Excrement from the living hen's feces was collected and bacteriophage were isolated. In the lab the isolated bacteriophage produced lysis in liquid cultures of chicken typhoid. While the laboratory experiments were underway, a curious thing happened at the surviving hen's coop. All the chickens recovered and no typhoid bacteria was present, but the typhoid lytic bacteriophage was now throughout the chicken coop.[7] Bacteriophage was reported as having caused the spontaneous cure. The effects described from the chicken coop are interesting for many reasons. First, bacteriophage are present in feces and could be transmitted between animals orally. Second, d'Herelle described a disease dynamic where a bacterial infection appears and a 'spontaneous cure' in the form of bacteriophage eventually presents. The 'spontaneous cure' was of course the evolution of a bacteriophage lytic for chicken typhoid. These interesting findings were beyond the early 20th century understanding of microbiology,

because Koch's postulates were thought to occur from static microbes and not from the evolving host pathogen interaction we now understand.[6,10,11]

d'Herelle then worked on human typhoid and dysentery patients in Paris, with promising results.[7,9] He showed bacteriophages had lytic ability against typhoid, cholera, dysentery, and staphylococcus.[9] The work with childhood dysentery was impressive, but bacteriologists in the US, Brazil, and Germany could not reproduce the work.[7] d'Herelle continued unabated and expanded on his dynamic theory of bacteriophage:bacteria. The control of bacteria by bacteriophage was dose and potency dependent on bacteriophage. In the laboratory he found that a dose sufficient to destroy all of the disease bacteria in a few hours was necessary, otherwise resistant bacteria appeared and complete lysis of cultures never occurred. This explained the variable results of different phage therapy trials. The Brazilian group armed with this knowledge found bacteriophage therapy of dysentery effective.[7]

Phage therapy became commonplace and d'Herelle's phage treatment for dysentery became widely accepted.[7] During the 1920s and 30s the use of phage therapy flourished and laboratories throughout the world appeared, leading to over 100 papers on bacteriophage being published in the Journal of Infectious Diseases between 1917 and 1940. Eli Lilly, Squibb and Sons, and Abbott Laboratories all sold therapeutic bacteriophage.[12] In Egypt, Compton was successful in combating bubonic plague,[13,14] and in India, Morison was successful in stopping large scale epidemics of cholera with phage therapy.[7] d'Herelle himself treated an epidemic of Asiatic cholera in 1927.[7] Staphlococcus infections were treated by Elivia, at the Tbilisi Institute in Georgia.[7] In parallel Larkum produced a treatment against staphylococcus.[8,15] Hauduroy produced tests and treatments for urinary infections and typhoid.[7] Finally, Tsouloukidsé developed a phage therapy for peritonitis, or perforated bowels.[7] During this time though, d'Herelle would only endorse treatments he oversaw because the variability in patient outcomes can be largely attributed to the phage preparation. Reports surfaced on the inactivity of commercial preparations and deaths in treated patients. A review in 1934 found that bacteriophage were only effective for staphylococcus, and cystitis.[12,16] The widespread use of antibiotics after World War II supplanted the use of bacteriophage in western

medicine, but the lack of antibiotics in Russia kept practitioners of phage therapy busy at the Elivia institute in Tbilisi Georgia that d'Herelle co-founded.[12,17]

Although a moot point by this time, Bacteriohpage were visualized using an electron microscope in 1940 by Helmut Ruska,[18] and was first documented in English by Luria in 1942.[19] Indeed bacteriophage was a virus. d'Herelle was correct in proposing that phage feed on bacteria, and were not simply an inanimate object. Phage faded from the limelight of therapeutics and became the model organism of choice for the soon to be named field of molecular biology, under the initial direction of Max Delbrück.[20,21] In the second half of the 20th century, bacteriophage would go on to be the tool of choice in molecular biology.[20-23]

As noted, with the discovery of antibiotics the choice of medicine for bacterial infections moved away from bacteriophages.[24] A combination of factors lead to the demise of bacteriophage therapy. The ease of producing standardized antibiotic pills versus the variability in phage preparations helped secure antibiotics as the treatment of choice, but the efficacy of antibiotics against a broad spectrum of bacteria was the final death knell for phage therapy. One strain of bacteriophage was only infective for one strain of bacteria. Vaccines continued to be important for many diseases, but new vaccines were primarily for viruses, as they lacked any other treatment option. In the 1960s the knowledge of infectious diseases had increased to such an extent that many believed microbes to be conquered. This complacency was helped by Salk's polio vaccines in the 1960's and by the eradication of Smallpox by1979.[25] The war on microbes appeared to be over and the focus of health research now shifted to diseases that were less prevalent in the former soup of microbial diseases.

1.2 Modern Phage Therapy

The 'war' on infectious disease was widely believed to be over in the 1980's, but antibiotic resistant forms of bacteria became increasingly common. With 'superbugs' becoming a problem, Western medicine was reintroduced to phage therapy.[12] Work never stopped on phage therapy at the Elivia Institute in Georgia, which was co-founded by d'Herelle, and together with the Institute of Immunology and Experimental Therapy in

Poland[26] they remained stalwarts of phage therapy. Now they have deep expertise and the most extensive data available for human treatments.

The Polish group published a key paper in 1987: The first English report on the progress of human phage therapy.[27] The work was a compendium of 550 patients recalcitrant to antibiotics for numerous infections.[27] Phage cocktails were delivered locally on wounds, in the form of drops for the eye, ears, or nose, or patients received phage cocktails orally before meals but after gastric acid neutralization.[27] Phage were found in the blood and urine of patients after oral administration, indicating that bacteriophage were widely disseminated throughout the body.[27,28] Phage therapy was effective for 75% to 100% of patients, depending on the type of infection, or a striking 92% overall.[27] Although impressive, the study would not be acceptable as an FDA trial for a few reasons. Foremost, the study was not a double blind experiment investigating the efficacy in treated versus non-treated patients. Regardless of the study design, these impressive results were reported for some of the most obstinate bacterial infections.

In a separate study of 131 patients with antibiotic resistant staphylococcal and pseudomonas infections, phage therapy cured 82% of patients.[12] Phage therapy was found to be most efficacious for *pseudomonas* infections, but efficacy cannot be reported as the phage isolates are not identified in these cocktails. Another study was done on 236 patients with antibacterial-resistant infections and a cure rate of 92% was reported.[12] Separately, a dysentery trial was performed on 6,520 kindergarten children, 3,210 patients received *Shigella* phage, and the remainder a placebo. When phage was administered prophylactically, the incidence of dysentery was 2.5 fold lower.[12] Again the study did not look at the type of phage in the phage cocktail administered. Typically preparations or cocktails are prepared from naturally occurring phage from the environment that are found to be hosted by the pathogen of interest. Without better classification, preparations have tremendous variability across batches. With parallel or pyrosequencing techniques classification could be achieved. Another concern was the extended time it took to treat patients. The average treatment was greater than 5 weeks, but for some rare patients treatment lasted up to 14 weeks.[12] Given the extended treatment regimen, little was done to describe the immune reaction to phage over this

time. There is an outside chance that the efficacy of phage therapy may have been due to non specific immune priming, which activated the immune response to the bacterial infections. Given the early 20th century work using bacteriophage this explanation seems improbable, but treatment control groups containing bacteriophage of different bacteria are necessary before eliminating the possibility. One finding that might better define the mechanism of action was the distribution of phage throughout the body after mucosal presentation to patients. With better understanding of the mechanism of phage therapy *in vivo*, the course of treatments could be decreased from five weeks, and the scientific community would be more receptive to the work.

In Western medicine, phage therapy has been studied using model animals.[12,29-38] Spraying calf bedding was effective for preventing enteropathogenic *E.coli* diarrhoea,[39] much as d'Herelle found in his chicken typhoid experiment.[7] Smith and colleagues went on to document the appearance of antibodies against phage after oral phage treatment.[40] Oral treatment of phage treatment has also proved effective for enteropathogenic *Salmonella typhimurium* in chickens.[41] Phage therapy has been effective in mice against *E.coli* K1, and the wound healing models of *Acinetobacter baumannii* or *Pseudomonas aeruginosa* parenteral infections.[12] Finally phage are effective against *V.vulnificus,* which originates in oysters and causes septicaemia and necrotizing fasciitis.[12]

Indeed, phage therapies have proven effective for many bacterial infections, but they are not the panacea first described at the turn of the 20th century. This is in large part because the efficacy of phage therapy has been affected by a poor understanding or acceptance of the evolution of the virus. Of note, the coevolution of our immune system with enteric bacteriophage has affected phage therapy. The immune response to phage therapy is poorly understood. Phage have been found in immune privileged tissues, such as the brain, and and are able to cross the placental barrier.[42-45] Antibody titers against bacteriophage have been measured in studies by Smith and Delmastro after oral innoculation.[35,40] Furthermore the lateral gene transfer of virulence factors between phage and bacteria could be a lethal complication in treatment and phage must be sequenced to protect patients.[12] The inability of bacteriophage to lyse a broad spectrum means that antibiotics will remain the treatment of choice for most infections. As

discussed, the key benefits of antibiotics will continue to provide therapeutic value for most bacterial infections as antibiotics have a broader spectrum, their activity can be easily tested, and they are chemicals that translate well into existing industrial production methods. All these features give antibiotics reproducibility and safety, however bacteriophage have a niche in modern therapeutics as a viable alternative for chronic bacterial infections that are recalcitrant to antibiotics.

1.3 Early Microbiology

The ancient Greeks believed disease was the work of toxins.[46] The toxin theory of disease was reasoned as the symptoms from alcoholic indulgence mimicked disease, namely vomiting, fever, and diarrhoea. In medieval Europe life was given and taken by God, but a belief in toxins causing disease either via poisonous vapours or from contact with contagions became prevalent.[6,46] The European bubonic plague of 1346 resulted in mortality on a new scale and planted the seeds for the concept that diseases could be transmissible.[6] In 1530, an Italian physician Girolamo Fracastoro wrote that *Syphilis* was a sexually transmitted disease spread by seeds.[6] With the advent of microscopy in 1683 by Anton van Leewenhoek, dental bacteria were visualized for the first time. In 1796, Edward Jenner made an amazing observation: milkmaids exposed to cowpox did not contract smallpox. Jenner's astute observation was eventually translated into the first vaccine. The miniscule pharmacopoeia was expanding.

Investigations into infectious disease only intensified after Jenner's seminal work. The theory of toxins or a contagion was lent weight by Albrecht von Haller and Francois Magendie, who independently showed that animals become sick after the injection of decomposed meat.[46] On the other hand, fresh meat did not cause disease therefore something in the putrid matter caused sickness. In 1849, John Snow observed the transmission of Cholera through a water well, but the toxin or contagion was not pinpointed.[47] It was around this time germ theory was proposed and proven by Louis Pasteur and Robert Koch.[6,46] The term microbe was coined to define a contagion, and microbes were necessary and sufficient to cause disease. Notably, Pasteur identified bacteria in souring milk and fermenting sugar, produced a veterinary vaccine for anthrax in the 1870s, and a human vaccine for rabies in 1885.[6] 'Koch's postulates' defined early

microbiology, one of which was a belief that each disease was the result of one microbe. Using this hypothesis, Koch identified the bacterium responsible for tuberculosis in 1882, and cholera in 1884.[6,46] With proof of germ theory the golden age of immunology and microbiology began.

At the turn of the 20th century the average adult life was 47 years.[6] By 1950, life expectancy had increased to 68 years, or 48%. Most of the increase in lifespan can be attributed to advances from immunology and microbiology resulting in the prevention and treatment of infectious disease.[6] In the second half of the 20th century the war on microbes was believed to be over. With the rise in lifespan entire hospital wards were emptied, but afflictions of the aged began to fill hospitals. The new scourge was diseases of the aged.

1.4 Immunology

At the start of the 20th century the fundamental theories of immunology were described. The distinction between natural immunity, or the innate immune system, and acquired immunity, the adaptive immune system had been made.[4] The discovery of phagocytosis and macrophages by Metchnikoff, propelled the idea of cellular immunity, whereas Ehrlich's work with the agglutination of sera after the addition of toxins proved humoral immunity.[4] The idea was that anti-toxins, coined antibodies, were produced in response to toxic components of microbes. Humoral immunity was corroborated by the work of Behring and Roux who proved passive immunization; antibodies from serum could be used prophylactically to protect against diphtheria toxin. The works described were groundbreaking and garnered the first and eighth Nobel prizes. Of course the theories needed refinements, as Almroth Wright found that antibody treated bacteria were phagocytosed more efficiently. Opsonization, as it was called, was a synthesis of both theories.[4] This idea laid the foundation for immunology as we know it today.

The fundamental question following early immunology was the idea of self and non-self.[48,49] These questions revolved around how the body reacted to non-self and prevented infection without damaging itself. In the last half of the 20th century it became known that innate immune reactions were the primary response which activated Metchnikoff's cellular immunity and Ehrler's humoral immunity.[48-56] The theory has

been honed from the early days when the model of clonal selection explained all. In the clonal selection model, self recognizing clones were deleterious to T and B cell development. These models were later adapted by the addition of the two signal model, which lead to the co-stimulatory model, and finally into pattern recognition theory and danger models of present day.[48,49]

1.5 Adjuvants

Adjuvants, or stimulators of the adaptive immune response, have been widely used since the turn of the 19th century. Adjuvants were identified separately from antigen, as adjuvants activated antigen presenting cells and enhanced the costimulatory signal which allowed for optimal antigen presentation. Remarkably, until recently their mechanism for effect was not understood.[57,58] It is now understood that adjuvants signal through pattern recognition receptors (PRRs) which activate immune responses.

One of the oldest, and one of the few currently approved adjuvants is alum.[57,59,60] Alum stimulates the NALP3 inflamasome,[57] which results in interleukin 1β (IL-1β) production. Alum does not induce IL-6 or tumour necrosis factor α (TNFα), unlike lipopolysaccharide (LPS) and other *toll*-like receptor (TLR) ligands.[57] The use of alum as an adjuvant results in T helper 2 (Th2) polarized immune responses.[61]

LPS is a potent adjuvant.[62,63] LPS signals through TLRs, and also activates NOD-like receptors NLRs.[64-67] LPS will be discussed more fully in the following section, but it is not approved for use as an adjuvant due to serious and potentially fatal toxicity issues in patients. [68] The monophosphoryl lipid A (MPLA) form of LPS removes the negative side effects associated with LPS and restricts LPS mediated TLR4 signalling to the TRIF2 pathway (Fig. 1.1).[69] As such, MPLA is 100 fold less toxic than the lipid A component of LPS.[46]

Another TLR ligand commonly used as an adjuvant is hypomethylated CpG DNA.[70] CpG DNA can be from bacterial, viral, or eukaryotic sources, which all signal through TLR9. TLR9 signalling results in a T helper 1 (Th1) polarized immune response.[70]

Many other adjuvants are used for vaccines. The mechanisms and receptors for many adjuvants remain unknown. Some notable adjuvants are diphtheria toxin, cholera

toxin, and synthetic variants on these, such as CRM197.[71] For more information on adjuvants an excellent review by Aguilar is recommended.[72]

1.6 Lipopolysaccharide

The presence of evil humors or toxins was postulated in ancient times, to which we now attribute some of this activity to LPS.[46] In the 17th century it was proven that putrid matter caused symptoms of illness.[46] At the turn of the 19th century Pfeiffer found a non-protein toxin in cholera that produced fever. This molecule was later described as lipopolysaccharide (LPS).[46]

Gram negative bacteria are surrounded by an asymmetrically organized phospholipid bilayer. LPS is the primary component of the outer leaflet of the phospholipid bilayer.[73] The structure of LPS can be described as a hydrophilic heteropolysaccharide covalently bound to a lipid component, called lipid A.[46,73] The heteropolysaccharide can be further subdivided into the O-antigen and the core oligosaccharide. Tremendous variation in the structure of the O-antigen is seen across bacterial strains.[46,73-76] Tremendous variability also exists even within a single bacterial culture.[73]

The O-antigen has been found to be dispensable to LPS function, as mutants to the *rfb* locus lack the O-antigen but are viable. O-antigen deficient bacterial colonies appear rough and as such are called rough or R-mutants, whereas smooth LPS, S-form, contains O-antigen and bacterial colonies appear smooth. Biologically this distinction becomes important as *Salmonella* containing O-antigen are protected from phagocytosis and complement mediated lysis.[73] TLR4 signalling by LPS will be discussed later, but the R-form of LPS has been shown to be equivalent to lipid A in the ability to stimulate the production of IL-6 and TNFα.[77] The S-form of LPS cannot stimulate inflammation unless the co-adaptors CD14 and LPS binding protein (LBP) are present.[77]

The core oligosaccharide region of the heteropolysaccharide can be further subdivided into an outer and inner component. The core region is structurally more conserved than the more diverse O-antigen region. The core region has only a single core type present in all *Salmonella* serotypes, and *E.coli* have only five different core types.[73]

E.coli core types are classified as R1 to R4, and K-12. K-12 being the core type present in most laboratory strains of *E.coli.*

With the chemical production of lipid A it was determined that it is the endotoxic region of LPS, as lipid A contains identical immune stimulatory activity as bacterially isolated LPS.[46] Lipid A contains two phosphorylated glucosamines that are connected by a β(1-6) linkage and are acylated by six lipid chains.[78] Biological recognition of lipid A is mediated by MD2 and TLR4.[78] Upon binding lipid A, TLR4 molecules dimerize through interactions between lipid A and loops on MD2 molecules. The end result is an MD2-LPS-TLR4 complex bound to another MD2-LPS-TLR4 complex. The residues of lipid A responsible for this structure are the two phosphate groups and the lipid chains. A large hydrophobic pocket in MD2 binds up to five acyl chains on lipid A, leaving the 6th acyl chain to interact with the second TLR4 molecule. Loss of one acyl chain results in lipid A being 100 times less immunogenic.[78,79] Loss of two acyl chains stops TLR4 signalling. The other binding domains on lipid A are the two phosphate groups. The 4' phosphate interacts with positive residues on the MD2 that has bound the lipid chains of lipid Aas well as positive residues on the TLR4 receptor that are directly bound to MD2. The 1' phosphate interacts with MD2, and both TLR4 molecules in the supramolecular MD2-LPS-TLR4 dimer. Loss of the second phosphate in lipid A, also known as MPLA, results in a 100 fold less active lipid A molecule.[78]

1.7 *Toll-like* Receptors.

LPS is the most potent TLR ligand,[80] and as a result the LPS receptor (TLR4) was the first *Toll*-like receptor to be characterized. The potency of low concentrations of LPS in serum at eliciting an immune response was postulated to be due to a receptor of high affinity.[46] TLR4 remained an orphan receptor until 1998 when it was discovered that the mutations rendering C3H/HeJ and C57BL/10ScCr mice susceptible to Gram-negative infection were due to defective LPS binding.[64,65,67] LPS is the prototypical TLR ligand and the signalling of TLR4 will be discussed herein as a model for other TLRs.

In a Gram-negative bacterial infection a defined series of events occur. The liver produces LPS binding protein (LBP) which binds plasma LPS, or LBP extract LPS directly from Gram-negative cell membranes.[46] Specifically, LBP binds the lipid A

component of LPS through its acyl chains..[81,82] LBP then shuttles LPS to TLR4 expressing cells, thereby enhancing the detection of LPS. The LBP-LPS complex then becomes bound by CD14, which can be in an outer membrane bound or soluble form.[81,83] Using deletion mutant analysis it has been shown that the amino-terminal 65 amino acids bind LPS. This region contains a hydrophobic pocket which is postulated to bind the lipid component of lipid A.[82] The exact mechanism of delivery to the TLR4 receptor complex is not understood, but CD14 delivers LPS to the TLR4-MD2 receptor complex.[82] LPS is then be bound to the TLR4 receptor complex as discussed previously. Many details are lacking as all LPS binding molecules appear to bind the same lipid component of lipid A. Each subsequent LPS binding molecule may have higher lipid binding affinities.

Increasing affinity in LPS transfer proteins may be responsible for delivery of LPS to TLR4, but an alternative is suggested by the R and S-forms of LPS.[77] The R-form of LPS acts in similar fashion as lipid A and causes binding of TLR4-MD2 directly without the involvement of CD14.[77] The S-form LPS, which contains O-antigen, is CD14 dependent for TLR4 signalling.[77] Therefore, CD14 may bind the glycosylated O-antigen of LPS. In binding the O-antigen, the acyl chains of lipid A become accessible for MD2 binding.

After the ligation of LPS to the supramolecular TLR4 receptor complex, intracellular adaptor molecules are recruited (Fig. 1.1). Two adaptor molecule pairs are used by TLR4, MyD88 and TIRAP operate together at the cell surface, and after receptor internalization TRIF and TRAM operate on endosomal TRL4.[84] TLR4 is the only one in the TLR family which uses both TRIF and MyD88 adaptor proteins. MyD88 results in signalling through TRAF6/IRAK to TAK1, which activates the NF-κβ and MAPK pathways: ERK, p38, and JNK.[80,85] TRIF signalling results in TRAF6/RIP1 signalling to TAK1, which also leads into the NF-κβ and MAPK signalling pathways. In parallel, TRIF signalling also activates TRAF3 to produce IRF signalling and stimulate type 1 IFNs.[85]

Although similar intracellular signalling cascades are produced, MyD88-dependent and TRIF-dependent cytokines are distinct.[69] MyD88 results in IFNγ, IL-1β,

IL-6, and MIP-1α being produced. In contrast, TRIF-dependent signalling results in G-CSF, MCP-1, IP-10, and RANTES production. This dichotomy in cytokine expression was discovered using MyD88$^{-/-}$ and TRIF$^{-/-}$ mice.[69] Using these knockout mice, the adjuvant activity of MPLA has been found to be TRIF dependent, and *wt* mice produce the following cytokines: IL-6 early during stimulation, G-CSF, MCP-1, IP-10, and some RANTES.[69]

MPLA only engages one TLR4 molecule in the TLR4 dimer and signalling is TRIF-dependent.[69] As discussed previously, CD14 is necessary for smooth LPS binding but dispensable for rough LPS.[77] As MPLA is a lipid A variant, it can stimulate TLR4 in a CD14-independent manner, yet MPLA is TRIF-dependent; even so, lipid A in CD14 KO mice is reported to be MyD88-dependent.[86] The difference in MyD88 as compared to TRIF-dependent signalling must relate to the engagement of two TLR4 molecules for lipid A molecules and only one for MPLA. Obviously slight variations in ligands result in large differences in adaptor recruitment. MPLA producing a TRIF response may be attributable to a delay in receptor signalling which results in endosomal TLR4 signalling vs. cell surface signalling for lipid A. Alternatively, lipid A binding of TLR4 might be possible in CD14$^{-/-}$ mice, but CD14 contributes to the lipid A-TLR4 signalling complex when present.

Another variation in TLR4 signalling is receptor ligation to vesicular stomatitis virus g protein (VSV-g). VSV-g engages CD14/TLR4 to produce a MyD88-independent and TRAM-dependent signalling cascade, which activates IRF7.[87] In this situation TRIF activation was found to be nearly absent and no NF-kB signalling was seen. This response was found to be in myeloid DCs and macrophages, but not pDCs.

Of interest to the work described in this thesis is the mutation of C3H/HeJ mice. This strain contains a proline to histidine substitution present in the TIR domain at amino acid 712.[64,67] The TIR domain is cytoplasmic and this mutation results in defective or absent MyD88 binding.[88] The effect on TRIF remains unknown.

This section outlined the prototypical signalling cascade for TLR4 and some variations on the paradigm. More variations will undoubtedly be found as TLR4 appears to be a promiscuous receptor. Currently it is known to bind LPS, viral capsid proteins

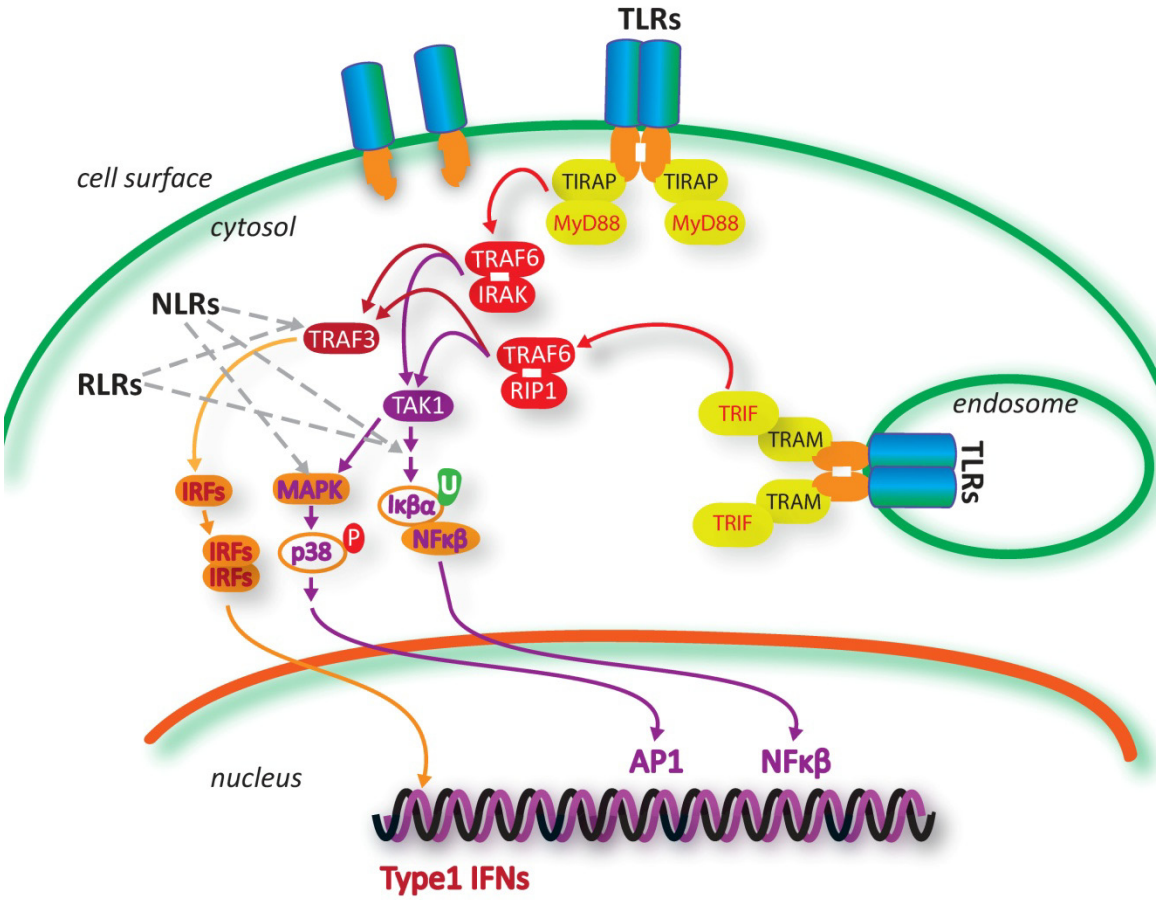

Figure 1.1: TLR signalling cascade

from respiratory syncytial virus and mouse mammary tumor virus,[85] a dust mite protein,[89] and host derived factors. Several variations in signal propagation and cytokine production have been highlighted as TLR4 is implicated in the work described in later chapters.

1.7.1 Other Toll-like receptors

There are at least 13 members in the TLR family of receptors.[90] These are named TLR1 to TLR13. The ligands for most are known except for TLR10.[91] Of particular interest for the work in this thesis are TLR9, TLR5, and TLR2. The prototypical ligand for TLR9 is hypomethylated CpG DNA.[85] TLR9 is located in the endosome and therefore signals through the TRIF/TRAM adaptor pair. Stimulation of TLR9 during vaccination or infection produces Th1 polarized immune responses.[92] B cells and plasmacytoid DCs express TLR 9.[54,93] Flagellin is the prototypical TLR5 ligand, and lipoproteins are bound by TLR2.[85] TLR5 and TLR2 signal from the cell surface through the MyD88/TIRAP adaptor pair.

1.7.2 NOD-like receptors and RIG-I-like receptors

A new cytoplasmic pattern recognition receptor family has been discovered called the nucleotide-binding and oligomerization domain (NOD) -like receptors (NLR).[94] As intracellular PRRs, NLRs are expressed primarily by phagocytes, including macrophages and neutrophils.[94] Many more questions remain than for TLRs but they are known to signal into the NF-κβ and MAPK pathways, via downstream signalling molecules distinct from TLRs. Whereas TLRs utilize the TIR domain for the recruitment of downstream signalling proteins, NLRs downstream effectors are recruited via amino terminal domains.[94,95] Four types of amino terminal domains are seen in the NLRs: caspase activation and recruitment domain (CARD), pyrin domain (PYD), baculovirus inhibitor repeats (BIR), and acidic domains.[94] NLRs are a large family of PRRs but in general they are organized as follows: a protein-protein interaction domain on the amino terminus, a NACHT domain necessary for nucleotide binding and self oligomerization, and a carboxy terminal leucine rich repeat motif of variable length. The signal transduction cascade from any given NLR is poorly defined especially for those proteins

responsible for the propagation of NOD2 signalling to IFNβ,[94] but many NLRs converge on the inflammasome.[96] The inflammasome has been found to be crucial for the adjuvant activity of alum, and in the production of IL-1β.[57]

The most poorly described PRR family are the retinoic acid-inducible gene I (RIG-I)-like receptors (RLR). Similar to NLRs, RLRs are cytoplasmic family of proteins. Unlike the restricted expression of TLRs which produce large amounts of Type I IFN responses, RLRs seem to be present in most cell types and are responsible for virus detection.[97] RLRs are known to signal to the IRF and the NF-κβ pathways.[98]

1.8 Antigen Presentation

The adaptive immune response is initiated by antigen presenting cells. Antigen is processed by the lysosome or the proteasome and epitopes are displayed on MHC II by antigen presenting cells (APCs) (Figure 1.2). APCs are macrophages, dendritic cells, B cells, and in allergic responses basophils.[99-101] Theoretically, the adaptive immune response could select a T cell receptor (TCR) or B cell receptor (BCR) for any antigen presented, but in reality the receptor diversity is restricted by the genomic loci of the TCR and immunoglobulin genes respectively. This restriction has remarkable diversity, as each loci undergoes somatic mutation to produce hypervariable regions to recognize the proper ligand. The number of possible variations is staggering. The process of genomic rearrangement and clonal selection produces non-self TCR and BCRs. The clonal selection model was first proposed in the 1950s, but questions surrounding how clonal selection is initiated or what caused APC activation remained.[48]

The activation of APCs was found to be a costimulatory signal from pattern recognition receptors (PRRs) that recognizes a pathogen associated molecular pattern (PAMPs) and results in the production of pro-inflammatory cytokines.[48,51] Janeway's pattern recognition theory has since been proven to be the activating signal responsible for the transmission of an innate immune signal into an adaptive immune response.[102] Immunologists had long known that adjuvants, such as LPS and alum, could produce pro-inflammatory cytokines that result in adaptive immune responses but the discovery of the PRRs responsible has produced a new understanding of disease.

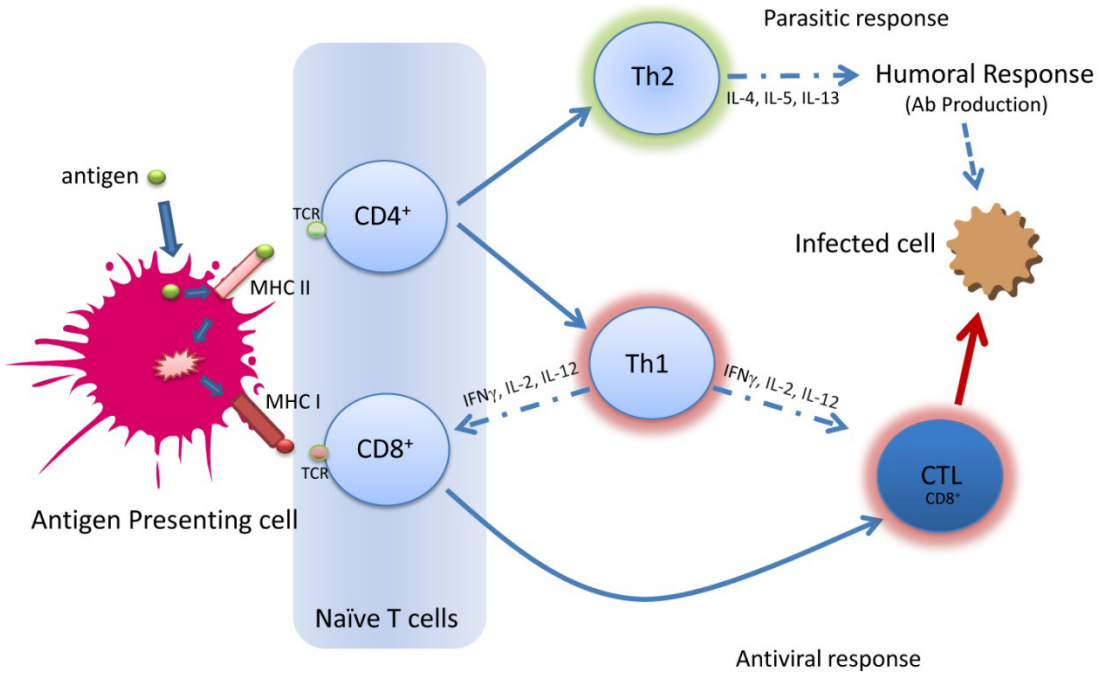

Figure 1.2: Adaptive Immune response.

1.9 T cells

B and T cells are integral components of the adaptive immune response (Figure 1.2). Two primary outcomes are possible with an adaptive immune response: 1) a humoral immune response, which is produced by B cells, and 2) a cellular immune response, which is produced by T cells. Within this framework T cells are the workhorses as they produce T helper (Th) cells and cytotoxic T lymphocytes (CTL). Th cells direct effector cells during infection or damage, while CTLs are effector cells of the cell mediated immune response that kill infected cells.[103-107] In general terms, the humoral immune response is produced for a parasitic response, whereas the CTL response is produced as an antiviral response.

Immature thymocytes (T cells) possess CD4 and CD8 receptors on their cell surface. With maturation, T cells become restricted to one receptor; $CD4^+$ T cells are called T helper (Th) cells, and $CD8^+$ Tcells become CTLs. Th cells are subdivided into four distinct lineages: Th1 which regulate cell mediated immunity, Th2 which regulate humoral immunity, regulatory T cells which downregulate immune responses, and the newly described Th17 cells.[104,106,108] By definition Th1 cells produce interferon gamma (IFNγ), Th2 cells produce IL-4, and Th17 cells produce IL-17.[106,108] All T cell responses to infection can be described as three phases, growth, contraction, and memory.[109,110] At the start of an infection, T cell populations expand to provide the diversity and numbers to combat infection, as the infection continues the specificity of T cells increases and the infectious particles are cleared. After an infection most effector T cells die, and memory T cells are retained to protect against future infections.

The prototypical delineation of T cells is Th1 cells and Th2 cells (Figure 1.2). Naive $CD4^+$ cells express low levels of IL-2, which has been shown to increase upon activation in a subset of multipotential Th cells, that are non-committed toward either IFNγ or IL-4.[106] Other subsets of Th cells become committed to IL-4 or IFNγ very quickly. As a result of these subsets being present, early in differentiation there is considerable heterogeneity at the single cell level for cells producing the Th1 defining and Th2 defining cytokines, IFNγ and IL-4.[106] During an immune challenge, before the expansion phase occurs IL-2 is beneficial for Th cell survival, but during the expansion

phase when the number of T cells increases, IL-2 becomes detrimental to survival.[111] The differentiation program begins with IL-4 causing Th2 differentiation and IL-12 initiating Th1 cells.[112] The polarization or commitment of Th cells can be defined further by the presence of different transcription factors (TFs), T-bet in Th1 cells and GATA-3 in Th2 cells.[113,114] Each TF acts as a master regulator of Th cells with Th1 cell commitment being T-bet dependent and GATA-3 being necessary and sufficient to produce Th2 restricted cells. GATA-3 has proven to be a true master regulator as committed Th1 cells transfected with GATA-3 convert into Th2 cells.[114] In parallel to TF master regulators being expressed during lineage commitment, the genomic loci for IFNγ and IL-4 become acetylated, resulting in the down regulation of the appropriate gene during the differentiation program.[112]

Immune reactions in response to challenge are dictated by several parameters including the type of pathogen, the PRRs stimulated, and the presentation of antigens. When a Th1 polarized response is produced, large quantities of IFNγ are secreted, Tc cells mature into CTL cells (Figure 1.2), and B cells differentiate into IgG2a plasma cells.[115] Alternately, when IL-4 dominates an immune reaction, the Th2 specific cytokines IL-5 and IL-13 are produced, and IgG1 along with IgE producing B cells result.[106,116] Following the immune clearance of pathogen, IL-10 is produced to down regulate activated immune cells. This is defined as the contraction phase of the immune reaction and many T cells undergo apoptosis. During this phase of the response the presence of IL-2 becomes beneficial for pathogen specific T cell survival and the retention or production of antigen specific memory T cells.[106,111] After apoptosis of effector T cells, the immune system enters the memory phase of response, whereby antigen binding TCR memory cells are maintained in anticipation of another challenge.

The new recruit to the Th cell paradigm is Th17 cells. Surprisingly many of the same characteristics and paradigms defining Th1 and Th2 cells are also applicable to Th17 cells. The defining pro-inflamatory cytokine for Th17 cells is IL-17 and the differentiation from naive $CD4^+$ T cells or multipotential IL-2 secreting $CD4^+$ T cells is initiated with IL-23.[104,108] Although TGF-β, TNFα, and IL-6 are also involved in Th17 differentiation.[108] As of yet no transcription factor has been identified that defines the

Th17 cellular program, but IFNγ and IL-4 are inhibitory for mature Th17 cells.[108] Th17 cells are intimately linked with autoimmunity, and involvement in multiple sclerosis, psoriasis, and rheumatoid arthritis have been documented.[117-119] Since the discovery of Th17 cells, models of protective immunity against pathogens have been described for the mucosa of the gut and lung.[120-123] Interestingly, when Th17 cells are stimulated to defend against pathogens, IFNγ and IL-17 are implicated in host responses.[104,121] This evident overlap in protective immunity between Th1 and Th17 cells is highlighted in the Th1/Th17 axis of polarization being distinct from Th2 cells during Th cell differentiation.[124] However, Th1 and Th17 remain distinct as IFNγ is inhibitory for Th17 cells.[108]

1.10 Immunity: Memory and Location

An incredible observation was made regarding immune memory in 1846.[110] A measles outbreak occurred and no one aged 65 or greater was affected even though 75-95% of the general population suffered from infection. After some investigation, Ludwig Panum found that a measles outbreak had occurred in 1781 which conferred immunity on these individuals. This was an incredible observation and sixty five years of immune memory is a feat all vaccines should aspire to.

Memory B cells have been a controversial story.[125] B cells are produced in the bone marrow, where they undergo immunoglobulin (Ig) rearrangements and mature into IgM and IgD expressing B cells. Once mature, B cells migrate to secondary lymph organs upon the loss of the CD45R/B220 receptor. In the secondary lymph organs mature B cells undergo clonal selection with follicular DCs whereby Ig class switches can occur resulting in the diversity of IgG, IgA, and IgE antibodies. After disengagement with follicular DCs, B cells are directed by Th2 cells to proliferate and/or differentiate. B cells do not secrete antibody until they become plasma cells. After infection, stimulated lymph nodes produce large numbers of B and T cells. After antigen clearance, most B cells die, but classic experiments have shown that 8% of the originally expanded plasma cells persist past 6 months in secondary lymph organs.[125] It was later found that antigen specific plasma cells are present far longer in the bone marrow. Controversy surrounds the existence of memory B cells vs. long lived plasma B cells, but data suggests memory

B cells express CD45R while plasma cells do not.[125] *Ex vivo* plasma cells are difficult to culture and only survive when fused to myeloma cells or cultured in the presence of a combination of cytokines, including IL-6.[126] *In vivo* long lived plasma cells are present in the bone marrow and the spleen.[125,127] It was shown that after an intraperitoneal (IP) infection with lymphocytic choriomeningitis virus (LCMV) the largest numbers of long lived plasma cells are present in the bone marrow, ~10^4, with approximately an order of magnitude less plasma cells present in the spleen. On the other hand, 10^4 to 10^5 memory B cells are present in the spleen after LCMV, while bone marrow memory B cells are below the detection limits of the assay.

Memory T cells are produced after a primary infection. Memory T cells are distinguished as central memory T cells (T_{CM}) if they express the homing molecules CCR7 and CD62L, or effector memory T cells (T_{EM}) when these homing molecules are absent.[106,107,128] This paradigm is present in both $CD4^+$ T cells and $CD8^+$ T cells. The expression of homing molecules results in T_{CM} cells being secondary lymph node resident, whereas T_{EM} cells remain non-lymphoid tissue resident. However both T cell subsets are present in the blood and spleen.[128] The spleen is the largest reservoir of T cells in the body, and therefore has the largest number of systemic memory T cells. Long term survival factors for T cells vary for $CD8^+$ and $CD4^+$ T cells. $CD8^+$ T cells rely on IL-7 and IL-15, but $CD4^+$ cells are dependent on IL-7, although this is controversial.[106,107,128] The evidence suggests that both effector and central memory cells are effective at cytokine production but T_{CM} cells proliferate more upon antigen presentation.[128] This might be explained by the homing of tissue resident DCs and macrophages to secondary lymph nodes after local infections. The location and expansion of memory cells is relevant for vaccination as long term memory requires large numbers of antigen specific memory T cells to survive; therefore as more T cells are activated, larger numbers of memory cells could ensue. Hence, secondary immune challenges, or boosting, should be done after T_{CM} cells are produced following a primary immune challenge.[128]

Classic experiments on T activation in delayed type hypersensitivity (DTH) models provided examples of how the spleen and local lymph organs interact.[129] When a

secondary immune challenge is provided IV, the proliferation and resolution of the immune response progresses more quickly in a local lymph node than when an inoculation occurs in the local tissue. Local immune responses, measured in the footpad, are prolonged in splenectomised mice when secondary immune challenges are provided intravenously (IV). Therefore a systemic challenge is mitigated by the presence of the spleen, but local secondary lymph organs also become stimulated in systemic immune challenges. Interestingly, if the secondary immune challenge is provided locally, contralateral lymph nodes do not respond. Therefore local immune reactions are cleared by draining lymph, and not systemically.[129] In a different model, where an oral vaccination with a keyhole limpet hemacyanin (KLH) - cholera toxin conjugate was provided, systemic and local lymph organs generated KLH specific memory cells.[130] Secondary challenges in vivo resulted in proliferation of local lymph node cells. Given our current understanding of T cell migration, it appears memory T cells populate tissues throughout the body following immune challenge.[131]

1.11 Cytokines

Cytokines are a diverse set of small (5-20kDa) secreted proteins that are key mediators of the immune system. Cytokines are responsible for many effects including cellular differentiation, inflammation, proliferation, anti-inflammatory responses, activation of cells, co-stimulation, histamine release, and chemotaxis.[132-135] The secretion of cytokines can produce autocrine, paracrine, and endocrine effects. Some cytokines are central to specific immune responses, and/or defending against specific pathogens that occupy immune niches. Various cytokines are necessary for protective immunity against pathogens. Most notable is interferon gamma (IFNγ), which is necessary to fight bacterial, and protozoan infections, such as *Leishmania major, Leishmania donovani, Listeria monocytogenes, Mycobacterium tuberculosis*, and *Bordetella pertussis*.[136,137]

The first cytokine found was interferon. These were later called type I interferons, or interferon α/β (IFNα/β). The seminal work with type I interferon showed an ability to inhibit, or interfere, with influenza A growth.[138,139] Since this time type I IFNs are used as a general antiviral and as an immune system activation drug for cancer treatment. Type I IFNs trigger the expression of over 100 genes and the products have

many roles in antiviral immunity.[115] A myriad of cells produce type I IFN including antigen presenting cells (APC), such as macrophages and dendritic cells (DC), as well as other cell types, such as fibroblasts.[98] Signal transduction which results in IFN expression occurs through Toll-like receptors (TLRs) via the TRIF adaptor protein.[140] In addition, type I IFNs have been shown to be downstream of NLRs, and RLRs.[94,98,141]

Interferon gamma (IFNγ) is the prototypical macrophage activator.[142] It is secreted primarily by Th1 cells, NK cells, and $CD8^+$ T cells,[106,135,143,144] but macrophages, DCs, and B cells have also been shown to secrete large amounts of IFNγ.[143,145,146] As mentioned above IFNγ is a correlate of protective immunity for many bacterial pathogens, [136,137] as it is involved in Th1 polarization (refer to section 1.8 for further discussion).[143,147] Briefly, IFNγ and IL-4 are generally viewed as antagonistic to each other as they are the differentiation signals for Th1 and Th2 respectively.[112,147-149] Upon innate immune activation, $CD8^+$ cells, Th1 cells, and NK cells produce IFNγ which results in: 1) the activation of macrophages and NK cells, and 2) the genomic rearrangement of B cells into IgG2A producing cells.[115,144,150] IFNγ production results from Myd88-dependent signalling downstream of TLR activation.[69]

The existence of tumour necrosis factor alpha (TNFα), had been postulated for a long time. In a screen to find host factors responsible for septic shock, TNFα was isolated and cloned.[46,151] TNFα binds the TNF receptor complex, which propagates its signal through two opposing signalling cascades: one that leads to cytochrome c release and apoptosis, and the other which causes NF-κβ translocation to the nucleus and cell survival.[152] The primary sources for TNFα are macrophages, monocytes, and T cells, among others. Some of the target cells that respond to TNFα are neutrophils, macrophages, monocytes, endothelial cells, and cells in the hypothalamus and liver.[134] TNFα, along with IL-6, and IL-1 produces systemic inflammation, including fever as a result of prostaglandin expression in the hypothalamus, and production of acute phase proteins by the liver.[153,154]

Interleukin-6 (IL-6) has been found to be elevated in the serum after immune challenge with LPS, local inflammation, restraint, electrical foot shock, and exercise.[51,153-155] The response in the latter three is the result of the acute phase response,

which is induced by IL-6.[132,156] LPS has been shown to be a potent inducer of IL-6.[51,155,157] Indeed, the pro-inflammatory cytokine IL-6 is commonly produced after TLR receptor ligation, and has been found to be MyD88-dependent.[69,140,158] IL-6 is produced by many cell types, such as macrophages, T cells, and fibroblasts. Many cells respond to extracellular IL-6 including B cells, T cells, hepatocytes, thymocytes, myeloid cells, and osteoclasts.[132] Upon exposure to IL-6, B cells differentiate into antibody secreting plasma cells, and IL-6 induces already differentiated plasma cells to secrete antibodies.[132] As a prognostic indicator, high serum IL-6 correlates with patient death in meningococcal disease.[155] Temporally, IL-6 secretion occurs after TNFα. IL-6, TNFα, and IL-1 are host derived disease factors responsible for septic shock.[155]

Interleukin-2 (IL-2) is a Th1 cytokine. During the early differentiation of T helper (Th) cells, IL-2 and IL-12 synergize and result in the production of IFNγ.[143] Naive T cells have low level expression of IL-2 but after stimulation IL-2 becomes upregulated in multipotential Th cells.[106] Following viral infection $CD4^+$ and $CD8^+$ effector cells undergo a contraction phase, where many cells die, but the addition of IL-2 increases the proliferation and survival of virus specific T cells.[111] Therefore, IL-2 has been cited as an indicator of T cell memory.[106] IL-2 is produced by T cells, and it acts upon T cells, B cells, NK cells, and macrophages.[132]

Interleukin-4 (IL-4) is the defining cytokine of Th2 cells.[106] IL-4 is responsible for the early differentiation of Th2 cells from 0 to 4 hours after immune challenge.[148] IL-4 is present in many early Th cells before polarization (Th0),[112,148] unlike IFNγ,[149] and is expressed along with IFNγ in the rare cell population of natural killer T cells (NKT).[159] IL-4 is produced by T cells and mast cells, and the target cells are T cells, B cells, macrophages, and monocytes.[132] IL-4 causes proliferation and differentiation of B cells into IgG and IgE clones, and inhibits cell mediated immunity and Th17 development.[108,124,132]

Interleukin-10 is a potent anti-inflammatory cytokine.[160] It is expressed by Th cells, subsets of regulatory T cells (Tregs), B cells, appropriately stimulated macrophages, DCs, eosinophils, mast cells, keratinocytes, epithelial cells, and tumour cells.[132,160] The exact strength of IL-10 production by any given cell type is being

determined but as with many cytokines, it is believed to be ligand and dose specific. To date, macrophages have been found to produce large amounts of IL-10 relative to DCs, and plasmacytoid DCs produce no IL-10.[160] Most hematopoietic cells express low levels of the IL-10 receptors, but expression is up regulated in response to appropriate stimuli.[160] Beyond hematopoietic cells, fibroblasts, epithelial cells, and many other cell types contain components of the IL10 receptor complex and these are up regulated with appropriate stimuli.[160] In target cells, inflammatory signals are inhibited via multiple pathways including suppressor of cytokine signalling 3 (SOCS3) inhibition of cytokine gene transcription, and blocking of NF-κβ translocation into the nucleus.[160] The primary target cells for IL-10 are antigen presenting cells, which down regulate major histocompatibility complex II (MHC II) expression and causes the inhibition of antigen presentation.[160]

In contrast to IL-10, interleukin-17 (IL-17) is a potent inflammatory cytokine.[161] It is expressed by Th17 cells.[161] The founding member of the IL-17 family was IL-17A, but the family now consists of IL-17A, IL-17B, IL-17C, IL-17E (also known at IL-25), and IL-17F.[161] Some family members have tissue restricted expression while others are cell restricted. IL-17 was discovered as part of the inflammatory response for many autoimmune diseases such as rheumatoid arthiritis, asthma, and lupus.[119,124,162] The distinction between IL-17 expression and other pro-inflammatory cytokines has resulted in IL-17 being the defining feature of a newly described T helper subset called Th17 cells. Expression of IL-17 can be found in Th17 cells, T cells, smooth muscle cells, epithelial cells, macrophages, the thymus, and the spleen.[133,163] The target cells are epithelial or endothelial, and the target tissues are mucosal.[133] IL-17 signalling leads to IL-6 expression.[161] Recently IL-$10^{-/-}$ peritoneal macrophages have also been shown to produce IL-17.[163] Beyond autoimmune disease, Th17 cells have proven instrumental in the protective immune response against many lung pathologies.[104,120,123] In these models, the bacteria *M.tuberculosis*, *P.aeruginosa,* and *B.pertussis* have been shown to have IL-17 as a protective immune correlate. Of particular interest to this thesis was the finding that *B.pertussis* was TLR4 dependent for the differentiation of Th1 and Th17 cells, and that IL-17 activates macrophage killing of *B.pertussis.*[104,123] IL-17 is maintained in a

subtle equilibrium as a key regulator of autoimmunity and protective immunity; low level expression promotes protective immunity while too much can lead to autoimmunity.

1.12 Vaccination

Vaccines remain one of the most effective medicines. Since Jenner's smallpox vaccine in 1796,[6] more lives have been spared by vaccination than any other medicine. With great success comes great complacency. Entering the last two decades of the 20th century it was believed the war on microbes was over. Antibiotics had been discovered and they were controlling bacterial diseases well.[24] Large leaps in lifespan over the course of the 20th century had been made, and the eradication of smallpox in 1979 left humanity feeling smug about their ability to control infectious disease. The arrival of acquired immune deficiency syndrome (AIDS) in 1981, and the discovery of the causative agent, HIV, revealed a new reality; [164-166] infectious diseases would prove more difficult to control than previously thought. Concomitant with the arrival of the HIV pandemic, recurring influenza pandemics, and new emerging pathogens, such as SARS, have proven viruses are more adaptable and tougher to eradicate than originally believed. New more effective vaccines are necessary to prevent the viral bane.

Jenner's original cure was an attenuated vaccine, a non-virulent form of a pathogen. In Jenner's case cowpox was relatively inert in humans, but contained epitopes homologous to smallpox, which conferred protective immunity. Isolation or manipulation of a pathogen into an avirulent form is specific for each disease. The yellow fever virus was attenuated by passaging it through mice resulting in the YF17D vaccine.[167] Attenuated forms of virus can be replication competent, which results in a stronger immune response. The measles vaccines currently produced are live attenuated virus, but originally they were produced as an inactivated vaccine. The inactivated form had poor T cell response and only provided short term protection, whereas the live attenuated form has overcome these shortcomings and is successful at providing protective immunity after two doses.[168] Attenuated vaccines can produce humoral and cellular immunity.

Attenuation is not always possible and an alternative is to produce dead pathogens. Some methods to kill pathogens are heat, ultraviolet light, or formaldehyde.

The latter was used for Salk's polio vaccine.[169] Attenuated or inactivated vaccine efficacy varies according to pathogen. Some common problems for both types of vaccine are the isolation of pathogen, growth of pathogen to produce sufficient quantities for vaccines, and effective methods for inactivation of virulence. In these types of vaccines good manufacturing practice and quality control are vital as virulent forms of the vaccine can evolve. This unfortunate scenario occurred when some manufacturers of Salk's polio vaccine improperly formaldehyde inactivated vaccine preparations, resulting in thousands of deaths. When vaccines are produced with non-replicative pathogens, they are ineffective at providing cytotoxic T lymphocyte responses.[170]

Subunit vaccines benefit from easy manipulation and production. After the initial isolation and characterization of a pathogen, recombinant components of a pathogen can be added to another vector or preparation. One strategy could be to use a subunit on the capsid of a recombinant virus, or subunit delivery as a DNA element delivered by a vector. A few examples of subunit vaccines are vaccinia virus,[171] adenovirus, baculovirus,[172] and virus like particles (VLPs).[173,174] VLPs are the platforms used for display of the L1 epitope from the human papillomavirus and the Hepatitis B surface Antigens for Hepatitis B vaccines. Both vaccines are approved by the Food and Drug Administration in the United States. The greatest benefit of this approach is the speed of production. Once the platform has passed clinical trials, any epitope can be added and tested for efficacy to new pathogens.[175] The drawback of subunit vaccines is the challenge of selecting epitopes to use. The more epitopes added to the vaccine the higher the chance protective immunity occurs and the less likely resistant forms of the pathogen will escape immunity.[176] The likelihood of resistance is dependent on the type of pathogen. HIV replication is degenerate and gives rise to a large population of virus within a host as an immune evasion strategy.[177] In subunit vaccines the formulation is the key to provide a strong immune reaction appropriate for protective immunity against the chosen pathogen. The modulation of the immune response in this type of vaccine is primarily dependent on the formulation as specific antigens added to the vector could have negligible effects.

Conjugate vaccines are a variation on subunit vaccines where the vaccine components are chemically linked. One example of a conjugate vaccine is the isolation of an oligosaccharide from a virus or bacteria with subsequent conjugation to an immune response enhancing adjuvant.[71] The most effective example of this system is the haemophilus influenza B (HiB) conjugate vaccine developed in the 1980's.[178] Typically the oligosaccharide coat of viruses and bacteria are poorly immunogenic and the immune response remains limited to the production of IgM antibodies.[71] The new HiB conjugate vaccines were a breakthrough, as they provided >95% protective immunity. The premise of these new vaccines was the coupling of the sugar molecules to an adjuvant, such as diphtheria toxin, tetanus toxin, a non-toxic variant of diphtheria toxin called CRM197, or a complex outer-membrane protein mixture from *Neisseria meningitidis*. These conjugates resulted in higher efficacy, longer immune memory, and most importantly protective immunity.[71,178] This approach is now being pursued for *Streptococcus pneumonia, Neisseria meningiditis,* and *Salmonella typhi*[71,178]

Cellular vaccination is another method of raising protective immunity. It may be carried out *ex vivo* or antigen presenting cells could be loaded *in vivo*. DCs are the usual target cell, as they are the most potent antigen presenting cells. The discoverer of DCs is an avid proponent for DC vaccines, as they are integral to most immune responses and could be used to treat most pathologies.[179] As such, vaccination with DCs could prove effective in the treatment of infectious disease, autoimmunity, cancer, or transplant rejection. One of the main benefits of this approach is cross presentation, which would result in the activation of naive T cells into CTL cells. A myriad of experiments are currently being undertaken, but no vaccines have been produced using DCs. If it becomes necessary for *ex vivo* cell work to produce DC vaccines, the cost will be prohibitive for developing countries where many vaccines are most needed. As such, it will not be feasible to protect developing or developed countries from infectious disease with cellular vaccination, as pathogens will persist and evolve in permissive conditions of non-immunized countries.

A variation of subunit or DC vaccination is DNA vaccination. In this method, recombinant DNA is delivered to cells in the body for expression of antigen. DNA

vaccination can produce CTL, T helper, and humoral immune responses.[170,180] The major hurdle for DNA vaccination is the poor memory immune response; as a consequence complex booster schemes are necessary to provide immunity.[181] DNA vaccination is not currently being used to treat human disease,[180] however, clinical trials are underway. As with subunit vaccines, DNA vaccination is accomplished with a vector to deliver DNA to an organ or cell type. Some targets include the liver, spleen, lymph nodes, or dendritic cells.[182] Vectors currently being investigated are viruses, liposomes, bacterial ghosts,[183] VLPs, bacteriophage,[184-186] or synthetic systems such as nanoparticles.[187-189]

Inoculation route affects the resulting immune response. With the appropriate formulation, an intravenous (IV) inoculation will deliver large amounts of vaccine to the spleen and liver, and systemic memory responses result. A drawback of an IV inoculation can be the rapid clearance of vaccine via the spleen and liver, which can attenuate or inhibit and adaptive immune response. This scenario combined with the need for a healthcare professional to administer IV injections, makes IV inoculation an unfavourable method. An intramuscular (IM) injection is most common; this stimulates Langerhans cells and tissue resident macrophages which results in draining lymph nodes processing the antigens. As muscle contains many physical barriers a depot effect can occur in which the clearance of the vaccine is physically inhibited, and longer immune stimulation results. As a benefit, if toxicity of vaccine components are an issue, IM inoculation can restrict necrosis and prevent systemic acute phase responses. This scenario may arise if stronger adjuvants are necessary for immune stimulation. With the appropriate formulation IM inoculation can produce systemic memory responses.

Ideally, vaccines could be delivered to the extremities or the mucosa. These inoculation methods are particularly well suited for mass vaccination programs. From a biological perspective, oral or mucosal vaccines could help produce a local immune response that could mimic the normal infectious pathway of most pathogens.[35,190,191] For example, when nasal sprays are used the production of mucosal and serum IgA are stimulated.[35,190,191] The presence of IgA increases the effectiveness of the mucosal immune barrier. Mucosa are highly specialized tissues that have evolved complicated defences which contain many physical, chemical, and biological components to prevent

infection.[90,190,192-195] They are an effective immune barrier, and hence presentation of vaccine to immune cells is difficult across the mucosa. Most vaccines cannot provide a consistent dose of antigen along with adequate costimulatory signals to immune cells. Therefore mucosal vaccines suffer from inconsistent immunity due to inconsistent delivery. In contrast, the full dose of vaccine is delivered to the immune system in IM inoculations, as immune cells are the only mechanism to remove the challenge from the local tissue. Mucosal or oral inoculations can result in an entire vaccine dose never encountering the adaptive immune cells as physical and chemical barriers should prevent interaction. For these reasons oral and mucosal vaccines are not common. The Dukoral™ vaccine is an anomaly, but with an effectiveness of only 2-3 weeks against *E.coli* and cholera, few other afflictions are reasonably inoculated in such a manner.

Vaccine development is very time intensive. Having correlates of immunity can expedite the process. Protective immunity remains the best proof of effective immunization, but immune challenges in patients or animal models are not always feasible, let alone ethical. Clinical data on cytokine expression, viral loads, and cell populations together with patients known to be resistant are key to developing a vaccine. With an appropriate animal model, further insights into disease progression can be gathered. With this knowledge vaccine trials in animals can be performed and appropriate immunological criteria can be established which correlate with a protective immune response. For example, in tuberculosis (TB) vaccines it is necessary and sufficient to produce high levels of IFNγ in order to confer protective immunity.[104,136] In HIV it has been found that RANTES, MIP-1α, and MIP-1β are suppressive cytokines produced by $CD8^+$ T cells to fight HIV.[196] For many pathogens, the identification of protective immune correlates is inhibited by the lack of effective disease models. With infectious diseases establishing effective disease models is difficult owing to the specificity of pathogen and host. The production of humanized mice will surely drive more optimal development strategies.[197,198]

The future of vaccine research is promising. The goal of designer vaccines that produce protective immunity, a robust immune memory response, and few, if any side effects can be achieved, as the tools available for rational vaccine design continue to

evolve. Though the vaccine methods discussed in this section seem extensive, under the current state of the art most pathogens are still recalcitrant to therapy. There is great diversity in pathogens and as of yet no one vaccine method is a panacea.

1.13 Phage vaccines

Bacteriophage has been widely used in molecular biology because of their safety, utility, and flexibility. Of particular interest to immunology and vaccine research is the ability to screen libraries for bioactive proteins or peptides. Phage libraries are regularly screened for peptides that bind APCs, tumours, or lymph organs.[182] Patient sera can also be screened using phage libraries to find protective immune epitopes.[199]

The first phage vaccine trial was performed in 1988.[29] Phage proved to be an effective subunit vaccine. No immune dominant epitopes were present in f1 filamentous bacteriophage when rabbits or mice were immunized, and displayed antigen resulted in serum antibodies after 1 to 2 inoculations. Unfortunately, the antibody response was only measured using dot blots or relative absorbance. The approach was promising but the inoculations were performed with Freund's adjuvant. It would have been interesting to examine the results of inoculations completed without Freund's adjuvant.

Since the first phage subunit vaccine study, many animal trials have been performed. Two studies have been performed with Freund's adjuvant,[34] and seven experiments without the use of adjuvant.[35,43,186,200-203] In the more recent Freund's adjuvant experiment antigen specific titers of 10^4 and 10^5 antibodies were found after immunization.[34] When no adjuvant was added to bacteriophage subunit vaccines, antigen specific titers of ~10^2 are produced after IP, oral, or nasal inoculation.[35,43] In contrast, bacteriophage antibody titers of 10^3-10^4 were measured in the saliva and serum of oral and nasally immunized mice.[35] No other studies measured antibody titers against antigen or phage, but antigen specific antibodies were produced[202] and robust absorbance values were measured using ELISAs for phage and antigen.[186,201,203] Bacteriophage therefore have natural adjuvant activity. In one of these studies polymyxin B beads were used to remove LPS after phage preparation.[201] Mice were inoculated subcutaneously and significant increases in protective immunity resulted following immune challenge with lethal doses of Herpes Simplex-2 virus.

The ability to immunize via an oral or nasal route would be a boon for the fight against infectious disease.[190] Bacteriophage are enteric bacterial viruses present in all alimentary tract organisms, such as humans and worms. Given the co-evolution of bacteriophage with various organisms it is interesting to note the presence of serum antibodies in response to oral inoculations of phage.[35,40] It is also surprising given the general suppressive environment of the gastrointestinal tract.[90,204]

Beyond oral immunization, the distribution of bacteriophage has been well documented. After oral, intravenous (IV), intramuscular (IM), or intraperitoneal (IP) inoculation, bacteriophage virions accumulate quickly in the spleen and liver.[30-33,38,205,206] In Geier's classic study, IM inoculation resulted in rapid clearance of all traces of bacteriophage λ in < 50hrs.[38] When $2x10^{12}$ PFU of λ are inoculated IV, IM, or IP, spleen was the primary reservoir of λ, which continued to have 10^5 PFU/g of wet tissue at 100hrs. In comparison, when T4 phage are radioactively labeled and administered 99% of phage clearance is performed by liver Kupffer macrophages within 30 minutes. Quick clearance of T4 may be virus specific or suggest contaminating PRRs were present in the T4 preparation administered. With an IP or IV inoculation of 10^{12} or 10^{10} PFU of λ, at 25hrs there are 10^4 PFU/mL of λ present in blood, and 10^1PFU/mL after 100hrs.[33,38] The serum concentration becomes constant by 100hrs, most likely due to viable phage that remain at a much higher concentration in the spleen and liver. Circulating or splenic bacteriophage may be beneficial and tolerated as sentinels of immune defense for infection. In contrast, IM inoculation of λ resulted in the rapid clearance of λ from blood and *per os* inoculations with the same titer resulted in complete clearance of all λ from all tissues within 20hrs. Non-tolerant immune cells are evidently activated in *per os* and IM phage delivery.

The use of subunit vaccines based on bacteriophage has been explored for a variety of pathogen epitopes including ones from malaria, *Plasmodium falciparium*, Hepatitis B surface antigen, Hepatitis B, Hepatitis C, Herpes Simplex virus, and human Respiratory Syncytial Virus.[29,35,44,186,200-203] Some of these experiments included models to test protective immunity. Given that bacteriophage are known to be immunogenic,

future studies should investigate their ability to confer protective immunity or their apparent adjuvant activity.

Two forms of vaccination are common in phage studies, peptide or mimotope display, and genetic immunization. The ease of manipulating the phage genome makes either approach relatively straight forward. Production of phage DNA vaccines in general necessitates less steps and fewer controls than are required for other vaccine types, with peptide or mimotope display many variables must be addressed, such as the valency of epitopes, the accessibility of fusions to solvent, and capsid stability. This will be discussed in more detail in a later section (Chapter 3). Currently, the work presented herein is the only report of a peptide/protein vaccination with a λ subunit vaccine. This is likely due to the technical hurdles in producing a λ phage display system, as there is no commercial system available. Other groups have been interested in the production of λ subunit vaccines for genetic immunization.[184,186,205,207,208] Although recombinant proteins generated in bacteria are often inadequately folded and/or post-translationally modified, significant success has been achieved in generating vaccines from virus-like particles (VLPs) cultured in insect cells after expressing self-assembling viral capsid proteins.[174,189] The choice of epitopes is key and as previously discussed, neutralizing antibody epitopes from resistant patients would expedite this process.[29,199,209,210]

Bacteriophage are one of the oldest genetic vectors, with reams of data on phage genomics/genetics and life cycle. There are also extensive studies showing human and animal therapeutic efficacy. The body of work on bacteriophage is lacking a deeper understanding of the bacteriophage-host immune system interaction. It is for the most part unknown how mammals recognize λ, what their adjuvant activity is, and how they stimulate the innate and adaptive immune systems.

1.14 Thesis Summary and Objectives

The λ display system developed for this thesis has been named Mashkiki. It is derived from the Algonquin name, mashkikì meaning medicine, with an alternative meaning of potion, or herbal brew. The name is fitting as bacteriophage have been used as a therapeutic since they were discovered by a French Canadian. The region where Felix d'Herelle and I are from was inhabited by the Algonquins. The material of this

thesis is based on utility of a λ display system. It is proposed that λ based therapeutics be called Mashkiki.

Hypothesis: Longer regions of homology delivered to ES cells can increase targeting efficiencies beyond the current rates of 10^{-6}.

Objective: The addition of a protein transduction domain will cause λ transduction into mammalian cells, facilitating delivery of long homology regions.

Mouse targeting vector construction is a rate limiting step for the discovery of gene function and production of disease models. Methods to expedite the process are necessary. As the laboratory has expertise in λ recombination for mouse targeting vector construction, a study was undertaken to test the utility of intact λ virions to transduce embryonic stem (ES) cells for gene targeting. It was previously shown that homologous recombination can be enhanced with longer homology regions, but a plateau is reached at 14kbp. Given λ capsids accommodate up to 50kbp, it was asked whether longer homology regions delivered by a non electroporation method would result in greater gene targeting efficiencies.

To test this hypothesis we set out to engineer bacteriophage λ to display a protein transduction domain and demonstrate its ability to be transduced into mammalian cells and deliver a genetic cargo. The results of this work are presented in chapter three, which is presented as a stand-alone chapter complete with an extensive introduction. Overall it describes the basis of much of the early work in this thesis, but was a separate line of reasoning than the immunological studies which form the bulk of this project.

This work is highlighted to present the construction of Mashkiki bacteriophage, and to present findings on the biological activity of λ that display the protein transduction domain of TAT. As the Mashkiki λ display system was built, it was postulated that λ could be an effective subunit vaccine platform. Phage had been previously shown to be immunogenic. The rapid development of vaccines for emerging diseases using a genetic approach would be an asset, as would the ability to biopan bacteriophage λ epitope libraries. With prior experience with recombineering and phage biology, it was a natural extension. The end result could be quick, cheap, and thermostable

vaccines.[29,35,147,205,209,211-213] Up to this time the study of bacteriophage vaccination had been limited to antibody production and survival models for protection. A comprehensive study of the immune challenge had not been previously undertaken.

Hypothesis: Bacteriophage lambda can be used to create effective subunit vaccines for mimotope or peptide vaccination.

Objective : To investigate bacteriophage lambda as a vaccination vector, and characterize the immune response to bacteriophage lambda challenge

Our aim was to undertake the first peptide vaccination study using bacteriophage λ. In parallel we also chose to investigate bacteriophage λ as a DNA vaccination vector. We set out to provide the field with a comprehensive understanding of the cytokine milieu in the spleen following immune challenge, along with an analysis of the antibody isotypes generated in response to challenge with Mashkiki.

Hypothesis: The adjuvant activity for bacteriophage lambda is provided by a Toll-like receptor ligand on the bacteriophage lambda capsid or provided by the hypomethylated bacteriophage lambda genome.

Objective A: Identify TLR/TLRs responsive to λ, and if the prototypical TLR ligand is present in λ preperations.

Objective B: Characterize the TLR intracellular signalling in response to λ to provide clues on differential cytokine expression and determine differential TLR activation from different ligands.

The detailed mechanism through which well known adjuvants function was poorly undersood. We endeavoured to characterize the adjuvant activity of λ, as it was unclear whether λ or a bacterial contaminant is responsible for the documented λ adjuvant activity. The understanding of adjuvant activity is necessary before Mashkiki subunit vaccines can be utilized in human trials. Hence, we decided to undertake a systematic analysis of λ immunobiology. With a better understanding of λ immunology, deficiencies and strengths can be adapted and taken advantage of to build better Mashkiki subunit vaccines. It remains to be seen how this knowledge will translate into protective immunity and immune memory, but the initiation and propagation of the immune

challenge is the foundation that builds an immune response. Overall the work presented herein will illustrate the basis for a new vaccine development platform based on bacteriophage λ.

Chapter Two: **Materials and Methods**

2.1 General Considerations

The protocols described herein are the optimized and final methods for each assay. Many variations were tested to arrive at the final procedure. Indeed, even within the data collected, slight variations were used in order to attain as unequivocal evidence as possible for a given experiment. This chapter will outline the standard operating procedures used to arrive at answers and thus more questions. Many of the techniques used below are described in Molecular Cloning 3rd edition by Sambrook and Russell.[211]

Some basic assumptions are that MilliQ purified water was used, except in some situations where the water was simply distilled water from the distilled water source for the building. In many cases the milliQ water was further sterilized by autoclaving, and this is referred to as ddH_2O. Two exceptions are for RNA work and LPS work. Both procedures require water free of contaminants still present in ddH_2O. For RNA work, DNAse/RNAse free, Ultrapure™ water, was purchased from Invitrogen. For LPS assays it was necessary to have LPS free H2O. In preparation of the polymyxinB column, Ultrapure™ water was used, as it has <0.25 endotoxin units (EU)/mL. When the LAL assay was performed, LPS free water was used, this was quality tested by Lonza and was provided in the LAL kit.

2.2 DNA based Methods

The basis of this thesis was to test synthetic bacteriophage for efficacy in reprogramming stem cells, and the immune system. Plasmids and bacteriophage genomes were modified to produce the various products in order to test these hypotheses. The DNA specific techniques for plasmids will be discussed in the section below and in section 2.5, a method called recombineering will be discussed which utilizes a homology driven recombination system of mutagenesis. Recombineering was used on the gpD capsid protein of bacteriophage lambda (λ, or phage).

Plasmid DNA was purified from bacterial cultures (2.4.1) using Qiaprep spin columns (Qiagen). This resulted in very clean DNA that was low in RNA and protein contamination.

2.2.1 Restriction Digests

The age of molecular biology was ushered in with restriction digestion and ligation. The ability to selectively cut DNA elements brought about a new era in synthetic biology.[212] In this thesis, restriction digestion was used for the construction of plasmids and bacteriophage. Digestions were setup in the buffer suggested by the supplier. The amount of DNA digested was dependent on how much product was needed for ligation, each ligation usually being 50-100ng for a 5kbp plasmid. Therefore, the volume and amount of DNA to digest was adjusted accordingly. A typical reaction was to cut 1μg of DNA with 0.5μL of restriction endonuclease, 1X restriction endonuclease buffer, and H_2O was added to increase the volume to 20 μL. In a 1X reaction, no more than 2μL of endonuclease was used per 20μL reaction, as a greater volume would result in a concentration of glycerol, greater than 5%, and star activity could then occur; star activity being when enzyme specificity becomes promiscuous.[213] Other factors affecting star activity are: high units of enzyme to μg of DNA, ionic strength < 25mM, pH >8.0, presence of organic solvents, or substitution of Mg^{2+} with other divalent cations such as: Mn^{2+}, Cu^{2+}, Co^{2+}, or Zn^{2+}. Digestions were left for 4hrs. but generally 1U of enzyme will cut 1μg of DNA/hr.

2.2.2 EtOH precipitation

If precipitating less than 10μg of DNA, glycogen was used as a carrier molecule (Roche) to increase the yield. One tenth of a volume of 3M sodium acetate pH7, and 2 volumes of -20^{o}C 95% ethanol (EtOH), were added to the DNA solution. A minimum volume of 64.5μL of DNA was used for a total volume of 200μL, where the volume of DNA was increased by the addition of ddH_2O. The reaction was vortexed, and left on ice for 10min. The reaction was then centrifuged at 16,000x g for 30min, if less than 1μg, or 20min for samples with >1μg. This has been shown to increase yields more so than

incubation temperature or time.[214,215] Following centrifugation, the precipitate of DNA was visible at the bottom of the microfuge tube.

Ethanol was removed from the precipitated DNA, and was then washed to remove residual salts. This was accomplished by removing the supernatant with a P200 wide bore pipette tip. This decreased the vortex of suction from the tip and helped increase the yield of DNA. The DNA pellet was then centrifuged for 1 min at 16,000x g and any remaining liquid was removed with a P20 pipette. The DNA pellet was then washed once by the addition of 800µL of -20^{o}C 70% EtOH. The tube was vortexed to remove any salt residue left from the previous buffer, and then centrifuged at 16,000x g. The supernatant was removed, as described above, being careful to not lose the now translucent DNA precipitate.

The precipitated DNA was dried, and then resuspended. Briefly, the microfuge tube was left with the cap open to allow any residual EtOH to evaporate and the pellet was resuspended in a low volume of Tris-EDTA (TE) buffer (10mM Tris, 1mM EDTA, pH 7.5 to 8). When large fragments of λ DNA were used for this or any other reaction care was taken to not over-dry the DNA precipitate as it becomes difficult to dissolve when over-dried, and any vortex steps must be omitted as DNA >10kbp will shear. Yields >90% were attained with this technique, and DNA can now be used for later steps in a different buffer, or at higher concentrations, or with lower salt concentration.

2.2.3 Oligo annealing

Following DNA synthesis, lyophilized DNA was resuspended in TE buffer to a final concentration of 100µM. The 100µM oligo stock is then diluted a further 10fold with ddH_2O, to make working stock solutions of 10µM. Both dilutions were left at -20^{o}C until needed.

To anneal DNA the following was assembled in a mircrofuge tube: 1µL of 10µM sense strand oligonucleotide, 1µL of 10µM antisense strand oligonucleotide, 1µL of 10X buffer 3 (NEB), and 9µL of ddH_2O. The reagents were mixed with a micropipette and heated for 5min at 98^{o}C. After incubation the heating block was left to equilibrate to room temperature. Equilibration usually took 4hrs. To test for successful annealing, 1µL of the reaction was separated using an electrophoretic mobility assay (section 2.2.4) and

DNA was visualized using ethidium bromide (EtBr). Only double stranded DNA will intercalate EtBr.

2.2.4 DNA gels

DNA gels were used to visualize and separate DNA species. The percentage of agarose (Invitrogen, Ultrapure #15510-027) gel used depended on the size of DNA that was visualized or purified. For example 0.5% agarose separates 1-20kbp, but for 0.1 to 2kbp, a 2% agarose gel is ideal. For smaller DNA species or better resolution a polyacrylamide gel was used (see section 2.7.1),

2.2.4.1 Agarose gel electrophoresis

DNA was electrophoresed in agarose gels to analyze restriction enzyme digestion or to isolate specific bands following digestion (section 2.2.5). Agarose gels were usually prepared with 0.7% w/v agarose, molecular biology grade, in 1X TAE buffer (40mM Tris, 20mM glacial acetic acid, 2mM Na_2EDTA, at a pH of 8.0). Agarose was weighed and added to TAE, the solution was then boiled in a microwave, with repeated stirring, until dissolved. After the solution was ~60^{o}C, 0.2 to 0.5μL of 10mg/mL EtBr was added. The solution was gently mixed and poured into a gel tray. Air bubbles were removed and a comb was inserted. Polymerization occurred as the solution cooled, and was visually seen as the opacity increased.

Three gel systems were used: a mini gel system from BioRad^{TM}, a medium size gel tray/tank for larger numbers of samples and larger DNA species, and a large gel apparatus for running bacteriophage DNA. The mini and large systems were used for quick gel screening of many samples. After the gel polymerized, the comb was removed from the gel. The gel was immersed in a buffer tank containing 1X TAE, and the wells were loaded with DNA mixed with 1X DNA loading dye. Two versions of DNA loading dye were used in this thesis. 6X DNA loading dye was 0.25% bromophenol blue, 0.25% xylene cyanol, with 30% glycerol in TE. The other loading dye was 10X DNA loading dye made with 40% sucrose, 2mg/mL Orange G (Sigma). Gels were typically run at 50 to 110V for 30min to 2hrs. For isolation and visualization of bacteriophage λ genomic

DNA, ~2μg of DNA was necessary per well and electrophoresis was performed for 18 or more hrs. at 36V. This resulted in better resolution of the DNA species present.

One last agarose gel method used to visualize DNA, was the 'surface tension gel'. This method was used on samples with a low abundance, and/or low volumes after manipulation. Using a typical DNA gel 10ng of DNA cannot be visualized, although in theory the sensitivity of EtBr is 10ng/mL.[216] With a surface tension gel this sensitivity is possible. Briefly, all components are the same, but after boiling the agarose solution was poured onto a small glass plate. The liquid agarose was retained on the plate with surface tension and this results in a regular gel height. With a consistently thin gel, rare DNA species can be visualized.

DNA migration was monitored by watching the DNA loading dyes migrate, a final check was done with a handheld UV box before the electrophoresis was stopped. Gels were visualized on a UV box and photographed using the Kodak 1D imaging system.

2.2.4.2 Polyacrylamide gel electrophoresis

After large DNA oligos were synthesized by Operon (Eurofins MWG Operon), they were checked for purity by a polyacrylamide DNA gel. For a DNA polyacrylamide gel, the same apparatus was assembled as for a protein gel (section 2.7.1), but only a resolving gel of 12% acrylamide was poured, instead of a stacker and resolving gel. Also instead of TBS running buffer being used to run the gel apparatus, 1X TBE (45mM Tris Borate, 1mM EDTA) was used.. TBE was filter sterilized and stored at RT. In a polyacrylamide DNA gel TBE was the buffer used for loading the DNA. When the loading dye front migrated down the gel to the desired location, the gel was removed from the apparatus, and EtBr was used to stain the gel. The gel was destained using water, where EtBr was retained in DNA caught in the acrylamide matrix. The DNA was then visualized using the Kodak 1D system. EtBr was necessary to be used as a stain at the end of this procedure, as it will inhibit the polymerization of acrylamide.

2.2.5 Gel Purification

Gel purification was used following most PCR reactions before a fragment was cloned. Gel purification was done on DNA fragments extracted from an agarose gel using a razor blade and forceps on a UV light box. Gel volumes were minimized and samples were added to a microfuge tube. Two methods were generally used for gel extraction, the QIAquick gel extraction kit (Qiagen), or the freeze and squeeze method.

When the QIAquick gel extraction kit (Qiagen, #28706) was used the protocol was followed as suggested in the product literature for a microcentrifuge. DNA was eluted in 30 to 50µL buffer EB depending on the amount of DNA present.

The squeeze and freeze method is a cleaner method to isolate DNA fragments from an agarose gel. To perform this method low melt agarose gel was used to prepare an agarose gel (section 2.2.4.1), and following electrophoresis the desired fragment was removed as described above. For each gel slice, or fragment, added to a 1.5mL tube, 100µL of TE was added. The tube was incubated at 65^{o}C, until the gel was melted, with occasional vortexing. Melting typically took 15min. The tube was then added to an EtOH dry ice bath until the DNA-TE solution was frozen. The solution was then thawed at room temperature and centrifuged at 12,000x g for 10min. The DNA containing supernatant was removed, and care was taken to not disrupt the precipitated agarose. Finally, 100µL of TE was added to the tube with the precipitate. The agarose precipitate tube was then centrifuged again and the supernatant was then added to the supernatant from the first extraction. DNA was then EtOH precipitated to decrease the volume (section 2.2.2).

2.2.6 Modification of DNA fragment ends

The termini of linear DNA were modified as necessary for the appropriate cloning strategy. The following techniques were used: phosphorylation, de-phosphorylation, ‘end filling’, and ‘end polishing’.

It is necessary to phosphorylate oligos after DNA synthesis to increase cloning efficiency. The reaction was prepared in a volume of 100µL as follows: 20µL of 5x forward reaction buffer (Gibco-BRL), 10µL of 10mM adenosine triphosphate (ATP),

2μL of 10U/μL of T4 polynucleotide kinase (T4 PNK), and DNA. Care must be taken not to use ammonium acetate in previous steps leading into this reaction as ammonium ions inhibit T4 PNK. The DNA can be 68μL or 2-4nmol total oligonucleotide, 20μg, or 20-40μL of a 100μM stock of oligonucleotide. The reaction was performed at 37^{o}C for 60min., followed by heat inactivation at 65^{o}C for 20min. The oligonucleotide was purified from the reaction using either phenol chloroform extraction or gel purification.

Dephosphorylation was commonly used to decrease self ligation of compatible DNA ends on a vector. After restriction digestion 1μL of Calf Intestinal Phosphatase (CIP), or ~5-10U was added for every 5-10μg of DNA. Phosphatase or alkaline phosphatase was compatible with most restriction enzyme buffers. The reaction was incubated at 37^{o}C for 30min., and an additional 1μL of CIP (Roche) was added to the reaction which was then left for an additional 30min. The reaction was terminated by the addition of 1.5μL of 100mM EDTA for every 20μL of reaction volume, which was subsequently heated to 70^{o}C for 20min. After heat inactivation the DNA was purified by either gel purification or phenol chloroform extraction. The efficiency of the dephosphorylation was tested by using an aliquot of the reaction for ligation with and without an oligonucleotide insert. After which the ligation was electroporated and the number of colonies for each treatment, with and without an insert, was counted.

End filling is a method that will mutate the sticky ends of a restriction endonuclease site into a blunt end, by the addition of nucleotides to overhanging ssDNA ends.. End filling was used to make compatible ends for some cloning steps, or to destroy endonuclease target sequences. Another alternative is to use an adaptor oligo, but this will not mutate endonuclease restriction digest target sequences. A few different enzymes can be used for end filling, but T4 DNA polymerase has a lower error rate and was therefore utilized rather than the Large Klenow Fragment. Lower error rates are accompanied by 3'to 5' exonuclease activity in T4 DNA polymerase, but this can be mitigated by lowering the reaction temperature, the amount of dNTPs, and lower enzyme concentrations. If the strategy was to cut back overhanging DNA ends, or an end polishing reaction, the reaction is therefore changed to to favour the exonuclease activity instead of the polymerase activity. In a fill in reaction DNA was in a restriction enzyme

buffer or 1X T4 DNA polymerase buffer. This was supplemented with 100μM dNTPs, and 1 unit of T4 DNA polymerase per μg of DNA. The reaction was performed at 12^{o}C for 15min. and was stopped by the addition EDTA to a final concentration of 10mM. This was heat inactivated at 75^{o}C for 20min.

2.2.7 Ligation

DNA ligation is a central technique in modern molecular biology allowing different DNA fragments to be joined. After DNA was synthesized or cut, 2 species of DNA were added to a microfuge tube. Typically a reaction was 50 to 100ng of vector, with a 1:1 or 1:4 molar ratio of insert DNA, 1μL of ligase, and ligase buffer. The volume was kept to a minimum, and this was usually 10-20μL. ATP can also be added to the reaction at a 0.5mM concentration. The reaction was left at room temperature or in a 16^{o}C water bath over night. After ligation, products were electroporated into bacteria for long term storage.

2.2.8 Screening of ligation products

After ligation, and transfection of bacteria, bacterial clones were screened for the desired ligation products. This was done by an initial screen using restriction digestion (2.2.1), PCR (2.3), or hybridization (2.5.8). After the initial screen DNA sequencing (2.2.9) was performed to verify clones.

Restriction digestions were typically performed on 2mL overnight cultures that were prepared using the Qiaprep kit (Qiagen). Linearized DNA was electrophoresed on agarose gels (2.2.4.1) and DNA fragment patterns matching the predicted fragment sizes were kept for sequencing. This procedure was performed on 5 to 20 colonies from a ligation. If no positives were found more colonies were screened by PCR.

Alternatively, PCR was done directly from a single colony or 1μL of bacterial culture. In this method a colony was spotted onto a new plate, using a sterile pipette tip, and the tip was dipped into a PCR reaction mix (2.3). The spot was labelled together with the PCR reaction mix. As the PCR reaction was performed the agar plate with the corresponding spots were grown overnight. After PCR, the products were separated

using gel electrophoresis and the colonies with the desired amplimer size were chosen for DNA preparation and sequencing.

2.2.9 DNA Sequencing

DNA sequencing was performed at the University Core DNA Services in the Faculty of Medicine at the University of Calgary. The early sequencing was performed on an ABI non-capillary sequencer. All sequencing since 2003 was performed with the ABI 3730 XL DNA sequencer (Applied Biosystems). A tube containing the DNA template and sequencing primer was provided to the facility. Typically this was 0.5μL of a 10μM primer stock with either 100ng of plasmid DNA, or 2μg of genomic λ DNA.

Sequencing results were compared using a pairwise alignment BLAST to the expected cloning product.[217-219] Care was taken to monitor the reading frame using Gene Runner ver. 3.05 (www.generunner.net), and annotation was performed using Microsoft Word™.

2.2.10 Construction of pGEX-DLTgfp

pGEX-DLT is a general purpose vector for isopropyl-β-D-thio-galactoside (IPTG) inducible expression of gpD-fusion proteins. In pGEX-DLT, the fragment containing glutathione S-transferase (GST) gene, thrombin recognition sequence and *Sma* I-cloning site of pGEX-2T (Amersham-Pharmacia) has been replaced with sequences encoding the λ capsid protein, gpD, a linker peptide (GKYTSSGQAGAAASES , see 2.5.7), a thrombin recognition sequence, LVPRGS, and a multiple cloning site: *Not* I - *Pac* I – *Eco*R I. The three nucleotides, TTC, immediately preceding the translation initiation codon, ATG, of GST was mutated to CAT in order to introduce an *Nde* I-site, CATATG, and the linker was flanked by *Hpa* I- and *Pvu* II-sites. The first three nucleotides of the *Hpa* I-site, GTTAAC, encoded the last amino acid of D protein and latter 3 nucleotides, add an additional amino acid, Asn, to N-terminal of the linker. Likewise, first half of the *Pvu* II-site, CAGCTG, added an additional amino acid, Gln, to the C-terminal of the linker and the latter half encoded the N-terminal amino acid, Leu, of the thrombin recognition site. The sequence encoding the D protein was isolated by PCR from wild type λ DNA using the forward primer: 5'-CCA GTG TAA GGG ATG CAT ATG A-3'

and the reverse primer: 5'-AAC GAT GCT GAT TGC CGT TCC-3'. The sequence encoding EGFP was isolated from pEGFP-F (CLONTECH) by PCR using the forward primer; 5'-AGA AAA AAG CGG CCG CCA TGG TGA GCA AGG GCG AG-3' and the reverse primer; 5'-TCG AAT TCC TTG TAC AGC TCG TCC ATG CC-3'. The result was EGFP without a farnesylation site. Following this, a *Not* I/*Eco*R I-digestion of the PCR product, was inserted between the *Not* I- and *Eco*R I- sites of the pGEX-DLT vector. The resulting plasmid, pGEX-DLTgfp, expresses a "gpD-linker-thrombin recognition site-EGFP" fusion protein upon addition of IPTG.

2.2.11 Contruction of pDE

The plasmid pDE was built in pBluescript SK^+ (Stratagene) and incorporated all of gpD from λ, and 560 bp of the 5' end of gpE; the start codon to an internal *Eco*R I site. The multiple cloning site (MCS) of pBluescript was replaced with the following oligo. The sense strand 5' to 3': ACC TGC TAG CAA TTG CTT AAT TAA TAG GAG GTT TTC ATA TGA CGC GTT AAC CCG GGC GGT GCG GCC GCA TAA TGA ATT CCT AGA TCG GCA GGT GTA C. The antisense strand was 5' to 3': ACC TGC CGA TCT AGG AAT TCA TTA TGC GGC CGC ACC GCC CGG GTT AAC GCG TCA TAT GAA AAC CTC CTA TTA ATT AAG CAA TTG CTA GCA GGT AGC T. The gpD coding sequence was then cloned into the *Nde* I and *Hpa* I sites of the new MCS. The gpE coding sequence was then cloned using the *Eco*R I sites in gpE and the new MCS. After cloning gpE, the 3' *Eco*R I site in gpE was destroyed by doing an end filing reaction following a partial digestion with EcoR1. At this point the 16 amino acid linker sequence was inserted 3' of gpD and the stop codon was replaced with the amber stop codon (section 2.5.7). This construct was used to make the pDam-mTAT plasmid for recombineering.

2.3 Polymerase Chain Reaction (PCR) based methods

PCR is a key tool in the modern molecular biologists tool belt. It is used for the amplification of products for use in cloning or recombineering, for screening recombinant products, and for measuring the level of mRNA present in samples.

2.3.1 Primer Design

All primers for PCR were designed using the Primer3 software.[220] In some cases, it was necessary for one primer to be at a set position. This was accomplished using Primer3, or by handpicking one primer and testing it on Netprimer.[221] Using these algorithms it was possible to pick primers with a Tm of ~60°C. These programs also gave an indication of success by calculating self complimentarity, 3' complimentarity, and any complimentarity; all indications of primer dimer or dimer product formation. In some experiments the specificity of primers were tested using a BLAST of a genome or a pairwise alignment BLAST of a plasmid or phage genome.[217-219]

2.3.2 Primer sets

All primers were synthesized at the University Core DNA synthesis facility here at the University of Calgary. Following synthesis DNA was resuspend in TE buffer at a concentration of 100µM. Working stocks were then made from this in ddH_2O, at a concentration of 10µM for PCR, or primer sets were combined in a stock tube at 5µM for QRT-PCR. The following primers were used in this thesis.

Primer Name	Sequence (5'-3')
18s-smF	CCT TTA ACG AGG ATC CAT TGG A
18s-smR	ACG AGC TTT TTA ACT GCA GCA A
EGFP-1 LH	GTGAGCAAGGGCGAGGAG
EGFP-1 RH	GCGGATCTTGAAGTTCACCT
IFNγ-FW	TCA AGT GGC ATA GAT GTG GAA GAA
IFNγ-RV	TGG CTC TGC AGG ATT TTC ATG
IL-6 FW	GAGGATACCACTCCCAACAGACC
IL-6 RV	AAGTGCATCATCGTTGTTCATACA
IL-17a FW	GCTCCAGAAGGCCCTCAGA
IL-17a RV	AGCTTTCCCTCCGCATTGA
TNFα FW	CAT CTT AAA ATT CGA GTG ACA A
TNFα RV	TGG GAG TAG ACA AGG TAC AAC CC

gpDprimer1	GCACGTTCCGTTATGAGGAT
gpDprimer2	CCACGCTGACGTTCTACAAG
gpE RHprimer1	ACGGAAAAAGAGACGCAGAA
gpE RHprimer2	TCGGATCGAACACGATGATA

Table 1: PCR Primers

2.3.3 PCR technique

A typical PCR recipe contained 0.2µL of Taq polymerase (Invitrogen), 0.5µL of each primer from a 10µM stock, 13.5µL of 'supermix', 5µL of template, and 5.3µL ddH_2O. Supermix was made with 4mL of 10X PCR buffer, 80µL of each dNTP from a 100mM stock, 2mL of glycerol, 200µL of Tween20, 2.4mL of 50mM $MgCl_2$, and 11.08mL of ddH_2O. In rare situations where a PCR product was being cloned or was difficult to amplify, Phusion Taq polymerase (Finnzymes) was used as described in the product literature.

A standard PCR cycling program was an initial melt for 95^{o}C for 1min. Followed by 30 to 35 cycles of 95^{o}C for 30sec. to melt the template, 55^{o}C for 30sec. to anneal the primers, and transcription or elongation at 72^{o}C for 3min., after theses cycles there was a final elongation step at 72^{o}C for 7minutes. These were performed on the PTC-200 gradient PCR thermocycler (MJ Research). In any given reaction it was necessary to tweak the reaction conditions. For example if there was little product, adding more cycles would generally result in more product. Another common problem was non-specific priming. One solution was to increase the annealing temperature, which increased the specificity. Alternatively new primers were sometimes necessary. Many variations of any given component or condition were sometimes necessary for difficult PCR reactions, which needed to be adjusted on a case by case basis, but generally the reaction described above worked.

2.4 Bacteriological Techniques

Proper sterile, or aseptic, technique was essential for bacterial culture. Sterile technique consisted of first spraying all surfaces and gloves with 70% EtOH. After which all bottles to be used and glass pipettes were sterilized under a flame using a Bunsen burner. Following inoculations, lids and rims of bottles were flamed before storage. All micropipette tips were autoclaved or sterile. All growth media and liquid reagents were visually inspected for bacterial and fungal growth before use. When bacterial cultures were performed, media or buffer controls were done to test for contamination. If growth appeared in the negative growth control, all cultures were discarded, and new cultures were performed with fresh media.

2.4.1 Bacterial culture

Bacteria were grown in liquid culture or on agar plates to isolate individual colonies. Two growth mediums were used in this thesis: Luria broth (LB), and Luria broth with magnesium (LBM). LB was made with 10g/L Tryptone, 5g/L yeast extract, 5-10g/L NaCl, and the pH was adjusted to 7.0. LBM is 10g/L Tryptone, 5g/L yeast extract, 5g/L NaCl, and 0.94g/L anhydrous $MgCl_2$. Before LB and LBM were used they were autoclaved and allowed to cool.

A typical overnight bacterial culture was started from an isolated colony, picked from an agar plate, with a sterile micropipette tip. The colony was used to inoculate a 2mL overnight culture in a 14mL culture tube. It was grown in a shaking incubator set at 260rpm and 37^{o}C. The next day the culture tube contained a 2mL broth saturated with bacterial growth.

Overnight bacterial cultures were used to isolate DNA, for λ culture (2.5), or to inoculate larger bacterial cultures, such as those used in protein expression. Larger liquid cultures were inoculated with a 1:100 dilution of overnight culture to media, using sterile aerosol micropipettes, or sterile 50mL conical tubes to measure the volume. The volume of liquid never exceeded 1/5 of the total volume of the vessel, in order to keep the bacteria properly aerated.

Bacteria were also grown on LB or LBM agar plates. This was done to isolate individual colonies or clones. Agar plates, containing 1.5% w/v agar, were poured using proper sterile technique and left at 4^{o}C until streaked. Bacteria were added from a frozen glycerol stock, another agar plate, or following a bacterial transformation. When a frozen glycerol stock or agar plate was used to inoculate, serial dilutions were performed on a plate using a flame sterilized loop and overlapping streaks on the plate. This was done by spreading the bacteria on the plate with a sterile inoculation loop, in one area of the plate. The loop was then flamed, and left to cool. The loop was then streaked once across the area that was just spread out, and then streaked across the surface of a new area on the plate, being careful to always drag the loop over the agar plate, without breaking the surface of agar. This was repeated 3-5 times, depending on the number of bacteria that were in the initial inoculation.

An alternative dilution technique for culturing bacteria on agar plates was used after bacterial transformation. Dilutions were performed on the liquid transformation product and were spread onto plates using a glass rod. In this way many individual colonies were isolated for screening purposes.

Agar plates were prepared according to the bacterial strain or plasmid that was being isolated. Antibiotics, magnesium, and IPTG/Xgal were added to agar plates depending on the purpose of the experiment.

2.4.2 Bacterial strains

The following bacterial strains were used during this thesis:

Bacteria	Antibiotic Resistance
BL21 (DE3)	None
DH5α	None
DK21	None
DY330	None
LE392	None
LG75	None
P2392	None

MC1061	Ampicilin, Kanamycin, Tetracyclin
Rosetta (DE3)	Chloramphenicol

Table 2: Bacterial Strains

2.4.3 Bacterial Transformation

Bacteria were transformed using electroporation (EP), a more efficient method than chemical transformation. EP was performed on a BioRad gene pulser. This machine was set at a capacitance of 25 μF, with the resistance was set to 400 Ω, and a charge of 2.5 V.

Electrocompetent bacteria were prepared as follows. A bacterial culture was grown to 0.5 – 0.8 OD_{600}. Bacteria were collected by centrifugation at < 3,421x g for 5-10 min. The supernatant was poured off, and ice cold ddH_20 was used to resuspend the cells. The cells were then re-centrifuged, and the cell pellet was resuspended in ice cold 10% glycerol. The centrifugation was repeated and the cell pellet was resuspended in 1/100 the original culture volume with ice cold 10% glycerol. Ideally there was a final concentration of 2-3x10^{10}cells/mL, where 1 OD_{600} = ~2.5x10^8cells/mL. Aliquots of 25-40μL are then made in 0.5mL tubes and left at -80^{o}C until needed.

For a bacterial transformation the following reagents were assembled and left on ice: electrocompetent bacteria, electroporation cuvettes, 10% glycerol or ddH_20, and DNA. The transformation was done with either 5μL of a ligation, or 50ng of plasmid DNA. Five μL of DNA was added to 35μL of 10% glycerol, together with 10μL of electrocompetent cells. The solution was mixed by pipetting, and added to an ice cold cuvette. The cuvette was placed in the gene pulser, and a current was applied to it. The time constant for the electric pulse was monitored, as an efficient electroporation results in time constant of 7.9 to 9.4.

The cuvette was rinsed with 500μL of SOC (20g/L tryptone, 5g/L yeast extract, 0.58g/L NaCl, 0.19g/L KCl, and 10mL of 2M glucose, pH 7), a rich growth media, and the cells were grown for 30minutes in a 37^{o}C shaking incubator. This step allowed the bacteria to recover from the electroporation before growing them overnight on agar plates(section 2.4.1).

After the recovery incubation, a serial dilution was made of the culture. A 1% and 10% stock was made in 100µL total volume, the remainder of the cells were centrifuged and resuspended in 100µL of media, and this was the 100% plate. Each dilution was spread onto the appropriate agar plate for the transformed plasmid and was left to grow overnight. Any resultant bacterial colonies were then confirmed for the appropriate plasmid using restriction digests, PCR screening, sequencing, or radioactive probe hybridization (2.2.8).

2.4.4 Protein expression

Bacterial protein expression was performed in DE3 containing bacterial strains. Proteins were expressed from a variant of the pGEX-2T plasmid (GE Healthcare). Bacteria were grown to an OD_{600} of 0.4, at which point transgene expression was induced with the addition IPTG to a final concentration of 0.1mM. The culture was grown for an additional 1-3hrs. Transgene protein was collected from cells as cell lysates, or secreted proteins were collected from media.

2.4.5 Protein Purification

Bacterial proteins were crudely separated from the supernatant or cell lysate for sodium dodecyl sulfate polyacrylamide gel electrophoresis (SDS-PAGE). Alternatively, they were purified from bacteria together with bacteriophage during large scale bacteriophage preparation. In the later situation gpD-GFP fusion protein was isolated after ultracentrifugation in cesium chloride (section 2.5.5).

2.5 Bacteriophage Lambda Techniques

Bacteriophage λ are bacterial viruses that are temperature and pH insensitive.[205] As such they remain viable on many surfaces. In order to decrease the chance of cross contamination between bacteriophage λ strains, aerosol resistant tips were used. All glassware, and plasticware was sterilized, and work areas were cleaned with 70% EtOH. Media, buffers and reagents are checked for contamination every time a bacteriophage titration was performed.

2.5.1 Bacteriophage plating cells

E.coli bacteria are the host for the propagation of bacteriophage λ. Derivatives of *E.coli*, were grown as described herein and these preparations were defined as 'plating cells'. A 2mL LBM overnight culture was started (section 2.4.1). The next day the bacteria were subcultured using a 1/100 dilution into 30-50mL of LBM. The culture was grown until an OD_{600} of 0.6 to 1 was measured, typically <3hrs. The optical density was measured on a spectrophotometer, and the measurement was noted. The culture was transferred to a 50mL conical tube, and centrifuged at 3000x g for 10min. The supernatant was removed and the cell pellet was resuspended in 10mM $MgSO_4$ at ¼ the original culture volume. Plating cells are viable at 4^{o}C for up to 3 weeks.

2.5.2 Bacteriophage Titration

To measure the number of bacteriophage λ, a titration was performed. This was done using the top agar spot titration method. LBM agar plates were warmed to 37^{o}C, and top agar was boiled and allowed to cool to 55^{o}C. Top agar is LBM with agar at a concentration of 0.75%. In a sterile culture tube, 100-200μL or ~3.2x10^{8} of plating cells were added, followed by 4mL of top agar. The solution was swirled and then quickly dumped onto a pre-warmed LBM agar plate. Care was taken to spread the top agar around evenly and avoid bubbles, as both could affect the quality of the bacterial lawn. The top agar was allowed to cool for up to 20min. A variation of this method was when bacteriophage DNA was isolated, where agarose was added to LBM instead of agar.

Serial 1/10 dilutions were performed on λ with SM buffer (0.1M NaCl, 5mM $MgSO_4$, 50mM Tris pH7.5, and 0.01% gelatin). The LBM agar plate was then inverted and circles of 2cm diameter were drawn on the bottom of the plate. These were labelled with the dilution to be added to the top agar above the circle. Ten μL of each serial dilution was dropped onto the appropriately labelled top agar, and was allowed to dry at room temperature for a maximum of 60minutes. If the 10μL λ spot was not absorbed or dry at this point they could run when they are inverted. If the plate is left for >60min. the bacteria will not grow into a smooth lawn. Plates were carefully inverted and incubated at 37^{0}C overnight.

Eight hours later, plates were removed and λ plaques were counted. A plaque is a spot where bacterial lysis occurred, and therefore the agar is clear. Each isolated plaque was from a single bacteriophage. Looking at the lowest to highest dilution in the series, a dilution with 2-10 isolated plaques was found. The concentration of phage was calculated as the number of plaques at the power of the dilutions series multiplied by 100. Therefore if 5 plaques were seen at a dilution of 10^{12} then the titer was $5x10^{14}$ plaque forming units (PFU)/mL. The multiplication by 100 was necessary because only 10μL of a dilution was used and the concentration is denoted per mL.

2.5.3 Phage stocks

This section will describe how to make phage stocks from agar plates. Phage can be isolated from individual plaques, confluent top agar plates or from liquid culture. Liquid culture techniques will be dealt with in the next sections.

To isolate an individual plaque, the small bored end of a Pasteur pipette was pushed into the agar such that the plaque was encircled by the pipette. The pipette was pushed to the bottom of the agar. At this point the latex bulb that was inserted at the top of the Pasteur pipette was expanded to suck up the plug of agar containing the λ plaque. Agar plugs were added to 1mL of SM buffer, containing 1 drop of chloroform, killing any remaining bacteria. Each plaque contained 10^6 to 10^7 phage.

Pure λ clones can also be amplified from plates that have confluent bacterial lysis. In this situation λ was plated to cover the whole plate, not just a spot on the plate. If a 90mm plate was used, adding ~25,000 phage was sufficient to cause confluent lysis. After the plate was incubated overnight, 4mL of SM buffer was added. This was left rocking for 1hr. at room temperature. The SM was removed and 2mL of SM was added to the surface to rinse. Six drops of chloroform was then added to the 6mL of phage in SM buffer. The solution was left overnight at 4^oC. The next day the clear phage containing SM was removed leaving behind the chloroform and bacterial debris that precipitated. This stock was usually at ~10^8PFU/mL.

2.5.4 Small scale phage preparation

A typical small scale phage preparation was performed in a 10mL volume of LBM. Alternatively, if more or less λ was necessary, small scale preparations were modified by adjusting the volumes of the steps listed below accordingly. Small scale phage preps were performed to isolate phage DNA, but they could also be used for the crude isolation of intact phage.

The phage culture was started by adding 100µL of plating cells to 10µL of plaque lysate. λ were left to adsorb at 37°C for 20min. and were then added to 10mL of LBM. The culture was left to grow for 6-9hrs at 37°C on a shaking incubator. At the end of growth, any non-lysed bacteria were killed with the addition of 100µL of chloroform.

λ were isolated from the bacterial debris by centrifugation at 8000x g for 20min. The supernatant was kept and 15µL of a 10mg/mL DNase1 was added. The DNase1 reaction was incubated at 37°C for 30min. λ was then precipitated using 2.5mL of a 2.5M NaCl/40% polyethylene glycol 8000 (PEG) solution and the mixture was incubated at 4°C for 2hrs. The solution was centrifuged at 3000x g for 10min. and the supernatant was removed. The pellet was resuspended in 500µL of SM buffer.

PEG was removed by adding a volume of chloroform equal to the solution volume, and extracting the phage containing aqueous phase. Care was taken to not disrupt the white PEG precipitate at the interface. If too much PEG was present, a second chloroform extraction was performed. RNaseA was then added, 15µL of a 10mg/mL stock. The reaction was left at 37°C for 30min. At this point the isolated phage are relatively pure, and can be kept at this relatively high titer. Alternatively if phage DNA was needed, this protocol can be continued.

To prepare phage DNA, the capsid of the virus was broken open by the addition of 5µL of 10% SDS and 5µL of 0.5M EDTA. This was incubated at 68°C for 15min. Protein was removed by performing one phenol chloroform extraction followed by two chloroform extractions. In each case the aqueous, or DNA phase was retained.

Ethanol precipitation was performed, by the addition of 50µL of 3M sodium acetate, and 1mL of 95% EtOH. See section 2.2.2 for full details on EtOH precipitation. Care must be taken to not shake or vortex the DNA as phage genomes are ~50kbp, and

shearing is possible. At the end of the precipitation 25-100µL of TE was added to resuspend DNA. One last RNaseA step was used to remove any residual RNA. This was performed by the addition of 5µL of 10mg/mL RNaseA and incubation at 37^{o}C for 30min. DNA concentration was measured by the absorbance at 260nm on a spectrophotometer.

2.5.5 Large scale phage preparation

Large scale λ preparations were performed for the amplification and isolation of λ for use in cell culture and *in vivo* experiments. These preps were tested for their titer, section 2.5.2, and the percentage of gpD fusion proteins displayed, section 2.7.1.5. Some of these preparations were also tested for TLR signalling (2.13) or LPS contamination (2.14).

2.5.5.1 Intact phage preparation

Large scale phage preparations were performed in 400mL of LBM. To make phage for a vaccination experiment and the subsequent terminal assays, four 400mL LBM cultures were processed and pooled together.

The large scale prep was seeded with plating cells as described in section 2.5.1. For one 400mL culture, $3.2x10^{10}$ cells were mixed with $8x10^{7}$PFU of phage, a 1:400 multiplicity of infection (MOI). Phage were left at 37^{o}C for 20min. to adsorb to plating cells. This solution was added to 400mL of pre-warmed LBM contained in a 2L Erlenmeyer flask. The culture was incubated at 37^{o}C at 260rpm. The culture was left for 18 to 29hrs, depending on when lysis was observed. When sufficient growth or lysis was attained, the remaining bacteria were lysed using 23.4g of NaCl and 1.5mL of chloroform, which was shaken for an additional 30minutes.

The isolation of bacteriophage begins with the removal of bacterial debris by centrifugation at 11,325x g for 15min. The phage containing supernatant was kept and 200g of ammonium sulfate was used to precipitate phage. The solution was put on ice and kept overnight at 4^{o}C. The next day phage were collected by centrifugation at

11,325x g for 40min. The supernatant was removed and the phage containing pellet was resuspended in 16mL of SM buffer.

Dialysis was performed to remove ammonium sulfate from λ preparations after precipitation. Regenerated cellulose dialysis tubing (Spectrum Medical Industries, #S732700) was filled with bacteriophage in SM buffer. The tubing was immersed in 4L of SM buffer and was gently stirred and left at 4^{o}C for 2-5hrs. The dialysis buffer was changed 4 times to equilibrate the phage buffer with SM.

Ultracentrifugation was performed to purify λ further. Before ultracentrifugation, cesium chloride was added to λ after dialysis at a concentration of 0.75g/mL, at this density λ was successfully isolated during ultracentrifugation. Samples were sealed in 5.1mL polyallomer tubes (Beckman, #342412), and were centrifuged for 4hrs at 354,413x g in a VTi65.2 rotor (Beckman Coulter). After centrifugation, a grey/white λ band was visible. An 18G needle and syringe was utilized to extract 1-3mL of λ. The samples from the polyallomer tubes were pooled, and an equal volume of SM buffer with 0.75g/mL CsCl was added. This process was repeated for a total of 4 ultracentrifugation steps. On the last occurrence the λ bands were extracted in 1mL. The samples were subsequently desalted with microcon ym30 centrifugal filters (Millipore, #42410). Phage were then titrated, and western blotted to measure the percentage display of gpD fusion proteins. In parallel, a qualitative analysis of purity was done by looking at total protein in the preparation with sypro ruby (Invitrogen, S-11791) staining of SDS-PAGE.

2.5.5.1.1 3D Display of gpD fusion proteins

Multiple gpD fusions can be displayed on bacteriophage λ by using recombineered λ, section 2.5.7, and bacterial host cells containing the pGEX-DLTgfp plasmid, section 2.2.10 to produce fusion protein in *trans*. The protocol was nearly identical to section 2.5.5.1, but the plating cells were prepared as described below.

LE392 are freshly transformed with pGEX-DLTgfp that was frozen in a glycerol stock. This was used to grow an agar plate overnight, the next day a colony was picked to start an overnight 2mL bacterial culture. A 50mL LBM culture with 50μg/mL of ampicillin was started with 500μL of the overnight culture. This was grown for 1.5hrs

and then 100μM IPTG was added, and the culture was grown for 2 additional hrs., to an OD_{600} of 0.8 to 1.0. The optical density was measured and used to calculate the volume necessary to subculture $3.2x10^{10}$cells.

When large scale preparations were seeded, ampicillin was present at a concentration of 50μg/mL in a 400mL broth, but IPTG was not added. At 4hrs and every 4hrs afterwards, 100μM IPTG was added to the culture. After the IPTG induction, all other steps in the preparation were the same.

2.5.5.1.2 DNA isolation from phage prep

To prepare DNA from a large scale λ preparation, a similar protocol was performed as described in 2.5.5.1. The exception in this protocol was that as with the small scale DNA preparation, PEG was used to precipitate λ after bacterial debris was removed following lysis. In the large scale DNA preparation 10% w/v PEG 8000 was added. λ were left overnight on ice and were collected by centrifugation at 11,325x g. Λ was resuspended in SM buffer and PEG was removed by multiple rounds of chloroform extraction. λ was further purified using ultracentrifugation, as described in section 2.5.5.1. After the procedure of section 2.5.5.1 was complete, λ capsids were broken open using an equal volume of phenol, and SDS at a concentration of 0.02%. This solution was gently mixed by slow inversion for 40 to 60min. The phases were then separated by centrifugation at 3000x g for 15min. The aqueous phase was removed and the DNA was precipitated by EtOH. DNA was removed after precipitation by spooling on a glass rod and was resuspended in TE buffer.

2.5.6 Cloning λgfp10

λ DNA can be cloned as with other types of DNA, except one must be careful in handling it to minimize shearing. λgt10 has a convenient *Eco*R I cloning site at 32,710bp.[211] This vector can accommodate up to 7.6kbp. The process for λ cloning will be described below, but the exact conditions were described in section 2.2.

To construct λgfp10, pEGFP-F (Clontech) was cloned into the *Eco*R I site of λgt10. Briefly, after digestion of λgt10 with *Eco*R I, λ DNA was dephosphorylated. *Eco*R I digested pEGFP-F was ligated to the digested and dephosphorylated λgt10. After

ligation λ DNA was packaged using the gigapackIII packaging extract (Stratagene). 200ng of DNA was added to 500μL of packaging extract. This was left at 4°C for ~2hrs and 100μL of SM was then added. λ was then amplified by growth on a top agar plate.

One method necessary for cloning λ phage was the annealing and melting of the COS ends. These contain a 12bp sticky overlap at the end of the linear genome that anneal to form the circular DNA genome. When electrophoresis was performed on λ genomes the COS ends are melted by heating λ DNA for 10min. at 65°C. In order to ligate into λ phage, the COS ends were ligated together to increase the efficiency of cloning. Before ligation, the COS ends were annealed after melting, by the addition of TE containing 10mM $MgCl_2$, this was left at 42°C for 1hr. COS ligation was then performed as for a typical ligation. After ligation, the reaction was heat inactivated. This product could then be digested and dephosphorylated.

2.5.7 Recombineering

Recombineering was performed to insert DNA into the non replaceable sequence of λ.[222-225] Previous attempts to utilize retro recombinant screening, transplacement mutagenesis, and orpheus recombination for the construction of Mashkiki λ, but none of these systems proved effective.[226-229] The lack of recombinants using recombination systems developed in the Rancourt lab, were probably due to large plasmid intermediaries being incorporated into the left arm of the λ genome during these recombination protocols. Recombineering on the other hand does not suffer from this shortcoming, as the oligonucleotide or plasmid is incorporated directly, and no condensation step was necessary. The only negative aspect of recombineering was that we had not developed a genetic system to screen for recombinants. As such, the only realistic method to find recombinants was by plaque hybridization.

The oligonucleotide that was recombineered into λ was designed to have a linker sequence, a myc tag, and the protein transduction domain of the TAT protein from HIV1, from 5' to 3'. The oligonucleotide was designed to be inserted on the 3' end of the gpD directly preceding the TAG stop codon. With this construct the last codon of gpD became a GTT codon. The stop codon became the amber stop codon, TAG, that could be suppressed in a $SupF^+$ host. The linker was inserted by cutting pDE with *Hpa* I and *Not*

I. The linker was a 16 amino acid sequence designed using LINKER.[230] The linker oligo sequence was: TAG GGC AAG TAC ACC AGC TCT GGC CAA GCA GGC GCC GCT GCG AGC GAA TCT GCG GCC GC. This was the 5' to 3' sense strand, and the antisense strand was the compliment. The oligo with the myc tag and TAT was: GGC CGC CGA GCA GAA ACT GAT CTC TGA AGA GGA TCT GTA TGG CCG TAA AAA ACG TCG TCA GCG TCG TCG TTA ATG. The antisense strand, 5' to 3', was: AAT TCA TTA ACG ACG ACG CTG ACG ACG TTT TTT ACG GCC ATA CAG ATC CTC TTC AGA GAT CAG TTT CTG CTC GGC. Everything was codon optimized for expression in *E.coli*. The c-Myc tag was based on the pCMV-Tag5 vector (Stratagene) where it was: EQKLISEEDL. The TAT PTD sequence was identical to Dr. Dowdy's which was: YGRKKRRQRRR.[231] All oligos were synthesized by Operon (Eurofins MWG Operon). They were gel purified by Operon, and checked on a polyacrylamide gels after annealing (2.2.3 and 2.2.4.2).

Before the oligo was recombineered into λ, it was cloned into the pDE plasmid. This was done to verify the sequence that would be used for recombineering, as well as to increase the homology of the insert, which increased the efficiency of the reaction. The pDE plasmid was cut with *Not* I and *Eco*R I (NEB), and dephosphorylated (2.2.6). The double stranded oligo was phosphorylated (2.2.6). Both DNA species were then ligated together. 100ng of plasmid was added to 1μL of 17nM oligo, together with 1μL of ligase, 4μL of 5X ligase buffer and 4μL of ddH_2O. This was left at 16^oC overnight. The reactions were then electroporated (2.4.3), and colonies were screened using PCR with gpDprimer2 and gpE-RHprimer1. Positive clones were sequenced and one was picked for recombineering. The resulting plasmid was called pDamE-mTAT.

The pDamE-mTAT plasmid was cut with *Nde* I and *Eco*R V to isolate 2μg of the gpD-mTAT-gpE fragment with gel purification. This fragment was then used for recombineering. The bacteria used for recombineering are DY330, which have a temperature sensitive mutation that at 30^oC results in no recombineering proteins being expressed, but the permissive temperature, ~42^oC, does cause recombineering proteins being expressed. DY330 was grown at 30^oC until log phase growth was reached. The cells were then centrifuged and resuspended in a 1/200 volume of SM buffer.

Bacteriophage λgfp10 was then adsorbed to DY330 cells at room temperature at a multiplicity of infection (MOI) of 1 λ particle to 3 bacteria.

Recombineering proteins were induced by moving the phage:bacteria solution to 5mL of 42^{o}C prewarmed LBM. This culture was grown for 15min. at 42^{o}C. The culture was stopped by adding the culture tube to an ice cold water bath. The cells were then made electrocompetent (2.4.3), and 600ng of the pDamE-mTAT plasmid was electroporated into them. The EP mixture was added to 5mL of pre-warmed 42^{o}C LBM, and was grown on a shaking incubator for 90min. At the end of this protocol bacteria were lysed with 0.25mL of chloroform. The resulting solution was then screened for recombinant bacteriophage that incorporated the oligo of interest. In the present work this was done by plaque hybridization.

2.5.8 Plaque hybridization

Plaque hybridization is a technique used to screen top agar plates for recombinant bacteriophage plaques. Basically, bacteriophage from plaques adhere to nitrocellulose membranes, which are probed with a complimentary oligo. Probes were labelled in this thesis using radioactivity. If a probe hybridized to a plaque, it was a positive for the oligonucleotide present. The plaque was then found on the plate, isolated and sequenced.

Plaques were produced on top agar plates (2.5.2). Large, 140mm, bacterial plates allowed more phage plaques to be screened, and therefore rare events could more easily be found. Amersham Hybond N+ (GE Healthcare, #RPN137B) membranes were layed on top agar. The orientation was marked on the membrane and agar by puncturing both with a needle. The membrane was removed and soaked for 5min. in denaturing solution, 1.5M NaCl and 0.5M NaOH. Membranes were then soaked for 5min in neutralizing solution, a pH 8 solution of 1.5M NaCl and 0.5M Tris. Finally membranes were dipped in 2X SSC to rinse, and were left to dry on Whatman^{TM} paper. They were labelled on the non-DNA side with a pencil. Care was taken not to touch membranes with gloves or fingers, all manipulations were done with clean forceps.

Hybridization of probe started with a prehybridization step. Nitrocellulose membranes were added to prehybridization solution and this was left at 65^{o}C for ~2hrs, with shaking. Prehybridization solution was 5 x SSPE, 5 x Denhardt's, 0.5% SDS, 0.1

mg/ml single-stranded salmon sperm DNA. At 2hrs, 50pmoles of end labelled probe was added to the membranes. The hybridization was left for a minimum of 5hrs but this could be left overnight.

Radioactive probe was prepared while the membranes were pre hybridizing. In the present study, as the oligonucleotide being recombineered was only 67bp, end labelling was necessary. This was done with either terminal transferase (NEB, #M0252S) together with α^{32}P dCTP, or T4 PNK (NEB) together with γ^{32}P dATP. The recipe was 5µL of 10X T4 PNK buffer (NEB), 2µL of T4 PNK (NEB), 5µL or 50pmoles of oligonucleotide, 10µL of γ^{32}P dATP (GE Healthcare), and 28µL of ddH_2O. First the oligonucleotides, sense and antisense, were boiled in a tube alone for 5 min. and left to cool down to room temperature for 1hr on a heater block. The isotope was then added together with the rest of the reagents outlined above. The kinase reaction was performed at 37^{o}C for 1.5hrs. The reaction was then boiled and unincorporated isotope was removed using the ProbeQuant G50 microcolumn (GE Healthcare, #27-5335-01). A Geiger counter was used to estimate the efficiency of the labelling reaction, by comparing the counts on the column to the counts in solution, the probe. The probe was added to membranes in pre hybridization solution and the mixture was left at 37^{o}C with circular agitation for a minimum of 3hrs.

After the probe was hybridized to the membranes, non-hybridized probed was washed off. Washes consisted of 1 rinse at room temperature with wash buffer, 2X SSC and 0.5% SDS, followed by 2 washes at room temperature with wash buffer for 15min. Finally, one last wash was done with wash buffer containing 0.2X SSC and 0.1% SDS, this wash was done for 30min. at 65^{o}C. The membranes were wrapped in Saran wrap (SC Johnson), and secured to a film cassette. Biomax MR X-ray film (Kodak) was then added to the cassette and was left for approximately 1 week at -80^{0}C, or until the proper exposure was attained. Films were then aligned with the agar plates, and positive plaques were picked and λ was grown.

2.6 Electron Microscopy

Electron microscopy was done at the Microscopy and Imaging facility in the Faculty of Medicine, at the University of Calgary. Phage samples were stained with 2% uronyl acetate, on a nickel grid, and imaged on an FEI Tecnai F20 HRTEM.

2.7 Protein Techniques

2.7.1 Western Blot

Specific proteins were visualized using western blots. These were typically done in denaturing conditions using a discontinuous buffer system.[211] Two sizes of western blots were used, mini gels, in the BioRad Protean III system, or large gels on 16cm x 18cm glass plates. Westerns were also run in semi-native conditions to investigate if λ proteins or 'free' GFP was present in phage preparations.

2.7.1.1 Mini Gels

Using the Protean III system polyacrylamide gels were produced. Glass plates were cleaned and wiped with 70% EtOH. These were assembled into the Protean III plate holders and 5.5cm of resolving gel was poured into them. Resolving gels varied in concentration depending on the product being investigated, but were typically 12% acrylamide. A 12% acrylamide gel has the following recipe for 10mL: 3.3mL ddH_2O, 4.0mL 30%Bis:Acrylamide (BioRad, #161-0156), 2.5mL of 1.5M Tris pH8.8, 0.1mL 0.1mL of 10% SDS, 0.1mL of 10% of ammonium persulfate. The solution was then mixed and 4μL of TEMED (EMD, #8920) was added. Methanol was poured on top of the gel as it polymerized, ~1hr. The methanol was removed and the gel was rinsed with ddH_2O before the staking gel was poured. The stacking gel was only 5% acrylamide and has a pH of 6.8, hence the discontinuous buffer. The stacking gel recipe was: 2.1mL ddH_2O, 500μL 30% Bis:Acrylamide, 380μL 1.0M Tris pH6.8, 30μL 10% SDS, 30μL 10% ammonium persulfate, this was mixed and 4μL of TEMED was added. The comb was inserted and the gel was left to polymerize for ~45min.

The polymerized gel was removed from the pouring apparatus and added to the buffer tank, containing SDS-PAGE running buffer. One litre of SDS-PAGE running buffer was made with 3.02g of Tris base, 14.4g of Glycine, and 1g of SDS. The comb was removed and protein samples in 1X loading buffer were heated to 98^{o}C for 5min. After heating they were added immediately to each lane. Six times protein loading buffer was 360mM Tris pH6.8, 36% v/v glycerol, 12% w/v SDS, 9.3% w/v DTT, and 0.012% w/v bromophenol blue. The voltage applied depended on the application, if higher resolution was necessary electrophoresis was performed at at 50V, this was the case for gpD densitometry work (2.7.1.5).

After the bromophenol dye front migrated to the desired distance, the gel was removed from the apparatus. At this point one can either stain total protein in a gel using Coomassie, Sypro Ruby (Invitrogen), or Silver Staining (BioRad), or the gel could be transferred to a PVDF or nitrocellulose membrane for a western blot.

To transfer the gel, it is incubated in transfer buffer for 15min. Transfer buffer was adjusted to a pH of 8.3 to 8.4 and contained the following for each litre: 3.03g Tris base, 14.4g glycine, 200mL methanol. Whatman^{TM} paper was cut to cover the gel as was Hybond nitrocellulose membrane (GE Healthcare, #RPN303D). Two ScotchBrite$^{®}$ pads, 4 Whatman^{TM} sheets cut to size, and 1 nitrocellulose membrane are incubated in the transfer buffer. All materials were then assembled, sandwiched on the gel, where the gel was at the negative electrode side and the membrane was on the positive electrode side. The sandwich was put into a transfer cassette, and electrophoresed at 150V or for 1.5hrs or until the voltage dropped.

At this point the proteins were transferred onto the membrane; this could be probed with antibodies. The membrane was removed from the transfer cassette and blocked for 10min. using 5% skim milk in TBS-T. One litre of TBS-T contained 8g NaCl, 0.2g KCl, 3g Tris base, 0.1% Tween20(Sigma) adjusted to pH 7.5. The primary antibody was added to this at an appropriate dilution and the solution was left overnight at 4^{o}C.

The following day the blot was shaken for 1hr at room temperature, and was then rinsed 3 times in 20mL of TBS-T for 5minutes. The appropriate secondary antibody, or

streptavidin, conjugated to HRP was then added to 20mL of 5% skim milk in TBS-T. The blot was shaken in 2^{o} antibody solution at room temperature for 1 to 4hrs. The blot was washed 3X as before. The blot was then immersed in ECL reagent (GE Healthcare, #RPN2106) for 1 min., the corner of the blot was dabbed with a kimwipe (Kimberley-Clark), and the blot was covered in Saran-Wrap (SC Johnson). The blot was then either imaged using ECL film, Hyperfilm (GE Healthcare, #28906838), or a on a digital imager, Versadoc (BioRad). If film was used the image was scanned into a TIFF file using the Epson Perfection 4870 scanner. When the Versadoc^{TM} was utilized images were saved as TIFF files, and densitometry (2.7.1.5) was performed to measure protein intensities in a lane using the Quantity One Sofware (BioRad).

2.7.1.2 Semi-Native Gels

These gels were used to look at what other products were present in phage preparations (2.5.5). They were prepared identically to the mini gels (2.7.1.1), except for a few exceptions. Protein samples were not denatured or boiled before running the gels. Therefore no DTT or SDS was added to the loading buffer, but the samples were electrophoresed through an acrylamide gel containing SDS, as well as in gel running buffer containing SDS. In this way SDS coated the outside of the proteins, aiding in migration, but did not unfold proteins or protein complexes.

2.7.1.3 Large Gels

Western blotting on large polyacrylamide gels were done on BMDM cell lysates (2.11.3 and 2.13.3). A similar method was used as described in section 2.7.1.1. The changes to the method described above will be discussed. The resolving gels were made with 10% acrylamide, using 30% Bis:Acrylamide, adjusted for 10% instead of 12% acrylamide. The gel was poured into16cm x 18cm glass plates, resulting in better separation than mini gels.

Protein samples were thawed from -80^{o}C, and samples were prepared by heating to 70^{o}C for 8 min. This lower temperature was used as kinases are sensitive to high temperatures. The samples were loaded into the stacking gel wells, along with 1 lane with

a protein ladder (NEB, #P77086). Each gel apparatus was labelled for the samples loaded. Two different methods of loading gels were used: 1) all samples from 1 animal with different stimulants were loaded onto a gel, or 2) the same stimulant in 3 different animals was loaded onto the same gel. The gel is then electrophoresed for 1000 volt hours, over twelve or more hours. The voltage used to on a gel was calculated as = $\frac{1000\ volt\ hours}{number\ of\ hours\ to\ run} = volts$. When the electrophoresis finished the gel was then transferred to a nitrocellulose membrane, Protran (Whatman, #10401196C). For this method the transfer was performed at 830mA for 3hrs.

Following the transfer, membranes were cut and probed with primary antibody. After the transfer was stopped, the gel was checked for complete transfer by looking at the amount of protein ladder on the membrane, and gel. If necessary the gel was electrophoresed longer. Membranes were removed from cassettes and dried on Whatman™ paper. Membranes were labelled with a black permanent marker (Sharpie®), and sections were cut according to the protein size to be visualized. For the protein size see Table 3: Antibodies. Blots were blocked for 1hr with blocking solution, 5% w/v BSA FV (Roche, #735 108) in phosphate buffered saline (PBS). Where PBS was at pH 7.4, and contained the following for 1L: 8g NaCl, 0.2g KCl, 1.44g Na_2PO_4, and 0.24g KH_2PO_4. Primary antibody was then added at a concentration of 1/1,000 in a small volume of blocking solution and the blots were sealed in a vacuum pouch. Pouches were put onto a rocking platform and membranes were left in primary antibody overnight at 4°C.

Primary antibody was washed off blots and secondary antibody was added. The primary antibody solution was dumped and membranes were washed three times in TBS-T for 10min. Secondary antibody was then added at a 1/10,000 dilution in blocking solution. Membranes were incubated at room temperature for 1hr and then washed as for 1° antibody.

Membranes were then exposed to film. Before membranes were exposed they were first covered in ECL. Washed membranes were covered in ECL for 1min. and then dried on Whatman™ paper. Blots were sealed in Saran Wrap (SC Johnson), and added to a film cassette. Various exposure times were used to image membranes with Kodak

General purpose Blue medical X-ray film (Kodak, #822 5526). Film was developed using an automatic developer.

If a phospho-specific antibody was used on the membrane this was then reprobed, as was the case for p38 westerns. The first exposure was done with a phospho specific antibody. Then the membrane was stripped of antibodies by adding it to stripping buffer (100mM βmercaptoethanol, 2% SDS, 62.5mM Tris pH 6.7) and it was heated to 56^{o}C for 45min. . After a blot was stripped, it was washed extensively in TBS-T and then it was processed as after being transferred.

2.7.1.4 Antibodies

Antibody and organism	Aproximate band size	Antibody source and Isotype	Company and Product Number
Fc, Mouse			Bathe Lab, 24G2 clone
CD4-FITC, Mouse		Rat, IgG2b κ	BD Pharmingen, (GK1.5) L3T4 clone, 557307
CD4-PE, Mouse		Rat, IgG2b κ	BD Pharmingen, (GK1.5) L3T4 clone, 557308
CD8-Cy, Mouse		Rat, IgG2a κ	BD Pharmingen, 553034
CD11b (MAC1) -FITC, Mouse		Rat, IgG2b κ	eBioscience, M1/70 clone, 11-0112-85
CD11c, Mouse			
CD45R (B220)-FITC, Mouse	220kDa	Rat, IgG2a κ	eBioscience, RA3 6B2 clone, 11-0452-82
F4/80-PE,		Rat, IgG2a κ	eBioscience, 12-4801-

Mouse			82
GFP	dependent on rGFP	Mouse, IgG2A	Clontech, JL8 clone
gpD, Bacteriophage λ	11.6kDa	Rabbit, polyclonal	Nakanishi Lab, Japan
IgA-Biotin, Mouse		Rat, IgG1 κ	BD Pharmingen, 556978
IgG1-Biotin, Mouse		Rat, IgG1 κ	BD Pharmingen, 553441
IgG2a-Biotin, Mouse		Rat, IgG1 κ	BD Pharmingen, 553388
IgG-HRP, Mouse		Sheep	GE Healthcare, NA931V
IgG-HRP, Rabbit		Donkey	GE Healthcare, NA934V
IgG-HRP, Rabbit		Goat	Santa Cruz Biotechnology, SC-2054
IgM-Biotin, Mouse		Rat, IgG2a κ	BD Pharmingen, R6-60.2 clone, 553406
IκB-α, Mouse	39kDa	Rabbit polyclonal	Cell Signalling, #9242
p38 Map Kinase, Phospho (Thr180/Tyr182), Mouse	43kDa	Rabbit polyclonal	Cell Signalling, #9211
p38α, Total, Mouse, Rat, Human	38kDa	Rabbit polyclonal IgG	Santa Cruz Biotechnology, SC-535 and SC-728
Streptavidin-HRP			GE Healthcare, RPN2190
Tcell Receptor, Mouse			Bathe Lab, clone 2C11

Table 3: Antibodies

2.7.1.5 Densitometry

Samples from λ phage preparations (section 2.5.5.1) were equally loaded, 20μg protein/lane, and electrophoresed in an SDS-Polyacrylamide gel which was transferred onto nitrocellulose paper, as previously described. Blots were probed with either the JL8 GFP antibody or the gpD antibody. ECL detection was performed on the Versa-Doc (Bio-Rad) imaging system, and densitometry was done with the Quantity One software (Bio-Rad).

2.7.1.6 Thrombin Cleavage of Phage

A thrombin cleavage site in pGEX-DLTgfp was cleaved with thrombin (Amersham). 20μg of purified λgfp10 grown in pGEX-DLTgfp (2.5.5.1.1) was cut with 2U of thrombin, left overnight at 37^{o}C. A western blot was performed on the reaction products and a negative control, which were (2.7.1.1) probed with the JL8 antibody (2.7.1.4).

2.7.2 Total Protein Gel

Total protein gels were electrophoresed as for mini gels, except a non specific protein stain was used, instead of a specific antibody to probe. General protein stains were either sypro ruby (Invitrogen), or Silver Stain (BioRad). In either case the gel was stained as described by the manufacturer. With sypro ruby, the gel was stained and then non-protein conjugated sypro was washed from the gel using a 10% methanol, 7% acetic acid wash solution. The gel was visualized on the same UV trans-illuminator and Kodak 1D system as for a DNA gel (2.2.4.1).

Silver stained gels were developed using the silver stain plus kit (BioRad, #161-0449). They were visualized by eye and scanned into TIFF files using the Epson Perfection 4870 scanner.

2.8 Cell Culture

Cell culture was performed with proper aseptic technique. Manipulation of cells was performed in a laminar flow biosafety cabinet, and cells were grown at 37°C in a 5% CO_2 incubator with >95% humidity. All cells were continually checked for contamination by visual inspection, or by PCR of supernatants. Data was not collected if cells were not healthy.

2.8.1 Embryonic Cell Culture

Embryonic stem cells (ESCs) were cultured one of two ways: either with a feeder layer or with gelatin coated plates. The culture on feeder layers will be outlined first, as this is the best way to passage ESCs, and was necessary for healthy cells after thawing ESC cryotubes (2.8.4). Three ESCs lines were used in this thesis, $R1^n$, E14, and D3.

ESCs were grown in complete ESC medium (822mL DMEM high glucose (Invitrogen, #12100-061), 150mL FBS (Invitrogen), 10mL sodium pyruvate (Invitrogen, #11360), 10mL non-essential amino acids (Invitrogen, #11140), 5mL penicillin/streptomycin (Invitrogen, #15140), 1mL βmercaptoethanol (Invitrogen, #21985-023), and 2mL LIF (Chemicon, #ESG1107)). Note that FBS lots were tested before for their inability to differentiate ESCs, as some lots of FBS cause spontaneous differentiation.

ESCs were grown in 60mm tissue culture dishes (Falcon, #353002) coated with irradiated mouse embryonic fibroblasts (MEFs). Dishes were first coated with 0.1% gelatin, and then irradiated MEFs were quickly thawed in a 37°C water bath. The vial of MEFs was labelled with the surface area of cells, which was used to estimate the volume of MEFs to add. The dish was cultured overnight in an incubator. A plate of MEFs was good for up to 2 weeks if the media was changed as determined by phenol red. After MEFs settled and deposited an appropriate extracellular matrix (ECM), ESCs were then cultured on them.

ESCs were thawed from cryovials in a 37°C water bath for 1 to 2 minutes. As this was occurring, media from plates with MEFs were aspirated off, and 3.5 to 4mL of fresh complete ESC media was added. A plugged Pasteur pipette was used to gently resuspend

the cells. Cells were added drop wise to the top of the media around the plate. The plate was returned to the incubator. Media on ESC plates was changed daily, and ESC colony morphology was checked for density, size, and number. When the ESC clones began to differentiate they became too large, with the edges of the colony became ragged and not smooth; It was then time to split the ESCs.

ESCs were split by aspirating off all media, and adding 1mL of 0.25% trypsin (Invitrogen, #25200). The plate was returned to the 37^{o}C incubator and trypsin was left to digest ECM for 5 to 7 minutes. Trypsin was neutralized by adding an equal volume of complete ESC medium. Cell clumps were broken up by gently pipetting up and down with a Pasteur pipette no more than 10 times. Cells were then added to a fresh MEF coated plate. If the cells were needed for an experiment the next day they were plated at a 1/3 dilution, if they were needed later they could be diluted up to 1/10 on plates.

To grow cells without MEFs, ESCs were split as above but instead of adding cells to a MEF plate, the cells were pre-plated. Pre-plating consisted of adding 2mL of complete ESC media to trypsinized cells, and all cells were added to a fresh, sterile tissue culture plate, polystyrene vacuum gas plasma treated surface (Falcon). Cells were left for 30 to 45min. in an incubator. The media and ES cells were then added drop wise to a 0.1% gelatinized plate (Falcon). The adherent cells that were left behind during the pre-plating procedure were MEFs. Pre-plating removed ~99% of MEFs from the culture. The media was changed daily, and the morphology, density, and number of colonies were checked regularly. When using gelatinized plates ESCs clones had rougher edges than those grown on MEFs, but they became noticeably rougher as they began to differentiate. Passaging these cells was done the same way as MEF cultured ESCs except they were returned to gelatin coated plates when they were split.

For all post analysis assays where EGFP, or Alexa fluor were used to investigate transduction or transfection efficiencies, ESCs were grown on gelatin for 1 passage. In this way MEFs were removed from the culture, and values of efficiencies measured ESCs and not MEFs.

2.8.2 Mammalian cell culture

Mammalian cell culture was similar to ESCs culture except no feeder cell lines were necessary, and this made cell culture of non-ESCs easier. Also most cell lines used in this thesis were adherent, therefore morphology was noted but, essentially the cell density indicated when cells required passaging. Cell lines used in this thesis were: Cos7 and Hek293T (ATCC).

To passage cells the following protocol was used. When the desired density was attained, 80-90%, cells were trypsinized. To trypsinize cells, the media was aspirated off and cells were rinsed in a 1/5 volume of Dulbecco's phosphate buffered saline (DPBS), as compared to the original volume of media. Trypsin was then added for ~5min. or until all cells dislodged from the plate. Trypsin volumes for a given plate size were followed as suggested by BD Falcon. An equal volume of complete media was added to neutralize trypsin. Cells were collected by centrifugation at 500x g for 5min. Supernatant was removed, and cells were resuspended in complete media. Cells were counted on a hemocytometer. Cos7 cells were usually confluent when they reached a cell density of $10x10^4$cells/cm^2, whereas for Hek293T cells confluence was $30x10^4$cells/cm^2. An appropriate dilution of cells, 1/3 to 1/5 of confluent concentration usually, was then added to a new vessel for culture with the appropriate volume of complete media.

Complete media for Cos7 and Hek293T was 500mL of DMEM with high glucose (Invitrogen, #11965), 1% v/v penicillin/streptomycin (Invitrogen, #15140), with 10% FBS (Invitrogen). If complete media was older than 2 months fresh glucose was added in the form 1% v/v of glutamax (Invitrogen, #35050-061).

2.8.3 Cell Transfection

Two methods of transfection were used in this thesis: calcium phosphate, and Effectene® (Qiagen). In either case transfection efficiciency was best when the cells were growing rapidly and were healthy. The health of cells varied with the density, and the age of media, which were both were dependent on the cell line. For most cells 50-60% confluent plates resulted in highly efficient transfections, and allowed for cell growth.

As multiple treatments and conditions were used in transfections, cells were cultured in 6 well plates (Nunc, #140675). Cells were seeded the night before. If this was being done for the first time a dose response curve was performed to find the optimal concentration of DNA to add to each well. For Hek293T cells up to 1.6 or 2µg of a 6-8kbp plasmid could be transfected per well. Viability was checked using trypan blue staining for cell counting (2.8.5), or flow cytometry (2.8.7).

Effectene is a non-lipisomal transfection reagent that was used on cell to test transgene expression from reporter genes. The method used was described in the literature provided by Qiagen.

Calcium phosphate transfection was another method used in this thesis for plasmids, bacteriophage DNA, and intact bacteriophage. It is known to be particularly good for Hek293T transfections. Two solutions were prepared: 2X HeBS or HEPES buffered saline, and 10X $CaCl_2$. HeBS at 2X was 280mM NaCl, 10mM KCl, 50mM HEPES, 1.5mM Na_2HPO_4, and the pH was adjusted to 7.05 with 1M NaOH. Ten times $CaCl_2$ was at a concentration of 2.5M. Both solutions were filter sterilized and stored at 4^oC.

Before calcium phosphate transfection the solutions were equilibrated to room temperature. Media was removed from cells and 1.8mL of fresh complete media was returned to each well. A mixture of 100µL of DNA and 1X $CaCl_2$ was made. This was vortexed and spun down. 100µL of HeBS was then added dropwise to the DNA mixture, and air was blown into the mixture with the pipetteman after the addition of HeBS, for a total of 30-40 times. The mixture was then vortexed and left at room temperature. As the air was blown into the mixture, it became cloudy, due to precipitate of DNA-calcium phosphate forming. The tube was then mixed thoroughly was added evenly to the tissue culture plate drop wise.

Cells were then grown in the transfection media until desired, usually 1-2 days. After transfection flow cytometry was performed to quantify the number of positive transfected cells. This was possible as a GFP reporter gene was present in the constructs.

2.8.4 Maintenance of cell stocks

The following protocol describes how to thaw cells from cryovials in liquid nitrogen. Every cell stock was thawed it was replaced by 2 cryovials produced from the resulting cells after the first passage. Each cryovial was marked with the cell line, media, passage number, surface area, and date.. Cells were thawed quickly by adding them to a 37^{o}C water bath for 1 to 2min. Cells were then resuspended into an appropriate volume of media for the volume marked on the tube. Typically a ½ or ¼ dilutions of cells were added to a plate and left to grow overnight. Cells usually recovered from freezing and thawing after 1 to 2 passages.

For long term storage cells were kept in cryovials immersed in liquid nitrogen. Cells were first trypsinized (see above), and then collected by centrifugation at 200x g for 4min. Cells were resuspended in freeze media (90% FBS with 10% DMSO (Sigma, #D5879)). No more than 0.8mL of freeze media was used for each 1mL cryovial (Nalgene). Therefore for one 60mm plate grown to 80% confluence it would be split into 2 cryovials and this would be noted. Each cryovial would be used for one 60mm dish. Once the info was marked on the cryovial, the cells were frozen slowly in a Mr.Frosty (Nalgene) overnight in at -80^{o}C. The next day the cryovials were moved to a liquid nitrogen tank for long term storage.

2.8.5 Cell Counting

Cells were counted on a haemocytometer. Briefly, a single cell suspension of 10µL was added to 10µL of 0.4% w/v trypan blue. The solution was mixed and left at room temperature for 5min. Ten µL of cells was added to a clean haemocytometer, and 2-4 quadrants were counted. If too many cells were present, a dilution was made and then counted. After counting the total number of living cells, the following calculation was done: cell concentration (Y) = $\frac{total\ \#\ of\ cells\ counted}{\#\ of\ quadrants}$ = Y x10^{4}cells/mL. If a dilution was made this value was multiplied by the dilution.

2.8.6 TAT transduction

Transduction of λ was performed on cells and results were measured with fluorescent microscopy (2.8.8) or flow cytometry (2.8.7). A similar plating procedure was performed as with cell transfections (2.8.3). Two transduction experiments were performed. One with intact λgfp10-TAT and another with biotin-TAT conjugated with streptavidin alexafluor488. Dose response curves were measured for both experiments. 200nM streptavidin was optimal, whereas no concentration of λgfp10-TAT was effective. A typical λgfp10-TAT concentration was 10^9 per well in a 6well plate (Nunc, #140675).

When intact λ was utilized for a transduction experiment, a cell culture plate with 20% confluence was used as this allowed for 2-3 days of growth with λ present. Over the course of the transduction experiment, microscopy was performed to measure reporter gene production. Live cells were assayed for internalization using fluorescent microscopy and flow cytometry.

With streptavidin alexafluor488 (SA488) conjugated to biotin-TAT peptide, the process investigated was only internalization. The cell culture plates were 50-80% confluent and SA488-biotin-TAT was only pulsed for 3hrs. After this cells were trypsinized for 20min. to remove surface bound SA488-biotin-TAT. Cells were rinsed with PBS and viability was measured. Internalization was assayed using flow cytometry and fluorescent microscopy on non fixed cells.

2.8.7 Flow Cytometry

Flow cytometry, also known as 'fluorescent-activated cell sorting' FACS, was used to determine the number of cells in a population. This was done after TAT transduction of cell lines, section 2.8.6, and following isolation of various immune cell types, section 2.11. For freshly isolated cells, from immune tissues, $1x10^6$ cells were added to each FACS tube; a round bottomed 12x75mm polystyrene tube (BD Falcon, #352052). When working with bone marrow derived macrophages and at times with ES cells, a cell scraper was used to remove them from a tissue culture plate. Most other cell types were dissociated by trypsin digestion, 0.25% trypsin (Invitrogen). During this procedure, when it was possible, cells were covered from light exposure in all subsequent

steps to protect fluorochromes from photobleaching. Furthermore all FACS tubes were incubated on ice when not centrifuged.

When λ or streptavidin transduction experiments were performed, cells were brought live in a single cell suspension to the flow cytometer for sorting. They were gated in the first channel, FL1, to count the number of positive cells for the transduction of AlexaFluor488 (Invitrogen) or for expression of an eGFP reporter gene.

Immune cell sorting was different as it was necessary to label cells. Cells were washed once with FACS buffer (0.1% BSA fractionV (Sigma) in DPBS), and then centrifuged for 2-5minutes at 400x g. Supernatant was removed by inverting each tube quickly and dumping the liquid out in one swift motion, at the end of this motion the tube was stopped abruptly. Care must be taken to not jerk the tube a second time, in so doing the cell pellet was retained, and all but ~200µL of liquid was removed. The Fc receptor was then blocked using 50µL of an Fc antibody (a gift from the Bathe lab) that was incubated for 5min. The primary antibody was then added (Table 3: Antibodies) and incubated for an additional 20min. Each sample was then washed twice with FACS buffer as described above. At this point cells can be stained with 2-5µg/ml of 7AAD (Calbiochem) for 20min. to access viability. Following 7AAD staining cells were again washed twice in FACS buffer, as described above. Finally, the cell pellet was resuspended and fixed with 300µL of 1% formalin. Flow cytometry was then performed by the University of Calgary Flow Cytometry Core Facility.

2.8.8 Fluorescent Microscopy

Fluorescent microscopy was performed at the Microscopy and Imaging Facility in the Faculty of Medicine, at the University of Calgary. Deconvolution fluorescent microscopy was performed on live cells using a Leica DM RXA2 microscope. Cells to be imaged under oil immersion were grown on glass coverslips. Coverslips were kept in media on ice until imaged under oil immersion. Before imaging a glass coverslip was mounted with 10µL of 20% glycerol in DPBS on a microscope slide, sealed with clear nail polish. Images in fluorescent channels and DIC were taken to find GFP positive cells. Multiple cells per treatment were imaged. Live cell imaging was necessary for transduction experiments as fixed cell walls are punctured and artifacts of internalization

would then be seen with PTD containing proteins.[232-236] Cell images were analyzed using ImageJ (Rasband, NIH).

2.9 RNA Methods

RNA was handled using RNAse/DNAse free tubes and micropipette tips. All reagents used were also RNAse/DNAse free, and care was taken not to contaminate stocks by using proper RNA handling technique. This included the use of aerosol resistant tips and maintaining a clean work area.

2.9.1 RNA Isolation

RNA was isolated directly from tissue culture plates using Trizol® (Invitrogen, #15596-026). Qiagen RNeasy was also tested but the yield and quality of Trizol isolated RNA was superior. Cell culture and cell isolation methods were performed as described (2.8 and 2.11). Trizol isolation of RNA was performed as outlined in the product information provided by Invitrogen. As all cell types analyzed were adherent, supernatant was completely aspirated from wells, and 1mL Trizol was added directly to each well of a 6 well plate (Nunc, #140675) plate. Plates, were gyrated to swirl Trizol around wells, and allowed to sit at room temperature for 15 minutes. The Trizol/cell solution was then pipetted repeatedly and added to a 1.5mL microtube. Samples were left at -80^{o}C until being processed.

Samples were defrosted at 4^{o}C on ice. From this point all work was done with RNAse/DNAse free plasticware and reagents. 200µL of $CHCl_3$ was added to each tube, and they were mixed by inverting for 15 sec.. Subsequently tubes were left at room temperature for 2 min. Microtubes were centrifuged at 12,000x g for 15min. at 4^{o}C, and ~500µL of the aqueous phase was extracted carefully. To precipitate RNA, an equal volume of ice cold isopropanol was added to the aqueous phase and left at -20^{o}C for ≥1hr. Samples were then centrifuged at 12,000x g for 15min. at 4^{o}C. The supernatant was carefully removed and the RNA pellet was kept. RNA was washed with 1mL of ice cold 75% ethanol, and centrifuged at 7,500x g for 5min. at 4^{o}C. The supernatant was removed completely; this sometimes took a second spin to facilitate removal of all liquid. Microtubes were left with an open top at room temperature or at 37^{o}C briefly to

evaporate all remaining EtOH. Care was taken to keep the RNA pellet moist; as if it dried out it will not dissolve into solution. RNA pellets were resuspended into 30μL of Ultrapure H_2O (Invitrogen), heated to 65°C for 10 min. and then incubated on ice overnight. The quality of the RNA was checked and RT-PCR was performed. RNA was stored at -20°C, or -80°C for long term storage.

2.9.2 RNA quality check

RNA quality was determined for all samples using a NanoDrop (Nanospec) or a NanoVue™ (GE Healthcare). Samples with an absorbance ratio of 260nm/280nm greater than 1.8 were determined to be pure RNA, with no DNA contamination. Absorbance ratios of 260nm/230nm were used to determine if protein, guanidine or phenol were contaminants in samples. An absorbance 260nm/230nm ratio ~2 was determined to be free of contaminants.

The Agilent 2100 bioanalyzer (Agilent) was a second RNA quality control assay performed on selected samples. The protocol for this machine was followed as described in the manufacturer's protocol. Any sample the RNA quality algorithm deemed degraded and having a low RNA integrity number, was not used in QRT-PCR.

2.9.3 Reverse Transcription of RNA

Reverse transcription of RNA was performed with Quantitect Reverse Transcription Kits (Qiagen). Amounts of RNA were determined as described in section 2.9.2. One to two μg per reaction were used. If 2μg was used then the recipe was doubled. All components and samples were left on ice except during reactions. All reaction incubations were done with a dry heater block set to 42°C, and 95°C. The genomic DNA elimination reaction was assembled and incubated for 3 min. at 42°C. The reverse transcription reaction components were then added and incubated for 30min. at 42°C. Inactivation of enzymes was performed at 95°C for 3min.

2.9.4 Quantitative Real Time PCR

Quantitative Real Time PCR (QRT-PCR), was performed as described by BioRad for the iQ supermix system in an iCycler QRT-PCR machine (BioRad). The components

necessary were the iQ SYBR green supermix (BioRad, #1708884), iQ 96 well PCR plates (BioRad, #2239441), and microseal 'B' adhesive seal (BioRad, #MSB1001). All primers were synthesized at the University Core DNA Services (University of Calgary), and the water used in the reaction was UltraPure DNase/RNase free H_20 (Invitrogen). Reactions were performed on the BioRad iCycler running iCycler IQ software ver. 3.1 (BioRad)

Primer sets were chosen from either RTprimerDB,[237-239] from previously reported primer sets,[240-243] or were custom made. Custom made QRT-PCR primers were chosen using Primer3 (section 2.3.1).[220] They were picked such that they were ~100bp, had a Tm ~60^{o}C and spanned an intron exon boundary. The housekeeping gene used for QRT-PCR was 18s (NR_003278.1), because the expression level of 18s remained constant in stimulated T lymphocytes, relative to the cell number.[242,244]

All QRT-PCR reactions were performed within an experiment in triplicate, and were performed over 3 separate experiments. Before any primer set was used in an experiment the primers were tested with non-template controls (NTC), and cDNA. Primer sets were not used if the NTC were positive for a melt curve, nor were they used if more than a single peak was seen on the melt curve for a reaction containing cDNA template. These two parameters were also checked at the end of each experimental run to control for contamination or degradation of components.

Each well on a plate was setup to run with ½ the suggested reaction volume. The recipe consisted of 10µL of iQ SYBR green supermix, 2µL of a 5µM primer set, and 6µL of H_20. These were setup in master mixes and aliquoted into each well. cDNA samples were then aliquoted to their respective wells and the plate was sealed with the microseal 'B' adhesive. Plates were centrifuged and loaded onto the iCycler. The cycle parameters were as follows. The iCycler was heated to 95^{o}C for 3min. The iCycler then performed 40 cycles of: 95^{o}C for 1min., 60^{o}C for 1min., and 80^{o}C for 10sec. The last 80^{o}C step was where the data collection occurred during cycling. The iCycler then had one final extension step at 55^{o}C for 1min., and then the melt curve program was performed. The threshold position for each run was optimally set using the internal iCycler IQ software. From this data the threshold cycle (Ct) was taken.

2.9.4.1 Calculating fold increase

After data collection the relative fold change for each sample was calculated. Threshold cycle's within an experimental group were not used if the variance was >1 Ct. Fold change was calculated in Excel (Microsoft) with the REST method.[245,246] This method was utilized as it does not make the assumption that a primer set amplifies perfectly. The experiment was designed for the experimental reference sample to be the experimental group with no treatment at 6 hours. In this setup the experimental reference is set to 1 and all other samples were expressed as the relative fold change compared to the experimental reference.

Pfaffle Method

$$\Delta Ct_{treatment} = Ct_{untreated} - Ct_{treatment}$$

$$\Delta Ct_{housekeeping} = Ct_{untreated} - Ct_{treatment}$$

$$fold\ increase = \frac{(E_{treatment})^{\Delta Ct_{treatment}}}{(E_{housekeeping})^{\Delta Ct_{housekeeping}}}$$

E is the efficiency for the primer set being used. The efficiency was calculated using the average change in C_t over a log10 dilution series. The equation for efficiency was:

$$E = \left[10^{\left(\frac{-1}{slope}\right)}\right] - 1$$

2.10 Animal Work

All animal work was approved by the University of Calgary Animal Care committee. The Animal Care committee adheres to the Canadian Council on Animal Care. Two animal protocols were approved, one for the rabbit experiments, protocol #M03046, and one for the mouse experiments, protocol #M07085. All work was done in accordance to standard operating procedures outlined in the animal care course provided by the animal facility, and with the Canandian Association of Laboratory Animal Science (CALAS).

2.10.1 Rabbit protocol

2.10.1.1 Vaccination Regime

Polyclonal antibodies recognizing λ, or λD-GFP were generated by injecting rabbits with ~0.3 mg (Lowry Assay) of purified λ or λD-GFP together with 0.5 mL of Freund's adjuvant (Sigma). Two treatment groups of 2 rabbits were used. One group was given wt λ, and one group had λD-GFP. Injections were carried out thrice, with two weeks passing between injections. The first inoculation was a subcutaneous injection with complete Freund's adjuvant (Sigma, F5881); the next two were administered intramuscularly with incomplete Freund's adjuvant (Sigma, F5506). Before each animal injection test bleeds were collected by ear bleeding. Finally, two weeks after the last injection rabbits were bled terminally by cardiac puncture under anaesthetic by the Animal Resource center. Serum was isolated by centrifugation at 2,380x g for 5min. The clear translucent upper fraction, the serum, was kept. Antibodies were purified from the serum using the Pierce Seize Primary Immunoprecipitation Kit (Pierce, #45335), used in combination with Protein A and Protein G labelling kits (Pierce, #44893 and 44990).

2.10.1.2 Western blotting of immune serum

Phage proteins and *Hek293T*, *Cos7*, and *BL21 (DE3)* cell lysates were electrophoresed through 12% SDS-Polyacrylamide gels and electro-blotted to nitrocellulose membranes using the Bio-Rad™ electrophoresis apparatus. Cell lysates were from non-transfected cells, negative control, or from pCMV-GFP, or pGEX-DLT-gfp transfected cells. Membranes were incubated with pre-immune rabbit sera, or with anti-sera following injections, subsequently purified for Ig proteins, or with a monoclonal rabbit anti-GFP antibody, JL8 (Clonetech), or with an anti-gpD rabbit polyclonal (gift from Dr. Nakanishi). Bound antibodies were then detected with donkey anti-rabbit IgG-Horse radish peroxidise (GE Healthcare) or sheep anti-mice IgG-Horseradish peroxidise (GE Healthcare) using an ECL detection kit (GE Healthcare, #RPN2106).

2.10.2 Mouse protocol

All mouse experiments were performed on female mice. The following mouse strains were used over the course of this thesis: C3H/HeJ (JAX), C3H/HeOuJ (JAX), C57Bl/6 (a gift from Dr. Robbins), TLR4$^{-/-}$ (Akira), TLR2$^{-/-}$ (Akira), MyD88$^{-/-}$ (Akira), and CD1 (Charles River). The original mouse vaccination work, Chapter 4, was performed with our CD1 mouse colony. The subsequent peritoneal macrophage isolation, Chapter 5, was done with 8-15 week old CD1 mice from Charles River. In the C3H immunizations, mice were ordered from JAX. The subsequent BMDM were isolated from C57Bl/6, TLR4$^{-/-}$,[65] TLR2$^{-/-}$,[247] and MyD88$^{-/-}$.[248]

2.10.2.1 Vaccination regime

Mice were immunized with a 100µL intra peritoneal (IP) injection. After the initial inoculation, booster inoculations were performed at 14 and 28days. Over the course of 4 months the mice were given a final boost 7 days prior to collection. The final boost was given to one or two mice per treatment group. This was done to control for day to day variability in the experiment, as it was not feasible to harvest cells from all animals on the same day. Diurnal variability was also controlled by harvesting animals at the same time in the morning, 9am. Animals were then dissected in the same order each time. The vehicle control animals were always done first with subsequent treatments going from vehicle to the most immunogenic treatment group.

The first immunization experiment was performed with CD1 mice. This experiment had 7 treatment groups where each treatment group contained 5 animals. The antigen vehicle was DPBS. In this experiment no adjuvant was used as we had seen in previous experiments that a similar immunogenicity was attained in mice inoculated with λ alone as with λ and RIBI (Sigma). The immunization groups in this experiment were: A) 10^{10} PFU wtλ, B) 10^{10} PFU λgfp10 displaying GFP, C) 2µg rGFP, D) 2µg rGFP co injected with 10^{10} PFU wtλ, E) 10^{9} λgfp10 displaying TAT and GFP, F) 10^{9} PFU λgfp10 displaying TAT, and G) DPBS.

The second immunization investigated the effect TLR4 ligands could have on the immunization. It was performed in the TLR4 mutant mice, C3H/HeJ, that are hyposensitive to LPS. A total of 4 treatment groups were inoculated. The first three treatment groups contained 15 mice each and were done in C3H/HeJ mice. These inoculations were done with: 1) 10^9 PFU of λgfp10 displaying TAT and GFP, 2) 10^9 PFU λgfp10 displaying TAT and GFP in 50μL DPBS and 50μL Freund's adjuvant, and 3) DPBS. The last treatment group was a positive control performed on 5 C3H/HeOuJ. This immunization group was injected with 10^9PFU λgfp10 displaying TAT and GFP, but no Freund's adjuvant.

Freund's adjuvant was utilized as recommended by the manufacturer. Complete Freund's adjuvant (CFA) was only used for the initial inoculations. All subsequent inoculations were done with incomplete Freund's adjuvant. In all cases 50μL adjuvant was mixed with 50μL of inoculant for a total volume of 100μL. This mixture was then vortexed extensively to produce an oil emulsion for injection.

2.10.2.2 Mouse necroscopy

Mouse necroscopy was performed beginning on the mouse immunized with the vehicle control and ending with the most immunogenic treatment group. For a detailed description of the mice chosen and the order of dissections, refer to section 2.10.2.1. After serum collection, lymph nodes were isolated from mice. The first lymph node collected was the inguinal node.[249] This node is located outside of the peritoneal cavity below the epidermis. To harvest the inguinal node, an incision was made to cut the epidermis below the lungs on the abdomen, but not so deep as to cut the peritoneal connective tissue. This incision was then extended along the midline of the abdomen towards the tail. The abdomen was then exposed by peeling the skin off the peritoneum, out towards each leg. In order to remove the skin towards the legs a lateral incision at the base of the abdomen was also performed as necessary. The skin was then pinned on the dissection tray. The inguinal lymph nodes were identified based on their location at the junction of 3 sub-epidermal veins. Given the age of the, these were typically buried in fatty tissue that was co-localized at the junction of the veins. The node was slightly

browner than adipose tissue and can be separated from adipose tissue by squishing the adipose tissue on a paper towel. Whereby, the nodes will poke through and resist being crushed with forceps, unlike adipose which lost all structure. There are 2 inguinal nodes, one on the left side and one on the right side, and each was 1-4mm in diameter. After collection and isolation from adipose tissue, the inguinal nodes were added a 1.5mL microfuge tube with 1mL of complete RPMI media (section 2.11.1) that was kept on ice.

The spleen was collected next. Care was taken not to perforate the bowel, as we were performing assays that are sensitive to bacterial endotoxin. The upper left side of the peritoneum was pulled and an incision was made through the connective tissue. The spleen is a deep red coloured organ that is oval shaped, long and flattened. It was cut from the splenic artery and vein and added to 5mL of complete RPMI media in a 35mm dish, kept on ice.

The mesenteric lymph nodes (MLN) were collected next. The mesentery is a connective tissue containing, lymph nodes, nerves, lymph vessels, blood vessels and arteries. The blood and lymph vessels drain from the large and small intestine. As such the mesentery is the white connective tissue next to the intestines. There were multiple mesenteric nodes located in this tissue. Depending on the animal, they could be larger and oblong in shape, or there could be many smaller nodes. The nodes can be found inside the mesentery by squeezing it with forceps and looking for nodes that pop out of the tissue. They were found close to the large intestine or in clusters where the mesenteric tissue collected in bundles on its way to the portal vein. Nodes were cut out of the tissue and were kept on ice in 1mL of complete RPMI media contained in a separate 1.5mL tube from the inguinal nodes.

The last two lymph nodes removed from the mouse were the axillary and brachial nodes, where one pair of each are under the forelimbs. After removal they were added to the inguinal node containing microfuge tube. The inguinal, brachial and axillary nodes from an animal were collectively called the peripheral lymph nodes (PLN) for this thesis.

After the lymphocytes were isolated, as described in section 2.11.1, $1x10^6$ cells were sent for FACS as described in section 2.8.7. This was done see if the lymphocytes were being polarized into $CD4^+$, $CD8^+$, or $B220^+$ populations during immunization.

2.10.2.3 Serum collection

Mouse blood was collected by cardiac puncture.[249] To perform this method, the animal was euthanized using cervical dislocation. The chest was then sterilized with 70% EtOH, and the chest cavity was opened up with sterile surgical tools. A 1 mL syringe (BD) with a 24 or 25gauge needle was slowly inserted into the beating heart at a 25^{o} to 30^{o} angle. When blood began to pool into the tip of the syringe the plunger was slowly retracted, care was taken to stabilize the syringe with a second hand. The procedure was done when ~1mL of blood was collected. Blood was centrifuged at 2,380x g for 5min. to precipitate clotting factors, and cells. The translucent and liquid top fraction, the serum, was kept. Samples were stored at -20^{o}C. Cardiac puncture was performed on mice before mouse necroscopy as the heart would not be beating if done following the collection of the spleen and lymph nodes.

2.11 *In vitro* immune cell culture

2.11.1 Lymphocyte Cell Proliferation

Lymph nodes were isolated as described in section 2.10.2.2. Lymph nodes of only one animal were processed at a time. Once harvested from an animal, lymph nodes and spleens were kept on ice in 35mm tissue culture (TC) dishes (Falcon, #353001) containing 5mL of complete RPMI media (RPMI 1640 media (Invitrogen, #21870), 10% FBS (Invitrogen), 2% penicillin/streptomycin (Invitrogen, #15140), and 1X β-mercaptoethanol (Invitrogen, #21985-023)). Depending on the lymph organ, two different methods were used to isolate lymphocytes.

For splenocytes, the spleen was pulverized with the top of a sterile 1ml syringe. The media and cells were added to a 15mL conical tube (Corning). Care was taken not to remove large clumps of connective tissue from the TC dish. The 35mm TC dish was then rinsed with 5mL of complete RPMI media, and the liquid was added to the same 15mL conical tube. The media and cells were left to settle for 5min., and the supernatant was removed, leaving behind the tissue that settled. The supernatant was centrifuged for

3min. at 400x g. The cell pellet was retained and 1mL of ammonium calcium potassium (ACK) lysis buffer (0.15M NH_4Cl, 10mM $KHCO_3$, and 0.1m EDTA, at a pH of7.4, and filter sterilized) was added. Cells were resuspended in ACK buffer and left at 37^oC for 2-5min. until all red blood cells (RBCs) were lysed. After incubation, lysis was stopped by the addition of 9mL of DPBS. The solution was mixed and centrifuged at 400x g for 3min. to remove all RBC cell debris. The cell pellet was then resuspended in 10ml of complete RPMI media, and a 1/10 dilution was counted on a haemocytometer (2.8.5). Before counting, an equal volume of trypan blue was added to the cells, and only viable cells, those that excluded the dye, were counted. It should be noted that very few splenocytes were dead after isolation. The total number of splenocytes in each spleen was calculated from the volume and concentration.

For all other lymph nodes collected, an electric pestle motor (Kontes) and disposable 1.5mL pestles (VWR) were used to disrupt the lymph nodes and release lymphocytes. Lymph nodes were collected from animals in 1ml of complete RPMI media in a 1.5ml microfuge tube. Tubes were kept on ice until the mortar and pestle was used. To review section 2.10.2.2, mesenteric lymph nodes were kept in one group, and peripheral lymph nodes were the other group of lymphocytes. Peripheral lymph nodes consisted of the axillary, brachial, and inguinal lymph nodes. Each group was dissociated by mechanical separation using a fresh sterile pestle. After dissociation, the volume of liquid was measured and then resuspended in 5mL of complete RPMI media. Care was taken to leave behind connective tissue from the lymph node. There was no need to remove RBCs as these nodes do not have many RBCs present. Cells were counted as described previously. The viability of cells was not affected by using the mortar and pestle to dissociate lymphocytes. The total numbers of viable cells were calculated for each lymph node.

Lymphocytes were plated at a concentration of $1x10^6$cells/mL. The cell proliferation assay was done on NunclonΔ 96 well plates (Nunc, #167008), where they had 100µL of cells/well. Spleen, mesenteric lymph node (MLN), and peripheral lymph nodes (PLN) were plated in triplicate for each stimulant. This was done separately for each animal. One mL of cells were also plated onto 24 well NunclonΔ plates (Nunc,

#142475), for the collection of supernatants to be used in ELISAs and for collection of cells for QRT-PCR. The 24 well plates were not performed in triplicate for each sample from each animal.

After plating, all cell stimulants were added to the plates. Two experiments: CD1 mice and C3H mice were performed with different amounts of stimulant being added for each. For the CD1 mouse experiment the following stimulants were added: 10% v/v T cell Receptor antibody (2C11), 10^{10} PFU wtλ, 10^{10} PFU λgfp10-GFP, 2μg rGFP (Millipore), 2μg rGFP co injected with 10^{10} PFU wtλ, 10^{9} λgfp10-TAT-GFP, 10^{9} PFU λgfp10-TAT, rGFP (Millipore) at 2μg/well, BSA (NEB) 2μg/well, rTAT PTD peptide at 2μg/ml, or media alone. The media alone wells were the experimental control, and they contained no stimulant. The 2C11 wells were the positive control treatment group that caused all T cells to proliferate. Finally, the rGFP and BSA treatments were to measure if any cells responded to rGFP, rTAT, or BSA, and/or if there were contaminants in these recombinant proteins.

The C3H mouse experiment had the following reagents added. After plating they were then stimulated with the addition of 5% v/v T cell Receptor antibody (2C11), λ-TAT-gfp at 10^{9}PFU/mL, LPS at 100ng/mL, rGFP (Millipore) 0.2μg/well, BSA (NEB) 0.2μg/well, or media alone.

Forty eight hours after stimulation, lymphocytes were pulsed with tritiated thymidine for 18hrs. Cells were then harvested onto grade 934AH glass fiber filter paper (Whatman, #1827-889) using a 96 well plate cell harvester (Brandel). Scintillation vials were loaded with the glass fiber membrane from each well and cytoscint (MP Biomedicals, #882453). Vials were left overnight, and then the counts per min. (CPM) were read on the Beckman LS 6500 liquid scintillation counter (Beckman).

Two other sets of samples were also collected from the 24 well plates during the culturing of lymphocytes. Supernatant was removed at 48hrs to be used in ELISAs to measure cytokine levels (section 2.12.1) and RNA was collected from adherent cells 48hrs post stimulation (section 2.9.1).

2.11.2 Peritoneal Macrophage

Peritoneal macrophages were collected from CD1 mice. Five days before collection 3mL of thioglycolate was injected into the peritoneal cavity of each mouse. For each experiment, 6 to 8 female mice had injections in order to collect sufficient peritoneal macrophages for an *in vitro* stimulation experiment. On day 5, mice were euthanized and the skin was removed from the abdomen. Skin was removed by cutting through the epidermis, from a fold of skin pulled away from the midline on the abdomen. Care was taken not to cut into the peritoneum. After the skin was nicked it was torn back from the abdomen to reveal the peritoneal cavity. A 10mL syringe filled with room temperature DPBS was injected into the peritoneal cavity with a 26G needle. Care was taken not to hit the intestines, as this would release *E.coli*. The DPBS was massaged throughout the cavity, and the mouse was left on a shaker for 6min. Each mouse was processed, and then DPBS was collected from the mice. DPBS was removed using a 10mL syringe and an 18G needle. The needle was inserted into the cavity, the cavity was distended, and the media was aspirated by the syringe. Proper distension resulted in 10mL of DPBS being collected. DPBS was pooled from mice and kept on ice.

Macrophage were isolated from DPBS and plated for stimulation. Cells were collected by centrifugation at 500x g for 8min. The cell pellet was rinsed with an equal volume of ice cold DPBS and centrifuged again to collect cells. Cells were resuspended in 10mL of complete growth media. Peritoneal macrophage were grown in 500mL DMEM (Invitrogen, #11965) containing 10% FBS, and 1% penicillin/streptomycin (Invitrogen, # 15140). $2x10^6$cells were seeded into each well together with 1mL of complete media in a 6well tissue culture dish (Nunc, #140675). The dish was incubated for 2hrs and the media was aspirated off and was replaced with 1mL of fresh complete media. This removed non-adherent cells, which are not macrophages. Half the wells were then stimulated with 10ng/mL of IFNγ, and cells were grown for 15hrs.

Fifteen hours after the addition of IFNγ to plates, a time course experiment was performed on macrophages. For this time course 0hr, 2hr and 6hr time points were collected where 1/3 of wells had no stimulant added, 1/3 had λgfp10-GFP-TAT at 10^9

PFU/mL, and 1/3 were stimulated with100 ng/mL LPS. In this setup ½ of plates were stimulated 15hrs previously with IFNγ.

2.11.2.1 Terminal Assays of Peritoneal Macrophages

Supernatants and RNA samples were taken at 0hrs, 2hrs and 6hrs after stimulation. Supernatants were kept frozen at -80^{o}C, until they were used for cytokine analysis on a Luminex machine, performed by Eve Technologies Inc. RNA samples were processed as described in section 2.9.

2.11.3 BMDM

Bone marrow derived macrophages were isolated from *wildtype* C57Bl/6 mice, and C57Bl/6 knockout mice for TLR4$^{-/-}$, TLR2$^{-/-}$,and MyD88$^{-/-}$. To begin, the tibia, femur, and pelvis of each mouse was isolated and the bone marrow was flushed out with a needle and syringe containing BMDM media. The bones were isolated by cutting them out of the surrounding tissue with scissors and sterile cheesecloth. After successful flushing, bones appear white and devoid of red marrow. Media was filtered to remove large particles with a syringe containing an 18G needle. Approximately 90x10^{6} cells were collected per mouse, whereas peritoneal macrophage isolation resulted in only 2x10^{6} to 5x10^{6} cells per mouse.

Isolated bone marrow cells were grown in BMDM media (1L of DMEM (Invitrogen, 11960-069), 10% heat inactivated FBS (Invitrogen), 1% penicillin/streptomycin (Invitrogen, #15140), and 15% L929 conditioned media (gift from E.Long)). L929 media was a source of CSF-1, a chemokine necessary for macrophage differentiation of macrophage progenitors.[250] Bone marrow cells were plated at a density of 2x10^{6}cells in 2mL of BMDM media per well into 6 well plates (Nunc, #140675). Cells were grown for 5 days, and then supplemented with 1mL BMDM media. Cells were grown for an additional 2 days. On day 7, 2hrs before the start of the time course, media was removed from the wells and was pooled, and then 2mL of the pooled media was added to each well.

BMDM were stimulated *in vitro* with LPS (*E.coli* or *S.minn.*) (section 2.13.3), λgfp10-GFP-TAT (2.5.5.1.1), or S-FSL1 (EMC microcollections) (2.13.3). Stimulants

were added to plates from the longest time point down to the no treatment, or 0 time point. In this way all plates were stopped at the same time by putting them on ice. Media was dumped off, and ice cold DPBS was added to each well. This was then dumped off, aspirated and 400µL of protein loading buffer was evenly distributed to each well. Plates were kept at -80^{o}C.

Protein samples were collected and stored for western analysis. Plates were thawed on ice, and samples were collected into labelled microfuge tubes. Each tube was sonicated to shear DNA and make a homogenous lysate. Samples were kept at -80^{o}C until they were run on a large western gel (2.7.1.3).

In parallel, tissue culture plates were also seeded for BMDM stimulation to collect RNA samples for QRT- PCR (2.9), and supernatants for Luminex analysis (2.12.2). As signals downstream of the intracellular signalling cascade were being investigated, these samples were set up on separate plates to be collected over longer periods of time. The assay was setup to measure the resulting cytokines at the mRNA and protein level.

2.12 Antibody and Cytokine assays

2.12.1 ELISA

Many serum ELISAs were performed to identify antibody and isotype titers. All samples and standards were performed in triplicate on Nunc Maxisorp^{TM} F8 strip wells. Most solutions were prepared in PBS pH 7.2. Strip wells were first washed a minimum of two times with PBS before coating. Ligands to be measured were then allowed to coat at room temperature overnight in PBS or carbonate buffer (0.795g Na_2CO_3, 1.465g $NaHCO_3$, 0.1g NaN_3, dissolved into 500mL of ddH_2O and adjusted to pH 9.6). Following overnight incubation, the plate was washed three times with wash buffer (0.05% Tween20 in PBS pH 7.2). Wells were blocked with 350µL of 1% fraction V BSA (Sigma) in PBS, otherwise called blocking reagent, for a minimum of 1hr. Wells were washed three times with wash buffer. Primary antibody or serum samples were added to the wells. This was done after a dilution series was made for each sample or primary antibody using blocking reagent. Plates were incubated overnight at 4^{o}C.

The next day, plates were washed three times with wash buffer and secondary antibody was added. This was either an isotype antibody with HRP or biotin. If biotin was used another wash and incubation was necessary with streptavidin-HRP. Secondary antibody and/or streptavidin was incubated for a minimum of 2hrs at room temperature, and washed three times with wash buffer. One hundred μL of TMB, product T4444 from Sigma, was then added for 20 minutes. TMB was added 1 row at a time at 10 second intervals. At 20minutes 50μL of 2N H_2SO_4 was used to stop the reaction. Plates were read on a BioRad Benchmark Plus microplate reader run from Microplate Manager software version 5.2 (BioRad). In this program two channel readings were taken, whereby 450nm was subtracted from 540nm to correct for optical imperfections in plasticware.

2.12.1.1 ELISA Kits

Sandwich ELISA kits were purchased from R&D Systems (Minn. MN, USA) to measure IL2, IL4, and IFNγ. These were the Duoset™ kits for IL-2 (DY402), IL-4 (DY404) and IFNγ (DY485). The assays were performed as described in their respective protocols, using the same plasticware and plate reader as described in section 2.12.1. Furthermore the same wash, blocking, and stop solutions were used along with the same TMB substrate as in the previous section, 2.12.1. As this was a sandwich ELISA absolute quantities of a given ligand were calculated using standard curves setup as described in the protocols but calculated using the BioRad Microplate Manager software version 5.2.

2.12.1.2 Custom ELISAs

Bacteriophage λ and rGFP ELISA's were developed to measure the relative concentration of antibodies in mouse serum. These were adsorption ELISAs where the ligand of interest coated the surface of wells. Each well was coated with either 10^9 bacteriophage λ, or 50ng of rGFP (Upstate, #14-392). Two different lots were used during this thesis, lot# DAM1503313, and # R0704D0010. As any recombinant protein is never 100% pure, both aliquots were tested for reproducibility in an ELISA with a

selection of mouse serums. In an earlier experiment a different lot did not give reproducible results. The two lots chosen gave consistent and reproducible results with the same mouse sera.

The antibody titer was expressed as the limiting dilution. To calculate the limiting dilution, a dilution series was prepared for each sample. Each dilution was plated in triplicate and the limiting dilution was defined as the last triplicate to have an average value above an optical density of 1.5. For a complete list of antibodies used in custom ELISA's refer to section 2.7.1.4. Exact dilutions of detection antibodies or streptavidin will be described in the results chapters.

2.12.2 Luminex Analysis

Supernatants of *in vitro* stimulated BMDMs or Splenocytes were analyzed using xMAP^{TM} technology on a Luminex detection system. A seven analyte plate was used to detect concentrations of cytokines and chemokines in multiplex. Samples were measured in duplicate and the standard operating procedures of Eve Technologies were used to quantify concentrations of cytokines and chemokines. A 22 analyte plate was also used for a selection of samples, but these were not performed in duplicate.

2.13 TLR ligand assays

Three experiments were used to investigate if ligands from bacteriophage λ preparations bound TLRs.

2.13.1 TLR ligand screen

InvivoGen performed an *in vitro* screen for mouse TLR ligands. 600μL of λ were provided to InvivoGen (SanDiego) for their propriety NF-κβ reporter system in Hek293T cells. 20μL of sample was added to duplicate wells along with positive and negative controls for each cell line. The following panel of mouse TLRs were tested: TLR2, TLR3, TLR4, TLR5, TLR7, and TLR9.

2.13.2 In vivo C3H mouse immunization

Immunizations were carried out as described in section 2.10.2.1. Readouts for differential TLR stimulation were antibody and cytokine concentrations. Antibody titers

were determined as described in section 2.12.1.2 and cytokine concentrations were determined as described in section 2.12.2.

2.13.3 BMDM stimulation

Bone marrow was isolated from four C57BL/6 mouse strains: *wildtype*, TLR4$^{-/-}$, TLR2$^{-/-}$, and MyD88$^{-/-}$. Bone marrow was cultured to produce macrophages, as described in section 2.11.3. Amounts of stimulants varied depending on the experiment. The first experiment was performed to produce a dose response curve. LPS was tested at 10ng/mL, 100ng/mL, and 250ng/mL. Bacteriophage was tested at 10^6, 10^7,10^8, and 10^9PFU/mL. This led to the following concentration of stimulant being used: 10^9 PFU/mL bacteriophage λ, 100ng/mL of LPS (see below), and 100ng/mL of S-FSL1 (EMC microcollections).

The stimulants used for BMDM experiments were as follows. BMDMs were stimulated *in vitro* with LPS from *E.coli* (Calbiochem, #437627), but the first BMDM work (Figure 5.4 B) was performed with *Salmonella Minnesota* R595 LPS (List Biological Laboratories Inc. Campbell, CA, product#434). The TLR2 ligand s-FSL1 was purchased from (EMC microcollections). Bacteriophage λ stock used for stimulation was from a prep prepared on September 8th 2008, λgfp10-TAT-gpDgfp. The signal transduction cascade was analyzed using total p38, phospho p38 or IκBα (section 2.7.1.4). Cytokines and chemokines were also analyzed downstream of these signalling cascades using xMAP technology from Luminex (section 2.12.2). For more information on this procedure please refer to section 2.11.3.

2.14 Lipopolysaccharide assays

2.14.1 LPS Silver Stained Lipid Gel

In 1983, Hitchcock and Brown described a qualitative method of visualizing LPS on a polyacrylamide gel.[251] The gel was prepared as described in section 2.7.1, except no SDS was added to the resolving gel. The loading buffer was 2% SDS, 4% β-mercaptoethanol, 10% glycerol, and 0.002% bromophenol blue in 0.1M Tris at a pH of

6.8. 10µL of sample or control was added to 10µL of loading buffer and incubated at 100°C for 30minutes. Samples are cooled, and 30µg of proteinase K is added and incubated at 56°C for 2-4hrs. After digestion with proteinase K, each reaction was loaded into the polyacrylamide gel and electrophoresed at 150 to 180V. When the dye front migrated close to the bottom of the gel, electrophoresis was stopped, and the gel was soaked overnight in distilled water containing 40% ethanol and 5% acetic acid. The next day, LPS was oxidized in 0.7% periodic acid, 40% ethanol, 5% acetic acid for 30 minutes. The gel was rinsed 5 times for 5 minutes with distilled water. Following rinsing, the BioRad Silver Stained Plus kit was used to stain oxidized LPS. This was performed in a clean glass dish, and was imaged on an Epson Perfection 4870 scanner.

2.14.2 Limulus Amebocyte Lysate Assay

Quantification of LPS was done using the *Limulus Amebocyte Lysate* (LAL) assay. This assay was first approved by the FDA in 1973 as a sensitive method to quantify the amount of LPS in products used for humans and animals.[252] In this work the LAL assay was an endpoint chromogenic assay (Lonza, #50-647U). The kit contained *Limulus Amebocyte Lysate* (LAL), *E.coli* endotoxin, a chromogenic substrate, and endotoxin free water. Not included were the endotoxin free glass dilution tubes, 13x100mm (Lonza, #N207), and the 96 well microplate (Thermo Electron, #8220).

Briefly, endotoxin and samples were diluted in glass tubes and vortexed vigorously for 1 min. before subsequent serial dilutions. 50µL of these standards and samples were then added to the microplate. The plate was pre incubated before addition of samples at 37°C. LAL was then added, 50µL, and the plate was mixed and incubated for 10min. at 37°C. The chromogenic substrate was then added, 100µL, and this was incubated and mixed for 6 min. at 37°C. Ten percent SDS was used to stop the reaction and the plate was read at 405nm, on the BioRad Benchmark Plus microplate reader. The linear range of absorbance for this assay is between 0.1EU/mL and 1EU/mL. Samples were compared to the standard curve using a linear fit ‘curve’ using Microplate Manager ver. 5.2 (BioRad).

2.14.3 Polymyxin B CNBr Column purification of Bacteriophage Preparations

For methods on how to perform a polymyxin B CNBR column please refer to Issekutz *et al*.[253]

Chapter Three: **Mashkiki bacteriophage λ display; Transduction into ES cells**

3.1 Summary

The objective of this study was to test the use of large homology regions on gene targeting rates in ES cells. A plateau of efficiency is seen in gene targeting with homology at 14kbp. Furthermore, when DNA is microinjected into the nucleus, targeting occurs at a rate of 10^{-3} instead of the usual 10^{-6}. With technologies developed in the lab that streamlined the production of targeting vectors, it was postulated if gene targeting rates could be increased by using intact λ particles. As recent experiments with λ phage had documented them as mammalian transduction vehicles, and since λ can carry large DNA cargos (up to 50kb) into the nuclei of mammalian cells, it could be used as a delivery vector to stimulate homologous recombination. A λ display system, termed Mashkiki, was built using recombineering. Techniques were developed to optimize the preparation of Mashkiki displaying three forms of gpD. Displayed peptides were accessible to thrombin cleavage, proving gpD fusion partners folded separately from gpD and were accessible to solvent. A GFP reporter cassette was cloned into λ-TAT and was shown to be active in mammalian cells this construct was called λgfp10-TAT. With Mashkiki bacteriophage built, it was determined that TAT mediated transduction of λ does not result in reporter gene expression, as previous studies reported, but TAT does cause transduction into cells.

3.2 Introduction

3.2.1 Phage Display

Phage display has become a powerful tool for molecular biologists. First developed by G. Smith as a technique to clone proteins recognized by antibodies, this technology has quickly become synonymous with protein interaction studies.[254,255] Phage display, or more formally bacteriophage display, is now used in a plethora of studies including screening receptor-ligand interactions, affinity maturation of epitopes or proteins, and more recently as a means to investigate enzyme catalysis and protein folding.[256-258]

Filamentous bacteriophage (M13/fd) was the first phage strain to be used for phage display[255] and is still the predominant strain used today. It is useful for the assembly of small polypeptide libraries, and affinity maturation experiments where a few amino acids along a scaffold are evolved, such as for the *in vitro* evolution of hypervariable regions on antibodies.[259] However, filamentous phage display is not efficient at displaying large fusion proteins or libraries of complex cDNAs.[260] For this purpose the lytic λ phage is choice.[261-264]

λ phage has two life cycles: lysogeny and lytic growth.[265] The choice between life cycles is dependent on the multiplicity of infection (MOI) and the nutritional state of the bacteria.[211] The lytic growth cycle gives λ phage an advantage over filamentous phage, as λ can assemble in the cytoplasm and then escape bacterial hosts through lysis. Filamentous phage is dependent on proteins being secreted and assembled in the periplasm, which can result in proteolysis, and a bias to display secreted proteins. [260] λ phage libraries do not suffer from similar over representation.[264] There exist many differences between λ and M13 which suggested λ would be a better display platform. When λ and M13 are compared in a real world setting the result is 100 times more fusion protein displayed on each λ, and displayed proteins are not degraded.[266]

λ was first isolated in 1944 by Gray and Tatum, and has been intensively studied ever since.[267] With volumes of work published, it is the ideal candidate virus to do molecular engineering work. λ contains two structural components the head capsid and

the tail (Fig. 3.1).[265] These assemble separately, then following DNA packaging into the prohead, the tail is attached (Fig. 3.1 3. 2).[265,268] The three major protein components of the virus are gpE, gpV, and gpD; in descending order of size.[265,269] gpE (38.2kDa) and gpD(11.6kDa) are the major proteins of the head capsid, with 405 copies on each particle.[268] The major component of the tail is gpV. On the head gpD is an accessory protein that assembles as prominent trimers.[268] Functional studies have shown that assembly of gpD onto the viral head is needed to accommodate its 48.5kB genome.[263,268]

λ display has been done using either gpV [261,264] or gpD [262,263,269-272]. The phage head is attractive for display as the structure has been studied and gpD's crystal structure is known.[268,273] Previous studies have used N-terminal [262,263,269,272] or C-terminal display [262,270,271] of peptides on gpD. The N-terminal of gpD has been used to display β-lactamase (31.5kDa) in a catalytically active form.[262] New structural work suggests N-terminal display of peptides will not be as efficient in display as the native N-terminus is not accessible to solvent,[273] resulting in decreased incorporation of the fusion protein. The N-terminus may be amenable to large fusions, such as β-lactamase, but as a result of this study we decided to display peptides and proteins off the C terminal of gpD.

3.2.2 Gene Targeting

The purpose of constructing a λ display system was to investigate if the rate of gene targeting could be improved. This all began with Derrick and I discussing options for receptor mediated endocytosis of λ. These were brought about from preliminary experiments in his lab showing intact λ particles to be effective in gene targeting experiments; they were performed by one of his former students, Maria Mosaico. Concurrently with this work, effective targeting vector methods were established in the lab taking advantage of λ recombination, these techniques called transplacement mutagenesis (TM), and retro-recombination screening (RRS) make it possible to design large genomic targeting vectors.[226,227,229,274] The benefits of these systems are 3 fold. First, having large DNA constructs allows longer homology to be used for targeting, thus increasing the homologous recombination frequency,[275,276] but the usual two pitfalls of

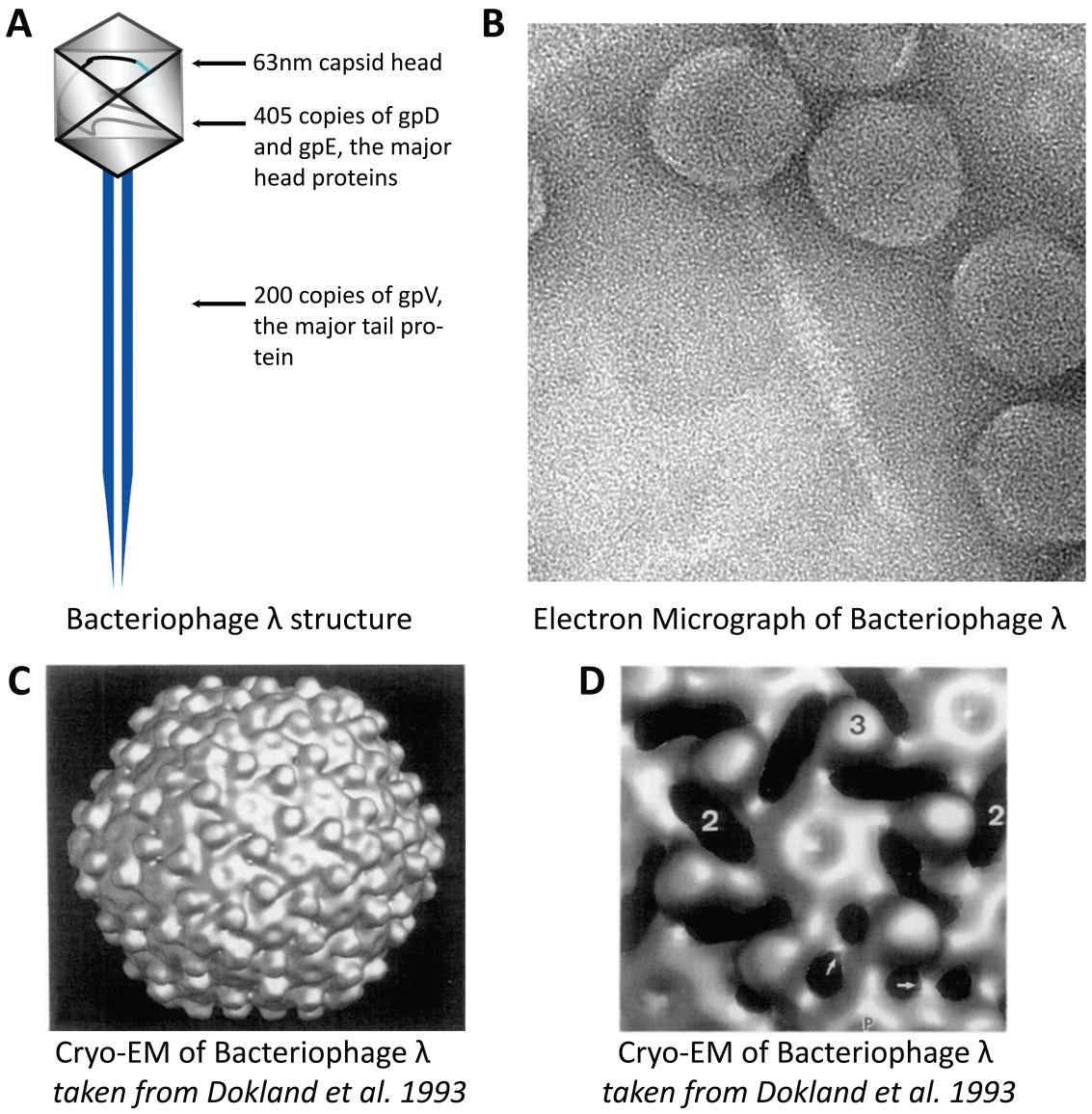

Bacteriophage λ structure

Electron Micrograph of Bacteriophage λ

Cryo-EM of Bacteriophage λ
taken from Dokland et al. 1993

Cryo-EM of Bacteriophage λ
taken from Dokland et al. 1993

Figure 3.1: Bacteriophage λ Structure.

Panel A is a graphical representation of λ. The major coat proteins are gpD, gpE and gpV. The tail is a spiral structure composed primarily of gpV, whereas the head capsid is composed of gpE with the accessory protein gpD forming trivalent spikes. Panel B is an electron micrograph of λ displaying TAT. Panels C and D are cryo-EM done by Dokland et al.[268] At high resolution the icosohedral shape of the head capsid is evident. The ring structures formed by gpE pentamers and hexamers are evident in C and D. The head capsid volume is increased with the addition of gpD trimers between gpE pentamers and hexamers.

working on large plasmids are avoided with this system. Second, as phage DNA is not manipulated in its naked form, without its capsid, vector shearing is not an issue, and third, restriction site availability is circumvented by using phage recombination. The original purpose of this thesis was to explore the possibility of transducing ES cells with intact phage; the rationale for these experiments will be outlined below.

In ES cells, gene targeting occurs at a frequency of approximately one event per million electroporated cells.[277,278] The rare event is selected for by positive-negative drug selection schemes, to purify ES cell clones containing the desired mutation.[279-285] ES clones are then screened, using PCR or genomic Southern blots, as many resistant clones do not contain the desired mutation. Interestingly, Dr. Capecchi's original work using microinjection reported a rate of 1 in 1000 cells undergoing targeting events to repair a defective *neo*^{r} gene.[284,286] With efficiencies of 10^{-3} it would seem one hurdle for targeting is efficient delivery of targeting constructs, but due to its labour intensive nature and rare occurrence, microinjection is not feasible for targeting experiments. With the advent of gene therapy vectors it seems more efficient delivery could result in a higher frequency of gene targeting events. Viral vectors could also be used as delivery vehicles that are modified with various moieties, or proteins, to increase the rate of gene targeting in somatic or ES cells. With this in mind, it is not surprising groups are actively investigating the utility of gene therapy vectors for the production of mutant mouse lines. The corollary is gene therapy labs are investigating targeted gene correction for monogenic diseases,[287] as random integration of genes can result in the development of cancer or further pathologies.[288]

One of the many benefits of λ is the large genomic cargo it can hold. The typical size of a genomic clone within flanking λ arms is usually >15kb. This is larger than either of the most common viral vectors, Lentivirus or Adeno-associated virus (AAV), can accommodate. In fact λ capsids can accommodate up to 48.5kb, larger than any viral vector currently available.[289] We believed we could increase the efficiency of gene targeting by using large regions of homology that would not suffer from previously reported plateaus of efficiency ~14kbp.[276] As it was known that by increasing the homology driving recombination from 1.3kbp to 6.8kbp a 250fold increase in targeting

frequency is seen.[275] We wondered what would result if we could get large pieces of DNA into mammalian cells without electroporation. Electroporation is a very effective method of transformation for small DNA fragments, but the efficiency decreases as the size increases past 14kbp.[290,291] Interestingly, this also correlates with the drop in gene targeting frequency.[275,276] Large DNA molecules, such as BACs are now routinely used in targeting experiments, but optimal entry of DNA using electroporation of large DNA constructs >80kbp, is only achieved when the construct is supercoiled. This is in contrast with linear DNA being optimal for transformation efficiency.[292] We believed that with λ we could use large flanking homology regions approaching 20kbp to increase targeting efficiency, but we did not know what effect intact λ particles would have on cellular entry, or transformation efficiency.

3.2.2.1 Gene Targeting: History

Gene targeting in the mouse has proved to be an excellent model for many diseases. The basic knockout mouse is achieved by the targeted insertion of a drug resistance marker, preventing normal gene expression.[293] Homologous recombination is the endogenous gene repair program utilized by gene targeting methods. The technique was developed in the 1980s by the research groups of Mario Capecchi and Oliver Smithies, and it was made possible with the discovery of murine embryonic stem cells by Martin Evans.[280-285,294-298] This technology, the knockout mouse, allowed forward genetics and the discovery of gene function. Once targeted mutations are designed, a phenotype is then analyzed in subsequent hetero- or homozygous mice. A variation on this theme is the knockin whereby a different gene, is inserted into a gene locus to investigate function with respect to spatio-temporal expression patterns. The gene to be knocked in can also be tagged to facilitate tracking. Tagging can be accomplished by fusing reporter genes, GFP or LacZ, to the inserted gene.

Using recombinases, Cre or Flp, along with inducible systems has given rise to new levels of control in gene targeting.[299,300] These conditional knockouts allow for spatio-temporal control. It is now possible to remove gene expression for a given organ or tissue, given the right promoter to drive expression of the recombinase.[301] Furthermore, the recombinase activity can be turned on or off with an inducer. This has

resulted in a better understanding of many phenotypes in adult mice, particularly in respect to the nervous system.[302] It is interesting to note this technological leap of using recombinases, was borrowed from the bacteriophage genome.

3.2.2.2 Gene Targeting and Double Stranded Breaks

We know that increasing homology in targeting vectors increases the efficiency of gene targeting,[275,276] but the reason this occurs is most likely due to a higher chance that a double stranded break occurs in the loci. The use of nucleases to cause double stranded breaks, and their concomitant repair, at genomic loci has been described in the literature since the early 90's.[303,304] Homology directed repair was seen to be 10 fold higher in human cells, and 100 fold higher in hamster cells, when a DSB was introduced to genomic loci.[305,306] When done on mouse ES cells a 5000-8000 fold increase is seen.[278,307] These experiments also documented a corresponding increase in non-homologous repair. This ranged from ½ of insertion events, in the best case scenario, to 100 non-homologous events for every targeted event in ES cells.[278,307] When hamster cell lines are investigated, a 1000 fold increase in non-homologous repair of DSBs is seen.[305] Obviously, cell type, mode of transfection and cell cycle play roles as to which DNA repair mechanism is used.[278,286,307]

3.2.2.3 Gene Targeting and Viral Vectors

Investigating the use of intact viral particles for gene targeting became more popular with increasing interest in gene therapy. Given the options outlined above there were a few parameters to investigate, and various moieties to test for their efficacy in gene targeting.

Lentiviral vectors were the first examples to be used for gene targeting by the Baltimore and Verma groups in 2002.[308,309] Six years ago, Dr. Baltimore's group published another example, this time using AAV.[307] This vector coupled with another causing double-strand breaks in the region of interest was used in an effort to investigate increasing the rate at which recombination occurs. The study documented gene targeting frequencies of 0.8%, an 8000 fold increase in recombination over previous rates for electroporation of 1 in a million. A striking finding was that homologous recombination

occurred in only half of the recombination events; where the other events underwent non-homologous integration.

Promoting homologous repair of double stranded breaks was effective in cell lines with engineered meganuclease sites, but how could it be adapted for wild type loci? Two papers presented similar strategies in 2003.[310,311] In both strategies, a one half of a meganuclease is fused to DNA binding proteins, zinc fingers, to 'home' the nuclease to a specific genomic loci. When two zinc finger-meganucleases are in close proximity the meganuclease dimerizes and cuts the DNA present. These have been termed 'zinc finger nucleases'. Recently this paradigm was used for gene therapy on human cells. This method resulted in 18% of cells having the desired correction in the appropriate loci. This was without any selection. Of the 18%, 7% had correction of both alleles. These seminal works were amazing, but one caveat is the earlier AAV work, as many of the cells will have non-homologous insertions, a fact not investigated in these studies.

AAV and Lentiviral vectors both have their merits and disadvantages. Retroviral integration is one issue to be considered. Lentivirus will integrate into dividing and non-dividing cells and integration is preferentially into intergenic regions.[17] AAV vectors on the other hand have a preference for integration into actively transcribed regions.[17] It is undetermined how a preference for actively transcribed genes will affect gene targeting with AAV vectors. Only cells expressing the gene of interest would be targeted, which is beneficial for some scenarios. More information is needed on the integrative mechanisms of both AAV and Lentiviral vectors, as analysis of targeting experiments may be complicated by their propensity for non-targeted integrations into the genome.

A new viral vector has recently come into the literature, Baculovirus, an insect virus.[312] Previously, it wasn't known if it infected mammalian cells but recent work has shown it does and could be used for targeting experiments.[312,313] This virus holds an extremely large genome of 150kb, approximately 3X larger than bacteriophage. The large size is both a benefit and a hindrance. The size is beneficial for gene targeting, as they can be used for similar work as BACs, but the lack of DNA recombination techniques is a hindrance to for engineering genetic mutations. In bacteriophage λ cloning is not the only way to produce mutations. Our lab has developed recombineering

methods to drop in mutations without the use of restriction enzymes.[229,274] We have also recently engineered mutations directly from dsDNA plasmid fragments, PCR amplimers, and ssDNA oligos using Donald Court's recombineering system.[222]

3.2.3 Reverse Genetics

Classic genetic model systems are synonymous with reverse genetics, or mutation screens. The prohibitive cost and the advent of forward genetic approaches in the mouse, resulted in these experiments becoming less prevalent. The saturation of mouse gene knockouts is a goal of the Gene Trap consortium, although it is not a phenotype driven screen, it is of interest as it is most similar to a reverse genetic approach,[314] and takes advantage of the 'random' integration of viral vectors. An even older method of reverse genetics is the use of the mutagen ENU, or *N-ethyl-N-nitrosourea*. This has been used to advantage in the phenotype screening system of Dr. Beutler,[315] which is of interest for the immunology chapters of this thesis.

3.2.4 Embryonic Stem Cells

Central to the study of mouse genetics, is embryonic stem cells. This cell type propelled gene function studies and was integral in deciphering mammalian developmental biology. As mentioned previously, their discovery by Martin Evans,[295,296] and later manipulation by Mario Capecchi's,[285] and Oliver Smithies' groups,[297] opened the doors of modern gene analysis. A new paradigm shift has recently come to the fore, as it has been shown that somatic cells can be reprogrammed, or dedifferentiated into pluripotent stem cells. This was lead by the seminal work of Dr. Yamanaka's group and was quickly recapitulated by Drs. Jaenisch and Thomson.[316-318] There is a shift in science as reprogramming is being used to discover new aspects of development, and autologous stem cell therapies are becoming possible.[319-321] More efficient systems of generating iPS cells are needed before the autologous stem cell therapies become widespread, and some of the same pitfalls seen for gene therapy still need to be addressed before human trials.[322-325]

3.2.5 TAT: A protein transduction domain

λ is inert in eukaryotic cells. The genome is not compatible for transcription, mRNA is not able to be translated, and it cannot enter eukaryotic cells as the *lamB* gene from *E.coli* is not present.[326-328] These characteristics are advantageous for genetic engineering of λ, as adverse effects from an endogenous viral proliferation lifecycle will not occur. As we wanted to use λ as a gene delivery vehicle for ES cells, we needed to cause transduction of λ into eukaryotic cells.

The first reported gene expression from λ DNA in eukaryotic cells was documented in 1971.[329] Interestingly, when cyclohexamide was used in this system, a chemical that only inhibits eukaryotic gene expression, the enzyme delivered by λ was still expressed in human fibroblasts. This leads one to believe that a bacterial contaminant in the culture or the cells was causing the transcription of λ DNA. Although controls were run to test for contamination, none was detected with 1971 methods. When the same group investigated λ RNA in fibroblasts, the amount increased over time, and this continued beyond 41days.[330] λ is inert in fibroblasts, and therefore cannot replicate and increase in numbers; further evidence that the effect was an artifact. The observation was never documented again in the literature, which is the final piece of damning evidence.

A better example of early λ transduction studies was the use of intact λ carrying a positive selection cassette.[331] This study documented a transduction efficiency of $1/_{2.3x10^5}$, as measured by TK^+ clones after HAT selection. Unfortunately a comparison between intact λ particles and similarly sized plasmids was not done.

The first barrier into eukaryotic cells is the cell membrane. The most promising technique for entry was the use of a protein transduction domain (PTD).[332] Protein transduction domains are contained on some proteins and are believed to cause cellular entry. The prototypical examples are: a domain on the *Drosophila* homeotic transcription factor *antennapedia*, a domain on the Herpes Simplex virus protein VP22, and a domain on the Human Immunodeficiency virus (HIV) protein TAT.[231,234] The characteristic common among these small regions was a net positive charge, and thus cationic peptides

were also found to contain PTD activity.[333] Using protein transduction domains displayed on the surface of λ, one study showed expression of an exogenous gene contained in the λ genome.[269] Another group tethered fusion proteins on gpD and saw uptake of bacteriophage λ into mammalian cells.[270] In this study the pentone base protein from the adenovirus capsid was used along with streptococcal protein G and staphylococcal protein A.

Phage was not the only cargo fused to PTDs. A whole field has developed around PTDs and investigating their utility in penetrating cell membranes to deliver pharmacologically active compounds. TAT fusion to HoxB4 was shown to expand the hematopoetic stem cell population.[334] This simplified the experiment as a viral vector was not necessary to deliver a transcription factor. TAT has also been fused to Cre, but Peitz *et al*. found that a nuclear localization sequence (NLS) was necessary for efficient Cre delivery.[335] Further experiments have shown that TAT transduction can be enhanced by using endosomal disruption agents. In one of these studies this resulted in a 23 fold increase in TAT-Cre delivery to the nucleus.[336] The mechanism of TAT transduction is controversial, but obviously the fusion partner, and what protein motifs it contains, affects intracellular trafficking.

When this work began it was decided that the best characterized PTD, TAT would be used for phage transduction into ES cells. The Tat PTD is an 11 aa, highly positively charged peptide.[332,337,338] The PTD field has had continual controversy, but these peptides seemed better suited than ever for our purpose. Originally, it was thought these domains caused transduction using a unique mechanism, that was energy and time independent.[332] Large cargos were transduced into cells, and even across the blood brain barier.[338] It was later found that many early TAT transduction studies were artifacts from the fixation of cells and this allowed TAT fusions to enter fixed, or permeabilized cells.[234] Some of these results will need to be re-evaluated, but knowing how these peptides worked, we thought would allow us to optimize the delivery of PTD-λ cargos. The mechanism of entry can now be described as follows. Tat and other PTDs are highly positively charged and adsorption occurs on the cell surface to the negatively charged heparan sulfate proteoglycans (HSPG).[233-236] PTDs and their cargo are subsequently

known to be internalized through endocytosis, macropinocytosis, or by caveolae.[232,233,339,340] As phage are large supramolecular complexes it is thought these are preferentially internalized through macropinocytosis,[340,341] but this effect may be cell type specific and claithrin mediated endocytosis could be involved.[232,233]

It should now be noted that in experiments on λ where Tat was displayed on gpD, transduction of λ was seen, as cells treated with Tat-phage resulted in exogenous reporter gene expression.[269] The use of this reporter gene assay to test for transduction proves this experiment was not an artifact. As mentioned, the previously mentioned artifact was due to cell fixation.[233-236] When cells are fixed their cell membranes are permeabilized and the highly positively charged PTD moves from the cell surface to the negatively charge molecules in the nucleus. Eguchi's data was not collected from fixed cells. It was a reporter gene that would only be transcribed if the phage entered the nucleus. Owing to these facts we proceeded with the experiment to test λ-TAT as a vector for ES cell gene targeting.

Since we began these experiments no studies on TAT and bacteriophage have reported efficiencies approaching those of Eguchi *et al*. In 2007, a study showed that similarly sized naked plasmid DNA was equivalent at internalization as *wt* λ, when both constructs had a CMV:luciferase cassette.[341] This study investigated if λ DNA exterior to the capsid was responsible for the effect. λ preparations were treated with DNAse1 and luciferase activity remained the same. When gpD displayed αvβ3 integrin, λ was marginally better at luciferase activity. $1x10^4$ RLU was seen for *wt* λ with the luciferase cassette whereas λ displaying αvβ3 had luciferase activity of $4x10^4$ RLU, this was statistically significant, but not a large difference. Given the initial reports seen by Eguchi and Piersanti,[269,270] this finding was unexpected and did not fit.

Given the controversy in the PTD field, it was not surprising the literature is peppered with studies and methods on how to enhance transduction. One belief was to find a more optimal PTD by using phage display projects to find new domains, the end result was new positively charged peptides.[342-344] Other ways of enhancing transduction that have been investigated are to coat PTD fusions with DOTMA,[345] or PEI,[346-348] both general transfection reagents, or by the use of the cationic peptide DEAE.[349] Other

strategies are to abrogate normal intracellular vesicle trafficking, using proteasomal inhibitors.[350] In this work a 5 fold increase in luciferase activity was seen after MG132, a proteasomal inhibitor, whereas the endosomal proton pump inhibitor, Bafilomycin A1, an endosomotropic inhibitor, had no effect. The MG132 result was shown to be phage specific, as it did not affect the same luciferase cassette in a plasmid. Another endosomotropic agent, chloroquine did affect luciferase activity, but it was at a level that this inhibitor affects lysosomal proteases. Lysosomal proteases, cathepsin B and L, also increase luciferase activity in this system.[350,351] We did not explore these other avenues of research for two reasons. First, when we were investigating λ transduction with TAT damning evidence against the efficacy was not prevalent,[341,351] and second, I wanted a robust system that would work as an *in vivo* gene therapy vector.

3.2.6 Recombineering

To build the gpD λ phage display system into the genome of λ a novel approach was used: recombineering. This is the only instance this technique has been used for this purpose, but given its elegance and simplicity, it is a paradigm for phage display vector construction that should be continued.

The Rancourt lab has developed methods of targeting vector assembly that take advantage of the *E.coli* RecBCD homologous recombination system. RecBCD is known to be enhanced by the λ gene *rap,* which is a nuclease that resolves holiday junctions.[227,352] These methods rely on the formation of co-integrants between λ or plasmids bearing homologous sequence. Another recombination process wholly in λ is Red. This system has been characterized to the individual λ proteins Exo, Beta, and Gam. λ Red can act independently of RecA, RecBCD and rap. Indeed if RecBCD is deleted and replaced with λ Red, *E.coli* become hyper-recombinant.[352] λ Red is a DNA double strand break repair pathway, and is ideal for genetic engineering as it relies on short oligos for repair. λ Red is very efficient at promoting recombination, as recombinants can occur at rates of 0.1-1%.[225] *Beta* has since been shown to be the only protein necessary for recombination to occur if single stranded oligos are used as a substrate for recombination. In this scenario *beta* binds the oligos and lagging strand invasion occurs during replication of the plasmid or λ genome.[222,353-355] Taken to the

extreme, only *beta* is needed and oligos of 36bps are sufficient to cause recombination, but with these parameters the recombination rate is lower than when longer homologies are used.[225,356-358] The λ Red recombination system has since been coined recombineering. We took advantage of recombineering to construct gpD-amber-TAT fusions into the genome of λgfp10.

3.2.7 Concluding Remarks

Given the possibilities of working on vector platforms to make gene targeting a more efficient process, many groups are now pursuing this goal in the gene therapy, cell therapy and gene targeting fields. The need for targeted gene therapy seems more necessary now than ever, given complications in therapies causing new pathogenesis from random integration.[289] The current media darling, stem cell therapy, holds much promise, especially for ex-vivo stem cell therapy, but methods are lacking to fix mutations in stem cells. We believed bacteriophage λ had many advantages over other viral vectors and would be suitable for this purpose. This whole project was conceived as Dr. Derrick Rancourt's lab was interested in improving gene targeting and I was interested in developing novel therapeutics.

3.3 Results

3.3.1 Bacteriophage λ structure

Bacteriophage λ is a 48.5kbp dsDNA virus that infects bacteria. The capsid, is composed of 2 major structural units, the icosohedral head capsid (Fig. 3.1 A), and the tail capsid. The tail is a coil structure composed primarily of the gpV protein, with the icosohedral head being made of gpE arranged in hexamers and pentamers separated by trivalent spikes of gpD (Fig. 3.1 C,D).[268,273] The major capsid proteins were important to study as these were the likely candidates for display of fusion proteins. An ideal phage display protein to produce fusion proteins on would be non-sterically constrained, allowing access to solvent, and would have large numbers on the capsid to maximize interactions. The Mashkiki phage display system was designed on the gpD capsid protein, as it had 405 to 420 copies per capsid and was accessible to solution. After the λ display system, Mashkiki, was built the morphology was then investigated by EM. The display of fusion proteins did not negatively affect the morphology of λ (Fig. 3.1 B).

3.3.2 λ phage display

After the capsid protein was chosen to display proteins and peptides, it was necessary to build the phage display constructs. Three different systems were developed (Fig. 3.2): 1) a '*trans* expression' system using the plasmid pGEX-DLTgfp (2.2.10), 2) 'direct mutation' using recombineering to make mutant phage displaying gpD-GFP (2.5.7), and 3) 'synthetic display' using TAT peptides conjugated to λ using biotin streptavidin chemistry.

The *trans* display system was built first for the display of gpD-GFP fusions off λ (Fig 3.2 E,F). Direct mutation of the genome was more difficult. The Rancourt lab developed phage recombination systems that take advantage of the *E.coli* RecABCD pathway, but unfortunately these all included the deposition of plasmid components into the phage genome before double recombinants are screened in non-permissive bacterial hosts.[226-229] Using variations on these systems, it was not possible to find viable mutants when the late polycistronic genes were targeted for mutation. In contrast, with λ Red

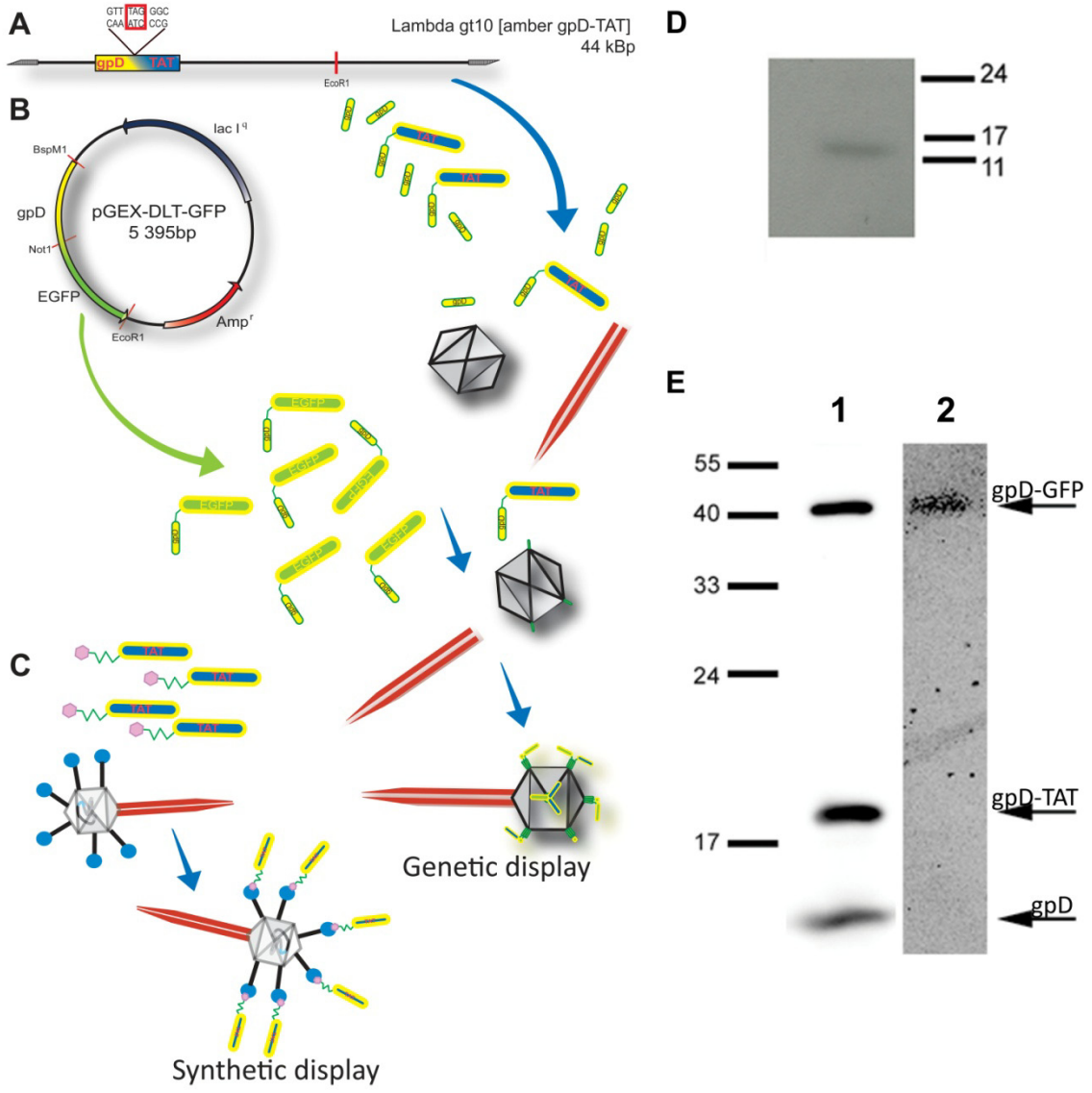

Figure 3.2: Phage Display.
Three methods to display peptides/proteins on λ were developed. The first system, panel B, was a *trans* expression system where gpD fusion proteins are produced by the pGEX-DLTgfp plasmid in bacteria, and become incorporated into λ during growth. Panel A is λ recombineered with a gpD fusion protein after the amber codon. In A, the phage genome produces *wt* gpD, and gpD-fusions when the supF tRNA is present. A third system, panel C, used synthetic peptides with biotin residues to decorate biotin/streptavidin/phage conjugates. In D, a biotin residue is seen on λGT10. Panel E is proof gpD, gpD-TAT, and gpD-GFP are present in Mashkiki phage. Mashkiki phage were visualized on a western blot probed with anti-gpD in lane 1, and anti-GFP(JL8) in lane 2.

recombination, or recombineering (Fig. 3.3), viable mutants were collected. In this system oligos of 35bps or greater drive incorporation of mutations, without the need for plasmid incorporation.[222,225] A consequence of the system we developed was a lack of genetic selection for recombinants. This resulted in the need to screen plaques using radioactive probe hybridization (2.5.8).

Synthetic display of TAT peptides was done using biotin-streptavidin chemistry. At the time there was no mono or divalent streptavidin available, and it was not possible to produce phage conjugated to TAT without making a large cross-linked mass. This line of investigation was stopped but interestingly, it appears there is a protein that is biotinylated and is approximately the same size as gpD (Fig. 3.2 D). For synthetic display, biotin-TAT peptides were synthesized, and were also useful the TAT-streptavidin transduction work (Figure 3.8 and section 3.3.6).

With various display systems built, we next tested if fusions to gpD suffered from steric hindrance. This could arise from an inappropriate linker, or because the C terminal of gpD is buried in the trimer.[230,273] The proteolytic cleavage of gpD-GFP with thrombin was used to test this. We engineered a thrombin site in the linker and successful proteolysis was proof that gpD and GFP folded separately (Fig. 3.4 C). As mentioned previously, the morphology of λ was not negatively affected by the display of proteins on gpD (Fig. 3.4 A,B).

The last question to ask is whether we can add multiple peptides/proteins onto λ using a combination of display systems (Figure 3.2 A) to produce Mashkiki phage. Using the optimized λ preparation protocol (sections 2.5.5, and Fig. 3.5) it is possible to display multiple moieties on gpD (Fig. 3.2 E). This was of interest for molecular therapy, as the more proteins displayed the more one can reprogram the function of the virus.

3.3.3 Optimization of λ preparation

Phage titers decreased in preparations (2.5.5) of λ displaying peptides, as compared to wild type λ. This lead to variability in the yields of phage prepared. The percentage display of gpD-fusions was also found to be variable in different preparations. These factors are compounded when *trans* expression is attempted together with recombineered phage, 3D display. An optimized protocol was necessary for consistent results.

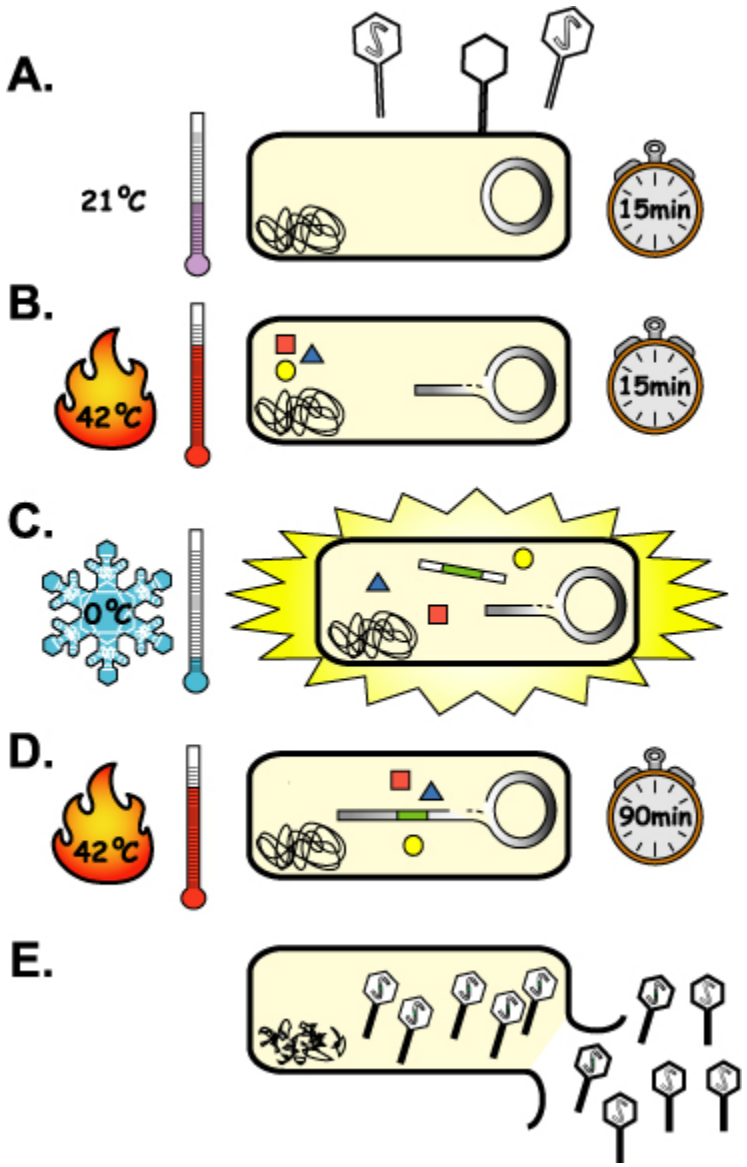

Figure 3.3: Bacteriophage Recombineering.
λ are adsorbed to DY330 cells for 15min. at 21^{O}C, panel A. The culture is then grown for 15min at 42^{O}C, whereby phage infect bacteria, and λ Exo, Beta and Gam proteins are induced, panel B. The culture is put on ice and homology containing DNA is electroporated into DY330, panel C. The culture is grown for a further 90min at the permissive temperature for λ Red expression, panel D, and bacteriophage are collected for screening recombinants, panel E. From: Knut Woltjen.

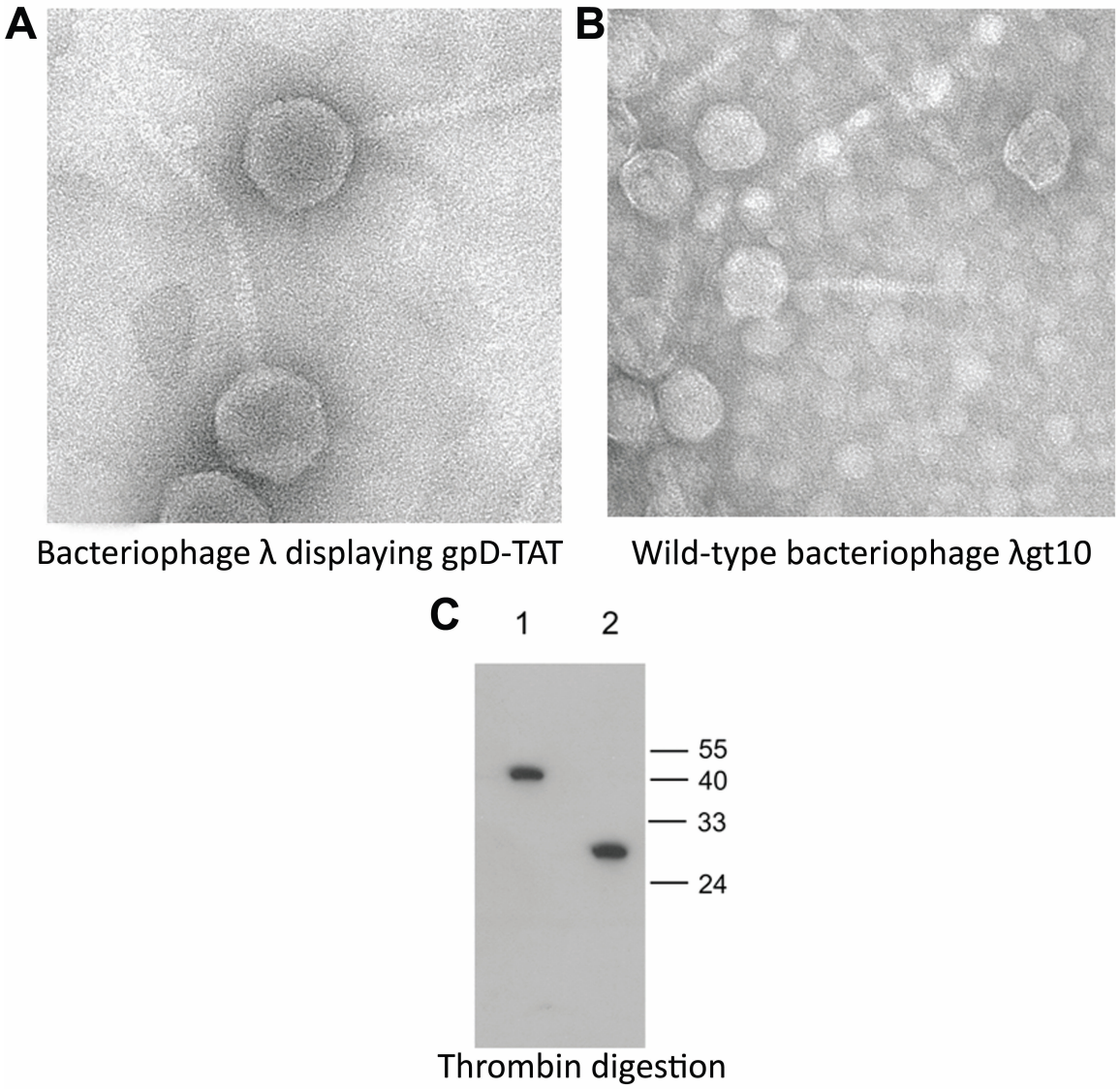

Figure 3.4 Phage Display Quality Control.
EM of bacteriophage λ preparations. A) λ-TAT has the stereotypical icosohedral head and coiled tail structure, as seen in the wild type λ preparation in B. Panel C is a western blot of a phage preparation probed with the JL8 GFP antibody. Displayed proteins are not sterically constrained. GFP displayed on gpD and containing a thrombin cleavage site is accessible for proteolysis. The western blot was probed with mAb to GFP (Clontech #632375). In lane 1 is λ-GFP uncleaved and lane 2 is λ-GFP cleaved with thrombin (Amersham). Lane 1 is full length gpD-linker-thrombin-GFP at 41kDa, whereas in lane 2 cleaved GFP is seen at 27kDa.

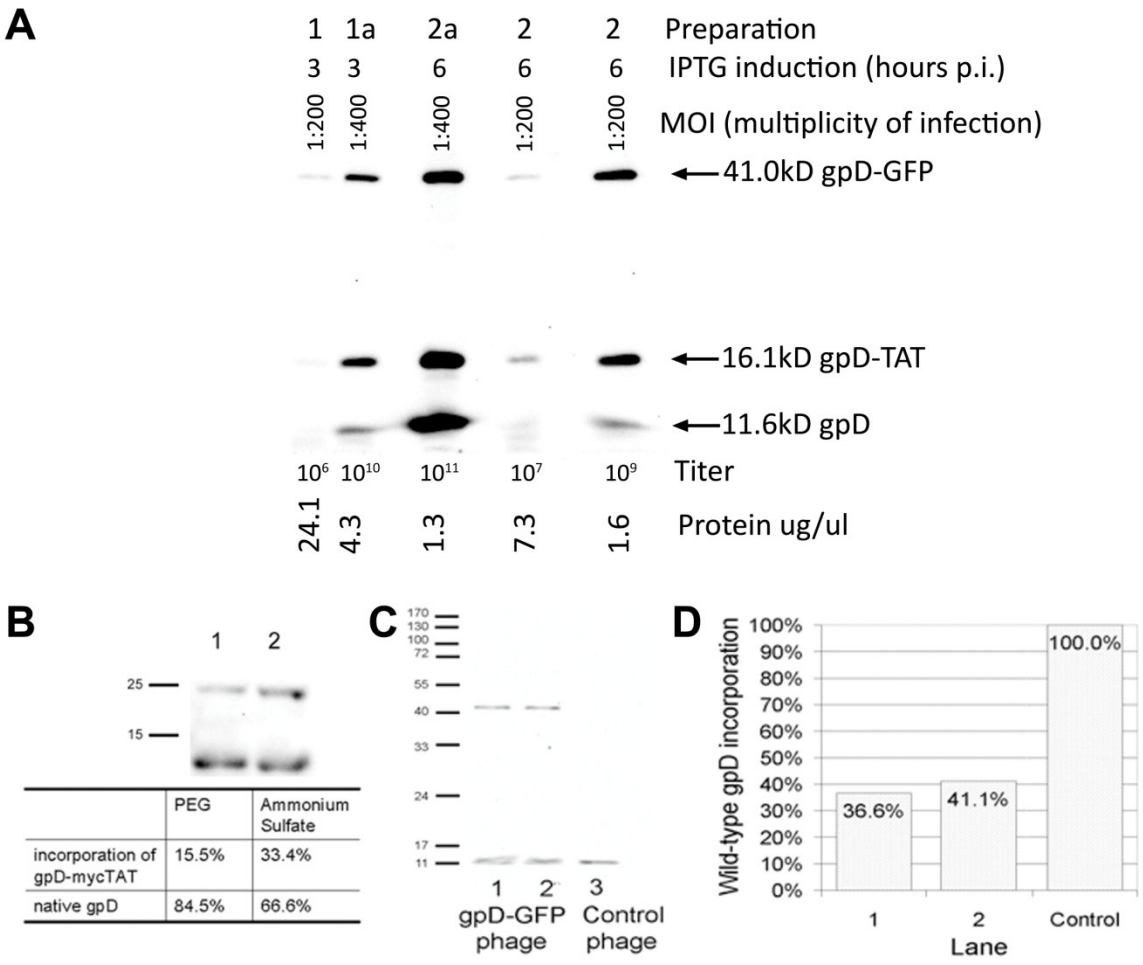

	PEG	Ammonium Sulfate
incorporation of gpD-mycTAT	15.5%	33.4%
native gpD	84.5%	66.6%

Figure 3.5: Optimization of λ preparation.
Bacteriophage λ preparation was optimized for the production of 3D display. A) Various multiplicities of infections were tested along with times for IPTG induction, each lane contained 10ug of protein. B) Two different precipitation methods were tested for λ phage purification. Ammonium sulfate gave the highest incorporation of gpD-mycTAT fusion protein. Panel C and D were the analysis of gpD display using a 1:400 MOI and 50% ammonium sulfate to precipitate. Lanes 1 and 2 are two separate *trans* expression preparations. In C we see the western blot and D is the gpD densitometry analysis.

Following phage culture with *E.coli*, lysis of bacteria was performed to release phage from cells, and bacterial debris was removed by centrifugation. Phage are then precipitated from solution. Precipitation can be done with 10% w/v polyethylene glycol 8000 (PEG). In this method PEG precipitates bacteriophage during an overnight incubation on ice. Centrifugation of precipitated phage allows for collection and a chloroform extraction removes contaminating PEG. This method was adapted from classic DNA preparation methods for λ, and had not been adequately tested for use in phage display. The concern was chloroform could strip gpD-fusions from virions. In order to address this issue an investigation comparing different concentrations of PEG, and ammonium sulfate was performed. Ammonium sulfate is a common precipitation chemical that produces salting-out of solubilised molecules, and is a commonly used in antibody purification. For PEG, 10% w/v produced the best yield of λ, whereas for ammonium sulfate 50% w/v resulted in the best yield of λ. PEG precipitation was superior for the quantity of phage collected, yielding 1 order of magnitude greater phage, or 10^{12} PFU/mL instead of 10^{11}PFU/mL. PEG was superior for the amount of phage isolated but was the percentage of gpD molecules displaying TAT or GFP affected. The purification protocol was followed as described (2.5.5), and densitometry was done. Although ammonium sulfate resulted in a lower yield of λ, a greater than two fold increase was observed for the amount of gpD-TAT displayed (Fig. 3.5B).

The next experiment was to find the optimal MOI and timing of IPTG induction for the best *trans* expression of gpD-fusions from plasmids. A large number of bacteria are necessary to support λ multiplication. For gpD-GFP incorporation the gene is induced with IPTG, but once induced bacterial reproduction is inhibited for protein production. With these two opposing forces constraining the bacterial culture conditions, a panel of preparations were performed to investigate varying the timing of IPTG induction and the MOI. A lower MOI, one λ in 400 cells, gave the highest titer of phage, 10^{10}-10^{11}PFU/mL, independent of the time of IPTG induction (Fig. 3.5A). This MOI also resulted in higher purity λ phage, where a 6 $\log_{10}$ difference is seen when comparing the least pure to highest purity preparation, lane 1 vs. 3 (Fig. 3.5A). Lane 1 had $4.1x10^5$ PFU/mg of protein as compared to $7.7x10^{11}$PFU/mg for lane 3. The difference between

lane purity for lanes 2 and 3 was not as great, and therefore 4hrs was then used for convenience. With an MOI of 1:400 and IPTG induction at 4hrs, λ preparations consistently had 10^{10} to 10^{11}PFU/mL purified phage with gpD-GFP supplied in *trans*.

Consistent yields of phage were achieved in preparations but it remained to be seen if the percentage display of gpD-GFP would also be consistent. In a separate experiment 3 cutlures were started with the optimized protocol (2.5.5), and λ was purified. Densitometry was done on samples of each where 36.6% and 41.1% of gpD were gpD-GFP supplied in *trans* (Fig. 3.5 C,D). This was consistent with most preparations were the amount of gpD-GFP was almost equivalent to the amount of *wt* gpD or had a similar percentage display as gpD-TAT (Fig 3.5, 3.2). A λ phage display system was thus built, Mashkiki, and we had an optimized method of production.

3.3.4 GFP reporter gene experiment

The original purpose of this project was to use λ as a viral means to increase the rate of gene targeting (3.2.2). The construct was now built with the TAT PTD and the hypothesis could be tested. To start the reporter gene in Hek293T cells was checked (Fig. 3.6). Hek293T cells are particularly efficient for transfection with calcium phosphate (2.8.3). We looked at the reporter gene activity in plasmid, λ DNA, and intact λ particles. Previous work had shown that as the size of the DNA construct increases the efficiency of transformation decreases.[331] The transformation efficiency for the TK gene in Hek cells was $1.2x10^{-6}$ to $1x10^{-5}$. In our system we saw 99.99% of cells transfected with pEGFP-N1 being GFP positive, and 98.13% of cells are GFP positive with pEGFP-F. The N1 plasmid proved to be 5.5X more fluorescent than the F plasmid which was cloned into pGEX-DLTgfp and λgfp10. When λgfp10 DNA is investigated we see 4.36% of cells are GFP positive, but intact phage that are calcium phosphate transfected only result in 0.14% or 0.23%, depending on the concentration of phage given. Intact phage gave equivalent transformation efficiency as the non treated cells, or background, but had an even lower mean fluorescence than background. This result was expected given Ishiura's work from 1982. [331] This experiment proved the reporter gene cloned into λgfp10 was active in mammalian cells, therefore if TAT worked as the literature described, GFP expression should result.

A

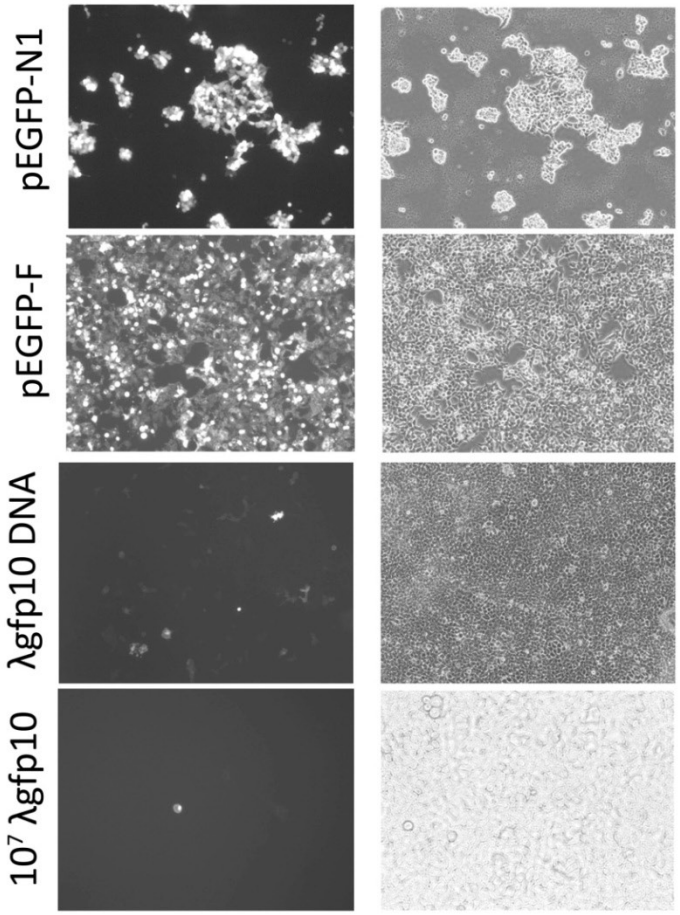

B

Treatment	Events Gated	%Gated	Mean Fluorescence
1. no treatment	24	0.18%	244.69
2. 1.6µg pEGFP-N1	12 456	99.99%	4941.34
3. 1.6µg pEGFP-F	13 907	98.13%	902.08
4. 1.6µg λgfp10 DNA	683	4.36%	99.86
5. 10^6 λgfp10	19	0.14%	11.92
6. 10^7 λgfp10	31	0.23%	43.55

Figure 3.6: Reporter Gene Experiment.
Testing the fluorescent reporter gene construct in Hek293T cells. A) Fluorescent microscopy and accompanying phase contrast microscopy, of 4 treatment groups. B) FACS analysis of 20 000 cells/treatment. The numbers of GFP positive cells are shown here as: events gated. Also depicted are the percentage of the total cells that are GFP positive and the mean fluorescence of the positive cells.

3.3.5 λ TAT transduction into ESCs

If the literature was correct, then λ displaying TAT will deliver its genetic cargo into the nucleus and reporter genes will be expressed.[269,270] In previous experiments an MOI of 10^3 to 10^6 λ for each cell was used.[269,270] In my experiment $2.4x10^5$ ESCs were added to each well of a 6 well plate. After 40hrs, various concentrations of λgfp10-TAT were added from 10^3 to 10^{11} λ per well. If we assume a doubling of ESCs every 24hrs we have an MOI from 10^3 to 10^5 λ per cell. There is no detectable GFP expression in cells transduced with λgfp10-TAT 47hrs post infection when investigate GFP fluorescence in ESCs using microscopy or FACS (Fig. 3.7). This is especially apparent when we look at the mean fluorescence of gated cells in λgfp10-TAT treatments as compared to the background level of GFP fluorescence (Fig. 3.7B). Parameters were tested including: different media types, these included media containing or without serum, different starting concentrations of cells, various times post infection, different plastic ware, but the result was always the same, no GFP was detected in ESCs transduced with λgfp10-TAT. This was not a cell line specific result, as E14, R1, D3, and Bruce4 ES cells were tested along with Cos7 and Hek293T cells. Mashkiki λgfp10-TAT will not transduce mammalian cells and produce GFP.

3.3.6 TAT transduction

No TAT transduction of Mashkiki phage was detectible as determined by the expression of a reporter gene. To investigate if this was a consequence of Mashkiki λ or of TAT a study with TAT and streptavidin was undertaken, in a similar manner as performed by Mai *et al*.[359] The experiment was performed as described by Mai *et al*, except in the data documented in figure 3.8, 200nM of TAT was added to Hek293T cells instead of 20nM as in the original paper. The result was surprising given all previous λ transduction experiments. Control cells had 1.39% of cells positive for GFP whereas SA488 with TAT was internalized at 90.18 and 90.64% in two different cell populations (Fig 3.8 A,B). When fluorescent microscopy was performed the amount of fluorescence in a given cell was very high, denoted by the white colour, as compared to control cells,

A

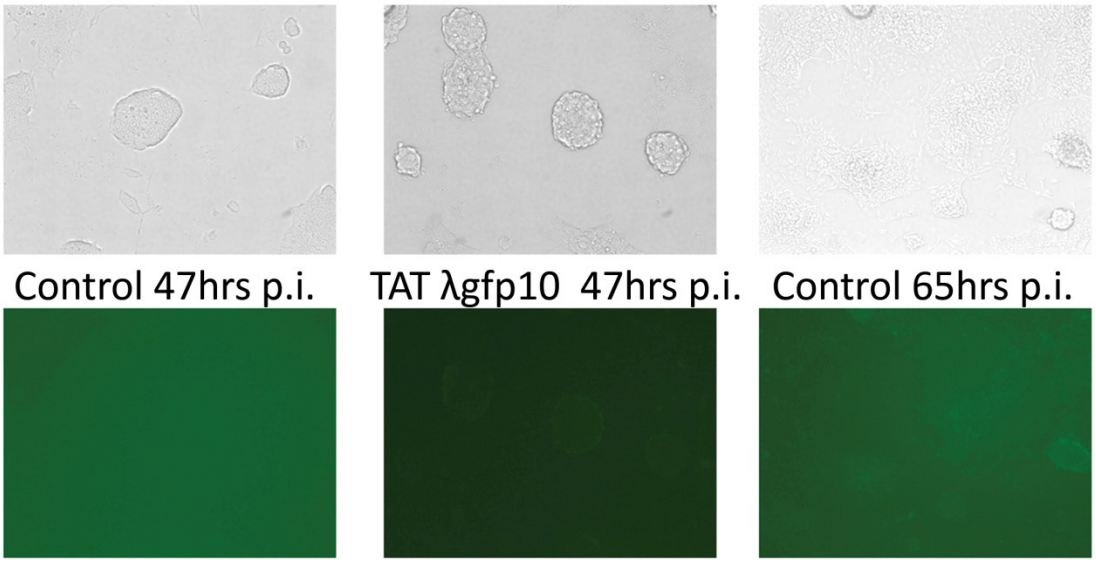

B

Sample	% Gated	Mean Fluorescence
Control (no phage)	1.1	34.67
$1.5x10^{11}$ λGFP10-gpDTAT	2.78	35.35
$3x10^{9}$ λGFP10-gpDTAT	2.87	34.95
$3x10^{6}$ λGFP10-gpDTAT	1.45	35.83
$3x10^{3}$ λGFP10-gpDTAT	2.57	37.18

Figure 3.7: Phage ESC Transduction.

Transduction of λgfp10-TAT into E14 embryonic stem cells. A) DIC and accompanying fluorescent microscopy of ESC at 47hrs., and 65hrs. post infection (p.i.) with λgfp10-TAT. B) FACs analysis of various amounts of λgfp10-TAT at 47hrs. p.i., 30 000 events were counted for each treatment.

which appear close to background (Fig. 3.8B). Obviously the TAT PTD was a potent transduction inducing molecule.

3.4 Discussion

This thesis would not be what it was without recombineering. Traditional molecular cloning was not versatile enough to accomplish the genetic engineering done herein. With recombineering λ DNA could be modified directly without the need for a plasmid integration step (sections 3.2.2, and 3.2.6). The incorporation of the plasmid into λ DNA disrupted the polycistronic late structural genes of λ and was the most likely reason the RecBCD *E.coli* based systems did not result in viable mutants. Instead, using recombineering and taking advantage of the lagging strand invasion of λ Red's *exo,* and *beta* genes, λ was engineered without co-integrants.

Although λ could have been engineered with small oligos, the pDE plasmid was used as an intermediary for oligo cloning and subsequent cutting; in this way longer regions of homology could be added to oligos and more efficient recombineering could occur. The minimum recombineering oligo length is 35bp,[225,357,358] but by first cloning synthetic oligos into pDE, the oligo sequence could be verified in clones before recombineering. This was beneficial as the mutant screening method was not a genetic based selection scheme, instead a more time consuming plaque hybridization screen was performed.

When λ morphology was investigated by electron microscopy, it was apparent that *wt* λ was overstained in Figure 3.4 B. This result could have been improved but as other studies have documented *wt* λ in electron micrographs, comparisons could be made between the data collected and previous reports. Furthermore, the display of GFP did not negatively affect the titer following preparation and after extended storage, indicating that once λ displaying gpD-GFP was assembled they are stable. For these reasons EM imaging was not redone as electron microscopy is an expensive procedure.

TAT and GFP can be displayed on the surface of λ (Fig. 3.2, 3.5, 3.4). It was debatable if TAT was displayed in a conformation that was accessible to solvent. GFP was proven to be accessible to proteolytic cleavage, but GFP is a large beta-barrel structure that has proven to be resilient to many different fusions. Less evidence is

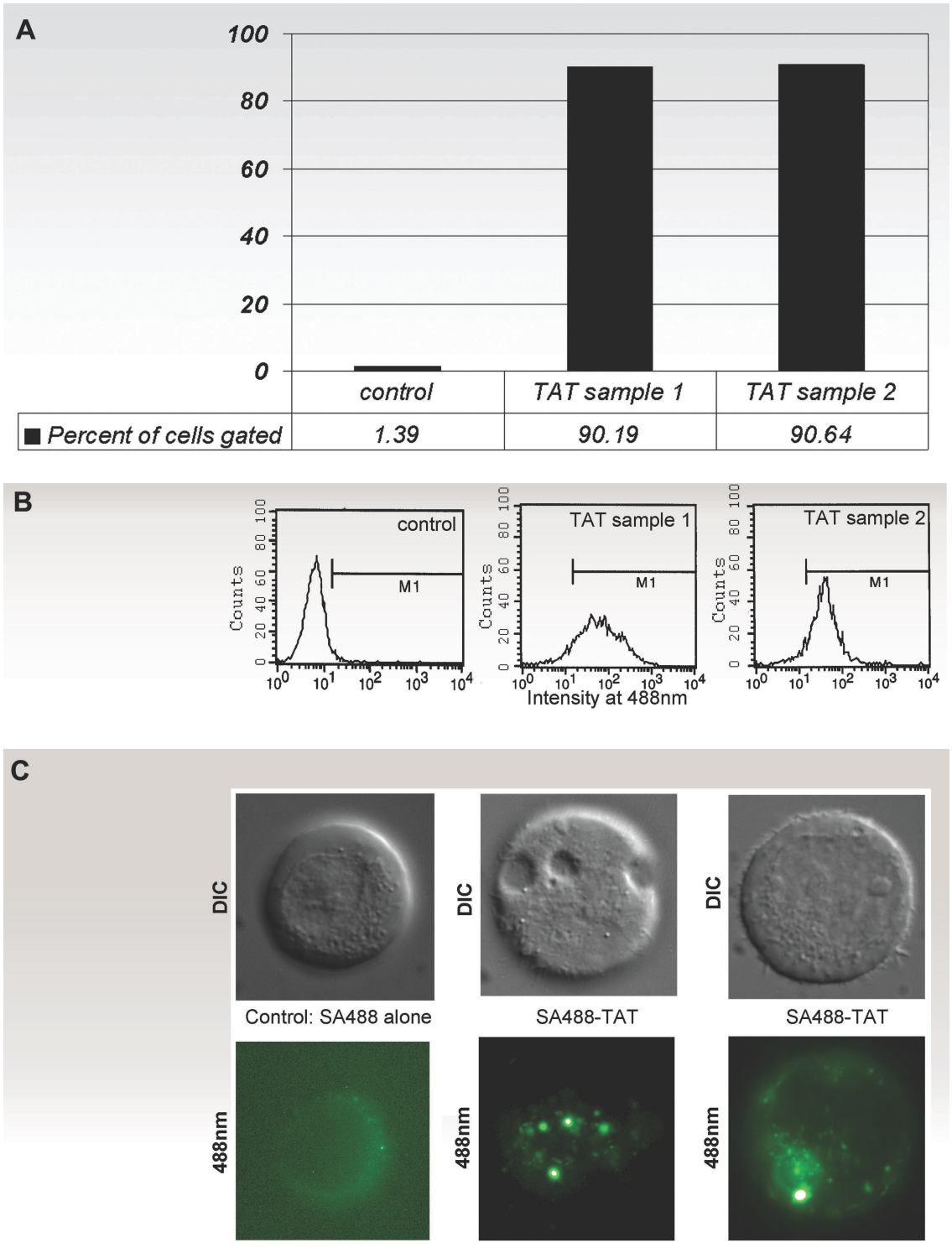

Figure 3.8: TAT Transduction into Hek293T cells.

Figure 3.8: TAT Transduction into Hek293T cells.
For each experimental group cells were treated with 200nM Streptavidin coupled with Alexafluor488, SA488 (Molecular Probes). TAT samples were SA488 incubated with biotin-TAT peptides. A) The percentage of cells above the fluorescent intensity cut off, M1. Three samples were analyzed, one control or SA488, and two samples of SA488-TAT (TAT samples 1 and 2). B) Histograms of fluorescent intensity in cell populations. Cell counts are depicted on the Y axis and the intensity of fluorescence at 488nm is on the X axis, in log scale. C) Microscopy of cells. The top three images are done in DIC, the bottom three images are the accompanying fluorescent images of the same cells. In panel C, the SA488 alone fluorescent image was one of the few that could be imaged. Notice the cellular fluorescence is similar to that of the background in the image. The fluorescence in the SA488-TAT cells shown is 20X greater than background fluorescence, as calculated with Image J.

available on TAT, and its display on the C terminus of gpD may not be optimal. This could account for the negative GFP expression for λgfp10-TAT transduction experiments (Fig. 3.7)

This work has documented that the display of proteins on λ decreases the yield of λ from similar cultures with *wt* λ. An optimized method of λ preparation was developed that increased yield of λ and provided consistent display of gpD fusion proteins. Therefore the phage structure is affected by the display of fusion proteins, but they are still viable and have a similar half-life once formed, as determined by the titration of λ stocks. As such it would seem that Gibbs free energy is increased with the addition of displayed peptides, which accounts for the lower yield, but the lowest energy state remains the assembled viral capsid.

Noteworthy for this chapter, is the ability to add multiple moieties to a single λ capsid. This will be beneficial for future studies where many different epitopes or proteins are required for a vector. This could prove helpful for manipulating the immune response to λ. One could envision λ being used in molecular therapy where multiple functions, or proteins, could be displayed on λ particles that would restrict its cell tropism and cause immune reactions to displayed epitopes.

3.4.1 TAT transduction

With λ displaying TAT and a GFP reporter gene cassette present, the utility of TAT transduction in ES cells was investigated. Piersanti reported robust GFP expression in Cos7, HuH7, and fibroblasts using an integrin binding protein as a PTD, and an MOI of 10^4 λ per cell. Eguchi used luciferase and GFP reporters and documented robust reporter gene activity in Cos1, NIH 3T3, HeLa, A431, Hek293T, and VA13/2RA cells when incubated with 10^3-10^6 λ-TAT per cell. This report also investigated endosomotropic agents, cationic lipids, and the use of nuclear localization signals. Interestingly Eguchi notes that integrin binding proteins do not work. Yet Piersanti provides evidence they do. These are the only 2 conclusive instances of robust reporter gene activity from λ transduction using a PTD.

The experiments documented by Piersanti and Eguchi make no mention of cells being fixed, by means of DMSO, paraformaldehyde, or EtOH, but cells were viable as

they grew, and expressed reporter genes. One criticism in the TAT transduction field that has come to the fore since the cell fixing artifact was reported, is the use of freshly trypsinized cells.[351] In both Piersanti's or Eguchi's studies cells are seeded 12 to 48hrs before applying λ to the culture, this is identical to the methods used herein, and yet no reporter gene expression is documented in chapter 3.

The next line of experiments was to investigate if the method of λ preparation was affecting the transduction of λgfp10-TAT. Whether λ was prepared with either PEG precipitation or ammonium sulfate, the result from the reporter gene assay remained negative. In a similar line of reasoning, were the λ preparations used herein or those of Piersanti or Eguchi's preparations contaminated with a molecule deleterious to transduction. One could imagine excessive λ DNA being present, or endotoxin. If λ DNA was present then expression from reporter genes would increase, but this would not be a drastic increase, as it would be similar to the λ DNA treatment in figure 3. Indeed in experiments outlined in the introduction, no difference in transduction was seen if λ is first DNAse1 treated. Alternatively, what effect would a contaminant, such as endotoxin have on transduction? Since this work was done, we have now documented LPS in our λ preparations, and presumably it would also be present in Eguchi or Piersanti's. To take this reasoning one step further, as Geier's work in the 1970s showed, could Eguchi and Piersanti's cells be contaminated? They make no mention of whether they tested their cells or not. If mycoplasma is present, endosomes will be leaky and this could account for the increased expression.

This chapter leaves only two scenarios for the negative transduction result: 1) our linker sequence is not displaying TAT properly, or 2) published experiments are reporting an artifact inherent to their experimental systems. Without re-recombineering the phage and trying the experiment again or using a different reporter cassette, it was decided that a new line of research would be pursued. During the work in this chapter, trial experiments were done to test Mashkiki phage as a subunit vaccine system and the data was very promising.

Another avenue of research that could have been followed would be to permeabilize the cells or endosomes. Cells could have been permeabilized by the

addition of DMSO, EtOH, or Hydroxycamptothecin,[360] or phage could have been coated with PEI, or other cationic lipids or peptides. As my interest was to eventually use phage as a gene therapy vector and not just as an *ex-vivo* cell therapy treatment, this was not attempted. This line of reasoning should have been pursued, as the main objective was to test the effect of longer homology regions on gene targeting, not to test conditions applicable for *in vivo* gene therapy. Although, it is unknown how ES cells would react to permeabilizing conditions.

Since these studies were undertaken, less literature is being published in the PTD field, and the TAT work has been challenged by a damning experiment. TAT is a protein of HIV which is believed to be able to infect adjacent cells. The trans-cellular activity should be present in cells that express a TAT PTD, yet no studies have documented this.[351] Indeed some are now saying that the TAT PTD is a nuclear localization signal with mild PTD ability. The PTD ability described in this body of work and in the literature was most likely due to it binding HSPG on the cell surface. The work presented in this chapter would corroborate this conclusion. When a reporter gene is packaged in λ, no gene expression is seen (Fig. 3.7), but TAT coated streptavidin readily enters cells (Fig. 3.8).

Chapter Four: **Vaccination with Bacteriophage λ**

4.1 Rationale

The previous chapters work was presented to highlight the construction of Mashkiki bacteriophage, and the biological activity of λ that display the protein transduction domain of TAT. As the Mashkiki λ display system was built, it was postulated that λ could be an effective subunit vaccine platform. Phage had been previously shown to be immunogenic, but no peptide based subunit vaccination had been attempted with λ. The rapid development of vaccines for emerging diseases using a genetic approach would be an asset, as would the ability to biopan bacteriophage λ epitope libraries. Having experience with recombineering and phage biology, it was a natural extension. The end result could be quick, cheap, and thermostable vaccines.[29,35,147,205,209,211-213] Up to this time the study of bacteriophage vaccination had been limited to antibody production and survival models for protection. We endeavoured to undertake a comprehensive study of the immune response to λ subunit vaccination.

Hypothesis: Bacteriophage lambda can be used to create effective subunit vaccines for mimotope or peptide vaccination.

Objective: To investigate bacteriophage lambda as a vaccination vector, and characterize the immune response to bacteriophage lambda challenge

Our aim was to undertake the first peptide vaccination study using bacteriophage λ. In parallel we also chose to investigate bacteriophage λ as a DNA vaccination vector. We set out to provide the field with a comprehensive understanding of the cytokine milieu in the spleen following immune challenge, along with an analysis of the antibody isotypes generated in response to challenge with Mashkiki.

4.2 Summary

A phage display platform was built for bacteriophage λ, called Mashkiki phage (Chapter 3). It did not yield ES cell transduction, our original endpoint, but when administered to *Oryctolagus cuniculis* (rabbit) it did produce a humoral immune reaction.

Being the first to document peptide immunization using λ display, the experiments lead to an investigation of the immune reaction to λ, λ displayed proteins, and λ DNA vaccination. To characterize the immune reaction two separate immunization experiments were undertaken in CD1 mice and C3H mice. From these experiments the concentration of serum antibodies recognizing λ or GFP were measured, and IgG subclass titers were determined. The percentage of B and T cells in various lymphoid organs was determined in order to investigate the immunization route and λ responding cell populations. Concurrently, experiments were performed on the effect λ had on lymphoid organ cell proliferation after being stimulated *in vitro* with various ligands. From this work cytokine secretion was measured to determine Th polarization and to characterize the type of immune response. From these experiments it has been determined that the responding lymphoid organ is the spleen regardless of prior immunization. The cytokines responsible for the immune reaction to λ have been identified. Finally, preliminary data suggests TLR4 is one receptor responsible for the observed adjuvant activity in λ, but the data also suggests TLR4 mutant mice are not sufficient to eliminate the immune response to λ.

4.3 Results

Oryctolagus cuniculis (rabbit) was inoculated with *Bacteriohpage* λ displaying gpD-GFP. The sera of 2 rabbits were collected before and after immunization. Antibodies were isolated from serum as described in section 2.10.1.1. Antibodies were used as probes for western blots of purified λ, bacterial lysates, Cos7 and Hek293T lysates (Fig. 4.1). In panel A, lanes 1 and 2 are purified λ and the three proteins that are most reactive to serum antibodies are the approximate size of the major coat proteins of λ, gpE, gpV, and gpD. Many proteins are reacting to λgfp10-GFP in lane 1, or λGT10 in lane 2, but there is one protein in lane 1 that is not present in lane 2, highlighted by the arrow. This protein is larger than 40kDa, and is present in DY330 *E.coli* expressing gpD-GFP, lane 3, at the identical size.

To determine the identity of the protein identified in panel A lane 3, an identical western blot was performed (panel B) but was probed with the GFP antibody JL8 (Clontech). A protein that corresponds in size with one seen in panel A, is present in lanes 1 and 3 in panel B. Importantly, no protein is recognized in lane 2, λGT10. A second positive control was run in lane 4 which consisted of EGFP-F, not fused to gpD, and this was over-expressed in Hek293T cells. A protein that matches the calculated size for EGFP-F is present in lane 4. In panel C, serum antibodies from a non-immunized rabbit were used to probe a similar western blot as in panel A and B. No proteins from λ, lanes 1 and 2, or from EGFP-N1, lane 3, were detected. The non-immunized animal serum used in panel C, was from one of the two rabbits that were subsequently immunized and raised an immune response for panel A.

Next an immunization experiment was performed where mice were inoculated with λgfp10-GFP in the presence and absence of the adjuvant Ribi. Western blots similar to figure 4.1 were performed and serum was found to contain IgG antibodies that recognized λ (data not shown). The intensity of recognition appeared similar in both the adjuvant and non-adjuvant serum (data not shown).

With data on antibody production in rabbits and mice, experiments were done to describe the type of immune response including the amplitude. For these experiments two mouse immunization trials were performed, one on the outbred CD1 strain (Charles

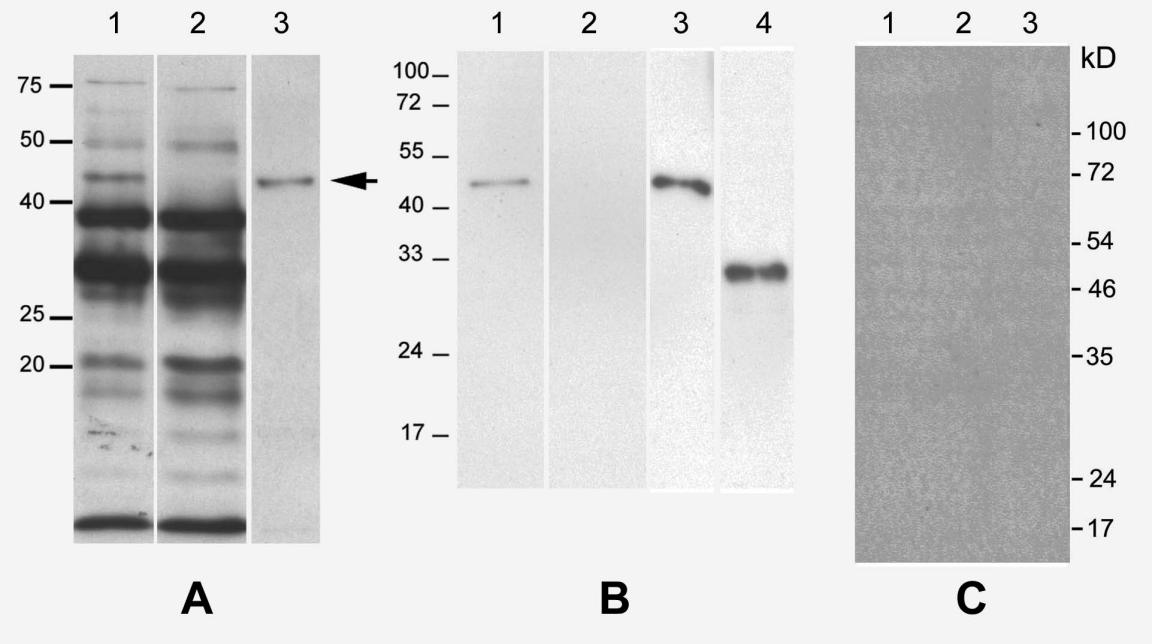

Figure 4.1: Rabbit Immunization.

GFP was displayed on λgfp10 and rabbits were inoculated. Three western blots were probed with A) purified immune serum post immunization, B) mouse mAb JL8 for EGFP, and C) pre-immune serum. A) Purified immune serum from both rabbits post immunizations was used to probe. Lane 1 is λgfp10-GFP and a protein band corresponding to the predicted 41kDa size of gpD-GFP (arrow) is seen. Lane 2 is wt λ where no protein is detected at 41kDa. Lane 3 is a positive control for gpD-GFP: bacterial lysates from DY330 expressing the fusion protein gpD-GFP (41kDa). Note the only protein detected corresponds to the same size as a protein in Lane 1. B) JL8 mAb for GFP was used as a probe. Lane 1 is λgfp10-GFP, and a protein with the size corresponding to gpD-GFP is present (41kDa). Lane 2 is wtλ, and no protein is detected. Lane 3 is cell lysate from DY330 cells expressing gpD-GFP (41kDa). Lane 4 is a positive control where lysates from Hek293T cells expressing EGFP-F (29.5kDa) were added. C) Pre-immune serum from one of rabbit was used to probe. Lane 1 is λgfp10-GFP, lane 2 is wt λ, and lane 3 is Cos 7 cells over-expressing EGFP-N1 (Clontech).

River) and another on the inbred C3H strain (JAX). The C3H stain investigated was C3H/HeJ, which is $H2^k$ and contains a point mutation of proline 712 to a histidine in the *tlr4* locus. For each immunization the serum antibody and isotype titers were measured, and *in vitro* cell proliferation assays were performed. A variety of immune stimulants were assayed for proliferative potential and the secretion of cytokines from lymphocytes.

When splenocytes were stimulated with a variety of ligands (Fig. 4.2) across immunization groups, λ caused the greatest cell proliferation. Whether the stimulant was *wt* λ (yellow column), GFP λ (green column), or TAT/gfp λ (red column), the response was heightened for any stimulant group that contained λ. This trend was observed even when CD1 mice were not immunized with λ. When cells were stimulated with rGFP, rTAT, or BSA alone, the response was similar in amplitude as the cell control (striped column) for the vaccination group.

CD1 splenocytes were sensitive to λ treatment, but it was unclear whether the response was strain specific. When C3H splenocytes were investigated, they were found to be sensitive to λ regardless of their immunization, in a similar manner to CD1 mice (Fig. 4.2, 4.3). In figure 4.3 the data was arranged to compare the stimulant used across the immunization groups, the opposite representation to figure 4.2. With the data in this orientation it was apparent that the stimulation of splenocytes with λgfp10-GFP-TAT had the greatest effect on proliferation. The overall trend was similar between C3H and CD1 mice but the amplitude was less in C than A. The greatest responders in C were C3H/HeJ mice immunized with λgfp10-GFP-TAT together with complete Freund's adjuvant (CFA), which were stimulated with λgfp10-GFP-TAT resulting in 1294 ± 761.8 CPM. Whereas in CD1 mice, panel A, the equivalent stimulation on the equivalent immunization group resulted in a maximal amplitude of 6928± 1536 CPM. The amplitude of proliferation was diminished in C3H mice, both for LPS hypo-responsive C3H/HeJ, and the non-TLR4 mutant C3H/HeOuJ. In lieu of making a direct comparison of these effects, the fold change was calculated by using the samples of the control cells from each immunization for normalization. When the data was normalized, λ was the only ligand that produced a fold change above 1.5 (Fig. 4.3 C, D). Interestingly, the

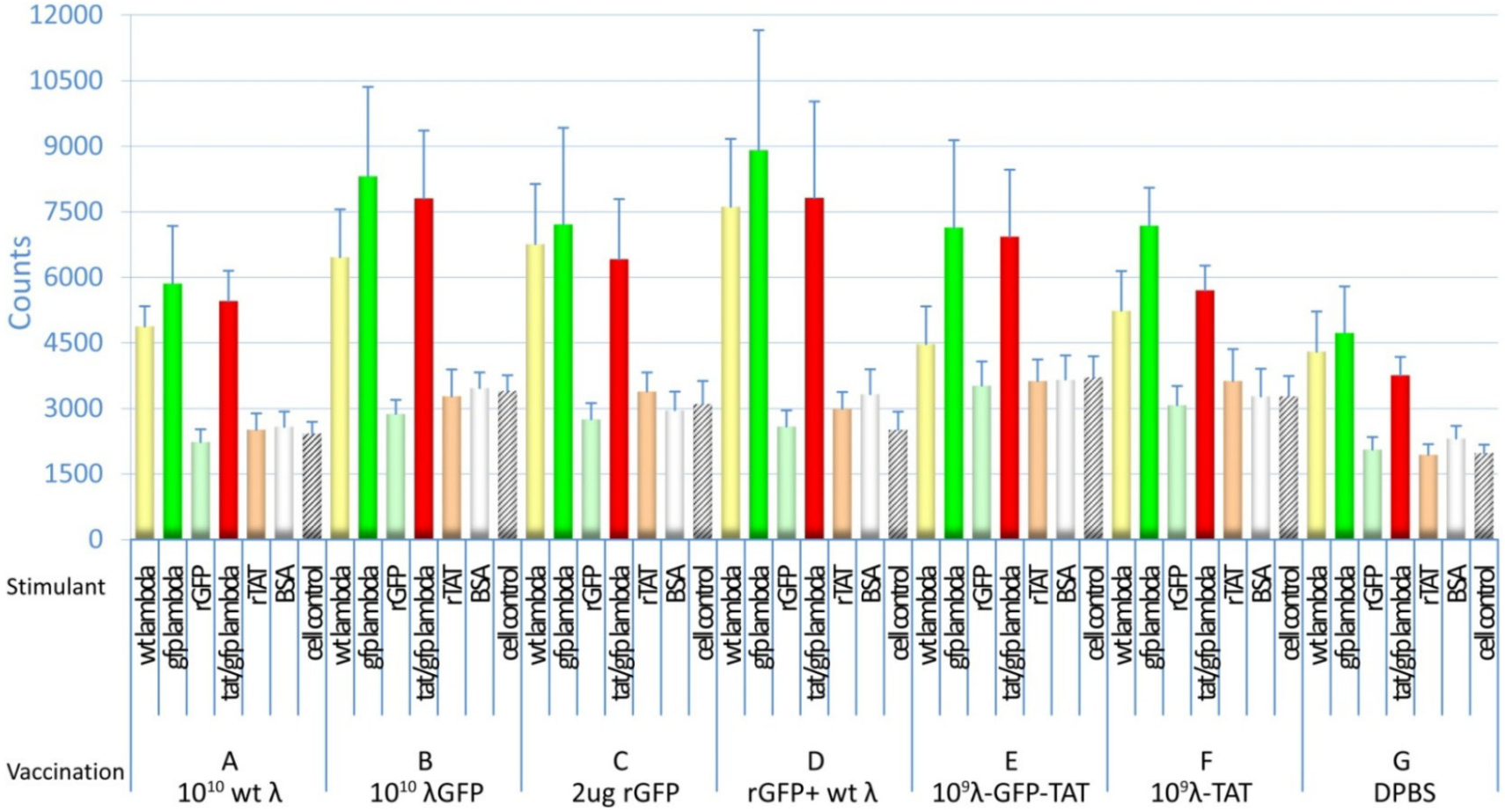

Figure 4.2: CD1 Splenocyte Proliferation.

Figure 4.2: CD1 Splenocyte Proliferation.

Splenocyte proliferation is shown in response to in vitro stimulation across the following immunization groups: A) 10^{10} PFU wtλ, B) 10^{10} PFU λgfp10 displaying GFP, C) 2ug rGFP, D) 2ug rGFP co injected with 10^{10} PFU wtλ, E) 10^{9} λgfp10 displaying TAT and GFP, F) 10^{9} PFU λgfp10 displaying TAT, and G) DPBS. For each immunization, splenocytes were stimulated in vitro with the following: 10^{10} PFU wtλ (wt lambda), 10^{10} PFU λgfp10-GFP (gfp Lambda), 2ug rGFP (rGFP), 10^{9} λgfp10-TAT-GFP (tat/gfp Lambda), 2ug rTAT PTD (rTAT), 2ug BSA (BSA), or a non-treatment control (cell control). N=5 for each column except rTAT where n=3, and all measurements were performed in triplicate and the standard error of the mean was shown for each average.

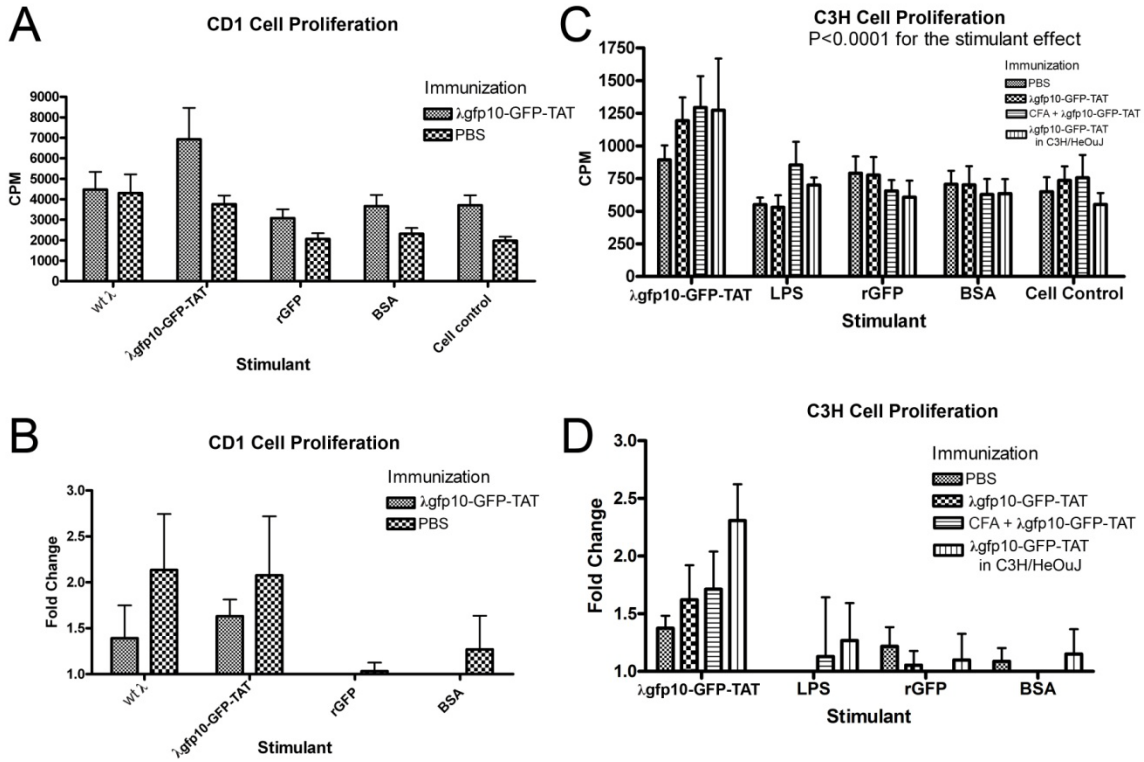

Figure 4.3: Comparison of CD1 and C3H Splenocyte Proliferation.
In vitro stimulation of splenocytes from immunized mice. A and B show results for splenocytes from CD1 mice following immunization. A is an abridged grouping from figure 4.2. In B the fold change in proliferation for each stimulation was calculated by normalizing each treatment to the cell control treatment group. In A and B n=5 for each stimulant group. C and D show results for splenocytes from C3H mice following immunization, whereby C3H/HeJ mice were investigated for the first three immunizations and C3H/HeOuJ mice were immunized in the last group. In D the fold change in proliferation for each stimulation was calculated by normalizing each treatment to the cell control treatment group. N=10 for each stimulation group except for C3H/HeOuJ mice where N=5. In panels A and C error was calculated as standard deviation, whereas in panels B and D the standard error of the mean was reported.

highest fold change in *wt* mice, CD1, was for non-immunized or naïve mice, whereas with C3H mice the opposite was observed. In fact the trend for fold change in C3H mice (Fig. 4.3 D) when splenocytes were stimulated with λgfp10-GFP-TAT, was similar to the average proliferation (Fig. 4.3 C), where PBS immunized mice were least reactive to λ, and the proliferation increased with each immunization group. The outliers of this trend are the C3H/HeOuJ mice which showed a hyper fold change.

To determine what type of cell was responding to λ, flow cytometry was performed. Lymph node Th, Tc, and B cell compartments were counted across immunizations (Fig. 4.4). No polarization was seen in the spleen, mesenteric lymph node (MLN) or the peripheral lymph nodes (PLN). MLN and PLN cell populations were similar, but spleen had more B cells and less Th and Tc cells.

The location of immune cells eliciting a memory or effector response was determined next. Spleen, MLN, and PLN cells were stimulated *in vitro* with various ligands after immunization (Fig. 4.5). With two-way ANOVA, no statistical significance was observed in PLN and MLN cells, although some treatments in the MLN compartment were significantly different when the stimulant effect was analyzed ($P = 0.0097$). Splenocytes did not respond in a statistically significant manner when immunizations are compared, however a statistically significant effect was noted when stimulants were compared across immunizations ($P<0.0001$). As it did not matter what immunization group was investigated, 2D phage (λgfp10-GFP-TAT) elicited a significant proliferative response in spleen.

The type of immune response in CD1 splenocytes was determined by cytokine production: IFNγ (Fig. 4.6), IL-2 (Fig. 4.7), and IL-4 (Fig. 4.8). For IFNγ, a Th1 cytokine, the highest responding group was TAT/GFP Lambda stimulated splenocytes from CD1 mice immunized with rGFP co-injected with *wt* λ (vaccination D), resulting in 2833 ± 636 pg/mL. The highest single response, averaged from a triplicate, was actually TAT phage stimulated splenocytes from the same group. Interestingly though, TAT phage was also the most potent ligand causing IFNγ release in mice immunized with λgfp10-GFP-TAT (vaccination E), and λgfp10-TAT (vaccination F). When rGFP was inoculated together with *wt* λ (vaccination D), all ligands had higher

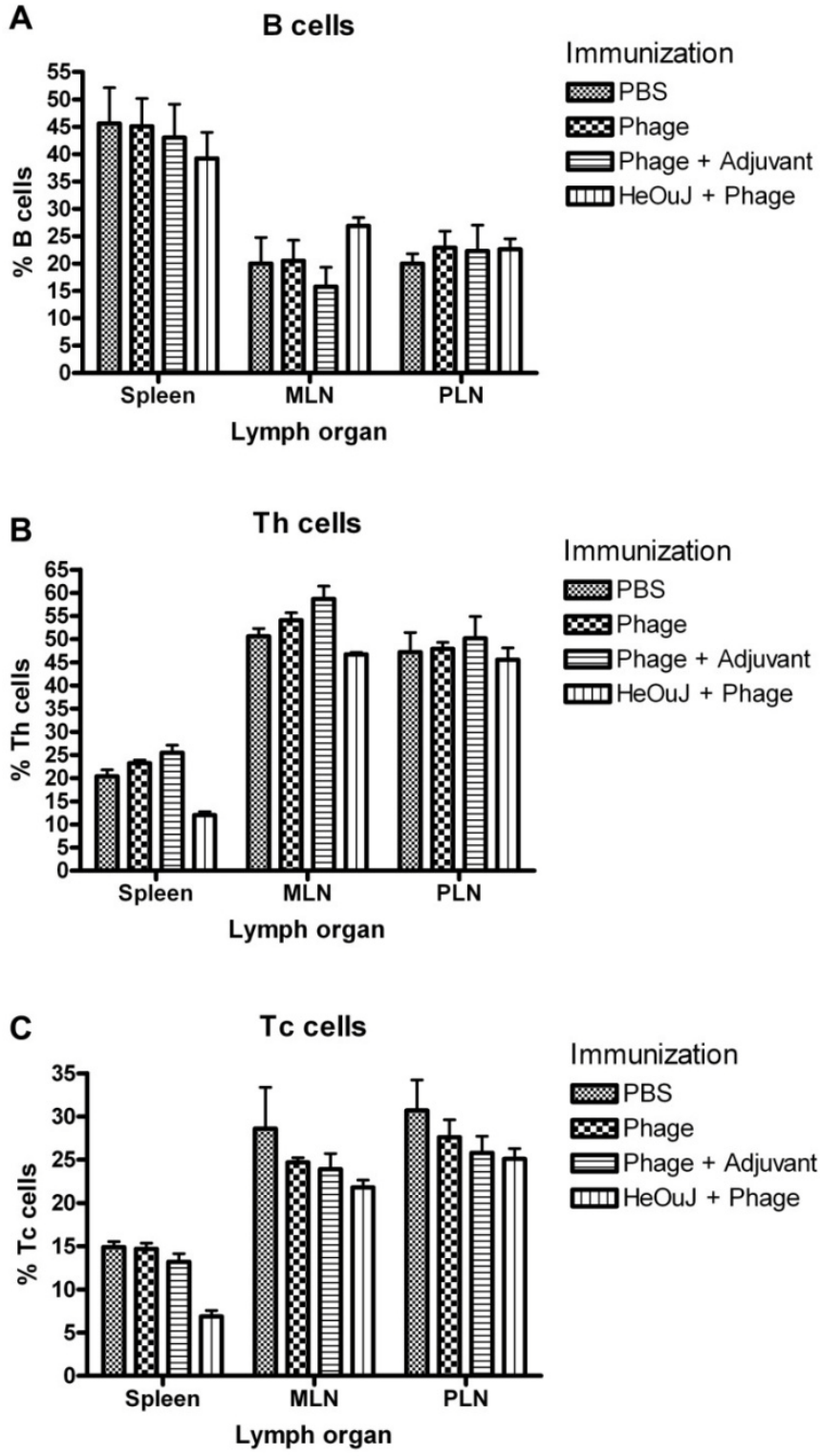

Figure 4.4: Cell Populations in C3H Lymph Organs.

Figure 4.4: Cell Populations in C3H Lymph Organs.

Flow cytometry was performed on isolated cells from the spleen, mesenteric lymph node (MLN), and peripheral lymph nodes (PLN). The immunizations were: PBS in C3H/HeJ mice, λgfp10-GFP-TAT (Phage) in C3H/HeJ mice, λgfp10-GFP-TAT with Freund's adjuvant (Phage + Adjuvant) in C3H/HeJ mice, and λgfp10-GFP-TAT in C3H/HeOuJ mice (HeOuJ + Phage). The number of positive cells was shown as a percentage of viable cells for each panel. The experiment was done in triplicate and the average from three separate animals, run on 3 separate days for each immunization group was shown. Error was reported as the standard error of the mean. A) B cells were counted with a B220-FITC antibody (eBioscience). B) T helper cells were counted with a CD4-PE antibody (BD Pharmingen). C) cytotoxic T cells were measured as $CD8^+$ cells using a CD8-Cy antibody (BD Pharmingen).

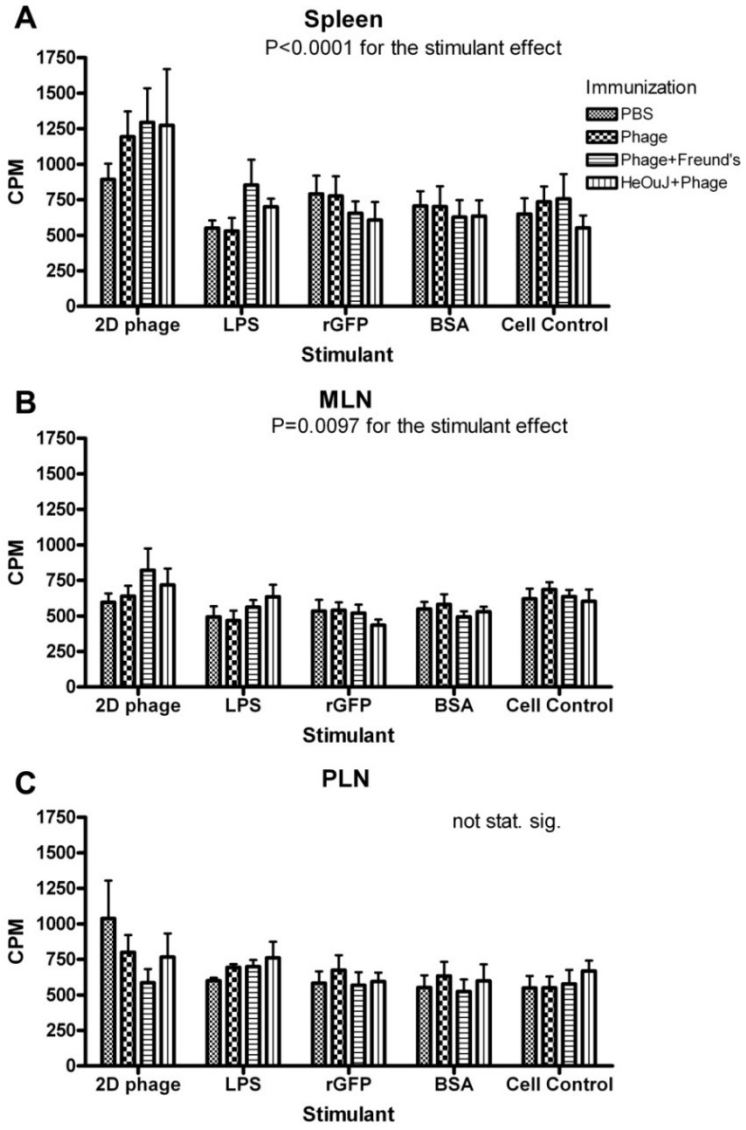

Figure 4.5: Cell Proliferation in Lymph nodes from C3H mice.

A) Splenocytes were isolated and then stimulated *in vitro* with 2D phage, LPS, rGFP BSA, or were not stimulated in the cell control group. Stimulations were done with λgfp10-GFP-TAT at 10^9PFU/mL (2D phage), LPS at 100ng/mL, rGFP (Millipore) at 0.2ug/well, or BSA (NEB) 0.2ug/well. B) Mesenteric lymph node (MLN) cells were isolated from the same animals and were treated with the same stimulants. C) Peripheral lymph nodes (PLN) were isolated and immune cells were treated as in A and B. The average of 10 animals for each immunization is shown except for the positive control C3H/HeOuJ mice, where the average of only 5 mice was used. In each panel, a two-way ANOVA analysis was performed to test for statistical significance (GraphPad Prism).

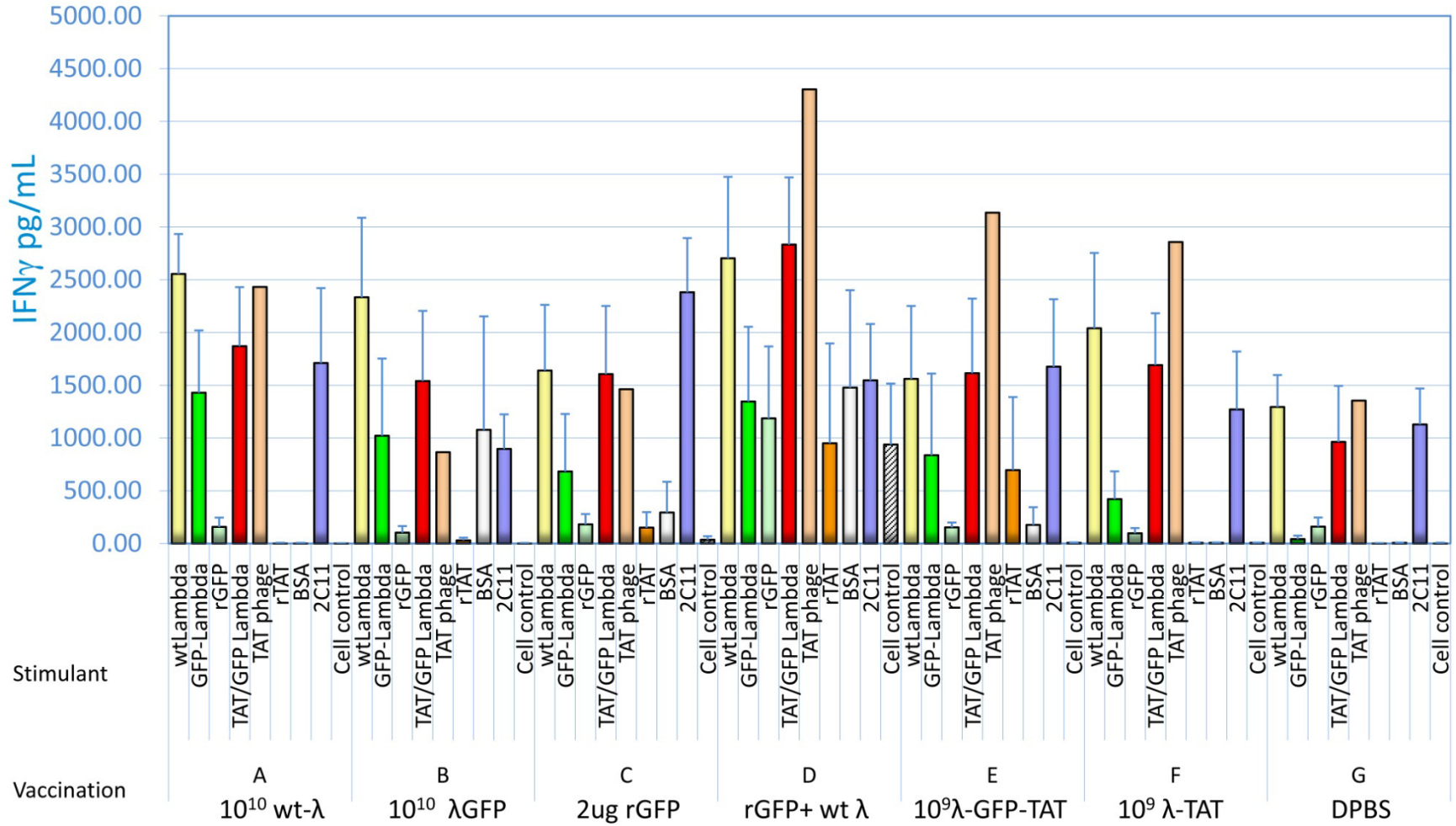

Figure 4.6: Interferon Gamma production in CD1 Splenocyte Proliferation.

Figure 4.6: Interferon Gamma production in CD1 Splenocyte Proliferation.

IFNγ was measured from supernatants from *in vitro* stimulation of splenocytes using a sandwich ELISA (R&D systems) across the following immunization groups: A) 10^{10} PFU wtλ, B) 10^{10} PFU λgfp10 displaying GFP, C) 2μg rGFP, D) 2μg rGFP co-injected with 10^{10} PFU wtλ, E) 10^{9} λgfp10 displaying TAT and GFP, F) 10^{9} PFU λgfp10 displaying TAT, or G) DPBS. For each immunization, splenocytes were stimulated *in vitro* with the following: 10^{10} PFU wtλ (wt lambda), 10^{10} PFU λgfp10-GFP (gfp Lambda), 2μg rGFP (rGFP), 10^{9} λgfp10-TAT-GFP (tat/gfp Lambda), 2μg rTAT PTD (rTAT), 2μg BSA (BSA), or a non-treatment control (cell control). N=5 for each column except TAT phage where N=1 and rTAT where N=3. All measurements were performed in triplicate.

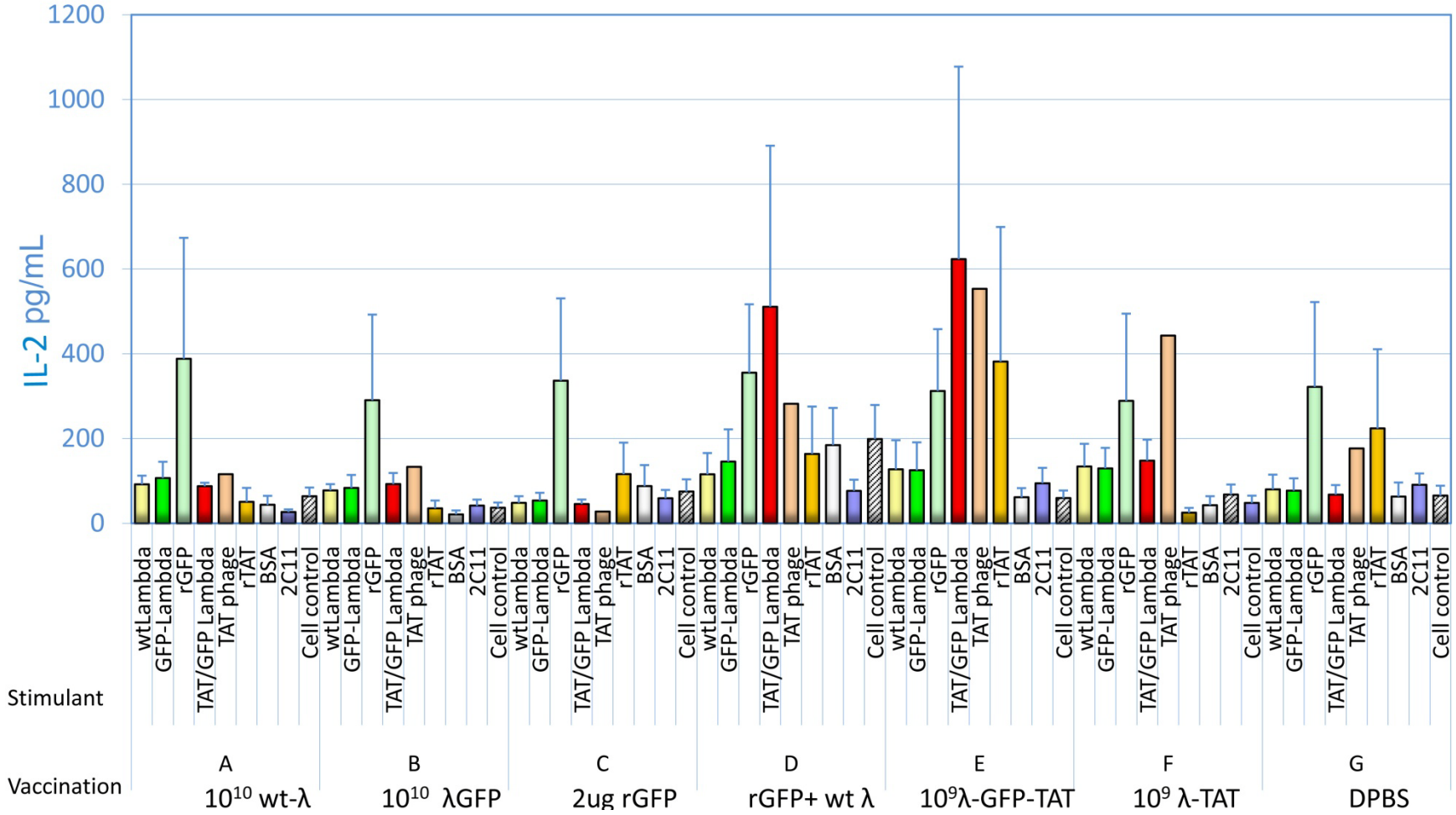

Figure 4.7: IL-2 production in CD1 Splenocyte Proliferation.

Figure 4.7: IL-2 production in CD1 Splenocyte Proliferation.

Supernatant from the *in vitro* stimulation of splenocytes were measured for IL2 produced using a sandwich ELISA (R&D systems) across the following immunization groups: A) 10^{10} PFU wtλ, B) 10^{10} PFU λgfp10 displaying GFP, C) 2µg rGFP, D) 2µg rGFP co-injected with 10^{10} PFU wtλ, E) 10^{9} λgfp10 displaying TAT and GFP, F) 10^{9} PFU λgfp10 displaying TAT, or G) DPBS. For each immunization, splenocytes were stimulated *in vitro* with the following: 10^{10} PFU wtλ (wt lambda), 10^{10} PFU λgfp10-GFP (gfp Lambda), 2µg rGFP (rGFP), 10^{9} λgfp10-TAT-GFP (tat/gfp Lambda), 2µg rTAT PTD (rTAT), 2µg BSA (BSA), or a non-treatment control (cell control). N=5 in each column except TAT phage where N=1 and rTAT where N=3. All measurements were performed in triplicate.

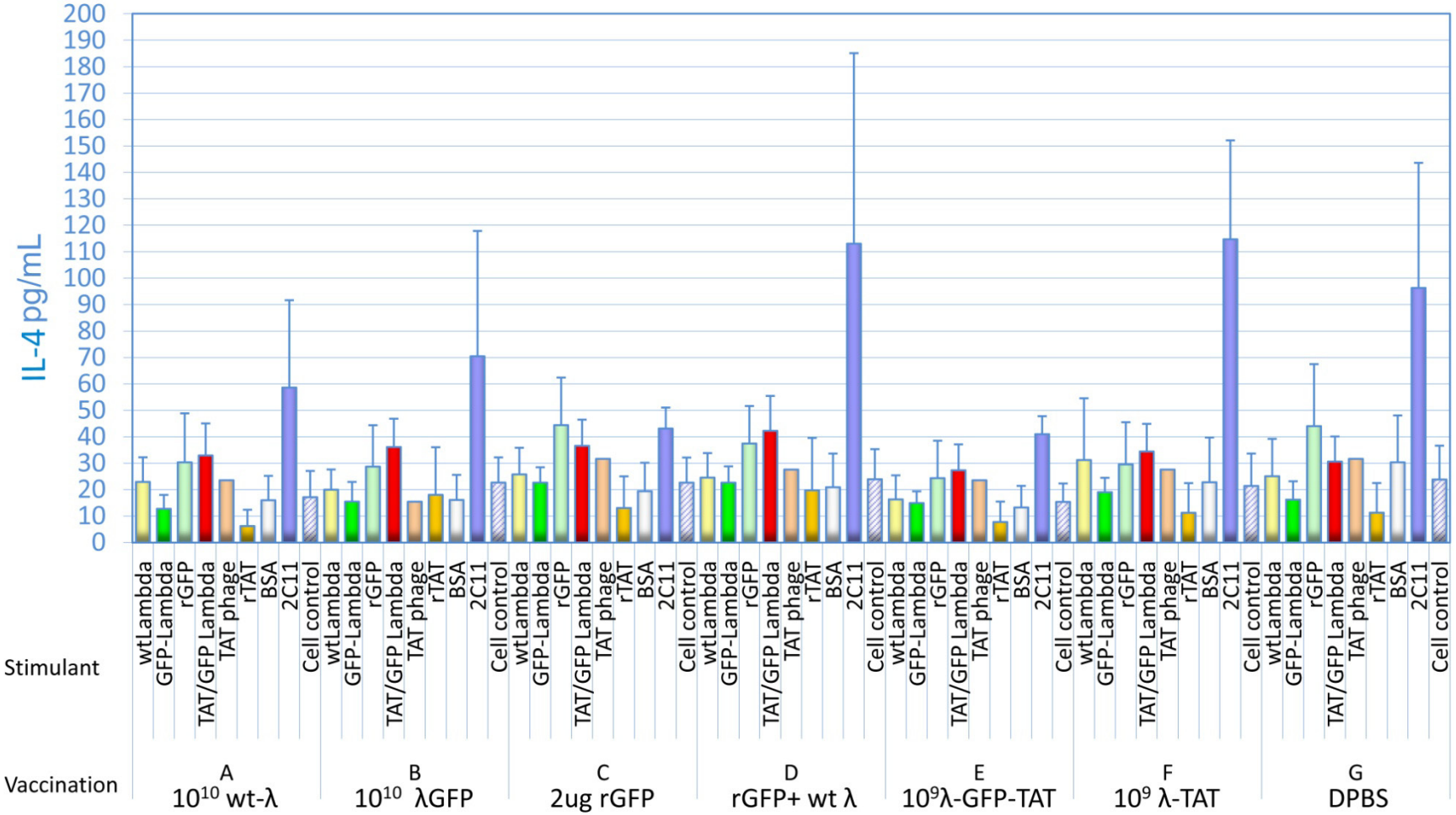

Figure 4.8: IL-4 production in CD1 Splenocyte Proliferation.

Figure 4.8: IL-4 production in CD1 Splenocyte Proliferation.

Supernatant from the *in vitro* stimulation of splenocytes were measured for IL4 produced using a sandwich ELISA (R&D systems) across immunization groups: A) 10^{10} PFU wtλ, B) 10^{10} PFU λgfp10 displaying GFP, C) 2μg rGFP, D) 2μg rGFP co-injected with 10^{10} PFU wtλ, E) 10^{9} λgfp10 displaying TAT and GFP, F) 10^{9} PFU λgfp10 displaying TAT, and G) DPBS. For each immunization, splenocytes were stimulated *in vitro* with the following: 10^{10} PFU wtλ (wt lambda), 10^{10} PFU λgfp10-GFP (gfp Lambda), 2μg rGFP (rGFP), 10^{9} λgfp10-TAT-GFP (tat/gfp Lambda), 2μg rTAT PTD (rTAT), 2μg BSA (BSA), or a non-treatment control (cell control). Each sample was run in triplicate and N=5 for each column except TAT phage where N=1 and rTAT where N=3. All measurements were performed in triplicate.

IFNγ secreted, as compared to other immunizations.

The greatest secretion of IFNγ (Fig. 4.6) was the result of stimulating *in vitro* with *wt* Lambda or TAT/GFP Lambda (λgfp10-GFP-TAT). One of these two λ ligands had a greater or equal response in every immunization than 2C11, an antibody that binds the T cell receptor. In the λgfp10-GFP-TAT immunization (vaccination E) the greatest stimulants for IFNγ were 2C11 with 1675 pg/mL ± 167, and TAT/GFP Lambda with 1614 pg/mL ±706. BSA was unusually high (>1000 pg/mL) in GFP Lambda (vaccination B) and rGFP+ *wt* Lambda immunizations (vaccination D), but well below 500 pg/mL in every other immunization. Stimulating with rTAT resulted in the highest IFNγ in the rGFP+ *wt* Lambda immunization (vaccination D), but this was lower than other recombinant or purified proteins, whereas rTAT was highest of all purified proteins, excluding intact λ ligands, in the TAT/GFP Lambda immunization (vaccination E).

IL-2 secretion was assayed across immunizations, and the data is shown in Figure 4.7. Like IFNγ, IL-2 is a Th1 cytokine. The immunization groups with the greatest IL-2 secretion across ligands were rGFP+*wt* Lambda (vaccination D) and TAT/GFP Lambda (vaccination E). The sample causing the greatest IL-2 secretion (623±454 pg/mL) was TAT/GFP Lambda immunized mice (vaccination E) stimulated with TAT/GFP Lambda. The next highest responding sample was TAT/GFP Lambda in TAT/GFP Lambda immunized mice (vaccination E). For all other immunizations, rGFP was the strongest stimulator of IL-2 secretion. GFP Lambda and *wt* Lambda were not strong stimulants in any of the treatments, as compared to BSA or cells with no stimulant. The T cell receptor ligand, 2C11, was also a poor stimulant for IL-2 secretion across immunization groups. In all treatments IL-2 was secreted at a lower concentration than IFNγ at 48hrs.

The Th2 cytokine IL-4 was measured using an ELISA (R&D systems) and the data is shown in figure 4.8. The highest IL-4 (115pg/mL ±37) was produced by stimulating with 2C11 in mice immunized against TAT Lambda (vaccination F). IL-4 had the lowest concentration of any cytokine measured in CD1 splenocytes when stimulated *in vitro*. Except for 2C11, all treatments were < 50pg/mL. Across immunizations the amplitude of reaction for stimulants were similar, rGFP and TAT/GFP Lambda were the second and third highest, with concentrations between 24.3pg/mL up to 44.4pg/mL, as compared to

15.3 to 23.9pg/mL for cells in media alone. No trends between immunization groups or stimulants were apparent.

The next step was to look at serum antibody titers to determine the quality of CD1 mouse immunization. In figure 4.9, panel A, the antibody titers against *wt* λ were greatest in animals immunized against *wt* λ, λ-GFP (inoculation B), and rGFP co-injected with *wt* λ (inoculation D), having average titers of $6.40x10^5$, $5.50x10^5$, and $7.75x10^5$ respectively. Not surprisingly these immunizations all contained λ. When rGFP was used alone to immunize mice (inoculation C), no titers >100 were observed; the same titer of antibodies observed in animals immunized IP with DPBS, our vehicle control. Animals inoculated with λ-GFP-TAT (λgfp10-GFP-TAT) and λ-TAT (λgfp10-TAT) each gave the same titer of anti-λ at $1x10^5$. It should be noted that these animals had only 10^9 PFU inoculated instead of 10^{10} as for the other λ immunizations.

Antibodies raised against GFP were also investigated (Fig. 4.9 B). In this capture ELISA, rGFP was coated on wells using carbonate buffer; as such it is described as being denatured. The highest titer observed was $2.2x10^5$, for animals co-injected with rGFP and *wt* λ (inoculation D), this was 3.5x less than the $7.75x10^5$ seen against λ for the same immunization. The next highest antibody titers against GFP were for animals immunized against λ-GFP-TAT (λgfp10-GFP-TAT), and λ-TAT (λgfp10-TAT), with $2.8x10^4$, and $3.0x10^4$ respectively, or a 3.6 and 3.3 times lower titer than that seen for anti-λ in the same immunization groups. Immunization against λ-GFP resulted in GFP antibody titers of $2.6x10^3$, or approximately 4x those seen in DPBS injected animals; this is a 210x drop in antibody titer as compared to anti-λ for the same treatment. Animals immunized against *wt* λ, or rGFP alone did not have GFP antibody titers above those observed in animals immunized IP with DPBS, our vehicle control.

With limited serum remaining, the titer of antibodies against GFP for IgA, IgM and IgG were determined (Fig. 4.9 C). IgA, the mucosal antibody, did not have significant serum titers as seen in panel A. In fact, the only group having a titer above baseline was λ-GFP. However, if multiple animal samples had been run this may have proven to be a false positive. Natural antibodies were investigated next in the IgG and IgM isotypes against λ (Fig. 4.9 D,E). In both cases no titer was seen above the limit of detection for

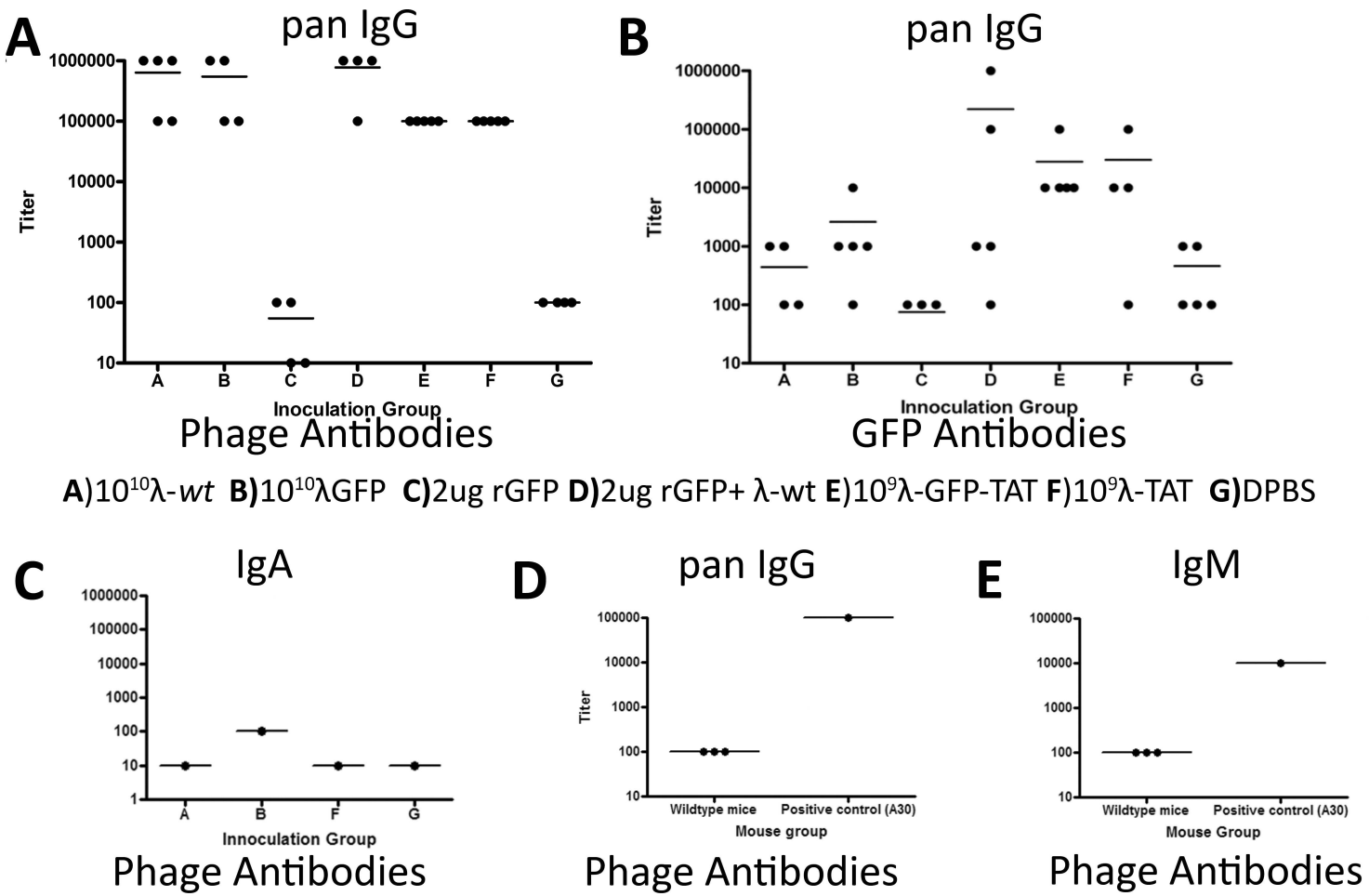

Figure 4.9: λ antibody titers after immunization in CD1 mice

Figure 4.9: Anti-Phage Titers in CD1 Immunization.

Panels A to E show the serum antibody titers raised against *wildtype* λ, or GFP. Pan-IgG (GE Healthcare) titers were measured in panel A and B, for λ and GFP respectively. In panels A, B and C the inoculation groups were A) 10^{10} PFU wtλ, B) 10^{10} PFU λgfp10 displaying GFP, C) 2μg rGFP, D) 2μg rGFP co-injected with 10^{10} PFU wtλ, E) 10^{9} λgfp10 displaying TAT and GFP, F) 10^{9} PFU λgfp10 displaying TAT, or G) DPBS. In panel C, the highest responder from panel A was measured for IgA (BD Pharmingen) antibodies. In panel D and E, three *wildtype* or non-immunized mice were tested for pan IgG and IgM (BD Pharmingen) antibodies against λ; as a positive control the highest responder in inoculation group A (#30) was used.

our assay (100). As TAT was present on λ in some immunization experiments, antibodies raised against the PTD of TAT were also investigated. No antibodies were detected that recognized TAT.

The amplitude and type of immune response against λ displayed GFP was determined by investigating serum antibody titers and isotype titers, together with cytokine expression of *in vitro* stimulated splenocytes (Figure 4.10). Antibodies to denatured GFP are shown in figure 4.10, panel B, and were also described in panel B of figure 4.9. In contrast to denatured GFP antibodies, native GFP antibodies were highest in the λgfp10-GFP-TAT immunization group, with an average titer of $2.8x10^4$, while mice immunized with rGFP and *wt* λ gave a native anti-GFP titer of $2.3x10^4$. Most other immunization groups were approximately equal to the vehicle control group, at an average titer of 62.0. The only other group that gave a response above baseline were rGFP immunized animals, at a titer of 277.5, but this was not as robust as compared to strong responders in panel A and B.

To this point only total IgG titers had been looked at when measuring anti GFP. By looking at IgG1 and IgG2a titers the type of Th response to λ displayed GFP was determined (Fig. 4.10 C,D). The number of samples remaining for this analysis was not high, therefore it may not be indicative of the whole population seen in panels A and B. IgG1 and IgG2a anti-GFP was at the lower limit of detection (100) for λgfp10-TAT immunized mice. For mice inoculated with rGFP co-injected with λ (inoculation D), the titers for IgG1 and IgG2a anti-GFP were $5.5x10^4$ and $5.1x10^4$. Phage that displayed GFP and TAT resulted in anti-GFP titers of $3x10^3$ for IgG1and $1x10^4$ for IgG2a. The immune reaction was polarized towards a Th1 response for λ displayed peptides, but was equal in the rGFP+ *λ-wt* immunized animals (inoculation D). To aid in interpreting the data, the cytokines measured during *in vitro* proliferation (Figs. 4.6, 4.7, 4.8) were distilled into the pertinent groups for panels E, F, and G of figure 4.10. IL-2 was secreted at 48hrs in a λ specific response for λgfp10-GFP-TAT, and rGFP + λ-*wt* immunizations (groups E and D), but this was not statistically significant. The other Th1 cytokine, IFNγ, shows a robust response to λ that was independent of the immunization and statistically significant. Lastly, IL-4 was secreted

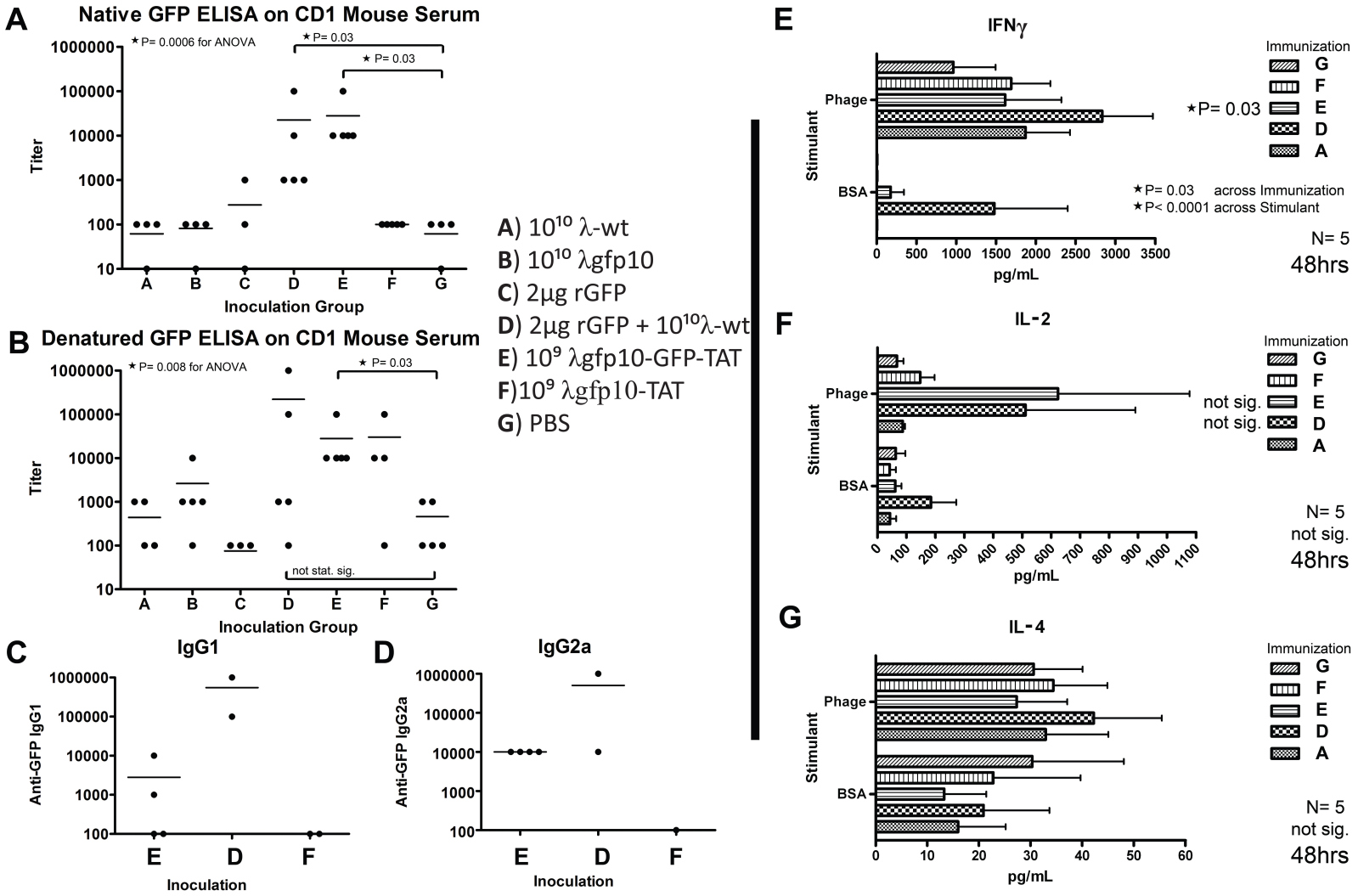

Figure 4.10: Th1 and Th2 immune response in CD1 mice.

Figure 4.10: Th1 and Th2 immune response in CD1 mice.

Panel A to D show serum antibody titers against GFP. In A and B the inoculation groups are: A) 10^{10} PFU wtλ, B) 10^{10} PFU λgfp10 displaying GFP, C) 2μg rGFP, D) 2μg rGFP co-injected with 10^{10} PFU wtλ, E) 10^{9} λgfp10 displaying TAT and GFP, F) 10^{9} PFU λgfp10 displaying TAT, and G) DPBS. Panels C to D have the same inoculations but not all groups were assayed. In A , GFP was in its native conformation, whereas ELISA plates were coated with denatured GFP in panel B. Panels A and B show pan IgG (GE Healthcare) titers recognizing GFP. In C and D, the IgG isotypes IgG1 (BD Pharmingen) and IgG2a (BD Pharmingen) recognizing GFP are measured. Panels E, F, and G are graphs derived from data in Figures 4.6 to 4.8. Horizontal columns correspond to immunization groups where 5 animals were measured in triplicate and the average is given along with the variation measured as the standard error of the mean. Top to bottom the immunization groups are: G) DPBS, F) 10^{9} PFU λgfp10 displaying TAT, E) 10^{9} λgfp10 displaying TAT and GFP, D) 2μg rGFP co injected with 10^{10} PFU wtλ, A) 10^{10} PFU wtλ. Shown are splenocytes stimulated *in vitro* with 10^{9} λgfp10-TAT-GFP or 2μg BSA. IFNγ, IL-2, and IL-4 are shown in panels E, F, and G respectively.

from splenocytes at 48hrs, but the response was approximately equal across immunization groups for stimulation with λ or BSA. To summarize, in CD1 mice there was a Th1 polarization after λgfp10-GFP-TAT immunization, as measured by IFNγ and IL-4 cytokines, or when IgG subclasses were measured.

C3H mice gave a severely depressed immune response to GFP displayed on λ (Fig. 4.11 A, C, D). The highest anti-GFP titer for an immunization group was for animals inoculated with adjuvant and λgfp10-GFP-TAT (Inoculation group 3). This resulted in a pan IgG titer of $8x10^3$; in contrast the same immunization in CD1 mice gave a pan IgG titer $2.2x10^4$. No other immunization group had any animal with a titer above 1000. When λgfp10-GFP-TAT were immunized in LPS responsive C3H/HeOuJ mice (Inoculation group 4) the resulting titer was 550, whereas in C3H/HeJ mice immunized against λgfp10-GFP-TAT (group 2) the titer was 77.5±14.73, or greater than three times that of the PBS immunized mice.

C3H mice reacted more strongly against λ itself than to a displayed protein (Fig. 4.11 A, B). The average titer of anti-λ across all immunizations was approximately $1x10^4$. C3H/HeJ mice immunized with adjuvant and λgfp10-GFP-TAT (group 3) resulted in the highest titer ($8.2x10^4$) whereas for λgfp10-GFP-TAT immunized in C3H/HeJ or C3H/HeOuJ mice, both had anti-λ IgG titers of $1x10^4$ but only titers of 78 and 550 for anti-GFP respectively. When the subclass of IgG in the anti-GFP response was measured the Th2 antibody IgG1 was absent, but IgG2a titers were nearly identical as those observed for total IgG recognizing GFP, as all averages were the same order of magnitude. The depressed immune response observed in C3H mice was therefore Th1 polarized.

To elaborate further on the type of immune response being observed, a panel of cytokines was measured using Luminex. IL-1α, IL-1β, IL-4, IL-6, IL-10, IFNγ, and TNFα were measured. No trends emerged for IL-1α, IL-1β, IL-4, IFNγ, or TNFα, but there was a difference in how IL-6 and IL-10 were secreted from splenocytes. In C3H/HeOuJ mice, IL-10 was secreted regardless of stimulation with λ or LPS, but IL-10 was only secreted upon stimulation with λ and not LPS in C3H/HeJ mice. IL-6 secretion in C3H/HeOuJ mice resulted in the same amplitude of response with either LPS or λ as stimulants,

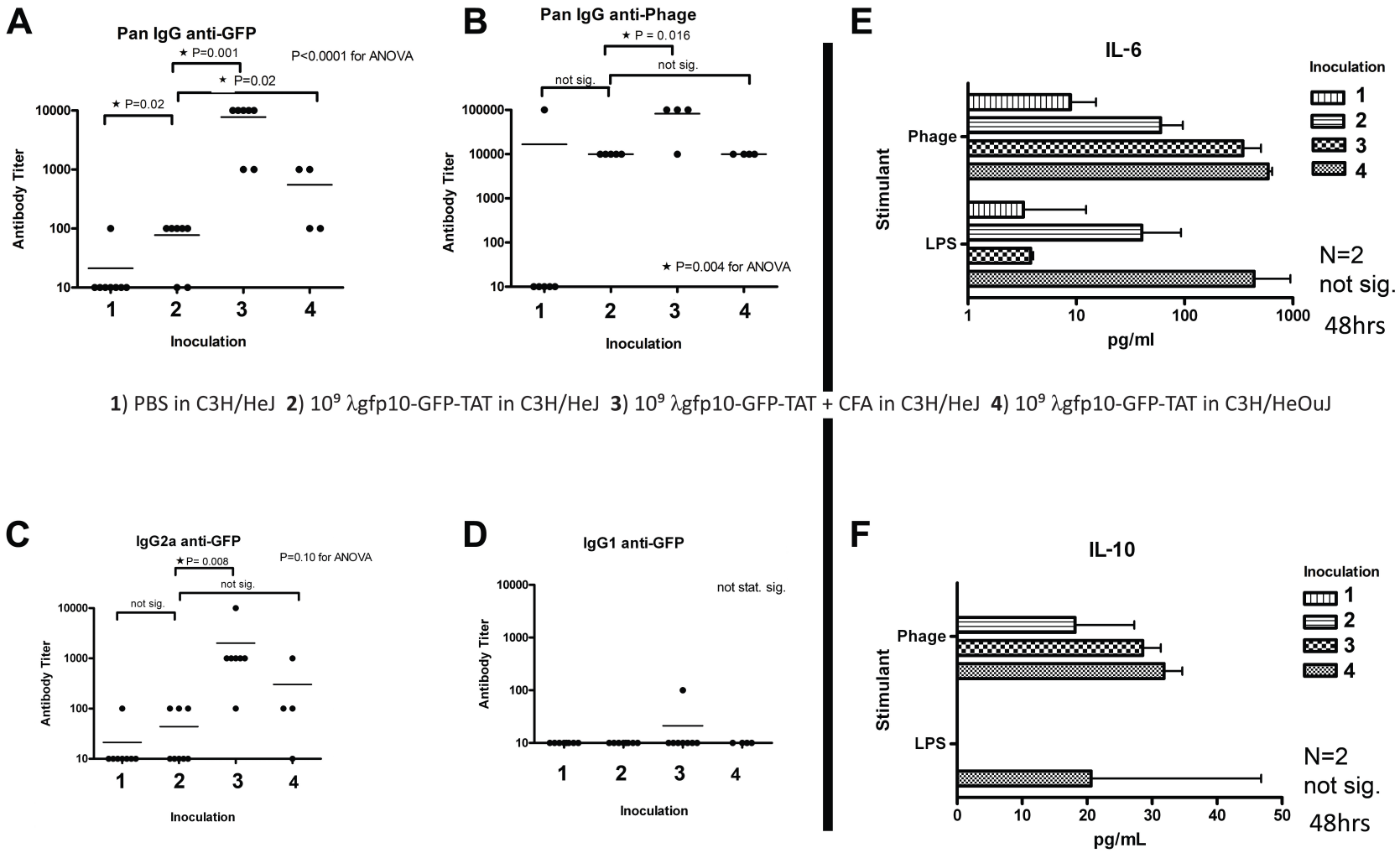

Figure 4.11: Antibody and Cytokine Response in C3H mice.

Figure 4.11: Antibody and Cytokine Response in C3H mice.
Panels A to D show serum antibody titers in four inoculation groups as follows: PBS, Phage, Phage + Adjuvant, and Phage in LPS responsive mice. The first 3 groups were done in C3H/HeJ mice and consisted of DPBS, 10^9 PFU of λgfp10 displaying TAT and GFP, 10^9 PFU λgfp10 displaying TAT and GFP in 50uL DPBS and 50uL Freund's adjuvant. The last group was done in C3H/HeOuJ mice with 10^9 PFU of λgfp10 displaying TAT and GFP. Panel A measures pan IgG (GE Healthcare) anti-GFP, and panel B measures pan IgG (GE Healthcare) anti λ. In panels C and D, the IgG isotypes that recognize GFP are measured; IgG2a in C and IgG1. Statistics were run in C and D, and the significance was determined across all groups using one-way ANOVA. In C, t-tests were also performed to compare two treatments; each anti-GFP IgG2a titer for phage inoculated animals were compared to each of the other inoculations individually. The statistical significance for each of these comparisons is shown. In panels E and F the amount of IL6 and IL10 was measured from *in vitro* splenocyte proliferation assays using a Luminex. N=2 for each column and these were done in duplicate. Horizontal columns are the same inoculation groups as in A to D that were stimulated with Phage or λ-TAT-gfp at 10^9PFU/mL, and LPS at 100ng/mL

but IL-6 expression was enhanced in the adjuvant and phage immunized mice when stimulated with λ as compared to LPS. PBS or Phage immunized C3H/HeJ mice resulted in identical responses to λ as compared to LPS.

4.4 Discussion

The studies undertaken on the immune reaction to λ and λ displayed epitopes have resulted in the most detailed analysis to date. The immune reaction to λ displayed epitopes will be described first followed by the general adaptive immune reaction to λ, the appearance of natural antibodies, and finally the discussion will close with a description of the innate response to λ.

4.4.1 Immune response to bacteriophage λ

λ displayed proteins elicit an immune response when injected into rabbits (Fig. 4.1). This was the first documented study showing antibodies produced in response to proteins displayed on λ capsids. Previous work had shown λ to be an effective delivery vehicle for DNA vaccination, but no studies had investigated λ as a scaffold for a subunit vaccine to present proteins and/or peptides to the immune system.[186] As this work in mice continued it was found that antibody production was not dependent on the addition of an adjuvant (Fig. 4.10). Of course, many studies have shown a variety of bacteriophage, notably M13, T4,[26] and ΦX174,[361] to be effective as treatments for a variety of pathologies including respiratory syncytial virus,[34] alzheimers,[43] and HIV.[361]

4.4.1.1 Cytokines

One method of evaluating the quality and strength of an immune reaction is by measuring the cytokines produced. The majority of vaccine studies measure the amount of IFNγ to 1) assess immunogenicity, and 2) as a correlate of protective immunity.[104,107,137,362] IFNγ is a Th1 cytokine that results in a cytotoxic T lymphocyte response to intracellular pathogenesis. The early initiator of a Th1 response is IL-12, which is enhanced by IFNγ, which in turn results in IL-2 being expressed for the

differentiation of memory T cells during the memory phase of the immune response after the expansion and contraction phases.[107,111,149]

In this study a strong IFNγ response was seen in splenocytes, with concentrations of 1675 ±167pg/mL, or 1614 ±706pg/mL for 2C11 and λ-GFP-TAT stimulation in λ-GFP-TAT immunized animals (Fig. 4.6). The highest responders were in the rGFP+ *wt* λ immunized animals with 2833 ±637pg/mL, and 2703±772pg/mL for λ-GFP-TAT and *wt* λ stimulated splenocytes, where 2C11 only resulted in 1547±534pg/mL. With these values it is apparent the spleen gives a strong Th1 effector response at 48hrs.

IL-2 secretion was very robust at 48hrs in splenocytes immunized with λ-GFP-TAT and rGFP+*wt* λ. IL-2 concentrations were high, being 623±454 pg/mL in the λ-GFP-TAT stimulated mice from rGFP+*wt* λ immunized mice (Fig 4.7). This was only 4.5 times less IL-2 as IFNγ, for the highest responders, and given the timing post stimulation, after the immunization regime undertook, it could be indicative of a strong memory response.[111] Further evidence for this statement was the fact that these two immunization groups resulted in the highest antibody titers against GFP (Fig. 4.10).

The possibility of immune memory after λ immunization was corroborated by the lack of IL-2 being secreted in splenocytes stimulated *in-vitro* with 2C11. 2C11 is a ligand that binds the T cell receptor. Given this data, it appears no effector cells have been produced for 2C11, and therefore no memory response was necessary and IL-2 was not secreted. Across immunizations, 2C11 stimulated cells have an equivalent IL-2 concentration as cells that have not been treated with any stimulant. Interestingly, stimulation with rGFP gave high concentrations of IL-2, regardless of the immunization. High IL-2 concentrations after stimulation with rGFP did not result in high titers of antibodies against GFP, as seen in TAT/GFP Lambda stimulant groups. This was most likely due to contaminants in the recombinant protein preparation, and was indicative of these animals having been exposed to a bacterial contaminant which lead to high IL-2 concentrations after our rGFP stimulation.

Other Th1 cytokines were not measured to further elaborate on how the Th1 response progressed. IL-12 could have been measured to describe the expansion phase of the Th1 response. IL-12 would have been measured at an earlier time point during the

stimulation, and at earlier time points in the immunization experiment.[106] With IL-12, IFNγ, and IL-2, and/or the transcription factor *Tbet* the study could have defined the time points for the expansion, contraction, and memory phases of the immune response for mice when presented with λ in a similar manner to the experiments that have been done on lymphocytic choriomeningitis virus (LCMV).[111] Alternatively, the study could also have investigated the number of cells positive for each of the above mentioned cytokines using intracellular cytokine analysis on a flow cytometer. This would have given a better view of the overall immune response, lending insight to how many and what types of cells are present at any given time.

When IL-4 concentration was measured in splenocytes (Fig. 4.8, 4.10 G) it was apparent the amplitude of the reaction was much lower than that seen for IL-2 and IFNγ. IL-4 was stimulated best by 2C11, and the highest concentration was 115 ±37 pg/mL, which was much lower than the highest concentrations of 623±454 pg/mL for IL-2, or 2833±637 pg/mL for IFNγ. In panel G of figure 4.10, IL-4 production was not found to be statistically significantly across immunizations after the addition of λgfp10-GFP-TAT (Phage) or BSA. A few scenarios potentially explain this result. The timing of IL-4 measurements may have been suboptimal for effective measurement of effector function in splenocytes, or the spleen might an inappropriate organ to effectively measure IL-4 concentrations in response to immune challenge. This could be a result of the spleen having a limited number of antibody secreting cells, even though it is the largest secondary lymphoid organ, filters the blood, and is the reservoir for systemic memory T cells and memory B cells.[125,127-129,363]

An alternative explanation for the low concentrations of IL-4 observed may be that its physiologic concentration may be lower than for IL-2 or IFNγ. The flat response in stimulant groups across immunizations does not lend itself to easy interpretation, and this analysis is no doubt complicated by the fact that IL-4 is produced not only to promote differentiation of Th cells into Th2, but also inhibits Th1 cell differentiation, and is involved in LPS signal transduction as an inhibitor to p38 phosphoryltation.[149,153,364] One could envision IL-4 in a negative feedback loop during the contraction phase of Th1 cells, as Th1 cell death occurs if sufficient IFNγ is not present.[364] Perhaps the effector

cytokine IFNγ was not the most favourable readout for discriminating the Th1 immune reaction in our immunization, and a memory cytokine for Th2 rather than the effector cytokine IL-4, would have been advisible.[106,107,111] There are no Th2 specific memory cytokines, but if IL-5 and IL-13 were used in conjunction with general T cell memory cytokines, such as IL-7 or IL-15, a better understanding of the immune response may have been obtained.[106,107]

To discriminate between Th1 and Th2 responses, perhaps the most conclusive measurement would have been to look at the transcription factors *GATA-3* and *Tbet.* The expression of these transcription factors is mutually exclusive,[113,114,365,366] and measuring *GATA-3* would be indicative of the number of Th2 cells, and not simply extracellular IL-4 protein concentration.[106] In measuring cytokines in cell media using an ELISA, protein concentration could be skewed by a few strong responders, and not indicative of the population of cells as a whole. This is one reason intracellular cytokine measurements are done using flow cytometry. To determine the Th polarization, the author eventually decided to investigate the IgG isotype *in vivo*, instead of working on the *in vitro* splenocyte assay as discussed here.

As for the cytokine assays performed herein, a few final points need to be addressed before moving onto other analyses. First, in figure 4.6 the λ-TAT stimulant effect was very high, but this was only performed in triplicate on the splenocytes of one animal. If done on multiple animals the stimulant effect would most likely be similar to λgfp10-GFP-TAT (stimulant TAT/GFP Lambda), as one animal in λgfp10-GFP-TAT stimulated animals for rGFP+*wt* λ immunized mice did have a concentration of IFNγ greater than that seen for the λ-TAT stimulant. This value fits within the range seen in λgfp10-GFP-TAT treatment (stimulant TAT/GFP Lambda). Due to time constraints this work was not repeated. Second, in figure 4.6 all stimulant responses were higher in immunization group D. This was interesting as these animals were inoculated with rGFP that was co-injected IP with *wt* λ. As such it was presumed that since rGFP gave a strong IL-2 response it was not pure, and the immune response in group D lead to Th2 memory for rGFP and any contaminants in the rGFP preparation. The contaminants in the commercial rGFP are presumably small particulate antigens that would normally be

opsonised, but given the presence of λ an adaptive immune response occurred, the result of which was a strong IFNγ response to all stimulants in D. This hypothesis applies to all stimulants used on immunization group D, but does not account for the non-stimulated splenocytes, or cell control group. Immunization group D appears hypersensitive to manipulation, which in this experiment could include the mechanical manipulation necessary for the *in-vitro* assay. These ideas are currently conjecture as this effect was not investigated further; however it was documented that rGFP and *wt* λ immunizations resulted in an additive effect on non-stimulated cells that caused a hyper IFNγ response. This hypersensitivity was not seen with any other inoculant including rGFP and *wt* λ alone

4.4.1.2 GFP antibody response

GFP is a known immunogen in mice and MHC are present in BALBc and C57Bl/6 that produce a cytotoxic T lymphocyte response (CTL).[367] When *wt* λ and DBPS immunizations were investigated in CD1 mice they had equivalent titers (Fig 4.10 A,B). This was the lower limit of detection for the anti-GFP ELISA performed. When the amplitude of the cytokine secretion was compared to GFP antibody production, the best indicator of high anti-GFP titers was IL-2 in response to λgfp10-GFP-TAT stimulation (Fig. 4.7, and panel A Fig. 4.10). Immunizations D and E were the highest IL-2 responders and have the highest native GFP antibody titers. This trend does not occur in panel B of figure 4.10, the denatured GFP ELISA, as compared to figure 4.7, but again the two highest responding IL-2 groups, immunizations D and E, had the highest anti-GFP titers.

In the CD1 immunization experiment there was roughly 10x more rGFP to inoculate each animal as compared to GFP delivered on λ. This number increased when immunizations with λ-GFP-TAT were compared to rGFP. The molecular weight of rGFP is approximately 27kDa. 20μg of rGFP was administered IP to each animal, which is equivalent to $4.46x10^{13}$ molecules:

$$20\mu g x \frac{1g}{1x10^{6}\mu g} x \frac{1\,mol}{27\,000g} x \frac{6.022x10^{23} molecules}{mol} = 4.46x10^{13} molecules$$

If we assume there are 405 gpD molecules for each λ plaque forming unit,[268] and if the

presentation of gpD-GFP was 40% of gpD molecules (162gpD molecules), then for immunizations A, B, and D where 10^{10}PFU of λ was used for each animal, there were approximately 10^{12} gpD-GFP molecules. In immunization groups E and F, where only 10^{9} PFU of λ was injected per animal there were approximately 10^{11} gpD-GFP molecules. With this in mind, it did not matter how much total GFP was present for native GFP antibodies, as λgfp10-GFP-TAT immunized animals had an equivalent titer against GFP as group D which had 100x more GFP. Furthermore, the response to λgfp10-GFP-TAT was more consistent compared to group D. When titers are compared between antibodies against native GFP and those against λ, there were 3.6x more anti-λ than anti-GFP in immunization E, whereas in immunization D there were 34.3x more anti-λ as compared to antibodies towards native GFP. Obviously the method of GFP presentation affects the quality of the immune response.

It was interesting to compare the type of antigen, small molecule vs. viral particle, and how mice responded. In figure 4.10 immunization group E gave the highest titers of antibodies recognizing native GFP, whereas group D gave the highest titers recognizing denatured GFP (Fig4.10 A,B). This effect must relate to how the immune system recognizes and presents rGFP to B cells as compared to λ displayed rGFP. This could be due to differences in opsonisation, phagocytosis, or MHC presentation. From the perspective of phagocytosis, the result could be due to the classic paradigm of a virus sticking to phagocytic cells readily whereas an isolated protein needs to be opsonised. Strangely, when rGFP was the only antigen inoculated IP into an animal, the only antibodies produced recognized native GFP, and not denatured GFP. The only treatments that gave native GFP antibodies were rGFP, with or without *wt* λ co-injected, and λgfp10-GFP-TAT. This lead to the presumption that TAT helped in the opsonisation or complement mediated response, during clearance. Figure 4.10 panel B documents titers of antibodies that recognize denatured GFP. A denatured epitope is typical of antigen processing and presentation on MHCII. High titers of antibodies for denatured GFP were seen in λgfp10-GFP, rGFP+*wt* λ, λgfp10-GFP-TAT, and λgfp10-TAT. In the case of group D, rGFP+*wt* λ, this was due to rGFP being present, but in all others it could be due to the GFP reporter gene being present. This will be discussed further in the next section.

4.4.1.3 DNA Vaccination

In figure 4.10 we clearly see that DNA vaccination using λ is possible (panel B). A previous group had documented this when λ was administered intranasally and intramuscularly; we now prove a similar result with IP injection.[186,203] In immunization group F, λgfp10-TAT, denatured anti-GFP titers were equivalent to those for λgfp10-GFP-TAT. In contrast, antibodies against native GFP (Fig 4.10 panel A) were absent in DNA vaccination groups. This result is not surprising as DNA vaccines need to be transcribed, translated, degraded in the proteasome, and finally loaded onto MHC on antigen presenting cells (APCs). Surprisingly, no native GFP antibodies are seen in group B, λgfp10-GFP. This could be a direct result of all antibodies being produced by the GFP reporter gene, but the necessary control, λgfp10 not displaying GFP, was not used to test this.

When the antibody titer generated via a peptide displayed vaccine and a DNA vaccine was compared, the result was roughly equivalent in the current study (Fig. 4.10 B). The efficacy of our DNA vaccination indicated by denatured ELISA was impressive as previous studies documented that peptide vaccination, without λ, was caused 8x higher antibody titers as compared to λ DNA vaccination.[203] Our data suggests IP injection of rGFP, results in a very low titer of anti-GFP, but very high titers when λ was the subunit vaccine platform for DNA or protein vaccination. GFP is a known immunogen,[367] as is the HepB antigen,[186,203] therefore the epitopes should have resulted in similar responses. The divergence in response maybe the result of the immunization route, IP vs. IM, or may have been due to the concomitant display of TAT which enhanced the immunogenicity (see the next section, 4.3.1.4).

Vaccination with a λ displayed peptide elicits native GFP antibodies which could be neutralizing antibodies, whereas λ DNA vaccination did not give native antibodies. For this reason we believe peptide immunization using λ will be more effective than λ DNA vaccination. Peptide immunizations have proven to be more potent than DNA vaccinations in other contexts and our λ data supports this conclusion.[368]

4.4.1.4 TAT immune response

The PTD of TAT was displayed on λ, and this may have enhanced the immune reaction. We did not test the direct effect TAT had on immunization further than that seen in the CD1 immunization (Figs. 4.9, 4.10). In this experiment it appeared that TAT enhanced the immunogenicity of a λ displayed protein, but *caveat lector*. In the CD1 experiment immunization groups A to D were performed with PEG precipitated λ, whereas groups E and F were performed with ammonium sulfate precipitated λ. Groups A to D were shown to have contamination with ligands for TLRs 2,3,4,7,9 and a non-TLR NF-κβ stimulating ligand. As such, no conclusions regarding TAT's effect on the immune response can be made. Claims have been made in reference to the PTD of TAT with regards to the immune response,[369-373] but as TAT was not effective when we investigated other published properties (Chapter 3) this avenue of research was not continued. We did continue with TAT λ constructs for the C3H experiments, as λ with TAT gave the strongest immune reactions as measured by antibody titer and cytokine response, but no direct comparison to non TAT λ can be made for CD1 or C3H mice.

One aspect of TAT immune response that was investigated was the titer of antibodies recognizing TAT. ELISAs were done as per previously described and many variations on this were also performed (section 2.12.1).[374,375] No IgG antibodies to the 11 amino acid PTD,[337,338] otherwise known as the basic domain, were measured in CD1 mouse sera. It may be presumed that the result is because either this epitope not being seen by the immune system due to steric hindrance from λ proteins or the epitope was not available in the HLA population of the mouse strains. Alternatively as the sequence is highly positively charged it may be similar enough to an endogenous protein leading to its removal during the negative selection of B cells. A recently published human phase I trial for HIV using a TAT vaccine reported IgM titers recognizing the basic and RGD regions of TAT, whereas the acidic domain was recognized primarily by IgG antibodies.[376] The lack of IgG titers recognizing the basic domain of TAT, suggest that IgM titers for the PTD of TAT should have been examined.

4.4.2 Immune reaction to λ

In figure 4.1 the primary proteins recognized by rabbit serum antibodies are gpE 38.2kDa, gpV 25.8kDa, and gpD 11.4kDa.[261,268] In the rabbit immunization the major coat proteins of λ are more immunogenic than gpD-GFP, while in figure 4.9 λgfp10-GFP-TAT immunized mice (group E) gave titers of $2.8x10^4$ for anti-GFP which were the same order of magnitude as those for anti-λ ($1.0x10^5$). This was most likely achieved due to the optimized purification protocol developed in chapter 3. In published vaccination experiments using filamentous bacteriophage, the titer of bacteriophage antibodies were many orders of magnitude higher than those for displayed peptides. This might be explained as a valency issue as f1 bacteriophage display proteins on the pIII coat protein, which only contains 3-5 molecules per virion.[29,377] With our system, similar numbers of major coat proteins and GFP were present, resulting in similar titers.

High titers of antibodies were raised against λ in CD1 and C3H immunized mice (Fig. 4.9A, Fig. 4.11B). In CD1 mice titers of 10^5-10^6 antibodies were raised against λ, whereas in C3H mice, 10^4-10^5 antibodies were produced. In a previous study, BALBc and C57BL/10 mice raised antibodies against f1 bacteriophage after immunization with Freund's adjuvant.[29] In that study C57BL/10 mice produced a humoral immune reaction to displayed peptides, but BALBc mice never responded.[29] In our CD1 immunization a strong anti-GFP humoral immune response was documented (Fig. 4.10), but a severely depressed or absent anti-GFP response was observed in C3H mice (Fig 4.11). We know the percent gpD-GFP in our λgfp10-GFP-TAT vaccine was equivalent in both CD1 and C3H immunizations (data not shown). With the addition of an adjuvant, anti-GFP titers of $7.8x10^3$ were observed, and antibodies against λ were at titers of $8.2x10^4$ in the same immunization group. This response decreased to only $5.5x10^2$ anti-GFP in the LPS responsive C3H/HeOuJ mice, and only $7.8x10^1$ anti-GFP in C3H/HeJ mice immunized without adjuvant but with the same λgfp10-GFP-TAT vaccine, or approximately 18 and 129 times less anti-GFP than anti-λ respectively. The discrepancy between anti-GFP and anti-λ for C3H mice may be similar to that seen in BALBc mice where these strains have robust anti-λ but poor responses to displayed proteins. The divergence in response may be due to MHC haplotype: BALBc have an $H2^d$ MHC haplotype and C3H have an $H2^k$

haplotype, whereas C57BL/10 are $H2^b$ and CD1 mice are outbred. The different haplotypes may have circulating natural antibodies that result in the immune dominance of the anti-λ epitopes instead of displayed proteins.

Interestingly, if we compare IgG titers recognizing λ in C3H mice it appears there was an outlier for in the PBS immunization group (Fig. 4.11 B). This could be due to the presence of natural antibodies recognizing λ in C3H mice, and would reinforce the immune dominance theory. Alternatively, this one PBS immunized mouse may have had its bowel perforated during IP inoculation, which released large numbers of λ into the peritoneum and resulted in a strong anti-λ titer. Given the consistency of anti-λ titers for λ immunized mice it is unlikely perforated bowels accounted for the observed high anti-λ titers for these immunizations.

In conclusion, λ immunization in TLR4 deficient mice was effective at eliciting a robust antibody response to λ, regardless of genotype. In contrast, the humoral immune response to a λ DNA vaccination or λ displayed proteins and/or peptides were dependent on mouse genotype and were sensitive to TLR4 signalling. With the addition of Freund's adjuvant, λ subunit vaccines are more effective in TLR4 mutant mice (Fig. 4.11 A).

4.4.3 Antibody Isotypes

The presence of IgG antibodies against λ and GFP were described above, but other immunoglobulin isotypes and subclasses might be present and could describe the immune reaction to a λ subunit unit vaccine further. After measuring IL-4 concentration *in vitro* during splenocyte proliferation (Fig4.8) it would be tempting to conclude a Th2 immune response did not occur, and instead our immunization was Th1 polarized.

Individual clones of Th precursors undergo differentiation into either Th1, or Th2, by the mutually exclusive expression of either IFNγ, or IL-4. Th1 cells can be defined by the master regulator transcription factor *Tbet*, whereas Th2 cells can be defined by their master regulator transcription factor *GATA-3*.[113,114,365,366] Each transcription factor is necessary and sufficient for its Th phenotype, even in previously polarized Th cells. If we take a holistic view of infection, instead of a clonal view, polarization is not necessary for an immune response, or even for memory, and in fact most vaccines elicit a heterogeneous response as measured by cytokines which is time and epitope

dependent.[148,378-380] HIV is well documented for its Th1 and Th2 response.[381,382] In fact, very few vaccinations produce protective immunity when only one Th response is stimulated. Two notable exceptions are *Leshmania major*, and *Mycobacterium tuberculosis* where Th1 vaccines produce protective immunity.[106]

In order to better characterize the Th cells present after λ vaccination, IgG1 and IgG2a subclasses were measured. IgG1 being produced predominantly in Th2 responses and IgG2a in Th1.[147] In figure 4.10, mice immunized against rGFP + λ-*wt* (group D), had high IgG1 and IgG2a titers, with $5.50x10^5$, and $5.05x10^5$ recognizing GFP respectively. For mice immunized with λgfp10-GFP-TAT, the titer of anti-GFP subclass IgG1 was $2.8x10^3$, while IgG2a was $1x10^4$. No antibodies against GFP were detected in λgfp10-TAT immunized mice, as these ELISAs were done in native GFP conditions. It appears that complete Th polarization did not occur when a λ subunit vaccine was inoculated into mice.

Taken together, the splenocyte cytokine data suggests a complete Th1 polarized response (Fig. 4.10), but serum IgG subclasses suggest both Th1 and Th2, though depending on the inoculant stronger Th1 polarization was observed. Given this data it appears IL-4 was not the appropriate cytokine to measure Th polarization. It has been documented that when mice have viral infections they frequently lack IL-4 secretion, and IFNγ predominates resulting in a class switch to IgG2a and predominant Th1 phenotypes.[10] Alternatively, the result may also be an artifact of the splenocyte cytokine measurements being performed *in vitro*, as most plasma B cells do not survive past 3 days.[126]

When IgG subclasses are investigated in the hypo-responding C3H mice, no IgG1 was seen (figure 4.11). IgG2a titers against GFP are produced and the average value for each immunization is on the same order of magnitude as in panel A, but the distribution of values in a given immunization renders this small sample size statistically insignificant when immunizations are compared. In C3H mice, a Th1 response predominates as a definite IgG subclass polarization is seen, but secretion of IL-6 and IL-10 suggests a Th2 response is also present. The Th2 response may become evident after antibodies recognizing λ are measured for IgG2a and IgG1.

4.4.4 Cell compartments and Lymph Organs.

The proliferative capacity of cells in lymph organs and the number of B and T cells are indicative of an immune response. In order to characterize the immune response after immunization with a λ subunit vaccine both were measured. The number of cells in the B, Th, and Tc compartments of the spleen, MLN, and PLN were shown in figure 4.4. Each cell compartment was consistent across immunization groups for a given lymph node. If an immune reaction was polarizing towards a humoral or cell mediated response the B or Tc cell compartments would have increased significantly. As an example, when CpG DNA was used as an adjuvant in a vaccine regime, the percentage of B cells in the draining lymph doubled from 29% to 58%.[70] A similar level of expansion was not observed in any lymph organ 5 days after boosting C3H mice. Our timing may not have been optimal to measure this effect as every pathogen has a different timecourse for the T cell expansion, contraction, and memory phases, and the coincidental B cell population dynamics.[109] However, five days was sufficient to measure splenocyte proliferation (Fig 4.2, 4.5). It would have been interesting to document this effect in the CD1 immunization, where a robust antibody response was documented for GFP and λ.

The lack of B or T cell expansion in lymph organs (Fig 4.4) may relate to the method of immunization, inoculation into the peritoneum, as the above mentioned experiment injected into footpads and measured the draining lymph.[109] Differences exist between local lymph nodes and the spleen, which is the largest secondary lymph organ, a reservoir for systemic memory and a filter for the circulatory system.[128] When we measure cell numbers from various lymphoid organs in C3H mice (Fig 4.4), the MLN and PLN cell populations were identical; in contrast the spleen had more B cells, but fewer Tc and Th cells.

Next the reactivity of immune cells in each lymph organ was measured (Fig. 4.5). In this experiment the PLN and MLN cells did not respond to *in vitro* stimulation in any immunization group. This was expected as these lymph nodes were not exposed to the λ vaccine after IP inoculation. In a classic experiment on contralateral lymph nodes, no proliferation was seen in the non-draining lymph nodes.[129] It is noteworthy to highlight the only increase in proliferation for the PLN and MLN was for λgfp10-GFP-TAT

stimulated cells. Also, the MLN may have been previously exposed to λ via the gastrointestinal tract, since these cells are in an immunosuppressive milieu which is responsible for the oral tolerance of food.[90,204] As such, in this experiment a possible prior exposure in the MLN and PLN did not result in a strong proliferative response.

When the spleen was investigated for a proliferative response, one was observed that dependent on the stimulant, but was independent of the immunization (Fig 4.5 A). In animals stimulated with λgfp10-GFP-TAT (2D phage), the proliferative capacity increased as the 'immunogenicity' of the inoculant increased. As such, after an IP immunization with λ, the primary reservoir of responding cells was splenocytes. This corroborates earlier experiments where intramuscular, intravenous, and intra-peritoneal inoculation resulted in the spleen being the primary location where bacteriophage accumulate.[38]

When we compare our IP immunization to another study where an IM inoculation was used, our DNA vaccination was more effective (Fig. 4.10 B).[203] Given the propensity for IM bacteriophage to quickly move into the spleen, one would expect a similar result. Beyond the local immune milieu, the purity of the λ preparation or the presence of TAT might be responsible for enhancing the immune response. In our immunization, DNA vaccination was more effective, while protein or epitope immunization alone (group C) was less effective for our IP experiment, when we compare our result to previous IM inoculation.[203] It might be that protein delivered IP was cleared more quickly than similar protein delivered IM. In the IM experiment a depot effect could be responsible for longer presentation and thus a heightened response.[72,185] A classic study where a vaccine was delivered via the footpad or IV found footpad inoculation was slower to respond, but resulted in a more sustained immune reaction to immunogens.[129]

The route of inoculation has been shown to affect humoral immune amplitude and isotype in bacteriophage vaccination.[35] Previous work described intranasal immunization as more effective than intragastric, but with both routes if IgG antibodies were produced concomitant serum IgA was also present. No IgA was measured in the present study

when the sera of high responding IgG animals was analyzed. IP inoculation of λ does not appear to cause mucosal immunity as measured by IgA titers.

4.4.5 Natural Antibodies

In figure 4.1, panel C, the sera from animals before immunization does not react to any proteins present within inoculants. We do not see natural antibody titers in figure 4.9 as determined by IgM isotypes recognizing λ. When IgG was investigated one non-immunized animal had a high titer to λ; as discussed previously (Fig. 4.11, panel B, PBS). We did not measure IgD titers, the other isotype that occurs before V(D)J recombination, as this isotype was not mentioned in the literature.[10] The possibility exists that λ becomes bound by a naturally occurring IgD, but given the kinetics of λ clearance, and the poor interaction between IgD and complement this appears unlikely.[33,38,206] Our IgM finding was in agreement with no IgM being found that recognized filamentous bacteriophage, a member of the bacteriophage family.[29,35] Apparently, any natural antibodies to bacteriophage were at a low level or were non-existent. Circulating IgM are defined by their constant regions, but also as a population of antibodies that are secreted at low concentration with cross reactivity to many epitopes, but poor affinity to any given epitope.[383] After a class switch clonal selection increases the binding affinity and concentration of adaptive immune isotypes, followed by clonal expansion; these adaptive isotypes are IgG, IgA, and IgE.

Low levels of natural antibodies are common in poorly cytopathic viruses.[10] As hosts have low evolutionary pressure on HLA sequences to recognize poorly pathogenic viruses, and virus have low pressure on themselves to enter equilibrium with their hosts and produce natural antibody epitopes on capsids to decrease virulence. Given the complete absence of any pathology associated with bacteriophage, it was not surprising that natural antibodies were not detected against λ Before this can be conclusively stated, further experimentation will be necessary.

In T7 bacteriophage, it has been determined that complement is responsible for its rapid clearance.[384] Complement was found to clear T7 bacteriophage via the capsid protein 10B. This was shown using cobra venom factor (CVF), and the EGTA dissociation assay, proving the classical pathway of complement is responsible. In the

classical complement pathway, C1q protein binds the Fc region of IgM or IgG. Sokoloff went on to prove the clearance was IgM dependent by depleting serum of antibody isotypes. A similar mechanism is most likely occurring with λ.

No natural antibodies have been identified for λ, but given the low number and high dissociation constant of any given IgM clone, this was not surprising. It is necessary to find a better assay before the presence of natural λ antibodies can be discounted. One clue to the ability of the innate immune system to recognize λ was the finding that when a lysine to glutamic acid substitution was made at amino acid 158 of gpE, λ becomes a 'long-circulating' variant in vivo.[33,206] 24hrs after the IP delivery of 10^{12}PFU λ, there were still 10^{9}PFU of λ in circulation compared with only 10^{6}PFU in *wt* λ. Undoubtedly a natural antibody in BALBc mice recognizes this region of gpE. It would be interesting to test *wt* λ inactivation and the gpE variant *in vivo* with CVF. An inactivation assay could be more sensitive than measuring relative antibody titers for IgM, which are always at low concentration before class switching.

4.4.6 Innate response to λ

The experiments discussed suggest a strong innate immune reaction to λ. In this section an expansion on the proof for an innate response to λ will be presented. These results then lead into the next chapter where the adjuvant activity of λ will be explored.

Splenocytes proliferate after stimulation with λ. In figure 4.2, it was apparent that regardless of the immunization group, λ typically caused double the proliferation of cells that were grown in media alone. In contrast, purified protein or peptides caused the same proliferation as splenocytes grown in media alone. Therefore something on λ, or in the λ preparations, caused enhanced proliferation in an immunization independent manner. It appears λ caused proliferation regardless of memory.

Bacteriophage have been investigated for use as a subunit vaccine platform since the late 1980's.[29] These experiments began with the use of an adjuvant to increase the immunogenicity of bacteriophage,[29,34] but it was soon found that adjuvants were not necessary for an immune response and protective immunity.[35,43,186,201-203] Irving et al. proposed that the adjuvant activity might be due to LPS.[385] Given the naïve mouse splenocyte proliferation experiment (Fig 4.2) an experiment was undertaken to

investigate λ adjuvant activity in the LPS hypo-responsive mouse C3H/HeJ.[65] In figure 4.3 a similar fold change in proliferation was observed regardless of the genetic background. Furthermore, when IL-10 was investigated in C3H/HeJ mice (Fig. 4.11F), IL-10 secretion was dependent on λ immunization followed by λ immune presentation, whereas when C3H/HeOuJ mice were used LPS was sufficient to elicit IL-10 secretion. Therefore, another TLR was most likely causing immunological activation for λ stimulated animals, and this was dependent on an adaptive immune response. These results lead to the conclusion that the innate immune response between mice and λ was not completely dependent on TLR4 as other factors contribute to the immune response.

In figure 4.11, C3H mice mount a strong humoral immune response to λ. The response was therefore TLR4 independent, but a severely attenuated antibody response to GFP was shown, unless Freund's adjuvant was used. TLR4 provided a large component of the immune stimulation for λ displayed peptides, but a weaker immune stimulation via other mechanisms was sufficient to cause a natural antibody to be selected for a response against λ. Interestingly, if CpG DNA is used as an adjuvant, a Th1 polarized response has been well documented.[386] We have documented that Th1 polarization does occur, as measured by IgG2a production.

The adjuvant activity of λ may not be based on LPS, as TLR2 and TLR4 are known to interact with viral capsid proteins.[85] Indeed it has been documented that the pIII capsid protein from filamentous bacteriophage can act as an adjuvant when fused to a protein.[184] This result must be tempered with the same caution all adjuvant experiments contain: the preparation may have contained contaminants that were responsible for the documented adjuvant activity. With this caution in mind it was interesting to note the strong response, above any recombinant protein or peptide, seen in figure 4.2 and 4.3.

Having outlined how the innate immune recognition for λ may be occurring, a model of λ immune recognition in mice can be proposed. The long circulating mutants of λ suggest natural antibody recognition of gpE.[33,206] IgM is then bound by complement, and is filtered by the spleen where it is recognized by marginal zone macrophages.[384] It was shown herein that splenocytes proliferate when presented with λ regardless of immunization which corroborates the complement finding, whereas draining lymph

nodes are not receptive to λ stimulation. The quality of splenocyte stimulation has been found to be TLR4 dependent, but is not necessary for λ antibodies. 48hrs after splenocyte stimulation, the λ immune reaction has been found to be directed by the secretion of IFNγ, IL-2, and IL-10. The final result of this reaction was the production of IgG antibodies that are both Th1 and Th2 in phenotype. When a TLR4 mutant was immunized with λ, a depressed antibody response with respect to a displayed protein, and Th1 dominant response was observed.

Chapter Five: **Adjuvant activity of Bacteriophage λ**

5.1 Rationale

Bacteriophage have been investigated as a subunit vaccine platform since the late 1980s.[29] As mentioned previously these experiments began with inoculations of bacteriophage together with an adjuvant,[29,34] but it soon became apparent that adjuvants were not necessary in order to stimulate protective immunity with bacteriophage subunit vaccines.[35,43,186,201-203] Given the explosive growth in understanding of innate immune activation since the first TLR4 studies,[64,65,67,158] and more recently as experiments were published which began to describe the mechanism of classical adjuvants,[59,387] we became interested in the adjuvant activity of λ. Given that naïve mouse splenocytes proliferate in response to λ, regardless of immunization (Fig 4.2) we undertook experiments to investigate λ adjuvant activity. Irving et al. proposed that the adjuvant activity might be due to LPS.[385]

Hypothesis: The adjuvant activity for bacteriophage lambda is provided by a Toll-like receptor ligand on the bacteriophage lambda capsid.

Objective A: Identify TLR/TLRs responsive to λ, and if the prototypical TLR ligand is present in λ preparations.

Objective B: Characterize the TLR intracellular signalling in response to λ to provide clues on differential cytokine expression and determine differential TLR activation from different ligands.

The mechanism describing how popular adjuvants function was poorly understood. We endeavoured to characterize the adjuvant activity of λ, as it was unclear whether λ or a bacterial contaminant was responsible for the documented λ adjuvant activity. The understanding of adjuvant activity is necessary before Mashkiki subunit vaccines can be utilized in human trials. Hence, we decided to undertake a systematic analysis of λ immunobiology. With a better understanding of λ immunology, deficiencies and strengths can be adapted and taken advantage of to build better Mashkiki subunit vaccines. It remains to be seen how this knowledge will translate into protective

immunity and immune memory, but the initiation and propagation of the immune challenge is the foundation that builds an immune response. Overall the work presented herein will illustrate the basis for a new vaccine development platform based on bacteriophage λ.

5.2 Summary

In this chapter the adjuvant activity of λ was analyzed by investigating TLR signalling. Recently, the classic human adjuvant, alum, has been shown to be Nalp3 dependent,[57,387] and new adjuvants have been developed based on derivatives of TLR ligands. As pattern recognition receptors are potent activators of adaptive immune responses used by many adjuvants,[388] a study was undertaken to determine the role of TLRs in λ adjuvant activity. Of particular interest to this study was the promiscuous ligand binding of TLRs, that suggested the adjuvant activity of λ could be from the direct binding of λ to a TLR, and not a bacterial contaminant.[85,87,89,389]

The work began by screening λ against a panel of mouse TLRs for NF-κβ activity. λGT10X was found to stimulate TLR4 ligation. When λgfp10-GFP-TAT was investigated TLR4, TLR5, and to a lesser extent TLR2 were stimulated *in vitro*. The increase in TLR signalling may have been due to the presence of GFP or TAT, or it was the result of bacterial contaminants from a sub-optimal preparation of λ. As TLR4 was the common receptor, an analysis of λ preparations for LPS was performed. After visualization of LPS on an electrophoretic mobility assay, λ preparations were found to contain LPS. Intriguingly, the chemotypes present do not match the pattern observed in bacterial LPS, suggesting λ selectively binds LPS chemotypes. The amount of LPS present in λgfp10-GFP-TAT, the preparation used in C3H/HeJ immunization, was ≅ 181.5 endotoxin units (EU)/mL.

In parallel to LPS quantification of λgfp10-GFP-TAT, TLR4 intracellular signalling was analyzed for the activation of MAPK and NF-κβ. λ was found to signal via MAPKs and NF-κβ in the absence of TLR4. In $MyD88^{-/-}$ bone marrow derived macrophages (BMDM), MAPK signalling was equivalent after the addition of either 100ng/mL *E.coli* LPS or 10^9PFU/mL λgfp10-GFP-TAT. In contrast, NF-κβ signalling in λ was more

sensitive to the presence of MyD88 than LPS. This was a novel finding, and might be explained by the presence of λ bound LPS chemotypes, another lipid moiety, or the direct ligation of TLR4 by the λ capsid.

Finally, cytokine expression and secretion was measured in λ stimulated BMDM, peritoneal macrophages, and splenocytes. This work was done concurrently with the studies in chapter 4 and 5. It was found that subtle differences exist between LPS and λ. In all situations λ and LPS produced the same cytokines, but λ produced higher cytokine expression and secretion than LPS. Notably, TNFα expression lasted longer with λ than LPS. In multiplex analysis, LPS and λ produce many MyD88 dependent cytokines,[69] including IFNγ, IL-1β, IL-6, and MIP-1α, whereas the only TRIF cytokine present was IP-10. From the present study, it can now be reported that λ produces TNFα, IL-6, IL-17a, IFNγ, and IL-2.

5.3 Results

5.3.1 Invivogen TLR panel

Bacteriophage λ cause TLR signalling. Two preparations of λ were given to Invivogen (California, USA) to screen on a panel of mouse TLRs. 20μL of 10^{12} PFU/mL λGT10X, a *wildtype* laboratory strain caused TLR4 signalling (Fig. 5.1), whereas 20μL of 10^{12} PFU/mL λgfp10-TAT not only caused TLR4 signalling at a similar value as λGT10X, but TLR5 and TLR2 were also stimulated. When TLR4 signalling was measured with λgfp10-TAT, an OD_{650} reading of 0.86±0.16 was seen, whereas 1 μg/mL of LPS resulted in nearly double this value at 1.57±0.05. TLR5 signalling for λgfp10-TAT gave a similar result with an OD_{650} of 1.27±0.03, whereas 1μg/mL of *S.typhimurium,* the flagellin positive control was more than double this value at 2.66±0.11 OD_{650}. With λgfp10-TAT there was TLR2 signalling but this was marginal at a value of 0.366±0.086 OD_{650}, whereas the positive control had a value of 1.89±0.08, and when the TLR2 cells are grown with no ligand they result in a value of 0.08±0.028 OD_{650}. None of the other TLR signalling complexes tested resulted in signalling with either λ preparation, these included, mouse TLR3, TLR7, and TLR9.

In the Invivogen TLR screen, $2x10^{10}$ PFU of λGT10X or λgfp10-TAT was added to each well of cells. This is 100 times more λ than used for inoculation of an animal. This amount is also 100 times more λ than was added to each well for *in vitro* stimulation experiments.

5.3.2 Hitchcock and Brown LPS imaging

TLR4 signalling was common to λGT10X and λgfp10-TAT preparations, therefore we investigated the amount of LPS present in purified λ. To visualize LPS in λ preparations, Hitchcock and Brown's method was performed (Fig. 5.2).[251] A dilution series of LPS is seen in panel A for lanes 2, 3 and 4, where 10μg, 1μg, and 0.1μg were added. The typical laddering pattern of LPS was seen in lanes 2 to 4. Laddering is due to LPS molecules having varying oligosaccharide polymers. A laddering pattern was absent in lanes where λ was present. As the same pattern was not present between lanes with

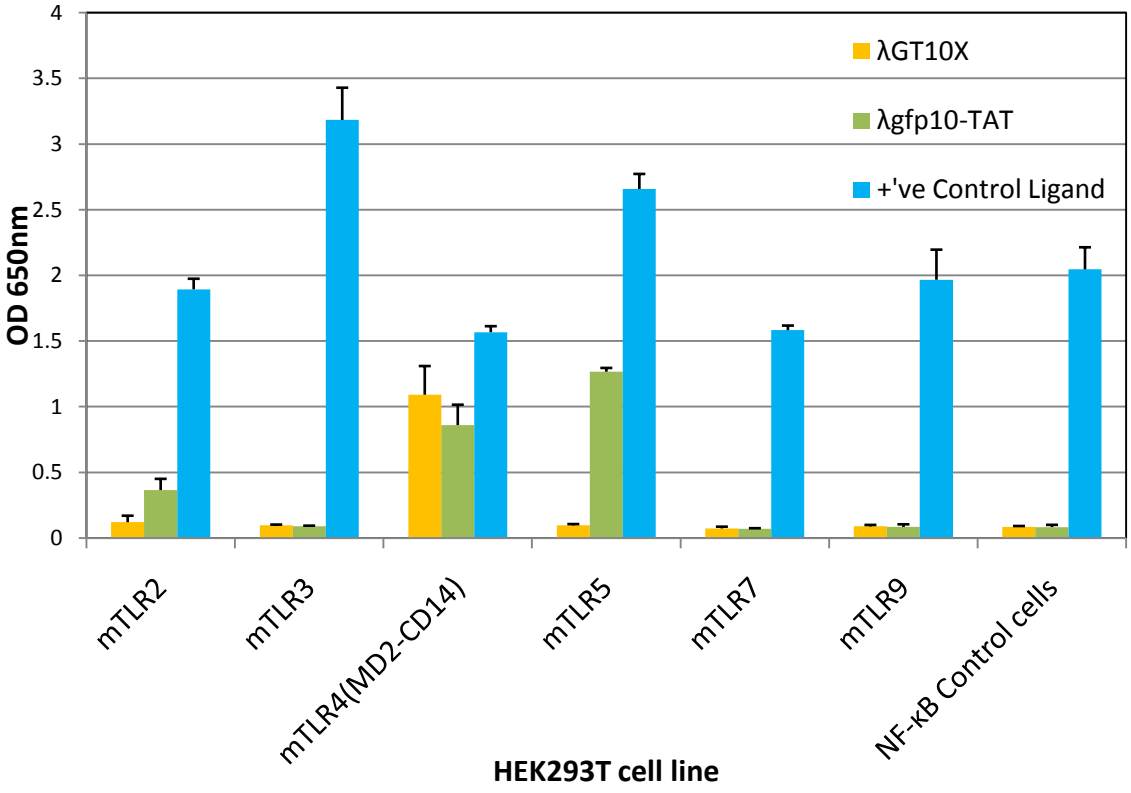

Figure 5.1: Invivogen TLR Ligand Screen.

$2x10^{10}$ purified Bacteriophage λ were added to HEK293T cells containing an Alkaline Phosphatase reporter gene with an NF-κβ promoter (Invivogen). Along the X axis are HEK293T cells containing the TLR signalling complex denoted, where these were absent in the NF-κβ control cells. TLR signalling was measured by Alkaline Phosphatase activity measured by the presence of a QUANTI-Blue™ product at 650nm. Three ligands were tested: the first column, yellow, is purified λGT10X, the second column, green, is purified λgfp10-TAT, and the third column, blue, are the positive control ligands. Each cell line contained 20µL of the following positive control ligand: heat killed *Listeria monocytogenes* at 10^8cells/mL for mTLR2, Poly(I:C) at 1µg/mL for mTLR3, *E.coli* K12 LPS at 1µg/mL for mTLR4, *S.typhimurium* at 1µg/mL for mTLR5, Gardiquimod at 1µg/mL for mTLR7, CpG oligonucleotide 186 at 1µg/mL for mTLR9, and TNFα at 1µg/mL for NF-κβ control cells.

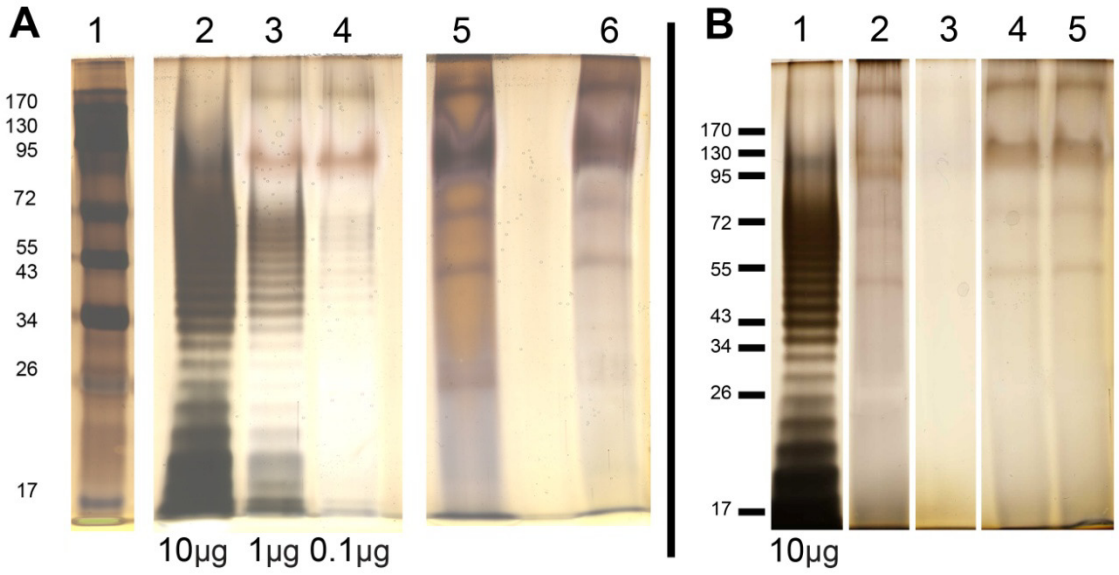

Figure 5.2: LPS in Bacteriophage Lambda Preparations.

LPS was detected in polyacrylamide gels by oxidation and silver staining. In panel A, λ was compared to various amounts of LPS. Lanes 2 to 4 contain a dilution series of LPS where lane 2 was 10µg, lane 3 was 1µg, and lane 4 contained 0.1µg. The last two lanes were 10^{10}PFU of λgfp10-TAT in lane 5, and 10^{9}PFU of λgfp10-GFP-TAT in lane 6. In panel B the amount of LPS was visualized in λgfp10-TAT after running it through a polymyxinB CNBr column.. Lane 1 contains 10µg of LPS, and lane 2 contains 10^{9} PFU λgfp10-TAT. Lane 3 contains the same sample as lane 2, λgfp10-TAT, diluted 1/100 in Ultrapure water (Invitrogen), the titer being 10^{7}PFU. Lanes 4 and 5 contain two fractions of λgfp10-TAT from a polymyxinB CNBr column. Lane 4 was fraction 4 and contained 10^{7}PFU λgfp10-TAT and lane 5 was fraction 5 which contained 10^{6}PFU λgfp10-TAT.

λ and those with LPS no relative quantification was possible. In lane 5, 10^{10}PFU of λgfp10-TAT was present, and lane 6 contained 10^{9}PFU of λgfp10-GFP-TAT. This was equivalent, or 10 times less λ than present in the Invivogen experiment (Fig 5.1).

LPS was removed from λ preparations using a CNBr sepharose column bound with polymyxin B, as previously described (section 2.14.3).[253] Fractions from the affinity chromatography were visualized in panel B of figure 5.2. Lane 4 contains fraction 4, and lane 5 contains fraction 5, both fractions are the same λgfp10-TAT preparation as seen in lane 2, except λ became more dilute following affinity chromatography resulting in a decreased titer. λgfp10-TAT is present at 10^{7} PFU in lane 4, and 10^{6} PFU in lane 5, whereas the original sample in lane 2 had 10^{9}PFU. In order to compare λgfp10-TAT before and after the polymyxin B column, the sample in lane 2 was diluted 1/100 in Ultrapure™ (Invitrogen) H_2O; this sample is seen in lane 3. Ultrapure H_20 was reported to have 0.25EU/mL. After dilution almost all visible staining, or LPS, is lost in lane 3. Lanes 4 and 5 appear equivalent in their staining whereas lane 2 may have more LPS.

The Limulus-Amebocyte Lysate assay was performed on λ preparations to quantify the amount of LPS (Lonza), see section 2.14.2. Double distilled H_2O from our lab was found to have 0.2 EU/mL. This is the water most reagents were made from. SM buffer, the buffer used for λ storage, was measured and found to have a 1.2 EU/mL of LPS. This value was above the standards used to calculate the standard curve and therefore more or less of this amount may be present. This stock of SM buffer was not freshly prepared. When λ preparations are compared, all samples were greater than 1 EU/mL for the dilutions measured. λgfp10-TAT was found to be ~1.5 EU/mL at a 1/121 dilution, whereas the λgfp10-GFP-TAT used in the C3H/HeJ vaccination experiments had >1.5 EU/mL at a 1/121 dilution. Fraction 4 from the polymyxin B affinity column had 1.35 EU/mL of LPS. LPS is evidently present even after the purification protocol developed in chapter 3.

5.3.3 TLR activation of p38 in Bone Marrow Derived Macrophages.

The intracellular signalling cascade from TLR ligation investigated in BMDMs in order to investigate if LPS was causing TLR4 ligation or a λ molecule. In figure 5.3 three panels, A, B, and C report results from: A) a dose response experiment performed

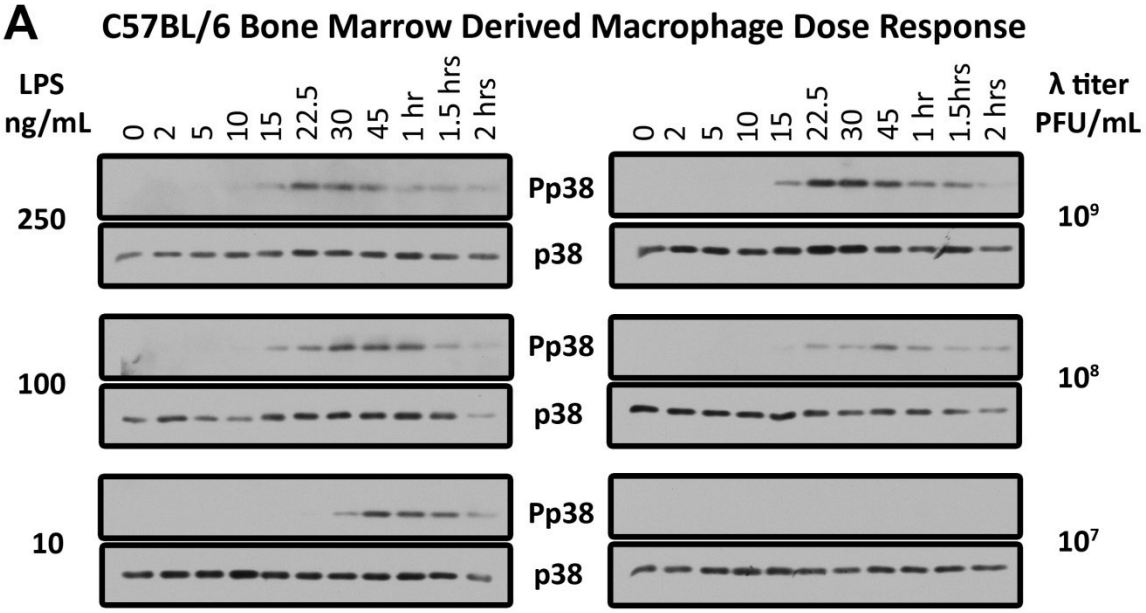

B

	F4/80 alone	F4/80 & Mac1	Mac1 Total	7AAD +
Wt	0.1	16.3	97.0	16.6
TLR2-/-	0.6	40.0	93.2	10.7
TLR4-/-	0.1	18.3	94.4	17.2
MyD88-/-	0.1	8.1	94.6	19.2

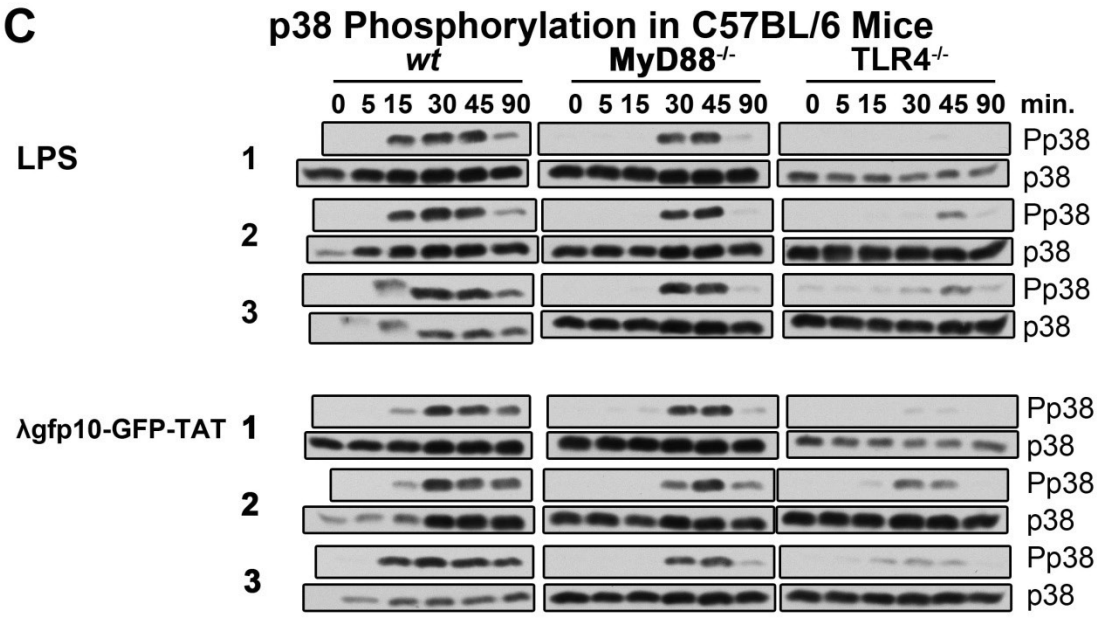

Figure 5.3: TLR activation of p38 in Bone Marrow Derived Macrophages.

Figure 5.3: TLR activation of p38 in Bone Marrow Derived Macrophages.

In panel A various doses of LPS or λgfp10-GFP-TAT were given to bone marrow derived macrophages (BMDM) from *wt* C57BL/6. LPS stimulated cell lysates are depicted on the left whereas λgfp10-GFP-TAT stimulated cells are shown on the right. Each concentration of LPS or λgfp10-GFP-TAT, was probed with phospho p38, Pp38, and then re-probed with total p38. The same animal was used to produce macrophage for all treatments in panel A. In panel B BMDMs were stimulated with 100ng/mL of LPS, or 10^9PFU/mL of λgfp10-GFP-TAT. Animal numbers are denoted on the vertical axis. For each animal samples were collected at 0, 5, 15, 30, 45, and 90 minutes. All samples were probed first with a phospho p38 antibody, then for total p38. For a given animal number, BMDM protein lysates from *wt*, MyD88$^{-/-}$, and TLR4$^{-/-}$ mice were visualized on the same blot. In panel C the flow cytometry data of all animals from the BMDM experiments where the number of cells positive for macrophage cell surface markers was measured after differentiation from bone marrow.

on *wt* BMDM, B) macrophage cell surface proteins measured on BMDM cells, and C) BMDM in response to LPS and λgfp10-GFP-TAT. Panels A and B were controls for figures 5.3 and 5.4, whereas panel C was done with the identical samples from figure 5.4, but a comparison across one animal in each of *wt*, MyD88$^{-/-}$, and TLR4$^{-/-}$ mice could be done for LPS or λgfp10-GFP-TAT with respect to the intensity of p38 phosphorylation.

Prior to performing the experiment outlined in figure 5.3 panel C and 5.4, a dose response experiment was first performed on *wt* C57BL/6 mice. In panel A of figure 5.3 the results of this experiment are shown. LPS and λgfp10-GFP-TAT was added at 3 different concentrations and the phosphorylation of p38 was measured. When 250ng/mL of LPS is added to a BMDM culture, p38 signalling occurred from 15 to 120min. where the peak response was seen at 30min. With only 100ng/mL of LPS added to BMDM cells signalling was present from 15 to 120min. but the peak signal was now at 45min. With only 10ng/mL of LPS present, p38 signalling only occurred from 30 to 120min. and the peak signal was seen at 45min. The overall trend for p38 signalling in response to decreasing amounts of LPS was a temporal shift of the peak signal to later times. For any given sample or time, the intensity of MAPK signalling was equal at the peak, and all samples adjoining looked identical in relation to the peak signal.

When λgfp10-GFP-TAT was added to BMDM cultures from C57BL/6 mice an identical response was seen for 10^9PFU/mL of λ as compared to 250ng/mL of LPS (Fig. 5.3 A). Signalling occurred from 15 to 120min. and the peak response was seen at 30min. The intensity of the Pp38 signal was greater with 10^9PFU/mL of λ as compared to 250ng/mL of LPS. When 10^8 PFU/mL of λgfp10-GFP-TAT was added to a culture, signalling occurred from 22.5 to 120min. The peak signal was at 45min and the amount of Pp38 decreased as compared to the higher titer of λ. At 10^7PFU/mL of λgfp10-GFP-TAT Pp38 was below the detection limit of the assay. 10^6PFU/mL of λgfp10-GFP-TAT was also tested and no Pp38 was present. All dilutions of λ for this experiment were done with SM buffer. From the results of figure 5.3 panel A, the decision was made to perform the TLR signalling experiments in BMDM cultures at 100ng/mL of LPS, and 10^9PFU/mL of λgfp10-GFP-TAT.

In order to determine the identity of cells *in vitro* were BMDMs, cultures were counted for the number of Mac1 and F4/80 positive cells using flow cytometry (Figure 5.3, B). All animals in figure 5.3 C and 5.4 were measured for the number of positive cells in population and were grouped according to mouse strain. 93.2% to 97% of BMDM cells are Mac1 positive, where 93.2% of cells were $Mac1^{+}$ for $TLR2^{-/-}$, and 97% of *wt* BMDM were $Mac1^{+}$. Cells were double positive for F4/80 and Mac1 from 8.1% to 40% across mouse strains, with the average being 21%. Only 0.1 to 0.6 % of BMDM cells were positive for only F4/80.

In panel C of figure 5.3 a comparison of LPS across mouse strains will be done first. BMDM from *wt* animals have p38 signalling from 15 to 90min. In $MyD88^{-/-}$ mice signalling only began at 30min. and very little was seen at 90min. $TLR4^{-/-}$ BMDM had very little signalling if any. Although some p38 signalling was seen in animal 2 at 45min, and in animal 3 signalling was apparent from 30 to 90min. but this was very weak as compared with *wt*, and $MyD88^{-/-}$ mice.

BMDM cultures from *wt*, $MyD88^{-/-}$, and $TLR4^{-/-}$ mice will now be compared in response to λgfp10-GFP-TAT (Fig. 5.3 C). For *wt* mice p38 signalling in response to λ was similar to that seen for LPS, Pp38 is present at 15min and this continued to 90min. $MyD88^{-/-}$ mice had attenuated signalling, where Pp38 was present from 30 to 90min, and a peak was observed at 45min. For $TLR4^{-/-}$ BMDM cultures, p38 signalling was present from 30 to 45min, but this was at lower level than that observed for *wt* and $MyD88^{-/-}$ mice. In animals 2 and 3 of the $TLR4^{-/-}$ mice, where λgfp10-GFP-TAT was added to the BMDM culture, signalling was present from 15 to 45min.

5.3.4 TLR signalling in BMDM

To determine the contribution TLR4 provides for immune activation in a λ subunit vaccine, two arms of the TLR signalling pathway (Fig. 1.1) were investigated using BMDM (Figures 5.3 C and 5.4). The phosphorylation of p38 measured the MAPK pathway, and total Iκβα measured activity in the NF-κβ pathway. Ligation of TLR4 results in both the phosphorylation of p38, which is a hallmark of MAPK signalling, and Iκβα is phosphorylated and then degraded which releases NF-κβ and promotes expression of NF-κβ dependent genes.[390,391] The results below, section 2.5.4, describe figure 5.4.

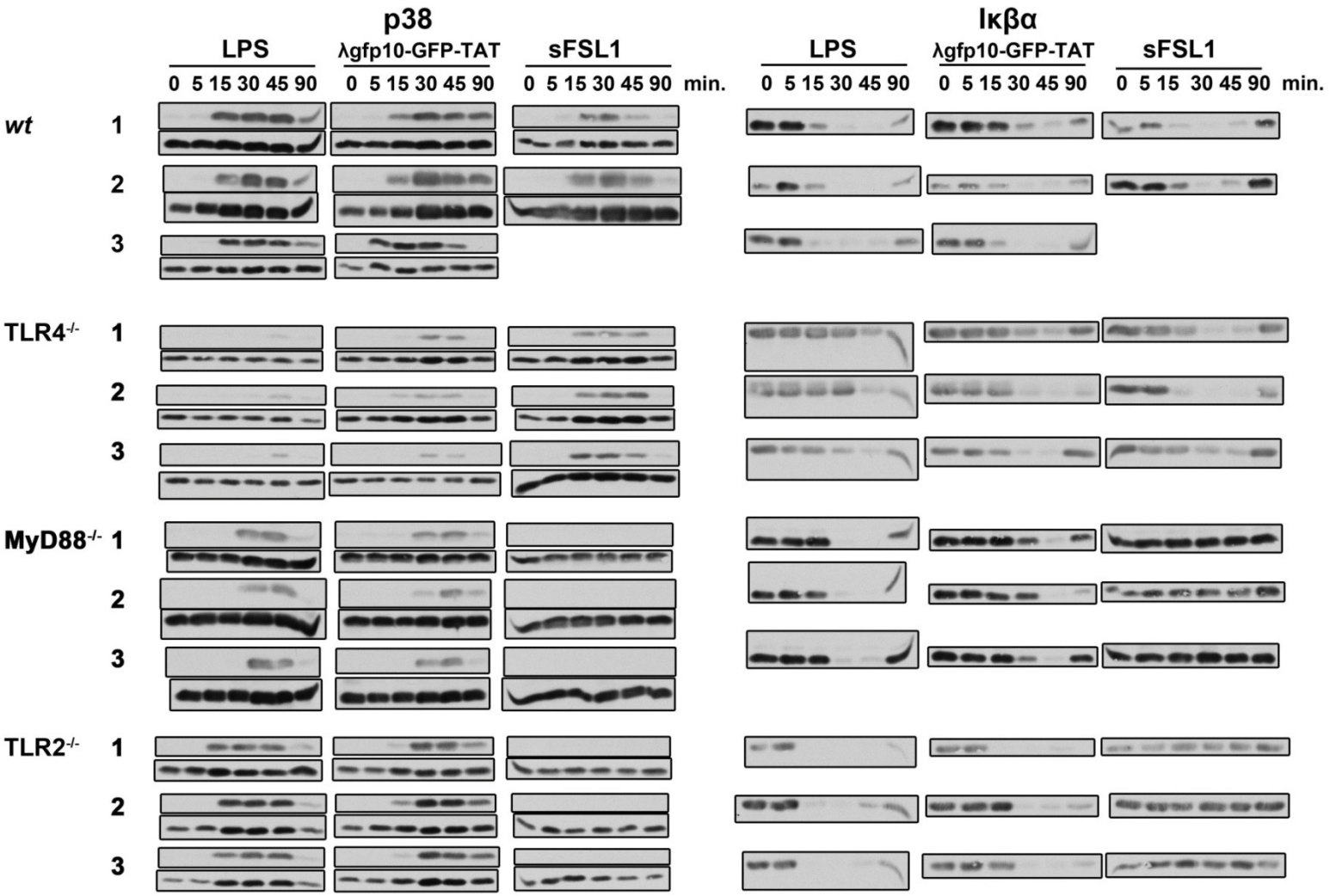

Figure 5.4: TLR Signalling in BMDM – Comparing ligands across an animal.

Figure 5.4: TLR Signalling in BMDM – Comparing ligands across an animal.

TLR signalling was measured by p38 and Iκβα in four mouse strains, each strain having three separate animals, as denoted on the vertical axis. BMDM from each animal were given three ligands: 100ng/mL of LPS, sFSL-1, or 10^9PFU/mL λgftp10-GFP-TAT. On the left side of the figure, p38, the top panel for each animal is phospho p38, and the bottom panel is total p38, whereas for Iκβα, the right side of the figure, only total Iκβα was measured. Samples were collected at 0, 5, 15, 30, 45, and 90 minutes. For each mouse LPS, λ, and sFSL-1 samples were visualized on the same blot with a given antibody.

5.3.4.1 NF-κβ signalling in BMDM

The amount of Iκβα in BMDM stimulated with either LPS, λgfp10-GFP-TAT, or synthetic Pam2CGDPKHPKSF (sFSL-1) will be reported first. The amount of Iκβα will be described first across animals with a given ligand; and then down a column in figure 5.4. As the samples being compared down a column were on different blots, no comparison of intensity can be made, but the timing of signalling can be compared across mice.

When λgfp10-GFP-TAT, referred to herein as λ, was added to BMDM cultures of *wt* C57BL/6 mice, NF- κβ signalling begins at 15 min. and ends at 90min. In Myd88$^{-/-}$ mice λ resulted in Iκβα degradation being delayed to 45min, although some degradation was seen at 30min, and Iκβα returned by 90min. TLR2$^{-/-}$ mice have a similar Iκβα response to λ as *wt*, except NF-κβ signalling was extended beyond 90min. TLR4$^{-/-}$ animals produce an NF-κβ signal in animals 2 and 3 which was similar to *wt* animals, but there was weak or non-existent signalling in TLR4$^{-/-}$ animal 1.

BMDM cultures supplemented with 100ng/mL of LPS will now be compared across animals for the presence of Iκβα. In *wt* mice, NF-κβ signalling began at 15min. and ended at 90min. The TLR2$^{-/-}$ mice were identical to *wt* with respect to NF-κβ signalling. As with λ stimulation, MyD88$^{-/-}$ mice have delayed NF-κβ signalling in response to LPS, Iκβα is degraded at 30min, but reappeared by 90min. TLR4$^{-/-}$ mice had little or no Iκβα degradation. In TLR4$^{-/-}$ animals 2 and 3 had Iκβα degraded at 45min, but at no other timepoint was any degradation seen.

sFSL-1 will be the last ligand discussed for Iκβa degradation across animals. *Wt* animals began to signal through NF-κβ at 15min. and Iκβα returned by 90min. In MyD88$^{-/-}$ and TLR2$^{-/-}$ mice no NF-κβ signalling was observed as determined by Iκβα. TLR4$^{-/-}$ mice responded to sFSL-1 by 15 or 30min, and this response stopped at 90min. TLR4$^{-/-}$ mice and *wt* mice had a similar signalling profile.

Figure 5.4 was prepared to compare the relative intensity of Iκβα for each animal in response to LPS, λgfp10-GFP-TAT, or sFSL-1. To accomplish this the time courses for a given animal for all three ligands were run on the same western blot. In *wt* animals LPS caused degradation of Iκβα by 15min and at approximately 90min Iκβα recovered. λ

is slightly more delayed as it caused degradation between 15 and 30min, depending on which *wt* animal, and recovery occurred at 90min. sFSL-1 presented a similar time course as λ, where NF-κβ signalling began at approximately 15min. and was finished by 90min. in *wt* animals.

Next Iκβα degradation was compared across TLR4$^{-/-}$ mice for all three ligands. LPS caused little or no signalling, but in 2 of 3 animals some degradation was seen at 45min. On the other hand λ and sFSL-1 resulted in NF-κβ signalling that was similar to one another. λ caused Iκβα degradation at 30 and 45min, as did sFSL-1. In TLR4$^{-/-}$ animal 2, sFSL-1 appeared to cause NF-κβ signalling from 15min to 90min. If animals 1 and 3 were switched, the Iκβα response between λ and sFSL-1 stimulated mice would be nearly identical.

For all three MyD88$^{-/-}$ mice, LPS caused NF-κβ signalling from 30 to 90min. When λgfp10-GFP-TAT was added to BMDM cultures, signalling was less at 30min. but did occur, and this continued to 90min. No signalling was present in MyD88$^{-/-}$ mice when BMDM were given sFSL-1. Nor did BMDM from TLR2$^{-/-}$ mice degrade Iκβα in response to sFSL-1. When TLR2$^{-/-}$ BMDM are cultured with LPS or λ, Iκβα degradation appeared similar to *wt* BMDM.

5.3.4.2 <u>p38 signalling in BMDM</u>

The phosphorylation of p38 in BMDM was measured using a phosphate specific p38 antibody, shown on the top panel of each time course, and an antibody for total p38 for the bottom panel of each time course (Figure 5.4). Total p38 was probed to show equal loading of samples. As with Iκβα, first a comparison of Phospho p38 (Pp38) will be made for a given ligand across animals, down a column.

First, λgfp10-GFP-TAT will be compared across mouse strains. λ caused robust p38 signalling from 15 to 90 min in 2 *wt* animals, with the 3rd animal responding to λ by signalling through p38 from 5 to 45min. BMDM from TLR4$^{-/-}$ mice had p38 signalling when λ was added after 30min. and this continued to 45min. for two animals. The third animal responded by 15min. and continued to signal up to 90min. In MyD88$^{-/-}$ mice, p38 signalling was seen from 30 to 90min, whereas in TLR2$^{-/-}$ mice, as with *wt* mice, p38 signalling began at 15min. and continued to 90min.

LPS will be the second ligand to be compared for the timing of p38 signalling across BMDM from various mouse strains (Fig. 5.4). LPS in *wt* animals caused p38 signalling from 15 to 90min. In TLR4$^{-/-}$ mice there was weak signalling at 45min. The lack of MyD88 did not stop p38 signalling in response to LPS, as robust p38 signalling was seen from 30 to 45min, but this response was attenuated as compared to *wt* BMDM as no signalling was seen at 15min, and very little signalling was seen at 90min. In BMDM from TLR2$^{-/-}$ mice LPS caused identical p38 signalling as with *wt* BMDM. The last ligand to be compared across mouse strains is sFSL-1. When sFSL-1 was added to BMDM cultures, p38 signalling was robustly seen from 15 to 45 min in BMDM cultures from *wt* and TLR4$^{-/-}$ mice, but signalling was completely absent in MyD88$^{-/-}$ and TLR2$^{-/-}$ mice.

A more comprehensive comparison can be made when comparing LPS, λgfp10-GFP-TAT, and sFSL-1 stimulation of p38 signalling across an individual animal. The relative intensity of Pp38 across an animal can be compared, because samples from each ligand for every time point were loaded onto the same blot for a given animal. In *wt* BMDM, LPS and λ resulted in similar signalling, where Pp38 was present for 4 time points. The amount of Pp38 present after the addition of sFSL-1 to BMDM cultures was less than for LPS, and λ. With sFSL-1 p38 signalling was robustly seen from 15 to 45min., and was barely present at 90min.

BMDM cultures from TLR4$^{-/-}$ mice will now be compared across an animal for Pp38. When sFSL-1 was added to a BMDM culture from TLR4$^{-/-}$ mice, p38 signalling was identical as *wt* BMDM. Signalling decreased in λ stimulated BMDM cultures, where the majority of signalling was only present from 30 to 45 min., as compared with 15 to 90min in *wt*. Noteworthy was animal 2 in the TLR4$^{-/-}$ group for λgfp10-GFP-TAT, which had signalling present from 15 to 90min, this was identical to *wt* BMDM after the addition of λgfp10-GFP-TAT. With LPS added to BMDM cultures from TLR4$^{-/-}$ mice signalling was nearly absent, although a small amount of Pp38 was visible at 45min.

In contrast to p38 signalling in TLR4$^{-/-}$ BMDM, MyD88$^{-/-}$ BMDM p38 signalling in response to LPS, and sFSL-1 was very different. sFSL-1 did not cause p38 signalling in MyD88$^{-/-}$, but LPS did cause phosphorylation of p38 from 30 to 45min. LPS had a

small amount of Pp38 at 90min in 2 of 3 animals. LPS in BMDM cultures from MyD88$^{-/-}$ mice resulted in an attenuated response as compared with *wt* animals, which had signalling from 15 to 90min. λgfp10-GFP-TAT caused more p38 signalling than LPS when added as a ligand in Myd88$^{-/-}$ BMDM culture. For λ, p38 signalling occurred from 30 to 90min.

TLR2$^{-/-}$ BMDM cultures will now be examined. When LPS was added to BMDM cultures, p38 signalling occurred from 15min to 90min, this was similar to *wt* animals, except the amount of Pp38 was weak at 90min. When λ was added to BMDM cultures, p38 signalling occurred from 15min to 90min, but in this situation the stronger Pp38 was seen at 30 to 90min. and at 15min the amount of Pp38 was less. When sFSL-1 was added to BMDM from TLR2$^{-/-}$ mice no p38 signalling was seen.

5.3.5 Cytokine response to BMDM stimulation

In figure 5.5 the cytokine induction data from C57BL/6 BMDM cells is shown in panel A. In panel B the cytokine gene expression from peritoneal macrophages in response to LPS and λgfp10-GFP-TAT stimulation is shown. When media from BMDM cells were collected at 2hrs and 6hrs following the addition of LPS or λgfp10-GFP-TAT, large concentrations of TNFα and IL-6 were measured. At 2hrs a titration effect was seen for the amount of TNFα produced in response to different titers of λgfp10-GFP-TAT, where 10^7PFU produced 73pg/mL, 10^8PFU produced 793pg/mL, and 10^9PFU produced 1742pg/mL. In contrast, a 25 fold difference between the amounts of LPS added did not change the order of magnitude of TNFα production at 2hrs, as 250ng/mL resulted in 1742pg/mL, and 10ng/mL produced 1633pg/mL. At 6hrs the amount of TNFα produced in BMDM cultures with LPS did not change appreciably. Whereas the highest titer of λ added to BMDM cells produced 32,306pg/mL, or 18 times more TNFα. Across λ concentrations at 6hrs, a titration effect was seen, where each log10 decrease in λ titer decreased the concentration of TNFα by an order of magnitude. When two-way ANOVA was performed a significant difference across time, treatment and their interaction was documented. Furthermore the addition of 10^9 λgfp10-GFP-TAT results in a significantly different amount of TNFα at 6hrs as compared to all other treatments, which highlighted the dichotomy between LPS and λ treatment in BMDM.

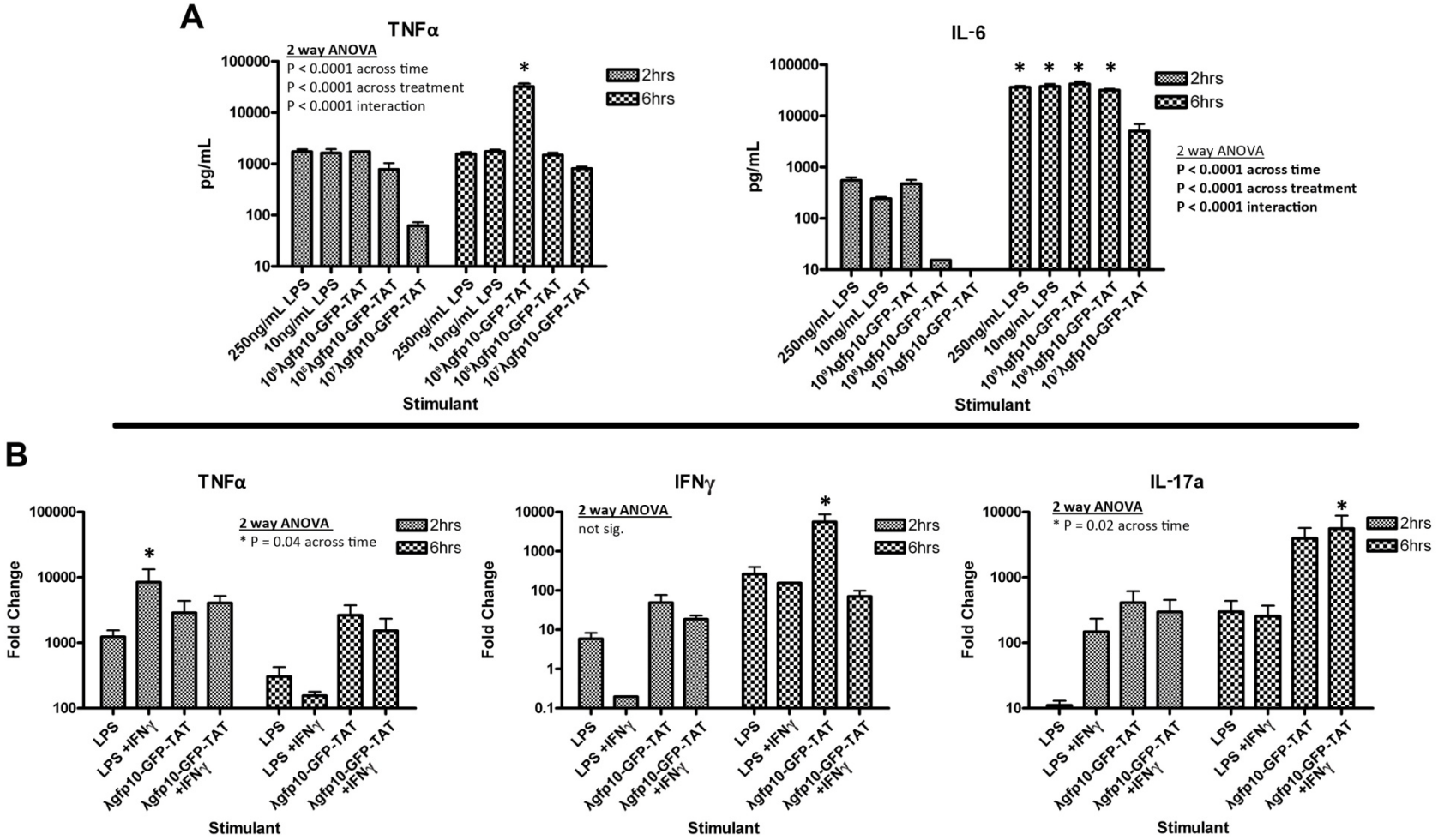

Figure 5.5: Macrophage Cytokine Expression/Secretion.

Figure 5.5: Macrophage Cytokine Expression/Secretion.

In Panel A, the concentration of TNFα and IL-6 secreted from C57BL/6 bone marrow derived macrophage were measured using a Luminex. Media was collected at 2 and 6 hrs, after stimulation with LPS or λgfp10-GFP-TAT. Along the X axis from left to right BMDM were stimulated with 250ng/mL, or 10ng/mL LPS, or 10^9, 10^8, or 10^7 PFU/mL λgfp10-GFP-TAT. In panel B quantitative real time PCR was performed on CD1 peritoneal macrophages. The expression of TNFα, IFNγ, and IL-17a was measured following stimulation of CD1 macrophage with 100ng/mL LPS, or 10^9PFU/mL λgfp10-GFP-TAT. Half of the samples were stimulated with 10ng/mL IFNγ 15hrs. prior to the addition of LPS or λ. Samples were collected at 2 and 6hrs. Two-way ANOVA was performed on each panel and the statistical significance of each factor (time and treatment), and their interaction was calculated. A Bonferroni post test was then performed to compare pairs of means to each other, and statistically significant means were highlighted with a star above the treatment or column.

IL-6 concentration after 2hrs of LPS treatment resulted in 584pg/mL and 276pg/mL for 250ng/mL and 10ng/mL of LPS respectively. At 6hrs IL-6 concentration from LPS treatment had increased to 36,155pg/mL and 37,558pg/mL, for 250ng/mL and 10ng/mL of LPS respectively. When λgfp10-GFP-TAT was added to BMDM, again a titration effect was observed for the concentration of IL-6 produced. For each time point the maximal value was in the same order of magnitude as that for 250ng/mL of LPS, but the lower concentrations of λ resulted in an order of magnitude less IL-6 being produced. IL-6 production was significantly different across time, treatment, and their interaction (Two-way ANOVA). Bonferroni post test proved the four highest concentrations of treatments were significantly different at 6hrs than all other samples in this experiment.

BMDM cells stimulated with LPS and λgfp10-GFP-TAT were also investigated for IL-1α, IL-1β, IL-4, IL-10, and IFNγ. No other cytokine gave as great a response as seen with IL-6 and TNFα, but some interesting effects were observed. IL-1α, and IFNγ concentrations were less than or equal to non treated BMDM cells at 2 and 6hrs. Whereas IL4 was completely absent at these times. IL-1B was above the non treated cells at 6hrs, the concentration of samples being between 30 and 59pg/mL, except for 10^7PFU/mL of λ which had a concentration equal to the non-treatment control cells. When IL10 concentration was measured at 2hrs, marginal values were recorded, but at 6hrs both LPS samples and the highest λgfp10-GFP-TAT samples resulted in concentrations between 45pg/mL to 56pg/mL.

In a slightly different type of experiment peritoneal macrophages from CD1 mice were cultured with LPS or λgfp10-GFP-TAT, and the relative expression of TNFα, IFNγ, and IL-17a were measured using QRT-PCR (Fig. 5.5B). When the relative TNFα expression was measured, LPS caused peak expression at 2hrs ($P<0.05$) which decreased by an order of magnitude at 6hrs. In contrast, λgfp10-GFP-TAT gave the relative expression of TNFα at 2hrs and 6hrs. With IFNγ expression, λgfp10-GFP-TAT alone gave the highest fold increase and was 1 order of magnitude greater than LPS at 2hrs and 6hrs. Two-way ANOVA proved there was a statistically significant difference in samples across time, but the variance was much higher in QRT-PCR than Luminex analysis and this contributed to decreased P values.

When IL-17a expression was compared, LPS alone had very little effect at 2hrs, but λ had 1 order of magnitude greater effect at 2hrs and 6hrs. In this experiment a statistically significant difference was observed across time, but again the variance in QRT-PCR was high. The presence of IFNγ had produced a statistically significant difference in the amount of IL-17a produced at 6hrs.

To further extrapolate on the aforementioned results a one off experiment was performed on a panel of 22 mouse cytokines. Splenocytes from the TLR4 hypo-responsive mutant, C3H/HeJ, were tested for cytokine secretion after LPS and λ stimulation. In this experiment samples were not measured in duplicate. No conclusions can be made with this data, but some interesting effects were seen. In splenocytes from C3H/HeJ mice λ induced IL-6, IL-9, IL-10, IL-13, IP-10, and MIP-1α at 6hrs. On the other hand no difference was seen in splenocytes stimulated with λ or LPS for IL-1α, IL-1β, IL-2, IL-4, IL-5, IL-7, IL-12p70, IL-15, IL17, TNFα, M-CSF, GM-CSF, and MCP-1. When cytokines are measured in response to LPS the six cytokines with high concentrations for λ are also induced, but at a lower level. A few cytokines, IL-2, TNFα, and KC, that were cited as negative for secretion are in fact positive, but they were inconsistent across the samples assayed. All cytokines that were inconsistent had greater concentrations in λ samples than LPS samples.

5.4 Discussion

After the results obtained in Chapter 4 the hypothesis for Chapter 5 was that TLR signalling was responsible for the adjuvant activity of λ. Innate immune signalling by TLRs has long been associated with the danger signal that leads to an adaptive immune response,[46,48-50,52,193,392-396] therefore this mechanism could be responsible for the adaptive immune response observed in Chapter 4. Alternatively, λ may use a similar mechanism as alum, which is not TLR dependent, but uses the NOD-like receptors (NLRs) to activate the NALP3 inflamasome.[57,387] Therefore λ could be using TLRs or NLRs for immune activation, or yet another pathway such as the retinoic acid-inducible gene I- like receptor (RLR) could be responsible for λ adjuvant activity.[98,141] Chapter 5 of this thesis was a study to investigate the role TLR signalling in the adjuvant activity of λ.

5.4.1 TLR screen

In figure 5.1 a panel of mouse TLRs were screened using the Invivogen™, *in vitro* TLR screening method. *Wt λ*, seen here as λGT10X, only stimulated the receptor that recognizes LPS, TLR4.[64,65,67,85] Whereas λgfp10-TAT stimulated TLR5, TLR4, and TLR2. In fact λgfp10-TAT caused stimulation of NF-κβ through TLR5 twice the intensity of TLR4 which was itself stimulated 2.3 times more than TLR2. These receptors are known to recognize flagellin, LPS, and lipoteichoic acid and peptidoglycan respectively.[85,247,397] No signalling was seen from TLR3, TLR7 and TLR9. This is interesting as these receptors signal from endosomes,[85,398] this may be an artifact of the Invivogen™ system, whereby surface displayed TLRs do not recognize intact virus, as their ligands have not been released from the viral capsid via endosomal processing. It is also possible that λ does not stimulate the endosomal TLRs.

The increased number of TLR molecules stimulated by λgfp10-TAT has a few possible explanations. In the simplest scenario, this preparation was contaminated with more bacterial TLR ligands than the λGT10X preparation and thus signalling was seen in more TLRs. The observed result could support this hypothesis, as flagellin is a common bacterial component, but TLR2 and TLR4 being stimulated was strange. *E.coli* are gram negative bacteria, therefore LPS is present, but TLR2 ligands are gram positive cell wall

components, and the preparation of λ was done with *E.coli.* Therefore, something beyond our samples being contaminated with bacterial debris must be occurring. This discrepancy may be TAT dependent, and if so it could be the result of TAT itself, via its positive charge or amino acid composition, or due to something it is binding during the preparation of λ. If TAT is responsible for signalling through TLR5, TLR2, and/or TLR4, then a new ligand has been found for these receptors. This possibility could also exist with respect to λGT10X, whereby λ itself is the ligand for TLR4. Given the co-evolution of our gut flora, and the innate immune system this may explain the adjuvant activity of λ and/or TAT. Many TLRs are now known to be promiscuous,[85,87,89,389,398,399] and new ligands for each receptor are being discovered.

5.4.2 LPS

As TLR4 was the receptor stimulated in both *wt* λ, and λgfp10-TAT preparations we investigated if LPS was present. To identify LPS, polyacrylamide gels were used to visualize lipids.[251] In figure 5.2, no λ samples were seen with the stereotypical laddering pattern indicative of bacterial LPS.[74-76,251,400] A ladder like pattern is typical of LPS as this molecule is composed of lipid A at its core, and oligosaccharide polymers of various lengths are assembled onto it.[46,73,251] Perhaps lane 4 of panel A, 0.1μg of LPS, was similar to lane 6, 10^9PFU/mL of λgfp10-GFP-TAT. Therefore, the amount of LPS in lane 6 might be comparable to 0.1μg of LPS, but there are two differences between these samples.

First, for λ in lane 6 no laddering was seen, whereas when less LPS was visualized in lane 4 the larger sizes of LPS remained visible and continue to show a laddering pattern from ~34kDa to 72kDa. Therefore, as the number of molecules of a given polymer size of LPS remains constant, with less LPS added only the larger LPS molecules were silver stained enough to remain visible. A more apt comparison might be lane 4 from panel B, 10^7PFU/mL λgfp10-TAT, to lane 4 from panel A, 0.1μg LPS. From this comparison we could say that 10^7PFU/mL of λgfp10-TAT in lane 4 contains 0.1μg of LPS. This is only an approximation though, as it is difficult to compare samples that are imaged separately. The comparison cannot be made as these samples were visualized on

different gels, and the exposures will not match, although the 10μg LPS samples for lane 2 panel A and lane 1 panel B are roughly equivalent.

The second difference between LPS and λ samples was the appearance of only a few major species for λ, the major one being ~95kDa. At 95kDa, the lipidA core is not the major species, as lipid A will have the greatest electrophoretic mobility in each lane. Lipid A nucleates the polymer and is thus the start of the chain, and the smallest molecule on the gel,[73,76] but as only sugar molecules will be stained by silver nitrate after periodic oxidation, lipid A was not seen in figure 5.2.[401] A large polymer ~95kDa could be indicative of an *E.coli* strain variant which changes the polymer size of LPS. This has been described for W3110 *E.coli*, which is the parental strain of K12, the laboratory *E.coli* strain that is parental to LE392.[76,402-404] Strangely, LPS molecules in λ preparations also have minor chemotypes with sizes ~26, ~55, ~72, and >170 kDa, together with a major species at ~95kDa. This is very different than previously described.[76] In W3110 *E.coli,* small chemotypes of LPS were absent, but at the larger polymer sizes the ladder pattern was still evident in a 12.5% to 14% polyacrylamide gel.[76] In figure 5.2, a 12.5% polyacrylamide gel was prepared, and no laddering was seen around 95kDa for λ samples.

In λ preparations LPS was present but the chemotypes are different varieties than seen in bacterial preparations (Fig 5.2). In a λ preparation (Section 2.5.5.1), specific chemotypes of LPS are co-purified with λ. This may be an artefact of the purification method, or it could be indicative of λ using LPS in the capsid. A study is necessary to determine if bacteriophage λ particles associate or bind LPS molecules for capsid stability. Few studies have described the chemotype of LPS as most experiments simply measure the amount of LPS using the LAL assay. The data in figure 5.2 could support the idea that λ has undergone two evolutionary pressures. One selective pressure was for stability, or to remain long lived and this could have caused the incorporation of LPS from bacteria during λ maturation. The binding of LPS is not without precedence in the bacteriophage family, as HI8A and HI8B adsorb LPS on *E.coli*.[400] In ϕX174, the spike proteins G and H bind LPS, and in particular the G protein has been found to bind lipid A.[405] Within the λ family, classic studies on T3, T4, and T7 have shown adsorption to be

LPS dependent, but the specificity to the O antigens or lipid A was not determined.[406,407] In each of these bacteriophage studies the work investigated adsorption to bacterial host by a bacteriophage protein, whereas the data in this thesis suggests capsid binding of LPS preceding adherence to the bacterial membrane, which may be contributing to stability or immune evasion. This hypothesis can then be incorporated into the other selective pressure on λ, to keep the mammalian host alive. The co-evolution of LPS incorporation into the λ capsid would result in a potent indicator of gastro-intestinal immune barrier maintenance.

Polymyxin B columns were not successful at purifying λ from LPS contamination. Using a previously described method,[253] LPS was not removed from λ preparations (Fig. 5.2 panel B). Some LPS appears to have been removed, as the amount of background staining decreased after elution from the polymyxin B column. Please note the nearly identical LPS staining in lanes 4 and 5 regardless of lane 5 containing less λ, by one order of magnitude. Strangely, when the original λ stock, lane 2, was diluted in Ultrapure™ water to an equivalent titer as for λ in lanes 4 and 5, LPS staining is nearly lost. The 95kDa LPS band did remain visible, but was almost undetectable to the human eye. Two explanations exist for this scenario. In the first, SM contains LPS, or a component of SM does. All components of SM are salts, except gelatine, which could be responsible for contamination. Gelatin is the hydrolyzed form of collagen and is used to increase the stability of λ in SM buffer. Collagen is a protein, therefore it, along with other proteins were not present after proteinase K digestion of λ preparations, but LPS may be present in the stock of gelatin. The presence of LPS in gelatin must be determined. In the second scenario, when λ was diluted by the addition of Ultrapure™ water, instead of SM buffer, λ could have been destabilized and may have been lost in processing, along with LPS. The loss of LPS after the dilution of λ in Ultrapure™ water was puzzling and so an LAL assay was performed to quantify the amount of LPS in λ preparations.

The LAL assay was one of the first to be approved by the Food and Drug Administration for measuring LPS concentration.[408] LPS was measured against a standard curve in the LAL assay, and the units of measurement are endotoxin units/mL,

or EU/mL. When an LAL assay was performed on the double distilled H_2O from our lab 0.2 EU/mL was measured. For comparison Ultrapure™ water from Invitrogen was cited as having 0.25EU/mL. Therefore, the LPS seen in λ preparations was not from the water in the laboratory. SM buffer had much higher LPS concentration (1.2 EU/mL) and this could explain the high levels seen lanes 4 and 5 of panel B in figure 5.2. As the amount of LPS measured in lanes 4 and 5 did not lower as the titer of λ did, the LPS present was from the buffer, or was diluted in the SM buffer of the column. In contrast the amount of LPS measured for λgfp10-GFP-TAT was found to be >1.5 EU/mL at a 1/121 dilution. After running the sample through the polymyxin B column this value decreased to 1.35 EU/mL for lane 4 of figure 5.2 panel B. Therefore, the polymyxin B column was successful at removing LPS, but the SM buffer may have contributed to the 'basil' reading of 1.2 to 1.35 EU/mL. The LAL assay is known to react to the lipid A molecule in LPS,[409] but it is unclear if the O antigen is measured. The identification of reactive species is important, as the silver staining method from figure 5.2 identified the O antigen, or sugar molecules, whereas the LAL assay is specific to lipid A.[409,410]

In previous studies it has been found that prior to ultracentrifugation in cesium, λ preparations have 50,000 EU/mL of LPS, whereas after ultracentrifugation samples varied from 3 to 1,000 EU/mL.[33] In the present study values of ≅ 181.5 EU/mL of LPS for the stock of λ used in vaccination and for stimulation experiments were observed. After a further purification using a polymyxin B column, λ was found to have only 1.35 EU/mL of endotoxin. This value would be acceptable for human treatment under current FDA guidelines which state that 5.0 EU/ng or 5.0 EU/mL of product can be administered per kilogram of each patient when delivered intraperitoneally.[408] The amount of LPS administered per mouse was greater than the FDA guideline, given the size of our animals. The average mouse was 32.0 ± 3.4g when euthanized. The amount of LPS administered to each mouse at each injection was 10μl of a 181.5 EU/mL solution containing λ, or 1.8 EU was administered, which is 11.25 times the acceptable limit for human consumption. We could decrease the amount of LPS further with an improved method for production of SM buffer, or by using a commercial column to remove LPS.[191,411]

The LAL assay is known to measure LPS and lipid A.[409] The LAL assay is characterized by its extreme sensitivity, which is due to its derivation from an immune reaction in *limulus polyphemus* to gram negative bacterial infections.[409,412] As mentioned previously λ has been shown to adsorb LPS.[406,407] Given the data herein this may occur not only during the infectious part of the λ lifecycle, as it adsorbs onto its host, but it could be occurring during the growth or lysogenic phase of λ. If this did occur it would result in the rapid clearance of λ from mammalian blood.[26-28,30,33,35,36,38,42,44,413] This does occur, but a basal level of λ was always present in blood, which suggests LPS was not present. Furthermore the presence of LPS on λ would preclude it from entering the CNS, but λ entering the CNS is well documented.[26,42,44] An intriguing mechanism used by another lipoprotein could be occurring. The bacteriophage lipoprotein genes for *bor/iss* are expressed on the surface of *E.coli*, and allow for serum complement resistance.[414-416] The Bor/Iss lipoproteins may also affect TLR4 binding of LPS. This effect needs to be defined further. Perhaps λ incorporates LPS, and evades immune detection with the Bor and Iss lipoproteins.

The amount of LPS and λ present in the peritoneal and BMDM experiments described hereafter used 10^9PFU/mL of λ, and were equivalent to lane 5 of panel A in figure 5.2 for the amount of LPS, or approximately 1.82 EU. Depending on the chemotype of LPS 1EU is generally seen as 100pg, therefore 1.82 EU will equal 182 pg. This amounts to 10x less λ and LPS than the λ sample given for the Invivogen assay.

5.4.3 Bone Marrow Derived Macrophages

A dose response experiment was first performed on BMDM to determine the optimal amount of LPS and λgfp10-GFP-TAT to measure MAPK signalling, as measured by p38 phosphorylation. BMDM were utilized as they can be grown in sufficient numbers to perform western blot analysis on protein phosphorylation. In figure 5.3, panel A, 100ng/mL of LPS gave an equivalent result as 10^9 PFU/mL of λgfp10-GFP-TAT, all subsequent experiments shown in figure 5.3 C and 5.4 utilized these amounts. As a corollary, 100ng/mL of LPS is a common concentration in many *in vitro* stimulation experiments, which facilitates the comparison of results.[64,80,417-423] In figure 5.3 A, when λ and LPS concentrations were decreased the phosphorylation of p38 occurred at a later

time, and a corresponding shift in the peak signal was observed. Given the discussion on LPS in the previous section, it is interesting to note that λgfp10-GFP-TAT was diluted in SM buffer, yet the concentration of LPS in this buffer did not result in p38 signalling being present at 10^7 and 10^6 PFU/mL. This experiment was done with SM buffer prepared before the LAL assay was performed therefore no comment can be made on the amount of LPS in this SM buffer, but given the amount of LPS in the laboratories ddH_2O and the amount measured in the SM buffer was most likely 0.2 to 1.35 EU/mL. Therefore p38 phosphorylation in figure 5.3 and 5.4 was dependent on the λ preparation and not on the buffer.

BMDMs were differentiated as previously described (section 2.11.3).[250,424] Macrophage are known to be the only cells viable after differentiation of bone marrow cells *in vitro* with colony stimulating factor (CSF),[250,424] but as with all experiments the appropriate control was necessary to prove no contaminating cells were present. Flow cytometry was performed to identify the phenotype after differentiation, using two myeloid cell markers: F4/80 and Mac1 (CD11b). All BMDM cultures in figure 5.3 were >93% $Mac1^+$, and 21% of cells were positive for both F4/80 and Mac1. This value was expected to be higher but a relative fluorescence gate of 100 was set, and this resulted in many F4/80 cells not being counted as positive. These values are similar to previous studies.[425] Other surface antigens could have been measured to count contaminating cells, these would include $CD3^+$ for T cells, and $DX5^+$ for NK T cells, NK cells, fibroblasts, and platelets.[425] As this work was done in collaboration with experts in the field, and cell morphology was consistent with previous experiments this was not performed. One troubling finding was the number cells dead in each BMDM culture. The BMDM cultures were grown at a higher cell density and for longer than described in some protocols, which most likely contributed to cell death. In future experiments this could be improved by decreasing the number of cells seeded in the culture, and/or by adjusting the number of days bone marrow cells were cultured before stimulation. In bone marrow derived cultures, cell death is normal and an expected result, as only macrophage or macrophage progenitors will be supported by BMDM culture media, therefore all other cells isolated from bone marrow perish.

TLR4 was the common receptor activated after the addition of λ (Figure 5.1), but this may be due to λ or LPS. When λ preparations were visualized for LPS using Hitchcock and Browns' method, an unusual pattern was observed, suggesting λ was binding specific chemotypes of LPS (Fig. 5.2). Using the LAL assay the amount of LPS present in λ preparations was found to be ~181.5 EU/mL. It was not known if these chemotypes of LPS would produce similar or different TLR signalling as determined by the kinetics of MAPK, and NF-κβ activity (Fig. 5.3,5.4).

It must be mentioned that the presence of LPS had yet to be determined when this study was undertaken. Therefore, the BMDM signalling experiment was to determine if λ was responsible for the direct ligation of TLR4. Many TLRs are known to have promiscuous ligand binding,[85,87,89,389,399] and the question remained whether λ could directly bind TLR4. LPS is the stereotypical ligand of TLR4, but viral capsid proteins from respiratory syncytial virus and mouse mammary tumour virus also cause TLR4 signalling.[85] Recently it was also shown that a dust mite protein could obviate the need for MD2-TLR4 binding in allergic asthma.[89] In parallel with these reports it was intriguing that oral immunization with λ can result in an adaptive immune response,[35] as LPS administered orally should not have an effect on immunization. Therefore, regardless of the presence of LPS in the λ preparations of the current study, a mechanism beyond simple bacterial contamination could account for oral adjuvant activity. In order to investigate the adjuvant activity of λ, multiple avenues of inquiry were therefore undertaken concurrently to investigate this hypothesis, including the analysis of TLR4, TLR2 and the adaptor protein MyD88 in the propagation of p38 and NF-κβ signals.

5.4.3.1 NF-κβ signalling in BMDM

The first analysis of BMDM signalling in knockout (KO) animals will be on Iκβα (Fig. 5.4); a signalling molecule specific for the NF-κβ pathway. The focus of these experiments was to analyze the effect λ had on signalling as compared to LPS, or sFSL-1, a synthetic TLR2 ligand used as a control. In *wt* C57BL/6 mice, there was less NF-κβ signalling in response to λ as compared to LPS, whereas λ and sFSL-1 were equivalent. Signalling in *wt* mice was the baseline to which all KO's were compared to. In a TLR4 KO mouse there was more NF-κβ signalling in λ as compared to LPS, but λ was again

equivalent to sFSL-1. In TLR4 KO mice LPS does not cause signalling,[64,65,67] and yet some was seen in figure 5.4. The genotype was correct for TLR4$^{-/-}$ mice (data not shown), but LPS and other TLR ligand preparations are notorious for having contaminating TLR ligands.[247,426,427] λ on the other hand could have multiple TLR ligands present, and given the TLR4$^{-/-}$ response this could be occurring. Whether signalling was due to contaminants in the preparations of λ or from λ directly is still to be determined. In figure 5.1 TLR5 and TLR2 were found to be activated, therefore in a TLR4$^{-/-}$ these could be responsible for NF-κβ signalling.

To prove the validity of our KO mice an ideal example of how the signalling should occur happens when TLR2, and MyD88 KO mice are investigated for sFSL-1. sFSL-1 is a ligand of TLR2, and TLR2 is MyD88 dependent for signalling.[85,247,422,423] In both MyD88 and TLR2 KOs no NF-κβ signalling was present when sFSL-1 was added to BMDM cultures. This suggests the stock only has sFSL-1 or a TLR2 dependent ligand. It also indicates that our BMDM study was clean and no signalling occurs in the absence of ligands, or as seen in figure 5.3C, when the concentrations of ligands were low.

In TLR2 KO mice, NF-κβ signalling was greater with the addition of LPS as compared to λ. These ligands in TLR2 KO mice were identical to the responses seen in *wt* mice, except it appears that λ contains more signalling at 90min than in *wt*. It is not apparent why this is occurring. It is apparent that in the absence of TLR2, Iκβα responds as in *wt* mice, therefore NF-κβ signalling from TLR2 was not responsible for λ adjuvant activity. These results contradict the λgfp10-TAT signalling observed in figure 5.1.

In MyD88 KO mice NF-κβ signalling was greater in BMDMs supplied with LPS as compared to λ. The adjuvant activity of λ appears to rely on MyD88 for the propagation of an NF-κβ signal more than LPS. Typically LPS causes delayed NF-κβ signalling in MyD88$^{-/-}$ mice,[158,422,428] as TLR4 and TLR3 signalling use both MyD88 and TRIF adaptor proteins.[85,422,428-431] In LPS stimulated MyD88$^{-/-}$ BMDMs a delay in NF-κβ signalling was observed. The lack of MyD88 had a greater effect on NF-κβ signal propagation in λ treated BMDMs, as λ in MyD88$^{-/-}$ have nearly lost NF-κβ signalling as compared to λ in *wt* BMDMs. BMDM supplied with λ have robust signalling at ~45min., but signalling was apparent between 30 to 90min, whereas in *wt* mice signalling occurred

from 15 to 90min. Even though separate westerns were used to visualize the samples, the λ effect was in stark contrast to that seen between LPS in *wt* and MyD88$^{-/-}$ mice. A more thorough analysis on the dependence of MyD88 signalling for λ adjuvant activity will be made in the discussion of p38.

5.4.3.2 MAPK signalling in BMDM

MAPK signalling was determined through the p38 pathway (Fig 5.3 A, C, and 5.4).[80,158,419,430] In *wt* C57BL/6 mice, phosphorylation of p38 from LPS and λ was equivalent in BMDMs, whereas sFSL-1 did not result in the same intensity or duration, although sFSL-1 began to signal at the same time. In TLR4$^{-/-}$ mice sFSL-1 signalling was unchanged from *wt*, as expected p38 phosphorylation was MyD88 dependent, as TLR2 ligands are MyD88 dependent. [85,422,428-431] In TLR4 KO mice LPS stimulated BMDMs have nearly non-existent signalling (Fig. 5.4), this should be negative for p38 phosphorylation as observed for sFSL-1 treated BMDMs in TLR2 KO mice, but obviously some bacterial contamination was present, as discussed previously in the NF-κβ signalling section. Interestingly, λgfp10-GFP-TAT continued to phosphorylate p38, although this was attenuated as compared to λ in *wt* animals. p38 signalling in response to λ in TLR4$^{-/-}$ animals suggested most p38 activation was TLR4 dependent. Whereas in MyD88$^{-/-}$ mice, LPS stimulated BMDMs were equivalent to those stimulated with λ. This suggested that TRIF signalling from LPS was equivalent to λ, and therefore TLR4 was responsible for TRIF signalling from λ. Finally, in TLR2$^{-/-}$ mice LPS and λ resulted in p38 phosphorylation at 4 time points and was equal to *wt* animals, when the intensity of the westerns were compared.

5.4.3.3 Summary of MAPK and NF-κβ signalling

Discussed herein will be the overall trends for MAPK and NF-κβ signalling with respect to the contribution from TLR4, MyD88, and TLR2 BMDMs. Particular attention will be made to the differences observed between ligands.

The kinetics of p38 phosphorylation between LPS and λ were nearly identical except in TLR4$^{-/-}$BMDM, where signalling was evident for λ. Given the results of figure 5.1, MAPK signalling in TLR4 KO mice in response to λ may be due to TLR2, or TLR5,

but MAPK signalling for sFSL-1 was different from λ in all mice. If a TLR2 ligand was present in λ it would be expected that sFSL-1 and λ would have identical MAPK signalling in TLR4 KO mice, this was not seen as λ had an attenuated response as compared to sFSL-1. Given the results of figure 5.3 panel A, the difference between sFSL-1 and λ in $TLR4^{-/-}$ mice could be from different concentrations of TLR2 ligand.

When the kinetics of NF-κβ signalling was investigated in *wt* and $TLR2^{-/-}$ BMDMs, LPS and λ were nearly identical. The degradation of Iκβα in $TLR4^{-/-}$ BMDMs stimulated with λ or sFSL-1 was also identical. NF-κβ signalling for λ in $TLR2^{-/-}$ BMDMs was equal to that seen in *wt* mice and therefore NF-κβ signalling in $TLR4^{-/-}$ BMDMs was most likely not from a TLR2 ligand in $TLR4^{-/-}$ BMDMs but could be from TLR5, as figure 5.1 suggests. Alternatively signalling in $TLR4^{-/-}$ mice might be from NLRs, or RLRs.[85,94] Experiments must be performed to determine the contribution of TLR5, NLRs, and RLRs have on NF-κβ signalling for the adjuvant activity of λ.

When the contribution of MyD88 was investigated for p38 and NF-κβ signalling, an interesting effect was observed. p38 signalling was identical for λ and LPS, as previously described, but the degradation of Iκβα was deficient in λ stimulated $MyD88^{-/-}$ BMDMs as compared to LPS. This suggested that Iκβα degradation was sensitive to the presence of MyD88 in λ stimulated BMDMs as compared to LPS. For both λ and LPS, the chemotype of LPS should be similar as both were produced by *E.coli*. It is strange to observe this dichotomy between MAPK and NF-κβ signalling in response to λ. Most studies report MAPK and NF-κβ signalling as being attenuated in $MyD88^{-/-}$ mice after stimulation, but no studies have described a difference between two ligands in $MyD88^{-/-}$ mice.[69,158,419,421,428]

Given the number of molecules in the TLR4 signalling complex a true comparison between two forms of LPS is lacking. A BMDM study is necessary to distinguish MyD88 and TRIF contribution to Iκβα degradation, especially given new data citing respiratory syncytial virus F protein, mouse mammary tumor virus capsid, dust mite Der p 2, and vesicular stomatitis virus glycoprotein g as TLR4 ligands.[72,85,87,89,389,399] Each of these new ligands may produce variations in the LPS to TLR4 ligation theme. In 2003 a study was published that described NF-κβ signalling from TLR4 as being MyD88

dependent, and not TRIF.[422] This was a strange comment as signalling was present in their figures, although it was attenuated in MyD88$^{-/-}$ peritoneal macrophage supplied with 10μg/mL of LPS from *Salmonella minnesota* Re 595. There are differences in experimental design as figure 5.3 C and 5.4 utilized *E.coli* LPS at 100ng/mL in BMDM. It was debatable whether TRIF was absent in this pathway as at this level of LPS, NF-κβ signalling may be saturated for the MyD88 pathway, and a difference in NF-κβ may not be observed. This observation was supported by the fact that other studies find NF-κβ signalling attenuated but not absent in peritoneal macrophages,[158,419,421] or BMDMs from MyD88$^{-/-}$.[428] In 2007 a study was done on the adjuvant activity of MPLA, where it was found to be TRIF dependent.[69] MPLA being a derivative of LPS. This was in contrast to what Yamamoto describes.[422] Furthermore in the MPLA study a comparison was done between LPS and MPLA in MyD88$^{-/-}$ BMDMs , and no difference was observed in IKKα/β signalling (Supplementary Figure 5).[69] What was observed in figure 5.4 is novel as p38 signalling in response to λ was MyD88-independent and partly TLR4-dependent, whereas NF-κβ signalling was TLR4-independent and largely MyD88 dependent. This profile was in contrast to LPS which was TLR4 dependent, and utilizes MyD88/TIRAP and TRIF/TRAM. In particular the effect of MyD88 on NF-κβ remains to be described in detail and suggests TLR4, or another PRR signalling through TRIF. Orphan adaptor molecules may be involved for NF-κβ signalling by λ, or various chemotypes of LPS could be responsible for differential activity, whereby variation in acylation, glycosylation or phosphorylation affect signalling.[69,79,86,87,432,433]

5.4.4 Cytokines expressed or secreted from Macrophage

APC cytokine expression is integral to Tcell priming and differentiation. To truly understand how an immune reaction progresses it was important to measure the cytokine profile, as cytokines are convenient correlates of protective immunity used for many vaccines.[104,107,137,362] Of primary importance for the current study was to decipher if λ was responsible for the described adjuvant activity or LPS. To further characterize the adjuvant activity of λ and LPS, the secretion and expression of cytokines by macrophages and splenocytes was measured.

A common method to distinguish immune responses to antigens or adjuvants is to measure cytokine production.[69,80,157] As described previously alum causes a Th2 polarized response,[57,434,435] which is characterized by IL-1β, and IL-18 cytokines.[436] The adjuvant activity of alum is dependent on the Nalp3 inflammasome.[57] On the other hand LPS is the most potent TLR adjuvant,[80,437] but suffers from toxicity issues when administered in humans.[72,434,438] LPS induces the greatest expression from TNFα, IL-1β, IL-1a, IL-12, and IL-6 cytokines at 1 and 4hrs.[157] The typical cytokines expressed and described for LPS are: TNFα, IL-6, IL-1β and IP10.[140,158,421,439] When the adaptor proteins in the TLR4 pathway are knocked out, MyD88 signalling is found to cause secretion of IFNγ, IL-1β, IL-6, and MIP-1α, whereas TRIF causes the secretion of G-CSF, MCP-1, IP-10, and RANTES.[69,157] Phenotypically this results in TRIF causing APC maturation and Tcell activation,[69,420] In general TLRs are thought to induce TNFα, IL-6, and depending on the presence of TRIF, the cytokines IFNα/β are also present.[140,158] Other cytokines are produced and these are modulated by the adaptor molecules recruited during signalling and by variations in the propagation of intracellular signalling.[80,157]

In *wt* C57BL/6 BMDMs the secretion of TNFα and IL-6 were observed after stimulation with LPS or λgfp10-GFP-TAT (Fig. 5.5 A). Both cytokines are pro-inflammatory and are common to TLR signalling. At 2hrs and 6hrs after stimulation with LPS the amount of TNFα was roughly equivalent. On the other hand at 2hrs λ stimulation was equivalent to LPS at a concentration of 10^9PFU/mL, but the amount of TNFα increased by 6hrs by a statistically significant amount as compared to all other samples. LPS appears to have saturated BMDM TNFα production at 2hrs and 6hrs, as 250ng/mL and 10ng/mL resulted in the same amount being produced. In contrast a dose response was seen in λ that parallels the titer added to the culture, and TNFα increased over time. This difference could be attributed to endosomal signalling by TLR4, TLR3, and TLR9. Endosomal processing of λ may be necessary to produce TLR ligands. As TNFα is not a product of TRIF signalling, this result suggests, TLR9 or TLR7/8 are responsible for the increase.

When IL-6 was measured, LPS and λ have nearly identical responses at their highest concentrations (Fig. 5.5A). Once again even though LPS was delivered across a 25 fold range, the values are in the same order of magnitude at 2hrs, and then at 6hrs. Suggesting the amount of LPS was at a saturating level. λ stimulation resulted in the same concentration of IL-6 at 2hrs and 4hrs as LPS, but again a dose response was seen across the 1000 fold range in λ concentration applied. This result would suggest that 10^9 PFU/mL of λgfp10-GFP-TAT had 10ng to 250ng/mL of LPS, but as the LPS concentrations were at saturation levels for IL-6 and TNFα, the amount of LPS or TLR ligand in λ may be less. Regardless of the amount of the presence or absence of LPS in λ preparations, there was a significant difference across all factors and nearly all samples in BMDM derived IL-6 production after LPS or λ, proving they respond differently.

The underlying gene expression driving early cytokine secretion was determined in peritoneal macrophages from CD1 mice (Fig. 5.5 B). Peritoneal macrophages are the most likely APC responding to λ in the vaccination experiments described in chapter 4, as they are the most numerous APC in the peritoneum. Unfortunately, even though they are the most prevalent APC, their numbers were insufficient for intracellular signalling experiments described in figures 5.3 and 5.4. As an alternative, the sensitivity of QRT-PCR allowed the quantification of gene expression, and cytokine gene expression is an accepted method to indirectly measure cytokine secretion.[240,243,439-442] In this experiment the activation of peritoneal macrophages was supplemented with IFNγ, as it was not known if they would respond to λ.[65,247,443,444]

When TNFα expression was measured (Fig 5.5B), it was apparent that LPS caused a peak fold increase at ~2hrs and by 6hrs expression was in retreat. Quick peak expression, at ~1200 fold increase, and a concomitant decrease of TNFα gene expression is indicative of LPS.[439] TNFα gene expression as a result of λ was different and it explains the continued increase in cytokine secretion seen in figure 5.5 panel A. At 2hrs and 6hrs, TNFα gene expression was >1000 fold after stimulation with 10^9PFU/mL of λgfp10-GFP-TAT.

The expression of IFNγ was much slower to respond than TNFα. In macrophages, IFNγ is not an early responding cytokine, but is instead a signal causing

activation of macrophages which results in the production of IL-12, IL-2, IFNα/β, or other PRR cytokines.[143,444] The primary source of IFNγ are Th1 cells and NKT cells.[143,439] Th1 and NKT cells are undoubtedly the major contributors to IFNγ concentration in the cell proliferation experiments (Fig. 4.6B). Our data shows IFNγ was expressed in peritoneal macrophages at 2hrs with λ and LPS at 2 and 3 orders of magnitude less than TNFα (Fig. 5.5B). At 6hrs LPS caused the fold expression of IFNγ to increase by two orders of magnitude to >100. The trend was identical for λgfp10-GFP-TAT where IFNγ increased to >1000 fold expression, and this was significantly different than other times and treatments.

When IL-17a expression was analyzed, it appeared LPS stimulated cells must have been activated with IFNγ at 2hrs, and at 6hrs this was dispensable. Autocrine stimulation of peritoneal macrophages by IFNγ could play a role. The IFNγ activation of macrophages was not necessary at 2hrs or 6hrs in λ treatments, and IL17a gene expression was 1 order of magnitude greater than LPS alone, but this was not statistically significant. This result was interesting as IL-17, or Th17 cells are proving to be instrumental in protective immunity against many lung pathologies.[104,120,123] The bacteria *M.tuberculosis*, *P.aeruginosa,* and *B.pertussis* have been shown to have IL-17 as a protective immune correlate. Of particular interest was the finding for *B.pertussis* that TLR4 is responsible for Th1 and Th17 cell differentiation and IL-17 activates macrophage killing of *B.pertussis.* In figure 5.5 we are measuring the expression of IL-17 in macrophages and not Th17 cells, but IL-17 has been shown to be expressed from macrophages and bone marrow mononuclear cells from aplastic anaemia patients.[163,445] Other cells types were likely responsible for IL-17a and possibly IFNγ expression in this experiment. The only requirement for a co-cultured cell was that it must be an adherent cell type. Typically IFNγ expressing cells are natural killer Tcells (NKT), classic NK cells, Th1 cells, and $CD8^+$ cells.[135,143,144,446] Conveniently many of these also express IL-17, except in Th cells where this variety is called Th17. The presence of IL-17 was noteworthy and expands our knowledge of λ or LPS as mediators of Th17 polarization. Bacteriophage λ can now be described as producing TNFα, IL-6, IL-17a, IFNγ, and IL-2, in their respective order of timing (Fig. 5.6). This is different from adenovirus or

respiratory syncytial virus which result in IL-4, IFNγ, and IL-6.[447] The presence of IL-4 in RSV infection was interesting as both RSV and λ cause TLR4 ligation.[389] In all the work of this thesis, IL-4 was never seen in BMDM, peritoneal macrophages, or splenocytes at anytime between 2 and 48hrs with λ, or LPS. Therefore the classic Th2 cytokine, IL-4, was not responsible for the immune response to λ (Fig 1.2). Taking into account BMDM and spleen cytokine expression, the presence of IFNγ, IL-6, IL-1β, and MIP-1α prove MyD88 was used in the immune reaction to λ.[69,157] Although the presence IL-1β is indicative of the Nalp3 inflammasome, or NLRs.[57,94] On the other hand, of all common TRIF cytokines, only IP-10 was present.[69,157] IP-10 is the product of IRF3 signalling,[421] which can be propagated from TRIF in TLRs or from the RLRs.[141] It remains to be seen if the expression of cytokines changes in LPS deficient λ preparations, or TLR4$^{-/-}$ BMDMs. In a test experiment, using C3H/HeJ splenocytes, which are hypo-responsive to LPS, it was found that λ produced higher concentrations of IL-6, IL-9, IL-10, IL-13, IP-10, and MIP-1α as compared to LPS. Noticeably absent from high responding cytokines in response to λ are IL-1α, IL-1β, IL-12, and TNFα, which were included in the analysis but did not produce a strong response. Further work will be necessary to determine the adjuvant activity of λ and better characterize immune correlates of infection.

Of particular interest to λ subunit vaccination was the cellular signalling of the adjuvant activity. It was interesting that studies describe oral immunization of λ resulted in an adaptive immune response and antibody production in the absence of an adjuvant.[35] Given the present study it would appear a TLR4 ligand whether this was λ, LPS, or a chemotype of LPS, was partly responsible for the adjuvant activity of λ. Given the immuno-suppressive environment of gastro-intestinal (GI) tract,[90,204] it would seem unlikely that LPS was responsible as an oral adjuvant. The mucosa of the GI or the lung would be interesting environments to further characterize the adjuvant activity of λ.

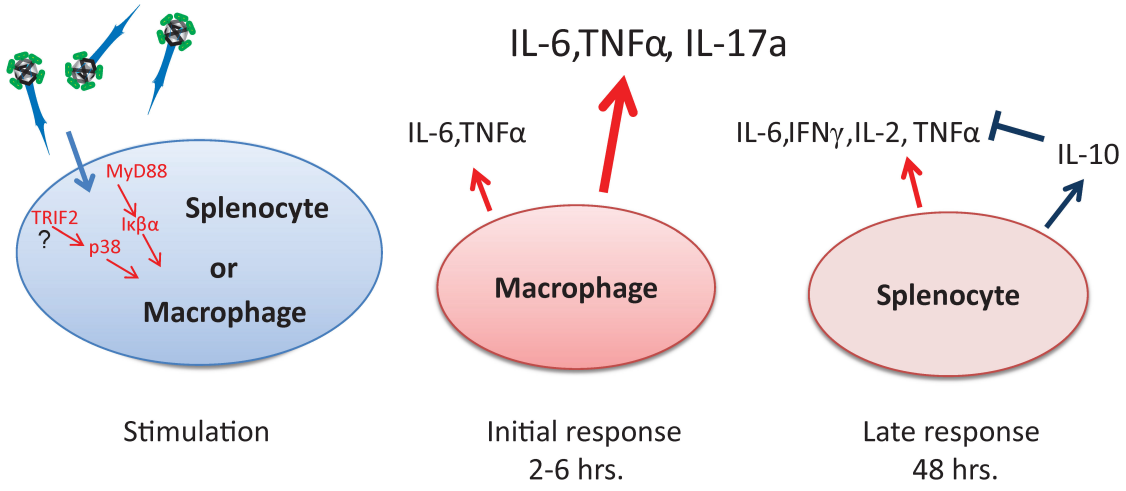

Figure 5.6: Immune Reaction to Bacteriophage.

Summary of immune reaction in splenocytes or macrophages in response to bacteriophage λ.

Chapter Six: **Mashkiki: Concluding Discussion**

6.1 Project Summary

The utility of λ phage display has been investigated. Mashkiki phage displaying TAT proved ineffective for delivery of recombinant genetic cargos. However, Mashkiki phage did prove effective for antigen presentation to the immune system. As a subunit vaccine vector, λ was shown to be a potent stimulus for splenocytes, regardless of immunization. The pro-inflammatory nature of Mashkiki was associated with IFNγ production. This co-stimulatory signal produced cellular and humoral immunity against λ and antigen. Antigen was effectively presented with λ as either a displayed peptide or by genetic immunization.

The adjuvant activity of Mashkiki phage was examined and was found to be intriguing. A study to find the pattern recognition receptor responsible for λ adjuvant activity ensued. *Wt* λ was found to cause TLR4 receptor ligation, whereas λ displaying TAT caused TLR4, TLR5, and to a lesser extent TLR2 ligation. TLR4 appeared to be a λ specific PRR, therefore a vaccine trial was performed with Mashkiki phage in the TLR4 hypo-responsive mutant C3H/HeJ. The humoral immune response to λ was found to be TLR4-independent, as titers of λ recognizing antibodies were equivalent between C3H/HeJ mice and the TLR4 responsive mouse strain C3H/HeOuJ. Interestingly, the adjuvant activity for a λ displayed antigen was 1 $\log_{10}$ weaker in C3H/HeJ mice than *wt* C3H/HeOuJ.

In order to determine the involvement of TLR4 in adjuvant activity, downstream signalling pathways from TLR4 were assayed for activity after λ treatment. TLR4 ligation with λgfp10-TAT-GFP caused activation of the NF-κβ pathway in a TLR4-independent fashion, but lack of MyD88 attenuated activation. In contrast, signalling through p38 was largely TLR4-dependent, but MyD88-independent. In the context of TLR signalling, MAPK signalling is therefore TRIF-dependent, and results in IP10 expression. On the other hand NF-κβ signalling was largely MyD88-dependent and signalling resulted in IFNγ and IL-6 expression. The cytokines produced from this response, which differ in timing and amplitude from LPS, the prototypical TLR4 ligand,

are: IFNγ, IL-2, IL-6, IL-10, IL-13, IL17a, IP-10, and MIP-1α. The initiation of an adaptive immune response from λ is therefore multifaceted. The adjuvant activity of λ is not TLR4 restricted. It is postulated that λ will provide immune stimulation through TLR9, a NOD-like receptor, and complement.

6.1.1 Bacteriophage Transduction into ES cells

The transduction of λ into mammalian cells resulting in expression of a reporter gene was not documented in the ES cell lines E14, R1, D3, or Bruce4, or for the immortalized cell lines Cos7 and Hek293T. TAT was effective for transduction of streptavidin, a 60kDa heterodimer. This was in contrast with two independent reports documenting successful expression of λ delivering DNA with the use of phage displayed protein transduction domains.[269,270]

The negative results for λ transduction documented in chapter 3 are concurrent with a recent report on the existence of possible artifacts in the PTD field.[351] Work in this field has been fraught with such reports. In 2003 it was determined that early reports documenting time and energy independent uptake of PTD molecules to the nucleus were artifacts of fixation, which permeabilized cell membranes.[234] At a similar time, it was determined that the PTD of TAT, also described as the basic domain, bound negatively charged molecules non-specifically.[233-236] In particular, it was found to bind the highly negatively charged molecules heparan sulfate proteoglycans (HSPG), dextran sulfate, and DNA.[232,234,235,359] Perhaps the most damning evidence for the transduction of λ by TAT is the fact that only 2 papers have been published, in 2001 and 2004. Nothing has been reported since. Evidence seems to support the hypothesis that the PTD domain of TAT should simply be called the basic domain, as the TAT-PTD fails to provide trans-cellular activity, a defining feature of full length TAT.[351] This conclusion is logical as many viral capsids that confer cell membrane penetration ability are large molecules and not simply short 11aa peptides. For example the hemagglutinin (PDB: 1ruz) protein is a dimer of peptides 328aa and 160aa in length. If a virus could save energy by the production of a smaller molecule it would have evolved a growth advantage.

Two positive outcomes were yielded from this line of study: 1) a λ protein/peptide display system was built, and 2) an optimized λ virion preparation technique was

determined. Both these would prove invaluable for results reported in chapters 4 and 5. The studies on λ phage display resulted in the development of three methods to display peptides or proteins on λ capsids. Mashkiki phage display can therefore be accomplished by expression of fusion proteins in *trans,* the genomic integration of gpD fusions using recombineering, or conjugation using biotin-streptavidin chemistry. The recombineering of gpD was a novel application of this technology, and proved necessary for engineering this structural gene in λ. The result of these systems has proven λ is effective at displaying proteins and peptides. In the present work, three forms of gpD were displayed on λ capsids. Indeed the benefit for molecular therapeutics is the number of different molecules that could be displayed on this vector.

6.1.2 Immunobiology of Bacteriophage λ

Similar to ΦX174 and M13 bacteriophage,[35,43,186,200-203] it was found that the display of a peptide on λ inoculated without an adjuvant resulted in an adaptive immune response. The response was measured by class switched Ig. Titers recognizing bacteriophage were greatest, but the presence of a co-displayed TAT protein improved the production of serum IgG recognizing a displayed antigen by 2 $\log_{10}$. The treatments which resulted in the highest responding anti-GFP IgG titers correlated with the production of IL-2 by splenocytes. This correlation was also seen when λ was used as a genetic immunization vector. Serum IgA was not produced in response to an intraperitoneal inoculation of λ. The production of serum IgM and IgG recognizing λ was dependent on immunization, as natural antibodies were either absent from CD1 mice, or were below detection limits in the ELISA performed. Interestingly, splenocytes produced high IFNγ after *in vitro* stimulation with λ. IFNγ production was not found to be dependent on prior immunization with λ, and is therefore, an innate response to λ.

The innate immune response to λ was intriguing. Bacteriophage λ, ΦX174, and M13 had proven to produce an adaptive immune response in the absence of an adjuvant, but the characterization of a cytokine responsible had not been previously shown.[35,43,186,200-203] A study was undertaken to determine the adjuvant activity of λ. The focus of this work was on TLR ligands, as LPS and CpG DNA are adjuvants proven to be effective in vaccination, and were likely present in λ preparations. Mouse TLRs were screened and

TLR4 responded to λ, whereas TLR4, TLR5, and to a lesser extent TLR2 responded to λ displaying TAT. As TLR4 was a λ specific response for either preparation, experiments were undertaken to investigate the contribution of TLR4 in λ adjuvant activity.

It was shown that TLR4 signalling occurs in the presence of λ. The prototypical ligand for TLR4 is LPS, but recently TLR4 ligation has been shown to be promiscuous, as it binds viral capsid proteins from respiratory syncytial virus and mouse mammary tumor virus,[85] a dust mite protein,[89] and host derived factors. The possibility existed that a λ capsid component was a new TLR4 ligand; alternatively TLR4 signalling could be the result of LPS in λ preparations. LPS was detectible after periodate oxidation and silver staining, a method which identifies oligosaccharides.[251,401] Interestingly, the chemotypes of LPS did not match the parental strain of *E.coli* used for the preparation of λ. This result suggests λ may incorporate specific chemotypes into the capsid. Unexpectedly, when λ was diluted in Ultrapure™ H_2O, LPS staining was lost. Furthermore, the dilution of λ in SM buffer removed p38 signalling at 10^7PFU/mL or less. Therefore the detection of LPS using periodate oxidation and silver staining may not represent LPS, but may indicate the presence of another oligosaccharide.

When the LAL assay was performed to detect LPS, or Lipid A,[409,410] λ preparations were positive. λgfp10-GFP-TAT, the preparation used in the second immunization trial on C3H mice and for TLR signalling experiments, was found to contain approximately 181.5 EU/mL of LPS. SM buffer, the buffer used for storage of λ, contained only 1.2 EU/mL. At 1.2 EU/mL of LPS, no p38 signalling was observed from λ diluted to 10^7 PFU/mL in SM buffer and added to BMDMs. The removal of LPS was shown to be possible using polymyxin B-sepharose chromatography, as eluted λ resulted in 1.35 EU/mL of LPS, a concentration equivalent to SM buffer. In contrast, laboratory MilliQ™ H_2O contained 0.2 EU/mL, and Ultrapure™ H_2O contained 0.25 EU/mL. If an equivalent concentration of LPS was present in the preparation of λ used in the inoculation of CD1 mice, and given an average mouse weight of 32.0 ± 3.4g for C3H mice, there was 11.25 times the FDA limit for human therapeutics. LPS undoubtedly affected the results in the CD1 vaccine trial, as LPS is a potent adjuvant. The effect of LPS is undetermined though, as a previously published study reported protective

immunity against herpes simplex B virus from filamentous bacteriophage displaying glycoprotein G, after removal of LPS with polymyxin B.[201] A similar result could occur with λ. Supporting this hypothesis, it was found that CD1 peritoneal macrophages and C57BL/6 BMDM express cytokines differently with the addition of LPS or λ. In particular it was observed that TNFα, IFNγ, IL-6, IL-10, and IL-17a differed between λ and LPS on the amplitude and timing of expression. These responses differed between CD1 and C57BL/6 mice most likely due to strain diversity in the TCR, and immunoglobulin loci.

In order to determine the TLR4 contribution to λ adjuvant activity, two studies were performed. The first study was a vaccine trial in the hyporesponsive C3H/HeJ mouse strain. The second study was to investigate the intracellular TLR signalling in BMDMs from TLR4, TLR3 and MyD88 KOs. ***These experiments lead to the conclusion that λ adjuvant activity is not solely TLR4 dependent, but TLR4 contributes to the immunogenicity of λ.*** Adjuvant activity in λ is therefore multifaceted due to multiple moieties in the virion.

When immunization with λgfp10-GFP-TAT was performed on C3H mice, the adjuvant activity of λ was not decreased with the proline 712 a.a to histidine mutation, as measured by antibody titers. In contrast the adjuvant activity or immune responsiveness against GFP did decrease, as C3H/HeJ mice mouse serum anti-GFP titer were 1 $\log_{10}$ lower than in C3H/HeOuJ mice. The discrepancy between λ and GFP titers could be due to how the ELISA measuring anti-λ was performed. Therefore, the higher anti-λ titer could be the result of the presence of other eptitopes in λ preparations as these would have coated ELISA plates and contributed to high anti-λ titers. Alternatively λ may have circulating natural antibodies, which contribute to a rapid Ig class switch in the presence of λ. The presence of natural antibodies was not detected in a separate anti-λ IgM ELISA, but these may have been below the detection limit of the assay.

Natural antibodies to λ may explain the proliferative capacity of the spleen as compared to the PLN and MLN organs. *In vivo* the spleen and liver are the primary clearance points for natural antibody opsonisation of antigen.[448,449] The primary responding cells of natural antibody opsonisation are marginal zone macrophages and

Kupffer cells. These cells could account for the enhanced proliferation of C3H/HeJ splenocytes in the presence of phage as compared to LPS. Convergent with IgM clearance is the complement system. Complement produces clearance of 99% of LPS or T4 phage to the spleen or liver.[38,448] Complement has been proven to bind T7 bacteriophage,[384] and ΦX174 is a T-dependent antigen,[450] but these effects have yet to be described in λ. Interestingly a long circulating variant of λ has been described which has a mutation in gpE,[33,206] which could be the binding site for IgM natural antibodies or complement. The complement effect was not tested for λ, or λ immunization, but could account for the enhanced proliferation of λ in splenocytes, especially in the absence of LPS. Complement and natural antibodies are known innate immune effectors that can produce co-stimulatory signals to activate adaptive immunity, therefore λ immunity could utilize these mechanisms in concert with LPS.[449-451] This hypothesis could explain C3H splenocyte proliferation described in this thesis. As a result marginal zone B1 cells and marginal zone macrophages should be investigated for λ activity in LPS free preparations.

When TLR signalling cascades were studied, it was proven that p38 and MAPK signalling were independent of TLR4 ligation. The response seen was attenuated as compared to *wt*, but signalling did occur. Activation of p38 was largely depedent on TLR4, but activation was close to *wt* in MyD88$^{-/-}$ BMDMs, suggesting that p38 signalling occurs independently of MyD88. In the context of TLR signalling, TRIF2/TRAM are the adaptor molecules responsible for most λ p38 signalling, but the appropriate KOs will need to be tested to prove this. Other PRRs also converge on p38, and therefore NLR KOs will need to be tested for p38 signalling as well. Therefore, λ stimulation of BMDMs results in p38 signalling that was largely dependent on TLR4-TRIF2 and resulted in IP-10 expression. In contrast NF-κβ signalling in TLR4$^{-/-}$ was roughly equivalent to *wt* BMDM, suggesting activation of NF-κβ is TLR4 independent. In contrast to p38 signalling, NF-κβ signalling was largely dependent on MyD88. This effect was not observed with *E.coli* LPS. The end result of NF-κβ signalling in response to λ was IL-6 and IFNγ. This dichotomy in p38 and NF-κβ signalling was the first evidence of this effect, whereby p38 is MyD88-independent and NF-κβ is MyD88-

dependent. Previously both pathways were believed to signal equally in response to a TLR signal. In the context of TLR signalling, NF-κβ was MyD88 dependent, and p38 was TRIF2/TRAM dependent. These signals produced a Th1 biased response based on IgG2a antibody production.

As discussed previously *wt* mice produced different cytokine patterns in response to λ as compared to LPS. Notably TNFα, IFNγ, IL-6, IL-10, and IL-17a are differentially expressed in response to λ. In C3H/HeJ splenocytes treated with λ or LPS the following cytokines were augmented in response to λ: IL-6, IL-9, IL-10, IL-13, IP-10, and MIP-1α. IFNγ, IL-17a, and TNFα are approximately equal in TLR4 mutant mice when splenocytes are stimulated with LPS or λ. Interestingly all three of these non-differentially expressed cytokines were differentially expressed in *wt* peritoneal macrophages and BMDM; this could be due to differences in the cells assayed or from variability in responses due to mouse strains. Therefore, correlates of λ immunity could be IFNγ, IL-2, IL-6, IL-9, IL-10, IL-13, MIP-1α, and depending on the strain or cell type IFNγ, IL-17a, and TNFα. These cytokines are involved in Th1 and Th2 responses but IL-4, the prototypical Th2 cytokine, is noticeably absent.

As discussed, the antibody response was Th1 biased in *wt* CD1 mice and for C3H/HeJ mice. Th2 antibodies were produced in CD1 mice but were absent in the C3H strains. This could be due to strain variability. No IgA was observed from any of the IP inoculations, and no serum IgM or IgG was measured in non-immunized mice. As discussed previously, natural antibodies may be present given the splenocyte proliferation data. One interesting effect documented for antigen recognition by λ immunization is the high avidity of anti-GFP in peptide immunization using λgfp10-GFP-TAT. This immunization produced antibodies that recognized GFP at pH 9.6, denatured conditions and pH 7.2, native conditions. This effect may result in neutralizing antibody production.

6.2 Synthesis and Conclusions

Bacteriophage λ immunization resulted in TLR4-independent immunity to λ and displayed peptides. Loss of TLR4 attenuated the response, but did not stop IgG antibody production. λ therefore has multiple adjuvant moieties resulting in robust immune

responses. It remains undetermined if LPS from λ preparations or a molecule from λ resulted in TLR4 ligation.

The multifaceted adjuvant activity of λ could be the explanation for λ crossing oral and mucosal barriers. It remains to be seen what effect any given phage adjuvant moiety has on mucosal transduction, but the oral or mucosal transduction ability of bacteriophage has been well documented since the beginning of phage therapy research. It is also interesting that a mucosal cytokine, IL17-a, is produced in response to λ. Other possibilities for λ adjuvant activity are TLR9, which is known to result in a Th1 response, TLR2, TLR5, NLRs, RLRs, natural antibodies, and complement. As previously discussed the adjuvant activity mediated by any of these receptors may be due to λ proper or the incorporation of bacterial components on the λ capsid. Given the current climate in vaccine research for the production of effective mucosal vaccines, this line of research could prove fruitful for therapeutics. Furthermore, the use of multiple adjuvants by λ could result in long term memory responses, an effect that has yet to be determined for bacteriophage vaccination.

One reason for λ crossing mucosal membranes and entering into the body may be due to our co-evolution with bacteriophage as we developed an alimentary tract. Bacteriophage may remain tolerated in the body as they are effective sentinels of infection. They may evade detection by binding the bacteriophage Bor/Iss lipoprotein, or smooth LPS. Electron microscopy of λ virions to detect capsid bound LPS, or Bor/Iss will be necessary to test this theory. Upon binding invading bacteria they may change conformation and allow complement, natural antibodies, and PRR recognition. In so doing, they could be acting as an exogenous opsonin.

In discussing opsonins it remains to be determined if natural antibodies or complement are involved in immune stimulation. Marginal zone B1 cells and marginal zone marcrophages remain to be studied in response to λ. In parallel to this work electron microscopy of λ-antibody complexes are necessary to determine the activity of complement or IgM. Cobra venom factor or C3 KO mice can also be used to investigate the involvement of the complement system in innate recognition of λ. Of course IgM and complement are synergistic and interact to form immune complexes which are efficiently

phagocytosed by marginal zone macrophages. Of course if this proves correct, as it has for brethren of the bacteriophage family, a strange paradox is occurring, as complement and natural antibodies are known to cause 99% of LPS and bacteriophage T4 clearance through the spleen and liver.[38,448] Yet viable bacteriophage are measured from the spleen or liver at relatively high titers, approximately 10^5PFU/g of wet tissue, and at 10^1PFU/mL of serum.[38] This result may corroborate the proposed immune sentinel properties of λ as it could prove beneficial for alimentary tract hosts.

No phage specific immune correlates were found when comparing λ to LPS, but large differences were observed between *wt* mice and C3H/HeJ mice in cytokine expression and secretion. Cytokine production during immune stimulation varies with ligand, but TLR4 remains a large part of λ adjuvant activity. In order to determine the magnitude of the TLR4 contribution to adjuvanticity, comparisons in TLR4$^{-/-}$, TRIF/TRAM$^{-/-}$, MyD88$^{-/-}$, C3H/HeJ, and C57BL/10ScCR are necessary. In this way variations in activity attributed to non-TLR4 effects could be analyzed. In parallel panels of NLRs and RLRs should be screened for λ specific stimulation in the absence of LPS.

With the excitement currently seen in the TLR signalling field it is interesting to have documented differential p38 and NF-κβ signalling. This is the first example of this effect and it is even more interesting to ask why MyD88 dependency is specific for NF-κβ, whereas TRIF2/TRAM appears involved exclusively for p38. Further experiments are necessary to determine the differences between λ and LPS in TLR4 signalling.

6.3 Concluding Remarks

This project was technically challenging but also intellectually stimulating. Given the pedigree of those who have studied molecular therapeutics, an apt quote is:

> *"Reasonable people adapt to the world around them; unreasonable people try to change it."* *~George Bernard Shaw*

Bacteriophage have proven to be a flexible tool for many different purposes. The utility of λ-TAT transduction into ES cells proved ineffective, but λ display is a viable platform for subunit vaccination. Many interesting paradigms remain to be discovered in bacteriophage λ biology. In studying λ a deeper understanding of the immune system is inevitable. The stimulation of the innate immune system and the translation of this signal

into an adaptive immunity have only recently been discovered, but the effects on adjuvant design and understanding have been profound. It remains to be seen how the minutiae of these mechanisms affect protective immunity. With a better understanding of protective immunity, a panacean vaccine may be possible using engineered phage. Many hurdles remain before the vision of Felix d'Herelle can be realized in 21st century medicine. Until that day, every bit of knowledge that can be gleaned from the immune system provides for better tools in rational vaccine design.

References

1. Duckworth, D. H. "Who discovered bacteriophage?" *Bacteriol Rev* **40**, 793-802 (1976).
2. Hankin, E. H. L'action bactericide des eaux de la Jumna et du Gange sur le vibrion du cholera. *Ann. Inst. Pasteur* **10**, 511 (1896).
3. Twort, F. W. An investigation on the nature of ultra-microscopic viruses. *The Lancet* **186**, 1241-1243 (1915).
4. Summers, W. C. On the origins of the science in Arrowsmith: Paul de Kruif, Felix d'Herelle, and phage. *J Hist Med Allied Sci* **46**, 315-32 (1991).
5. D'Herelle, F. On an invisible microbe antagonistic toward dysenteric bacilli: brief note by Mr. F. D'Herelle, presented by Mr. Roux. 1917. *Res Microbiol* **158**, 553-4 (2007).
6. Lederberg, J. Infectious history. *Science* **288**, 287-93 (2000).
7. Dublanchet, A. & Bourne, S. The epic of phage therapy. *Can J Infect Dis Med Microbiol* **18**, 15-8 (2007).
8. Booth, W. The Bacteriophage, Its Nature, Behavior and Use. *Bios* **3**, 37-44 (1932).
9. Beckerich, A. & Hauduroy, P. Le Bacteriophage de d'Herelle: Ses Applications Therapeutiques. *J Bacteriol* **8**, 163-71 (1923).
10. Hangartner, L., Zinkernagel, R. M. & Hengartner, H. Antiviral antibody responses: the two extremes of a wide spectrum. *Nat Rev Immunol* **6**, 231-43 (2006).
11. Carter, K. C. Koch's postulates in relation to the work of Jacob Henle and Edwin Klebs. *Med Hist* **29**, 353-74 (1985).
12. Duckworth, D. H. & Gulig, P. A. Bacteriophages: potential treatment for bacterial infections. *BioDrugs* **16**, 57-62 (2002).
13. Compton, A. Sensitization and Immunization with Bacteriophage in Experimental Plague. *The Journal of Infectious Diseases* **43**, 448-457 (1928).
14. Compton, A. Immunization in Experimental Plague by Subcutaneous Inoculation with Bacteriophage. *The Journal of Infectious Diseases* **46**, 152-160 (1930).
15. Larkum, N. W. Bacteriophage Treatement of Staphylococcus Infections. *The Journal of Infectious Diseases* **45**, 34-41 (1929).
16. Eaton, M. D. & Bayne-Jones, S. Review of the Principles and Results of the use of Bacteriophage in the Treatment of Infections. *JAMA* **103**, 1769-1776 (1934).
17. Sulakvelidze, A., Alavidze, Z. & Morris, J. G., Jr. Bacteriophage therapy. *Antimicrob Agents Chemother* **45**, 649-59 (2001).
18. Kruger, D. H., Schneck, P. & Gelderblom, H. R. Helmut Ruska and the visualisation of viruses. *Lancet* **355**, 1713-7 (2000).
19. Luria, S. E. & Anderson, T. F. The Identification and Characterization of Bacteriophages with the Electron Microscope. *Proc Natl Acad Sci U S A* **28**, 127-130 1 (1942).
20. Krisch, H. M. & Comeau, A. M. The immense journey of bacteriophage T4--from d'Herelle to Delbruck and then to Darwin and beyond. *Res Microbiol* **159**, 314-24 (2008).

21. Cairns, J., Stent, G. S. & Watson, J. D. *Phage and the origins of molecular biology* (Cold Spring Harbor Laboratory Press, Cold Spring Harbor, N.Y., 2007).
22. Hendrix, R. W. *Lambda II* (Cold Spring Harbor Laboratory, Cold Spring Harbor, N.Y., 1983).
23. Hershey, A. D. *The Bacteriophage lambda* (Cold Spring Harbor Laboratory, [Cold Spring Harbor, N.Y.], 1971).
24. Fleming, A. *On the antibacterial action of cultures of a penicillium, with special reference to their use in the isolation of B. Influenzae* (London, 1929).
25. Arita, I. Virological evidence for the success of the smallpox eradication programme. *Nature* **279**, 293-8 (1979).
26. Dabrowska, K., Switala-Jelen, K., Opolski, A., Weber-Dabrowska, B. & Gorski, A. Bacteriophage penetration in vertebrates. *J Appl Microbiol* **98**, 7-13 (2005).
27. Slopek, S., Weber-Dabrowska, B., Dabrowski, M. & Kucharewicz-Krukowska, A. Results of bacteriophage treatment of suppurative bacterial infections in the years 1981-1986. *Arch Immunol Ther Exp (Warsz)* **35**, 569-83 (1987).
28. Weber-Dabrowska, B., Dabrowski, M. & Slopek, S. Studies on bacteriophage penetration in patients subjected to phage therapy. *Arch Immunol Ther Exp (Warsz)* **35**, 563-8 (1987).
29. de la Cruz, V. F., Lal, A. A. & McCutchan, T. F. Immunogenicity and epitope mapping of foreign sequences via genetically engineered filamentous phage. *J Biol Chem* **263**, 4318-22 (1988).
30. Reynaud, A. et al. Characteristics and diffusion in the rabbit of a phage for Escherichia coli 0103. Attempts to use this phage for therapy. *Vet Microbiol* **30**, 203-12 (1992).
31. Inchley, C. J. & Howard, J. G. The immunogenicity of phagocytosed T4 bacteriophage: cell replacement studies with splenectomized and irradiated mice. *Clin Exp Immunol* **5**, 189-98 (1969).
32. Uhr, J. W. & Weissman, G. Intracellular Distribution and Degradation of Bacteriophage in Mammalian Tissues. *J Immunol* **94**, 544-50 (1965).
33. Merril, C. R. et al. Long-circulating bacteriophage as antibacterial agents. *Proc Natl Acad Sci U S A* **93**, 3188-92 (1996).
34. Bastien, N., Trudel, M. & Simard, C. Protective immune responses induced by the immunization of mice with a recombinant bacteriophage displaying an epitope of the human respiratory syncytial virus. *Virology* **234**, 118-22 (1997).
35. Delmastro, P., Meola, A., Monaci, P., Cortese, R. & Galfre, G. Immunogenicity of filamentous phage displaying peptide mimotopes after oral administration. *Vaccine* **15**, 1276-85 (1997).
36. Carlton, R. M. Phage therapy: past history and future prospects. *Arch Immunol Ther Exp (Warsz)* **47**, 267-74 (1999).
37. Keller, R. & Engley, F. B., Jr. Fate of bacteriophage particles introduced into mice by various routes. *Proc Soc Exp Biol Med* **98**, 577-80 (1958).
38. Geier, M. R., Trigg, M. E. & Merril, C. R. Fate of bacteriophage lambda in non-immune germ-free mice. *Nature* **246**, 221-3 (1973).

39. Smith, H. W., Huggins, M. B. & Shaw, K. M. The control of experimental Escherichia coli diarrhoea in calves by means of bacteriophages. *J Gen Microbiol* **133**, 1111-26 (1987).
40. Smith, H. W., Huggins, M. B. & Shaw, K. M. Factors influencing the survival and multiplication of bacteriophages in calves and in their environment. *J Gen Microbiol* **133**, 1127-35 (1987).
41. Berchieri, A., Jr., Lovell, M. A. & Barrow, P. A. The activity in the chicken alimentary tract of bacteriophages lytic for Salmonella typhimurium. *Res Microbiol* **142**, 541-9 (1991).
42. Carrera, M. R. et al. Treating cocaine addiction with viruses. *Proc Natl Acad Sci U S A* **101**, 10416-21 (2004).
43. Frenkel, D., Dewachter, I., Van Leuven, F. & Solomon, B. Reduction of beta-amyloid plaques in brain of transgenic mouse model of Alzheimer's disease by EFRH-phage immunization. *Vaccine* **21**, 1060-5 (2003).
44. Frenkel, D. & Solomon, B. Filamentous phage as vector-mediated antibody delivery to the brain. *Proc Natl Acad Sci U S A* **99**, 5675-9 (2002).
45. Blair, J. E. & Reeves, D. L. The Placental Transmission of Bacteriohpage. *Journal of Infectious Diseases* **42**, 440-443 (1928).
46. Beutler, B. & Rietschel, E. T. Innate immune sensing and its roots: the story of endotoxin. *Nat Rev Immunol* **3**, 169-76 (2003).
47. Snow, J. *On the mode of communication of cholera* (J. Churchill, London,, 1855).
48. Medzhitov, R. Approaching the asymptote: 20 years later. *Immunity* **30**, 766-75 (2009).
49. Matzinger, P. The danger model: a renewed sense of self. *Science* **296**, 301-5 (2002).
50. Sansonetti, P. J. The innate signaling of dangers and the dangers of innate signaling. *Nat Immunol* **7**, 1237-42 (2006).
51. Medzhitov, R., Preston-Hurlburt, P. & Janeway, C. A., Jr. A human homologue of the Drosophila Toll protein signals activation of adaptive immunity. *Nature* **388**, 394-7 (1997).
52. Janeway, C. A., Jr., Goodnow, C. C. & Medzhitov, R. Danger - pathogen on the premises! Immunological tolerance. *Curr Biol* **6**, 519-22 (1996).
53. Medzhitov, R. & Janeway, C. A., Jr. Innate immunity: the virtues of a nonclonal system of recognition. *Cell* **91**, 295-8 (1997).
54. Iwasaki, A. & Medzhitov, R. Toll-like receptor control of the adaptive immune responses. *Nat Immunol* **5**, 987-95 (2004).
55. Fearon, D. T. & Locksley, R. M. The instructive role of innate immunity in the acquired immune response. *Science* **272**, 50-3 (1996).
56. Vivier, E. & Malissen, B. Innate and adaptive immunity: specificities and signaling hierarchies revisited. *Nat Immunol* **6**, 17-21 (2005).
57. Eisenbarth, S. C., Colegio, O. R., O'Connor, W., Sutterwala, F. S. & Flavell, R. A. Crucial role for the Nalp3 inflammasome in the immunostimulatory properties of aluminium adjuvants. *Nature* **453**, 1122-6 (2008).
58. De Gregorio, E., Tritto, E. & Rappuoli, R. Alum adjuvanticity: unraveling a century old mystery. *Eur J Immunol* **38**, 2068-71 (2008).

59. Glenny, A. T., Pope, C. G., Waddington, H. & Wallace, U. Immunological notes. *The Journal of Pathology and Bacteriology* **29**, 31-40 (1926).
60. Lindblad, E. B. Aluminium adjuvants--in retrospect and prospect. *Vaccine* **22**, 3658-68 (2004).
61. Lindblad, E. B. Aluminium compounds for use in vaccines. *Immunol Cell Biol* **82**, 497-505 (2004).
62. Condie, R. M., Zak, S. J. & Good, R. A. Effect of meningococcal endotoxin on the immune response. *Proc Soc Exp Biol Med* **90**, 355-60 (1955).
63. Skidmore, B. J., Chiller, J. M., Weigle, W. O., Riblet, R. & Watson, J. Immunologic properties of bacterial lipopolysaccharide (LPS). III. Genetic linkage between the in vitro mitogenic and in vivo adjuvant properties of LPS. *J Exp Med* **143**, 143-50 (1976).
64. Poltorak, A. et al. Defective LPS signaling in C3H/HeJ and C57BL/10ScCr mice: mutations in Tlr4 gene. *Science* **282**, 2085-8 (1998).
65. Hoshino, K. et al. Cutting edge: Toll-like receptor 4 (TLR4)-deficient mice are hyporesponsive to lipopolysaccharide: evidence for TLR4 as the Lps gene product. *J Immunol* **162**, 3749-52 (1999).
66. Yamamoto, M. et al. ASC is essential for LPS-induced activation of procaspase-1 independently of TLR-associated signal adaptor molecules. *Genes Cells* **9**, 1055-67 (2004).
67. Qureshi, S. T. et al. Endotoxin-tolerant mice have mutations in Toll-like receptor 4 (Tlr4). *J Exp Med* **189**, 615-25 (1999).
68. Casella, C. R. & Mitchell, T. C. Putting endotoxin to work for us: monophosphoryl lipid A as a safe and effective vaccine adjuvant. *Cell Mol Life Sci* **65**, 3231-40 (2008).
69. Mata-Haro, V. et al. The vaccine adjuvant monophosphoryl lipid A as a TRIF-biased agonist of TLR4. *Science* **316**, 1628-32 (2007).
70. Lipford, G. B. et al. CpG-containing synthetic oligonucleotides promote B and cytotoxic T cell responses to protein antigen: a new class of vaccine adjuvants. *Eur J Immunol* **27**, 2340-4 (1997).
71. Ada, G. & Isaacs, D. Carbohydrate-protein conjugate vaccines. *Clin Microbiol Infect* **9**, 79-85 (2003).
72. Aguilar, J. C. & Rodriguez, E. G. Vaccine adjuvants revisited. *Vaccine* **25**, 3752-62 (2007).
73. Rietschel, E. T. et al. Bacterial endotoxin: molecular relationships of structure to activity and function. *Faseb J* **8**, 217-25 (1994).
74. Yeh, H. Y. & Jacobs, D. M. Characterization of lipopolysaccharide fractions and their interactions with cells and model membranes. *J Bacteriol* **174**, 336-41 (1992).
75. Goldman, R. C. & Leive, L. Heterogeneity of antigenic-side-chain length in lipopolysaccharide from Escherichia coli 0111 and Salmonella typhimurium LT2. *Eur J Biochem* **107**, 145-53 (1980).
76. Marolda, C. L., Lahiry, P., Vines, E., Saldias, S. & Valvano, M. A. Micromethods for the characterization of lipid A-core and O-antigen lipopolysaccharide. *Methods Mol Biol* **347**, 237-52 (2006).

77. Huber, M. et al. R-form LPS, the master key to the activation ofTLR4/MD-2-positive cells. *Eur J Immunol* **36**, 701-11 (2006).
78. Park, B. S. et al. The structural basis of lipopolysaccharide recognition by the TLR4-MD-2 complex. *Nature* **458**, 1191-5 (2009).
79. Rallabhandi, P. et al. Differential activation of human TLR4 by Escherichia coli and Shigella flexneri 2a lipopolysaccharide: combined effects of lipid A acylation state and TLR4 polymorphisms on signaling. *J Immunol* **180**, 1139-47 (2008).
80. Dowling, D., Hamilton, C. M. & O'Neill, S. M. A comparative analysis of cytokine responses, cell surface marker expression and MAPKs in DCs matured with LPS compared with a panel of TLR ligands. *Cytokine* **41**, 254-62 (2008).
81. Alexander, C. & Rietschel, E. T. Bacterial lipopolysaccharides and innate immunity. *J Endotoxin Res* **7**, 167-202 (2001).
82. Miyake, K. Roles for accessory molecules in microbial recognition by Toll-like receptors. *J Endotoxin Res* **12**, 195-204 (2006).
83. Wright, S. D., Ramos, R. A., Tobias, P. S., Ulevitch, R. J. & Mathison, J. C. CD14, a receptor for complexes of lipopolysaccharide (LPS) and LPS binding protein. *Science* **249**, 1431-3 (1990).
84. Kagan, J. C. et al. TRAM couples endocytosis of Toll-like receptor 4 to the induction of interferon-beta. *Nat Immunol* **9**, 361-8 (2008).
85. Kawai, T. & Akira, S. Signaling to NF-kappaB by Toll-like receptors. *Trends Mol Med* (2007).
86. Jiang, Z. et al. CD14 is required for MyD88-independent LPS signaling. *Nat Immunol* **6**, 565-70 (2005).
87. Georgel, P. et al. Vesicular stomatitis virus glycoprotein G activates a specific antiviral Toll-like receptor 4-dependent pathway. *Virology* **362**, 304-13 (2007).
88. Rhee, S. H. & Hwang, D. Murine TOLL-like receptor 4 confers lipopolysaccharide responsiveness as determined by activation of NF kappa B and expression of the inducible cyclooxygenase. *J Biol Chem* **275**, 34035-40 (2000).
89. Trompette, A. et al. Allergenicity resulting from functional mimicry of a Toll-like receptor complex protein. *Nature* **457**, 585-8 (2009).
90. Booth, J. S., Griebel, P. J., Babiuk, L. A. & Mutwiri, G. K. A novel regulatory B-cell population in sheep Peyer's patches spontaneously secretes IL-10 and downregulates TLR9-induced IFNalpha responses. *Mucosal Immunol* **2**, 265-75 (2009).
91. Takeda, K., Kaisho, T. & Akira, S. Toll-like receptors. *Annu Rev Immunol* **21**, 335-76 (2003).
92. Farkas, L., Kvale, E. O., Lund-Johansen, F. & Jahnsen, F. L. Plasmacytoid dendritic cells induce a distinct cytokine pattern in virus-specific CD4+ memory T cells that is modulated by CpG oligodeoxynucleotides. *Scand J Immunol* **64**, 404-11 (2006).
93. Krieg, A. M. CpG motifs: the active ingredient in bacterial extracts? *Nat Med* **9**, 831-5 (2003).
94. Franchi, L., Warner, N., Viani, K. & Nunez, G. Function of Nod-like receptors in microbial recognition and host defense. *Immunol Rev* **227**, 106-28 (2009).

95. Lamkanfi, M. & Dixit, V. M. Inflammasomes: guardians of cytosolic sanctity. *Immunol Rev* **227**, 95-105 (2009).
96. Martinon, F., Burns, K. & Tschopp, J. The inflammasome: a molecular platform triggering activation of inflammatory caspases and processing of proIL-beta. *Mol Cell* **10**, 417-26 (2002).
97. Kato, H. et al. Cell type-specific involvement of RIG-I in antiviral response. *Immunity* **23**, 19-28 (2005).
98. Takeuchi, O. & Akira, S. Innate immunity to virus infection. *Immunol Rev* **227**, 75-86 (2009).
99. Yoshimoto, T. et al. Basophils contribute to T(H)2-IgE responses in vivo via IL-4 production and presentation of peptide-MHC class II complexes to CD4+ T cells. *Nat Immunol* **10**, 706-12 (2009).
100. Sokol, C. L. et al. Basophils function as antigen-presenting cells for an allergen-induced T helper type 2 response. *Nat Immunol* **10**, 713-20 (2009).
101. Perrigoue, J. G. et al. MHC class II-dependent basophil-CD4+ T cell interactions promote T(H)2 cytokine-dependent immunity. *Nat Immunol* **10**, 697-705 (2009).
102. Janeway, C. A., Jr. Approaching the asymptote? Evolution and revolution in immunology. *Cold Spring Harb Symp Quant Biol* **54 Pt 1**, 1-13 (1989).
103. Altin, J. G. & Parish, C. R. Liposomal vaccines--targeting the delivery of antigen. *Methods* **40**, 39-52 (2006).
104. Cooper, A. M. & Khader, S. A. The role of cytokines in the initiation, expansion, and control of cellular immunity to tuberculosis. *Immunol Rev* **226**, 191-204 (2008).
105. Takahashi, H. Antigen presentation in vaccine development. *Comp Immunol Microbiol Infect Dis* **26**, 309-28 (2003).
106. Seder, R. A. & Ahmed, R. Similarities and differences in CD4+ and CD8+ effector and memory T cell generation. *Nat Immunol* **4**, 835-42 (2003).
107. Foulds, K. E., Wu, C. Y. & Seder, R. A. Th1 memory: implications for vaccine development. *Immunol Rev* **211**, 58-66 (2006).
108. Steinman, L. A brief history of T(H)17, the first major revision in the T(H)1/T(H)2 hypothesis of T cell-mediated tissue damage. *Nat Med* **13**, 139-45 (2007).
109. Kaech, S. M., Wherry, E. J. & Ahmed, R. Effector and memory T-cell differentiation: implications for vaccine development. *Nat Rev Immunol* **2**, 251-62 (2002).
110. Ahmed, R. & Gray, D. Immunological memory and protective immunity: understanding their relation. *Science* **272**, 54-60 (1996).
111. Blattman, J. N. et al. Therapeutic use of IL-2 to enhance antiviral T-cell responses in vivo. *Nat Med* **9**, 540-7 (2003).
112. Fields, P. E., Kim, S. T. & Flavell, R. A. Cutting edge: changes in histone acetylation at the IL-4 and IFN-gamma loci accompany Th1/Th2 differentiation. *J Immunol* **169**, 647-50 (2002).
113. Szabo, S. J. et al. A novel transcription factor, T-bet, directs Th1 lineage commitment. *Cell* **100**, 655-69 (2000).

114. Zheng, W. & Flavell, R. A. The transcription factor GATA-3 is necessary and sufficient for Th2 cytokine gene expression in CD4 T cells. *Cell* **89**, 587-96 (1997).
115. Medzhitov, R. Toll-like receptors and innate immunity. *Nat Rev Immunol* **1**, 135-45 (2001).
116. Webb, D. C., Cai, Y., Matthaei, K. I. & Foster, P. S. Comparative roles of IL-4, IL-13, and IL-4Ralpha in dendritic cell maturation and CD4+ Th2 cell function. *J Immunol* **178**, 219-27 (2007).
117. Fouser, L. A., Wright, J. F., Dunussi-Joannopoulos, K. & Collins, M. Th17 cytokines and their emerging roles in inflammation and autoimmunity. *Immunol Rev* **226**, 87-102 (2008).
118. Nair, R. P. et al. Genome-wide scan reveals association of psoriasis with IL-23 and NF-kappaB pathways. *Nat Genet* **41**, 199-204 (2009).
119. Dong, C. Regulation and pro-inflammatory function of interleukin-17 family cytokines. *Immunol Rev* **226**, 80-6 (2008).
120. Priebe, G. P. et al. IL-17 is a critical component of vaccine-induced protection against lung infection by lipopolysaccharide-heterologous strains of Pseudomonas aeruginosa. *J Immunol* **181**, 4965-75 (2008).
121. Smiley, K. L. et al. Association of gamma interferon and interleukin-17 production in intestinal CD4+ T cells with protection against rotavirus shedding in mice intranasally immunized with VP6 and the adjuvant LT(R192G). *J Virol* **81**, 3740-8 (2007).
122. Khader, S. A. et al. IL-23 and IL-17 in the establishment of protective pulmonary CD4+ T cell responses after vaccination and during Mycobacterium tuberculosis challenge. *Nat Immunol* **8**, 369-77 (2007).
123. Higgins, S. C., Jarnicki, A. G., Lavelle, E. C. & Mills, K. H. TLR4 mediates vaccine-induced protective cellular immunity to Bordetella pertussis: role of IL-17-producing T cells. *J Immunol* **177**, 7980-9 (2006).
124. Aarvak, T., Chabaud, M., Miossec, P. & Natvig, J. B. IL-17 is produced by some proinflammatory Th1/Th0 cells but not by Th2 cells. *J Immunol* **162**, 1246-51 (1999).
125. Manz, R. A. & Radbruch, A. Plasma cells for a lifetime? *Eur J Immunol* **32**, 923-7 (2002).
126. Cassese, G. et al. Plasma cell survival is mediated by synergistic effects of cytokines and adhesion-dependent signals. *J Immunol* **171**, 1684-90 (2003).
127. Slifka, M. K., Antia, R., Whitmire, J. K. & Ahmed, R. Humoral immunity due to long-lived plasma cells. *Immunity* **8**, 363-72 (1998).
128. Wherry, E. J. et al. Lineage relationship and protective immunity of memory CD8 T cell subsets. *Nat Immunol* **4**, 225-34 (2003).
129. Lagrange, P. H., Mackaness, G. B. & Miller, T. E. Influence of dose and route of antigen injection on the immunological induction of T cells. *J Exp Med* **139**, 528-42 (1974).
130. Vajdy, M. & Lycke, N. Stimulation of antigen-specific T- and B-cell memory in local as well as systemic lymphoid tissues following oral immunization with cholera toxin adjuvant. *Immunology* **80**, 197-203 (1993).

131. Starzl, T. E. & Zinkernagel, R. M. Antigen localization and migration in immunity and tolerance. *N Engl J Med* **339**, 1905-13 (1998).
132. Tato, C. M. & Cua, D. J. SnapShot: Cytokines I. *Cell* **132**, 324, 324 e1 (2008).
133. Tato, C. M. & Cua, D. J. SnapShot: cytokines II. *Cell* **132**, 500 (2008).
134. Tato, C. M. & Cua, D. J. SnapShot: cytokines III. *Cell* **132**, 900 (2008).
135. Tato, C. M. & Cua, D. J. SnapShot: Cytokines IV. *Cell* **132**, 1062 e1-2 (2008).
136. Flynn, J. L. et al. An essential role for interferon gamma in resistance to Mycobacterium tuberculosis infection. *J Exp Med* **178**, 2249-54 (1993).
137. Brady, M. T., Mahon, B. P. & Mills, K. H. Pertussis infection and vaccination induces Th1 cells. *Immunol Today* **19**, 534 (1998).
138. Isaacs, A. & Lindenmann, J. Virus interference. I. The interferon. *Proc R Soc Lond B Biol Sci* **147**, 258-67 (1957).
139. Isaacs, A., Lindenmann, J. & Valentine, R. C. Virus interference. II. Some properties of interferon. *Proc R Soc Lond B Biol Sci* **147**, 268-73 (1957).
140. O'Neill, L. A. The role of MyD88-like adapters in Toll-like receptor signal transduction. *Biochem Soc Trans* **31**, 643-7 (2003).
141. Creagh, E. M. & O'Neill, L. A. TLRs, NLRs and RLRs: a trinity of pathogen sensors that co-operate in innate immunity. *Trends Immunol* **27**, 352-7 (2006).
142. Steinman, R. M. & Moberg, C. L. Zanvil Alexander Cohn 1926-1993. *J Exp Med* **179**, 1-30 (1994).
143. Trinchieri, G. Interleukin-12 and the regulation of innate resistance and adaptive immunity. *Nat Rev Immunol* **3**, 133-46 (2003).
144. Biron, C. A., Nguyen, K. B., Pien, G. C., Cousens, L. P. & Salazar-Mather, T. P. Natural killer cells in antiviral defense: function and regulation by innate cytokines. *Annu Rev Immunol* **17**, 189-220 (1999).
145. Ohteki, T. & Koyasu, S. Role of antigen-presenting cells in innate immune system. *Arch Immunol Ther Exp (Warsz)* **49 Suppl 1**, S47-52 (2001).
146. Airoldi, I. et al. Expression and function of IL-12 and IL-18 receptors on human tonsillar B cells. *J Immunol* **165**, 6880-8 (2000).
147. Mosmann, T. R. & Coffman, R. L. TH1 and TH2 cells: different patterns of lymphokine secretion lead to different functional properties. *Annu Rev Immunol* **7**, 145-73 (1989).
148. Openshaw, P. et al. Heterogeneity of intracellular cytokine synthesis at the single-cell level in polarized T helper 1 and T helper 2 populations. *J Exp Med* **182**, 1357-67 (1995).
149. Smeltz, R. B., Chen, J., Ehrhardt, R. & Shevach, E. M. Role of IFN-gamma in Th1 differentiation: IFN-gamma regulates IL-18R alpha expression by preventing the negative effects of IL-4 and by inducing/maintaining IL-12 receptor beta 2 expression. *J Immunol* **168**, 6165-72 (2002).
150. Biron, C. A. Role of early cytokines, including alpha and beta interferons (IFN-alpha/beta), in innate and adaptive immune responses to viral infections. *Semin Immunol* **10**, 383-90 (1998).
151. Beutler, B. et al. Identity of tumour necrosis factor and the macrophage-secreted factor cachectin. *Nature* **316**, 552-4 (1985).

152. Papa, S., Zazzeroni, F., Pham, C. G., Bubici, C. & Franzoso, G. Linking JNK signaling to NF-kappaB: a key to survival. *J Cell Sci* **117**, 5197-208 (2004).
153. Bethin, K. E., Vogt, S. K. & Muglia, L. J. Interleukin-6 is an essential, corticotropin-releasing hormone-independent stimulator of the adrenal axis during immune system activation. *Proc Natl Acad Sci U S A* **97**, 9317-22 (2000).
154. Steensberg, A. et al. IL-6 and TNF-alpha expression in, and release from, contracting human skeletal muscle. *Am J Physiol Endocrinol Metab* **283**, E1272-8 (2002).
155. Waage, A., Brandtzaeg, P., Halstensen, A., Kierulf, P. & Espevik, T. The complex pattern of cytokines in serum from patients with meningococcal septic shock. Association between interleukin 6, interleukin 1, and fatal outcome. *J Exp Med* **169**, 333-8 (1989).
156. Castell, J. V. et al. Recombinant human interleukin-6 (IL-6/BSF-2/HSF) regulates the synthesis of acute phase proteins in human hepatocytes. *FEBS Lett* **232**, 347-50 (1988).
157. Hirotani, T. et al. Regulation of lipopolysaccharide-inducible genes by MyD88 and Toll/IL-1 domain containing adaptor inducing IFN-beta. *Biochem Biophys Res Commun* **328**, 383-92 (2005).
158. Kawai, T., Adachi, O., Ogawa, T., Takeda, K. & Akira, S. Unresponsiveness of MyD88-deficient mice to endotoxin. *Immunity* **11**, 115-22 (1999).
159. Burrows, P. D., Kronenberg, M. & Taniguchi, M. NKT cells turn ten. *Nat Immunol* **10**, 669-71 (2009).
160. Mosser, D. M. & Zhang, X. Interleukin-10: new perspectives on an old cytokine. *Immunol Rev* **226**, 205-18 (2008).
161. Dong, C. Diversification of T-helper-cell lineages: finding the family root of IL-17-producing cells. *Nat Rev Immunol* **6**, 329-33 (2006).
162. Lenarczyk, A. et al. Antigen-induced IL-17 response in the peripheral blood mononuclear cells (PBMC) of healthy controls. *Clin Exp Immunol* **122**, 41-8 (2000).
163. Gu, Y. et al. Interleukin 10 suppresses Th17 cytokines secreted by macrophages and T cells. *Eur J Immunol* **38**, 1807-13 (2008).
164. Gallo, R. C. et al. Isolation of human T-cell leukemia virus in acquired immune deficiency syndrome (AIDS). *Science* **220**, 865-7 (1983).
165. Jaffe, H. W., Bregman, D. J. & Selik, R. M. Acquired immune deficiency syndrome in the United States: the first 1,000 cases. *J Infect Dis* **148**, 339-45 (1983).
166. Barre-Sinoussi, F. et al. Isolation of a T-lymphotropic retrovirus from a patient at risk for acquired immune deficiency syndrome (AIDS). *Science* **220**, 868-71 (1983).
167. Barban, V. et al. High stability of yellow fever 17D-204 vaccine: a 12-year restrospective analysis of large-scale production. *Vaccine* **25**, 2941-50 (2007).
168. Griffin, D. E. & Pan, C. H. Measles: old vaccines, new vaccines. *Curr Top Microbiol Immunol* **330**, 191-212 (2009).
169. Salk, J. E. et al. Formaldehyde treatment and safety testing of experimental poliomyelitis vaccines. *Am J Public Health Nations Health* **44**, 563-70 (1954).

170. Alarcon, J. B., Waine, G. W. & McManus, D. P. DNA vaccines: technology and application as anti-parasite and anti-microbial agents. *Adv Parasitol* **42**, 343-410 (1999).
171. Kundig, T. M., Kalberer, C. P., Hengartner, H. & Zinkernagel, R. M. Vaccination with two different vaccinia recombinant viruses: long-term inhibition of secondary vaccination. *Vaccine* **11**, 1154-8 (1993).
172. van Oers, M. M. Vaccines for viral and parasitic diseases produced with baculovirus vectors. *Adv Virus Res* **68**, 193-253 (2006).
173. Stanley, M. A. Human papillomavirus vaccines. *Curr Opin Mol Ther* **4**, 15-22 (2002).
174. Mena, J. A., Ramirez, O. T. & Palomares, L. A. Population kinetics during simultaneous infection of insect cells with two different recombinant baculoviruses for the production of rotavirus-like particles. *BMC Biotechnol* **7**, 39 (2007).
175. Soborg, C. et al. Vaccines in a hurry. *Vaccine* **27**, 3295-8 (2009).
176. Klugman, K. P. et al. A trial of a 9-valent pneumococcal conjugate vaccine in children with and those without HIV infection. *N Engl J Med* **349**, 1341-8 (2003).
177. Bimber, B. N. et al. Ultradeep pyrosequencing detects complex patterns of CD8+ T-lymphocyte escape in simian immunodeficiency virus-infected macaques. *J Virol* **83**, 8247-53 (2009).
178. Rowe, J. E., Messinger, I. K., Schwendeman, C. A. & Popejoy, L. A. Three-dose vaccination of infants under 8 months of age with a conjugate Haemophilus influenzae type B vaccine. *Mil Med* **155**, 483-6 (1990).
179. Steinman, R. M. & Banchereau, J. Taking dendritic cells into medicine. *Nature* **449**, 419-26 (2007).
180. Donnelly, J., Berry, K. & Ulmer, J. B. Technical and regulatory hurdles for DNA vaccines. *Int J Parasitol* **33**, 457-67 (2003).
181. Lu, S. Immunogenicity of DNA vaccines in humans: it takes two to tango. *Hum Vaccin* **4**, 449-52 (2008).
182. Trepel, M., Arap, W. & Pasqualini, R. Modulation of the immune response by systemic targeting of antigens to lymph nodes. *Cancer Res* **61**, 8110-2 (2001).
183. Wang, X. & Lu, C. Mice orally vaccinated with Edwardsiella tarda ghosts are significantly protected against infection. *Vaccine* **27**, 1571-8 (2009).
184. Cuesta, A. M. et al. Enhancement of DNA vaccine potency through linkage of antigen to filamentous bacteriophage coat protein III domain I. *Immunology* **117**, 502-6 (2006).
185. Clark, J. R. & March, J. B. Bacteriophages and biotechnology: vaccines, gene therapy and antibacterials. *Trends Biotechnol* **24**, 212-8 (2006).
186. March, J. B., Clark, J. R. & Jepson, C. D. Genetic immunisation against hepatitis B using whole bacteriophage lambda particles. *Vaccine* **22**, 1666-71 (2004).
187. Caputo, A., Sparnacci, K., Ensoli, B. & Tondelli, L. Functional polymeric nano/microparticles for surface adsorption and delivery of protein and DNA vaccines. *Curr Drug Deliv* **5**, 230-42 (2008).
188. Patil, S. D., Rhodes, D. G. & Burgess, D. J. DNA-based therapeutics and DNA delivery systems: a comprehensive review. *Aaps J* **7**, E61-77 (2005).

189. Seow, Y. & Wood, M. J. Biological gene delivery vehicles: beyond viral vectors. *Mol Ther* **17**, 767-77 (2009).
190. Neutra, M. R. & Kozlowski, P. A. Mucosal vaccines: the promise and the challenge. *Nat Rev Immunol* **6**, 148-58 (2006).
191. Oma, K. et al. Intranasal immunization with a mixture of PspA and a Toll-like receptor agonist induces specific antibodies and enhances bacterial clearance in the airways of mice. *Vaccine* **27**, 3181-8 (2009).
192. Dubin, P. J. & Kolls, J. K. Th17 cytokines and mucosal immunity. *Immunol Rev* **226**, 160-71 (2008).
193. Rakoff-Nahoum, S. & Medzhitov, R. Innate immune recognition of the indigenous microbial flora. *Mucosal Immunol* **1 Suppl 1**, S10-4 (2008).
194. Aujla, S. J., Dubin, P. J. & Kolls, J. K. Th17 cells and mucosal host defense. *Semin Immunol* **19**, 377-82 (2007).
195. Zanvit, P. et al. Immune response after adjuvant mucosal immunization of mice with inactivated influenza virus. *Immunol Lett* **97**, 251-9 (2005).
196. Cocchi, F. et al. Identification of RANTES, MIP-1 alpha, and MIP-1 beta as the major HIV-suppressive factors produced by CD8+ T cells. *Science* **270**, 1811-5 (1995).
197. Denton, P. W. & Garcia, J. V. Novel humanized murine models for HIV research. *Curr HIV/AIDS Rep* **6**, 13-9 (2009).
198. Legrand, N. et al. Humanized mice for modeling human infectious disease: challenges, progress, and outlook. *Cell Host Microbe* **6**, 5-9 (2009).
199. Khurana, S. et al. Antigenic fingerprinting of H5N1 avian influenza using convalescent sera and monoclonal antibodies reveals potential vaccine and diagnostic targets. *PLoS Med* **6**, e1000049 (2009).
200. Demangel, C. et al. Phage-displayed mimotopes elicit monoclonal antibodies specific for a malaria vaccine candidate. *Biol Chem* **379**, 65-70 (1998).
201. Grabowska, A. M. et al. Immunisation with phage displaying peptides representing single epitopes of the glycoprotein G can give rise to partial protective immunity to HSV-2. *Virology* **269**, 47-53 (2000).
202. Greenwood, J., Willis, A. E. & Perham, R. N. Multiple display of foreign peptides on a filamentous bacteriophage. Peptides from Plasmodium falciparum circumsporozoite protein as antigens. *J Mol Biol* **220**, 821-7 (1991).
203. Clark, J. R. & March, J. B. Bacteriophage-mediated nucleic acid immunisation. *FEMS Immunol Med Microbiol* **40**, 21-6 (2004).
204. Weiner, H. L. Oral tolerance. *Proc Natl Acad Sci U S A* **91**, 10762-5 (1994).
205. Jepson, C. D. & March, J. B. Bacteriophage lambda is a highly stable DNA vaccine delivery vehicle. *Vaccine* **22**, 2413-9 (2004).
206. Vitiello, C. L., Merril, C. R. & Adhya, S. An amino acid substitution in a capsid protein enhances phage survival in mouse circulatory system more than a 1000-fold. *Virus Res* **114**, 101-3 (2005).
207. Sapinoro, R., Volcy, K., Rodrigo, W. W., Schlesinger, J. J. & Dewhurst, S. Fc receptor-mediated, antibody-dependent enhancement of bacteriophage lambda-mediated gene transfer in mammalian cells. *Virology* **373**, 274-86 (2008).

208. Zanghi, C. N., Sapinoro, R., Bradel-Tretheway, B. & Dewhurst, S. A tractable method for simultaneous modifications to the head and tail of bacteriophage lambda and its application to enhancing phage-mediated gene delivery. *Nucleic Acids Res* **35**, e59 (2007).
209. Motti, C. et al. Recognition by human sera and immunogenicity of HBsAg mimotopes selected from an M13 phage display library. *Gene* **146**, 191-8 (1994).
210. Yu, M. W., Scott, J. K., Fournier, A. & Talbot, P. J. Characterization of murine coronavirus neutralization epitopes with phage-displayed peptides. *Virology* **271**, 182-96 (2000).
211. Sambrook, J. & Russell, D. W. *Molecular cloning : a laboratory manual* (Cold Spring Harbor Laboratory Press, Cold Spring Harbor, N.Y., 2001).
212. Roberts, R. J. How restriction enzymes became the workhorses of molecular biology. *Proc Natl Acad Sci U S A* **102**, 5905-8 (2005).
213. Pingoud, A. & Jeltsch, A. Recognition and cleavage of DNA by type-II restriction endonucleases. *Eur J Biochem* **246**, 1-22 (1997).
214. Zeugin, J. A. & Hartley, J. L. Ethanol Precipitation of DNA. *Focus* **7**, 1-2 (1985).
215. Crouse, J. & Amorese, D. Ethanol Precipitation: Ammonium Acetate as an Alternative to Sodium Acetate. *Focus* **9**, 3-5 (1987).
216. Le Pecq, J. B. & Paoletti, C. A new fluorometric method for RNA and DNA determination. *Anal Biochem* **17**, 100-7 (1966).
217. Ye, J., McGinnis, S. & Madden, T. L. BLAST: improvements for better sequence analysis. *Nucleic Acids Res* **34**, W6-9 (2006).
218. Johnson, M. et al. NCBI BLAST: a better web interface. *Nucleic Acids Res* **36**, W5-9 (2008).
219. Tatusova, T. A. & Madden, T. L. BLAST 2 Sequences, a new tool for comparing protein and nucleotide sequences. *FEMS Microbiol Lett* **174**, 247-50 (1999).
220. Rozen, S. & Skaletsky, H. Primer3 on the WWW for general users and for biologist programmers. *Methods Mol Biol* **132**, 365-86 (2000).
221. http://www.premierbiosoft.com/netprimer/index.html. NetPrimer. *Premier Biosoft Inc.* (2009).
222. Oppenheim, A. B., Rattray, A. J., Bubunenko, M., Thomason, L. C. & Court, D. L. In vivo recombineering of bacteriophage lambda by PCR fragments and single-strand oligonucleotides. *Virology* **319**, 185-9 (2004).
223. Copeland, N. G., Jenkins, N. A. & Court, D. L. Recombineering: a powerful new tool for mouse functional genomics. *Nat Rev Genet* **2**, 769-79 (2001).
224. Friedman, D. I. & Court, D. L. Bacteriophage lambda: alive and well and still doing its thing. *Curr Opin Microbiol* **4**, 201-7 (2001).
225. Court, D. L., Sawitzke, J. A. & Thomason, L. C. Genetic engineering using homologous recombination. *Annu Rev Genet* **36**, 361-88 (2002).
226. Thomas, B., Woltjen, K. & Rancourt, D. E. Deep screening of recombination proficient bacteriophage libraries. *Biotechniques* **34**, 36-8, 40 (2003).
227. Woltjen, K., Ito, K., Tsuzuki, T. & Rancourt, D. E. Orpheus recombination : a comprehensive bacteriophage system for murine targeting vector construction by transplacement. *Methods Mol Biol* **435**, 79-94 (2008).

228. Woltjen, K., Unger, M. W. & Rancourt, D. E. Transplacement mutagenesis. A recombination-based in situ mutagenesis protocol. *Methods Mol Biol* **182**, 189-207 (2002).
229. Woltjen, K., Bain, G. & Rancourt, D. E. Retro-recombination screening of a mouse embryonic stem cell genomic library. *Nucleic Acids Res* **28**, E41 (2000).
230. Crasto, C. J. & Feng, J. A. LINKER: a program to generate linker sequences for fusion proteins. *Protein Eng* **13**, 309-12 (2000).
231. Schwarze, S. R. & Dowdy, S. F. In vivo protein transduction: intracellular delivery of biologically active proteins, compounds and DNA. *Trends Pharmacol Sci* **21**, 45-8 (2000).
232. Richard, J. P. et al. Cellular uptake of unconjugated TAT peptide involves clathrin-dependent endocytosis and heparan sulfate receptors. *J Biol Chem* **280**, 15300-6 (2005).
233. Richard, J. P. et al. Cell-penetrating peptides. A reevaluation of the mechanism of cellular uptake. *J Biol Chem* **278**, 585-90 (2003).
234. Lundberg, M., Wikstrom, S. & Johansson, M. Cell surface adherence and endocytosis of protein transduction domains. *Mol Ther* **8**, 143-50 (2003).
235. Tyagi, M., Rusnati, M., Presta, M. & Giacca, M. Internalization of HIV-1 tat requires cell surface heparan sulfate proteoglycans. *J Biol Chem* **276**, 3254-61 (2001).
236. Vives, E., Richard, J. P., Rispal, C. & Lebleu, B. TAT peptide internalization: seeking the mechanism of entry. *Curr Protein Pept Sci* **4**, 125-32 (2003).
237. Lefever, S., Vandesompele, J., Speleman, F. & Pattyn, F. RTPrimerDB: the portal for real-time PCR primers and probes. *Nucleic Acids Res* **37**, D942-5 (2009).
238. Pattyn, F., Speleman, F., De Paepe, A. & Vandesompele, J. RTPrimerDB: the real-time PCR primer and probe database. *Nucleic Acids Res* **31**, 122-3 (2003).
239. Pattyn, F., Robbrecht, P., De Paepe, A., Speleman, F. & Vandesompele, J. RTPrimerDB: the real-time PCR primer and probe database, major update 2006. *Nucleic Acids Res* **34**, D684-8 (2006).
240. Giulietti, A. et al. An overview of real-time quantitative PCR: applications to quantify cytokine gene expression. *Methods* **25**, 386-401 (2001).
241. Pan, J. Z. et al. Cytokine activity contributes to induction of inflammatory cytokine mRNAs in spinal cord following contusion. *J Neurosci Res* **68**, 315-22 (2002).
242. Kim, H. P., Korn, L. L., Gamero, A. M. & Leonard, W. J. Calcium-dependent activation of interleukin-21 gene expression in T cells. *J Biol Chem* **280**, 25291-7 (2005).
243. Overbergh, L., Valckx, D., Waer, M. & Mathieu, C. Quantification of murine cytokine mRNAs using real time quantitative reverse transcriptase PCR. *Cytokine* **11**, 305-12 (1999).
244. Bas, A., Forsberg, G., Hammarstrom, S. & Hammarstrom, M. L. Utility of the housekeeping genes 18S rRNA, beta-actin and glyceraldehyde-3-phosphate-dehydrogenase for normalization in real-time quantitative reverse transcriptase-polymerase chain reaction analysis of gene expression in human T lymphocytes. *Scand J Immunol* **59**, 566-73 (2004).

245. Pfaffl, M. W., Horgan, G. W. & Dempfle, L. Relative expression software tool (REST) for group-wise comparison and statistical analysis of relative expression results in real-time PCR. *Nucleic Acids Res* **30**, e36 (2002).
246. Pfaffl, M. W. A new mathematical model for relative quantification in real-time RT-PCR. *Nucleic Acids Res* **29**, e45 (2001).
247. Takeuchi, O. et al. Differential roles of TLR2 and TLR4 in recognition of gram-negative and gram-positive bacterial cell wall components. *Immunity* **11**, 443-51 (1999).
248. Adachi, O. et al. Targeted disruption of the MyD88 gene results in loss of IL-1- and IL-18-mediated function. *Immunity* **9**, 143-50 (1998).
249. Hoff, J. Methods of blood collection in the mouse. *Lab Animal* **29**, 47-53 (2000).
250. Winston, B. W., Chan, E. D., Johnson, G. L. & Riches, D. W. Activation of p38mapk, MKK3, and MKK4 by TNF-alpha in mouse bone marrow-derived macrophages. *J Immunol* **159**, 4491-7 (1997).
251. Hitchcock, P. J. & Brown, T. M. Morphological heterogeneity among Salmonella lipopolysaccharide chemotypes in silver-stained polyacrylamide gels. *J Bacteriol* **154**, 269-77 (1983).
252. FDA. 49 pages (Guideline on the Validation of the Limulus Amebocyte Lysate Test as an end-product Endotoxin Test for Human and Animal Parenteral Drugs, Biological Products and Medical Devices., Rockville, MD, 1987).
253. Issekutz, A. C. Removal of gram-negative endotoxin from solutions by affinity chromatography. *J Immunol Methods* **61**, 275-81 (1983).
254. Parmley, S. F. & Smith, G. P. Antibody-selectable filamentous fd phage vectors: affinity purification of target genes. *Gene* **73**, 305-18 (1988).
255. Smith, G. P. Filamentous fusion phage: novel expression vectors that display cloned antigens on the virion surface. *Science* **228**, 1315-7 (1985).
256. Lee, J. H., Engler, J. A., Collawn, J. F. & Moore, B. A. Receptor mediated uptake of peptides that bind the human transferrin receptor. *Eur J Biochem* **268**, 2004-12 (2001).
257. Hoess, R. H. Protein design and phage display. *Chem Rev* **101**, 3205-18 (2001).
258. Karlson, U., Pejler, G., Froman, G. & Hellman, L. Rat mast cell protease 4 is a beta-chymase with unusually stringent substrate recognition profile. *J Biol Chem* **277**, 18579-85 (2002).
259. Barbas, C. F., 3rd et al. In vitro evolution of a neutralizing human antibody to human immunodeficiency virus type 1 to enhance affinity and broaden strain cross-reactivity. *Proc Natl Acad Sci U S A* **91**, 3809-13 (1994).
260. Malik, P. et al. Role of capsid structure and membrane protein processing in determining the size and copy number of peptides displayed on the major coat protein of filamentous bacteriophage. *J Mol Biol* **260**, 9-21 (1996).
261. Maruyama, I. N., Maruyama, H. I. & Brenner, S. Lambda foo: a lambda phage vector for the expression of foreign proteins. *Proc Natl Acad Sci U S A* **91**, 8273-7 (1994).
262. Mikawa, Y. G., Maruyama, I. N. & Brenner, S. Surface display of proteins on bacteriophage lambda heads. *J Mol Biol* **262**, 21-30 (1996).

263. Sternberg, N. & Hoess, R. H. Display of peptides and proteins on the surface of bacteriophage lambda. *Proc Natl Acad Sci U S A* **92**, 1609-13 (1995).
264. Dunn, I. S. Assembly of functional bacteriophage lambda virions incorporating C-terminal peptide or protein fusions with the major tail protein. *J Mol Biol* **248**, 497-506 (1995).
265. Hendrix, R., Roberts, J., Stahl, F. & Weisberg, R. *Lambda II* (Cold Spring Harbor Laboratory Press, Cold Spring Harbor, New York, 1983).
266. Gupta, A., Onda, M., Pastan, I., Adhya, S. & Chaudhary, V. K. High-density functional display of proteins on bacteriophage lambda. *J Mol Biol* **334**, 241-54 (2003).
267. Hershey, A. D. *The Bacteriophage Lambda* (Cold Spring Harbor Laboratory Press, Cold Spring Harbor, New York, 1971).
268. Dokland, T. & Murialdo, H. Structural transitions during maturation of bacteriophage lambda capsids. *J Mol Biol* **233**, 682-94 (1993).
269. Eguchi, A. et al. Protein transduction domain of HIV-1 Tat protein promotes efficient delivery of DNA into mammalian cells. *J Biol Chem* **276**, 26204-10 (2001).
270. Piersanti, S. et al. Mammalian cell transduction and internalization properties of lambda phages displaying the full-length adenoviral penton base or its central domain. *J Mol Med* **82**, 467-76 (2004).
271. Santi, E. et al. Bacteriophage lambda display of complex cDNA libraries: a new approach to functional genomics. *J Mol Biol* **296**, 497-508 (2000).
272. Akuta, T. et al. Enhancement of phage-mediated gene transfer by nuclear localization signal. *Biochem Biophys Res Commun* **297**, 779-86 (2002).
273. Yang, F. et al. Novel fold and capsid-binding properties of the lambda-phage display platform protein gpD. *Nat Struct Biol* **7**, 230-7 (2000).
274. Unger, M. W., Liu, S. Y. & Rancourt, D. E. Transplacement mutagenesis: a novel in situ mutagenesis system using phage-plasmid recombination. *Nucleic Acids Res* **27**, 1480-4 (1999).
275. Hasty, P., Rivera-Perez, J. & Bradley, A. The length of homology required for gene targeting in embryonic stem cells. *Mol Cell Biol* **11**, 5586-91 (1991).
276. Deng, C. & Capecchi, M. R. Reexamination of gene targeting frequency as a function of the extent of homology between the targeting vector and the target locus. *Mol Cell Biol* **12**, 3365-71 (1992).
277. Sedivy, J. M. & Sharp, P. A. Positive genetic selection for gene disruption in mammalian cells by homologous recombination. *Proc Natl Acad Sci U S A* **86**, 227-31 (1989).
278. Donoho, G., Jasin, M. & Berg, P. Analysis of gene targeting and intrachromosomal homologous recombination stimulated by genomic double-strand breaks in mouse embryonic stem cells. *Mol Cell Biol* **18**, 4070-8 (1998).
279. Mansour, S. L., Thomas, K. R. & Capecchi, M. R. Disruption of the proto-oncogene int-2 in mouse embryo-derived stem cells: a general strategy for targeting mutations to non-selectable genes. *Nature* **336**, 348-52 (1988).
280. Hsiung, N. et al. Introduction and expression of a fetal human globin gene in mouse fibroblasts. *Mol Cell Biol* **2**, 401-11 (1982).

281. Kucherlapati, R. S., Eves, E. M., Song, K. Y., Morse, B. S. & Smithies, O. Homologous recombination between plasmids in mammalian cells can be enhanced by treatment of input DNA. *Proc Natl Acad Sci U S A* **81**, 3153-7 (1984).
282. Roginski, R. S. et al. Coordinate modulation of transfected HSV thymidine kinase and human globin genes. *Cell* **35**, 149-55 (1983).
283. Capecchi, M. R. High efficiency transformation by direct microinjection of DNA into cultured mammalian cells. *Cell* **22**, 479-88 (1980).
284. Thomas, K. R., Folger, K. R. & Capecchi, M. R. High frequency targeting of genes to specific sites in the mammalian genome. *Cell* **44**, 419-28 (1986).
285. Thomas, K. R. & Capecchi, M. R. Site-directed mutagenesis by gene targeting in mouse embryo-derived stem cells. *Cell* **51**, 503-12 (1987).
286. Capecchi, M. R. Gene targeting in mice: functional analysis of the mammalian genome for the twenty-first century. *Nat Rev Genet* **6**, 507-12 (2005).
287. Urnov, F. D. et al. Highly efficient endogenous human gene correction using designed zinc-finger nucleases. *Nature* **435**, 646-51 (2005).
288. Couzin, J. & Kaiser, J. Gene therapy. As Gelsinger case ends, gene therapy suffers another blow. *Science* **307**, 1028 (2005).
289. Kohn, D. B., Sadelain, M. & Glorioso, J. C. Occurrence of leukaemia following gene therapy of X-linked SCID. *Nat Rev Cancer* **3**, 477-88 (2003).
290. Kimoto, H. & Taketo, A. Studies on electrotransfer of DNA into Escherichia coli: effect of molecular form of DNA. *Biochim Biophys Acta* **1307**, 325-30 (1996).
291. Sheng, Y., Mancino, V. & Birren, B. Transformation of Escherichia coli with large DNA molecules by electroporation. *Nucleic Acids Res* **23**, 1990-6 (1995).
292. McNally, M. A., Lebkowski, J. S., Okarma, T. B. & Lerch, L. B. Optimizing electroporation parameters for a variety of human hematopoietic cell lines. *Biotechniques* **6**, 882-6 (1988).
293. Capecchi, M. R. Altering the genome by homologous recombination. *Science* **244**, 1288-92 (1989).
294. Capecchi, M. R. The new mouse genetics: altering the genome by gene targeting. *Trends Genet* **5**, 70-6 (1989).
295. Evans, M. J. & Kaufman, M. H. Establishment in culture of pluripotential cells from mouse embryos. *Nature* **292**, 154-6 (1981).
296. Kaufman, M. H., Robertson, E. J., Handyside, A. H. & Evans, M. J. Establishment of pluripotential cell lines from haploid mouse embryos. *J Embryol Exp Morphol* **73**, 249-61 (1983).
297. Koller, B. H. & Smithies, O. Inactivating the beta 2-microglobulin locus in mouse embryonic stem cells by homologous recombination. *Proc Natl Acad Sci U S A* **86**, 8932-5 (1989).
298. Smithies, O., Gregg, R. G., Boggs, S. S., Koralewski, M. A. & Kucherlapati, R. S. Insertion of DNA sequences into the human chromosomal beta-globin locus by homologous recombination. *Nature* **317**, 230-4 (1985).
299. Muller, U. Ten years of gene targeting: targeted mouse mutants, from vector design to phenotype analysis. *Mech Dev* **82**, 3-21 (1999).

300. Metzger, D. & Chambon, P. Site- and time-specific gene targeting in the mouse. *Methods* **24**, 71-80 (2001).
301. Tsien, J. Z. et al. Subregion- and cell type-restricted gene knockout in mouse brain. *Cell* **87**, 1317-26 (1996).
302. Sanes, D. H., Reh, T. A. & Harris, W. A. *Development of the nervous system* (Academic, San Diego, Calif. ; London, 2000).
303. Rouet, P., Smih, F. & Jasin, M. Introduction of double-strand breaks into the genome of mouse cells by expression of a rare-cutting endonuclease. *Mol Cell Biol* **14**, 8096-106 (1994).
304. Rouet, P., Smih, F. & Jasin, M. Expression of a site-specific endonuclease stimulates homologous recombination in mammalian cells. *Proc Natl Acad Sci U S A* **91**, 6064-8 (1994).
305. Sargent, R. G., Brenneman, M. A. & Wilson, J. H. Repair of site-specific double-strand breaks in a mammalian chromosome by homologous and illegitimate recombination. *Mol Cell Biol* **17**, 267-77 (1997).
306. Brenneman, M., Gimble, F. S. & Wilson, J. H. Stimulation of intrachromosomal homologous recombination in human cells by electroporation with site-specific endonucleases. *Proc Natl Acad Sci U S A* **93**, 3608-12 (1996).
307. Porteus, M. H., Cathomen, T., Weitzman, M. D. & Baltimore, D. Efficient gene targeting mediated by adeno-associated virus and DNA double-strand breaks. *Mol Cell Biol* **23**, 3558-65 (2003).
308. Pfeifer, A., Ikawa, M., Dayn, Y. & Verma, I. M. Transgenesis by lentiviral vectors: lack of gene silencing in mammalian embryonic stem cells and preimplantation embryos. *Proc Natl Acad Sci U S A* **99**, 2140-5 (2002).
309. Lois, C., Hong, E. J., Pease, S., Brown, E. J. & Baltimore, D. Germline transmission and tissue-specific expression of transgenes delivered by lentiviral vectors. *Science* **295**, 868-72 (2002).
310. Bibikova, M., Beumer, K., Trautman, J. K. & Carroll, D. Enhancing gene targeting with designed zinc finger nucleases. *Science* **300**, 764 (2003).
311. Porteus, M. H. & Baltimore, D. Chimeric nucleases stimulate gene targeting in human cells. *Science* **300**, 763 (2003).
312. Ho, Y. C., Chung, Y. C., Hwang, S. M., Wang, K. C. & Hu, Y. C. Transgene expression and differentiation of baculovirus-transduced human mesenchymal stem cells. *J Gene Med* (2005).
313. Kitagawa, Y. et al. Ligand-directed gene targeting to mammalian cells by pseudotype baculoviruses. *J Virol* **79**, 3639-52 (2005).
314. Nord, A. S. et al. The International Gene Trap Consortium Website: a portal to all publicly available gene trap cell lines in mouse. *Nucleic Acids Res* **34**, D642-8 (2006).
315. Georgel, P., Du, X., Hoebe, K. & Beutler, B. ENU mutagenesis in mice. *Methods Mol Biol* **415**, 1-16 (2008).
316. Takahashi, K. & Yamanaka, S. Induction of pluripotent stem cells from mouse embryonic and adult fibroblast cultures by defined factors. *Cell* **126**, 663-76 (2006).

317. Meissner, A., Wernig, M. & Jaenisch, R. Direct reprogramming of genetically unmodified fibroblasts into pluripotent stem cells. *Nat Biotechnol* **25**, 1177-81 (2007).
318. Yu, J. et al. Induced pluripotent stem cell lines derived from human somatic cells. *Science* **318**, 1917-20 (2007).
319. Wernig, M. et al. Neurons derived from reprogrammed fibroblasts functionally integrate into the fetal brain and improve symptoms of rats with Parkinson's disease. *Proc Natl Acad Sci U S A* **105**, 5856-61 (2008).
320. Hanna, J. et al. Treatment of sickle cell anemia mouse model with iPS cells generated from autologous skin. *Science* **318**, 1920-3 (2007).
321. Zhang, J. et al. Functional cardiomyocytes derived from human induced pluripotent stem cells. *Circ Res* **104**, e30-41 (2009).
322. Yu, J. et al. Human induced pluripotent stem cells free of vector and transgene sequences. *Science* **324**, 797-801 (2009).
323. Carey, B. W. et al. Reprogramming of murine and human somatic cells using a single polycistronic vector. *Proc Natl Acad Sci U S A* **106**, 157-62 (2009).
324. Woltjen, K. et al. piggyBac transposition reprograms fibroblasts to induced pluripotent stem cells. *Nature* **458**, 766-70 (2009).
325. Kaji, K. et al. Virus-free induction of pluripotency and subsequent excision of reprogramming factors. *Nature* **458**, 771-5 (2009).
326. Mount, D. W., Harris, A. W., Fuerst, C. R. & Siminovitch, L. Mutations in bacteriophage lambda affecting particle morphogenesis. *Virology* **35**, 134-49 (1968).
327. Thirion, J. P. & Hofnung, M. On some genetic aspects of phage lambda resistance in E. coli K12. *Genetics* **71**, 207-16 (1972).
328. Randall-Hazelbauer, L. & Schwartz, M. Isolation of the bacteriophage lambda receptor from Escherichia coli. *J Bacteriol* **116**, 1436-46 (1973).
329. Merril, C. R., Geier, M. R. & Petricciani, J. C. Bacterial virus gene expression in human cells. *Nature* **233**, 398-400 (1971).
330. Geier, M. R. & Merril, C. R. Lambda phage transcription in human fibroblasts. *Virology* **47**, 638-43 (1972).
331. Ishiura, M. et al. Phage particle-mediated gene transfer to cultured mammalian cells. *Mol Cell Biol* **2**, 607-16 (1982).
332. Lindgren, M., Hallbrink, M., Prochiantz, A. & Langel, U. Cell-penetrating peptides. *Trends Pharmacol Sci* **21**, 99-103 (2000).
333. Mi, Z., Mai, J., Lu, X. & Robbins, P. D. Characterization of a class of cationic peptides able to facilitate efficient protein transduction in vitro and in vivo. *Mol Ther* **2**, 339-47 (2000).
334. Krosl, J. et al. In vitro expansion of hematopoietic stem cells by recombinant TAT-HOXB4 protein. *Nat Med* **9**, 1428-32 (2003).
335. Peitz, M., Pfannkuche, K., Rajewsky, K. & Edenhofer, F. Ability of the hydrophobic FGF and basic TAT peptides to promote cellular uptake of recombinant Cre recombinase: a tool for efficient genetic engineering of mammalian genomes. *Proc Natl Acad Sci U S A* **99**, 4489-94 (2002).

336. Caron, N. J., Quenneville, S. P. & Tremblay, J. P. Endosome disruption enhances the functional nuclear delivery of Tat-fusion proteins. *Biochem Biophys Res Commun* **319**, 12-20 (2004).
337. Schwarze, S. R., Hruska, K. A. & Dowdy, S. F. Protein transduction: unrestricted delivery into all cells? *Trends Cell Biol* **10**, 290-5 (2000).
338. Schwarze, S. R., Ho, A., Vocero-Akbani, A. & Dowdy, S. F. In vivo protein transduction: delivery of a biologically active protein into the mouse. *Science* **285**, 1569-72 (1999).
339. Ferrari, A. et al. Caveolae-mediated internalization of extracellular HIV-1 tat fusion proteins visualized in real time. *Mol Ther* **8**, 284-94 (2003).
340. Kaplan, I. M., Wadia, J. S. & Dowdy, S. F. Cationic TAT peptide transduction domain enters cells by macropinocytosis. *J Control Release* **102**, 247-53 (2005).
341. Lankes, H. A. et al. In vivo gene delivery and expression by bacteriophage lambda vectors. *J Appl Microbiol* **102**, 1337-49 (2007).
342. Tilstra, J. et al. Protein transduction: identification, characterization and optimization. *Biochem Soc Trans* **35**, 811-5 (2007).
343. Kim, D. et al. Cytoplasmic transduction peptide (CTP): new approach for the delivery of biomolecules into cytoplasm in vitro and in vivo. *Exp Cell Res* **312**, 1277-88 (2006).
344. Kamada, H. et al. Creation of novel cell-penetrating peptides for intracellular drug delivery using systematic phage display technology originated from Tat transduction domain. *Biol Pharm Bull* **30**, 218-23 (2007).
345. Hodgson, C. P. & Solaiman, F. Virosomes: cationic liposomes enhance retroviral transduction. *Nat Biotechnol* **14**, 339-42 (1996).
346. Kleemann, E. et al. Nano-carriers for DNA delivery to the lung based upon a TAT-derived peptide covalently coupled to PEG-PEI. *J Control Release* **109**, 299-316 (2005).
347. Kim, Y. K. et al. Hybrid of baculovirus and galactosylated PEI for efficient gene carrier. *Virology* **387**, 89-97 (2009).
348. Ayame, H., Morimoto, N. & Akiyoshi, K. Self-assembled cationic nanogels for intracellular protein delivery. *Bioconjug Chem* **19**, 882-90 (2008).
349. Merril, C. R. & Geier, M. The effect of freezing and DEAE-D in spheroplast assays. *Virology* **42**, 780-2 (1970).
350. Volcy, K. & Dewhurst, S. Proteasome inhibitors enhance bacteriophage lambda (lambda) mediated gene transfer in mammalian cells. *Virology* **384**, 77-87 (2009).
351. Chauhan, A., Tikoo, A., Kapur, A. K. & Singh, M. The taming of the cell penetrating domain of the HIV Tat: myths and realities. *J Control Release* **117**, 148-62 (2007).
352. Poteete, A. R., Fenton, A. C. & Wang, H. R. Recombination-promoting activity of the bacteriophage lambda Rap protein in Escherichia coli K-12. *J Bacteriol* **184**, 4626-9 (2002).
353. Costantino, N. & Court, D. L. Enhanced levels of lambda Red-mediated recombinants in mismatch repair mutants. *Proc Natl Acad Sci U S A* **100**, 15748-53 (2003).

354. Zhang, Y., Muyrers, J. P., Rientjes, J. & Stewart, A. F. Phage annealing proteins promote oligonucleotide-directed mutagenesis in Escherichia coli and mouse ES cells. *BMC Mol Biol* **4**, 1 (2003).
355. Yu, D., Sawitzke, J. A., Ellis, H. & Court, D. L. Recombineering with overlapping single-stranded DNA oligonucleotides: testing a recombination intermediate. *Proc Natl Acad Sci U S A* **100**, 7207-12 (2003).
356. Yu, D. et al. An efficient recombination system for chromosome engineering in Escherichia coli. *Proc Natl Acad Sci U S A* **97**, 5978-83 (2000).
357. Mythili, E., Kumar, K. A. & Muniyappa, K. Characterization of the DNA-binding domain of beta protein, a component of phage lambda red-pathway, by UV catalyzed cross-linking. *Gene* **182**, 81-7 (1996).
358. Ellis, H. M., Yu, D., DiTizio, T. & Court, D. L. High efficiency mutagenesis, repair, and engineering of chromosomal DNA using single-stranded oligonucleotides. *Proc Natl Acad Sci U S A* **98**, 6742-6 (2001).
359. Mai, J. C., Shen, H., Watkins, S. C., Cheng, T. & Robbins, P. D. Efficiency of protein transduction is cell type-dependent and is enhanced by dextran sulfate. *J Biol Chem* **277**, 30208-18 (2002).
360. Jiang, H. et al. Development of efficient RNA interference system using EGF-displaying phagemid particles. *Acta Pharmacol Sin* **29**, 437-42 (2008).
361. Rubinstein, A. et al. Progressive specific immune attrition after primary, secondary and tertiary immunizations with bacteriophage phi X174 in asymptomatic HIV-1 infected patients. *Aids* **14**, F55-62 (2000).
362. Stoute, J. A. et al. Long-term efficacy and immune responses following immunization with the RTS,S malaria vaccine. *J Infect Dis* **178**, 1139-44 (1998).
363. Manz, R. A., Lohning, M., Cassese, G., Thiel, A. & Radbruch, A. Survival of long-lived plasma cells is independent of antigen. *Int Immunol* **10**, 1703-11 (1998).
364. Iribarren, P. et al. IL-4 down-regulates lipopolysaccharide-induced formyl peptide receptor 2 in murine microglial cells by inhibiting the activation of mitogen-activated protein kinases. *J Immunol* **171**, 5482-8 (2003).
365. Mayer, K. D. et al. Cutting edge: T-bet and IL-27R are critical for in vivo IFN-gamma production by CD8 T cells during infection. *J Immunol* **180**, 693-7 (2008).
366. Zhu, J. et al. Conditional deletion of Gata3 shows its essential function in T(H)1-T(H)2 responses. *Nat Immunol* **5**, 1157-65 (2004).
367. Stripecke, R. et al. Immune response to green fluorescent protein: implications for gene therapy. *Gene Ther* **6**, 1305-12 (1999).
368. Manoj, S., Babiuk, L. A. & van Drunen Littel-van den Hurk, S. Approaches to enhance the efficacy of DNA vaccines. *Crit Rev Clin Lab Sci* **41**, 1-39 (2004).
369. Patel, J. et al. HIV-1 Tat-coated nanoparticles result in enhanced humoral immune responses and neutralizing antibodies compared to alum adjuvant. *Vaccine* **24**, 3564-73 (2006).
370. Albini, A. et al. HIV-1 Tat protein mimicry of chemokines. *Proc Natl Acad Sci U S A* **95**, 13153-8 (1998).

371. Izmailova, E. et al. HIV-1 Tat reprograms immature dendritic cells to express chemoattractants for activated T cells and macrophages. *Nat Med* **9**, 191-7 (2003).
372. Leifert, J. A., Holler, P. D., Harkins, S., Kranz, D. M. & Whitton, J. L. The cationic region from HIV tat enhances the cell-surface expression of epitope/MHC class I complexes. *Gene Ther* **10**, 2067-73 (2003).
373. Boykins, R. A., Joshi, M., Syin, C., Dhawan, S. & Nakhasi, H. Synthesis and construction of a novel multiple peptide conjugate system: strategy for a subunit vaccine design. *Peptides* **21**, 9-17 (2000).
374. Goldstein, G., Manson, K., Tribbick, G. & Smith, R. Minimization of chronic plasma viremia in rhesus macaques immunized with synthetic HIV-1 Tat peptides and infected with a chimeric simian/human immunodeficiency virus (SHIV33). *Vaccine* **18**, 2789-95 (2000).
375. Zhao, J. et al. Enhanced cellular immunity to SIV Gag following co-administration of adenoviruses encoding wild-type or mutant HIV Tat and SIV Gag. *Virology* **342**, 1-12 (2005).
376. Longo, O. et al. Phase I therapeutic trial of the HIV-1 Tat protein and long term follow-up. *Vaccine* **27**, 3306-12 (2009).
377. Endemann, H. & Model, P. Location of filamentous phage minor coat proteins in phage and in infected cells. *J Mol Biol* **250**, 496-506 (1995).
378. Panus, J. F., McHeyzer-Williams, L. J. & McHeyzer-Williams, M. G. Antigen-specific T helper cell function: differential cytokine expression in primary and memory responses. *J Exp Med* **192**, 1301-16 (2000).
379. Bucy, R. P. et al. Heterogeneity of single cell cytokine gene expression in clonal T cell populations. *J Exp Med* **180**, 1251-62 (1994).
380. Kelso, A., Groves, P., Ramm, L. & Doyle, A. G. Single-cell analysis by RT-PCR reveals differential expression of multiple type 1 and 2 cytokine genes among cells within polarized CD4+ T cell populations. *Int Immunol* **11**, 617-21 (1999).
381. Fakoya, A. et al. HIV infection alters the production of both type 1 and 2 cytokines but does not induce a polarized type 1 or 2 state. *Aids* **11**, 1445-52 (1997).
382. Kidd, P. Th1/Th2 balance: the hypothesis, its limitations, and implications for health and disease. *Altern Med Rev* **8**, 223-46 (2003).
383. Ochsenbein, A. F. & Zinkernagel, R. M. Natural antibodies and complement link innate and acquired immunity. *Immunol Today* **21**, 624-30 (2000).
384. Sokoloff, A. V., Bock, I., Zhang, G., Sebestyen, M. G. & Wolff, J. A. The interactions of peptides with the innate immune system studied with use of T7 phage peptide display. *Mol Ther* **2**, 131-9 (2000).
385. Irving, M. B., Pan, O. & Scott, J. K. Random-peptide libraries and antigen-fragment libraries for epitope mapping and the development of vaccines and diagnostics. *Curr Opin Chem Biol* **5**, 314-24 (2001).
386. Abe, M., Tokita, D., Raimondi, G. & Thomson, A. W. Endotoxin modulates the capacity of CpG-activated liver myeloid DC to direct Th1-type responses. *Eur J Immunol* **36**, 2483-93 (2006).
387. Gavin, A. L. et al. Adjuvant-enhanced antibody responses in the absence of toll-like receptor signaling. *Science* **314**, 1936-8 (2006).

388. Palm, N. W. & Medzhitov, R. Pattern recognition receptors and control of adaptive immunity. *Immunol Rev* **227**, 221-33 (2009).
389. Awomoyi, A. A. et al. Association of TLR4 polymorphisms with symptomatic respiratory syncytial virus infection in high-risk infants and young children. *J Immunol* **179**, 3171-7 (2007).
390. Brockman, J. A. et al. Coupling of a signal response domain in I kappa B alpha to multiple pathways for NF-kappa B activation. *Mol Cell Biol* **15**, 2809-18 (1995).
391. Brown, K., Gerstberger, S., Carlson, L., Franzoso, G. & Siebenlist, U. Control of I kappa B-alpha proteolysis by site-specific, signal-induced phosphorylation. *Science* **267**, 1485-8 (1995).
392. Akira, S. Innate immunity to pathogens: diversity in receptors for microbial recognition. *Immunol Rev* **227**, 5-8 (2009).
393. Akira, S. Toll-like receptors: lessons from knockout mice. *Biochem Soc Trans* **28**, 551-6 (2000).
394. Medzhitov, R. Recognition of microorganisms and activation of the immune response. *Nature* **449**, 819-26 (2007).
395. Gallucci, S., Lolkema, M. & Matzinger, P. Natural adjuvants: endogenous activators of dendritic cells. *Nat Med* **5**, 1249-55 (1999).
396. Matzinger, P. Tolerance, danger, and the extended family. *Annu Rev Immunol* **12**, 991-1045 (1994).
397. Hayashi, F. et al. The innate immune response to bacterial flagellin is mediated by Toll-like receptor 5. *Nature* **410**, 1099-103 (2001).
398. Koyama, S., Ishii, K. J., Coban, C. & Akira, S. Innate immune response to viral infection. *Cytokine* **43**, 336-41 (2008).
399. Rassa, J. C., Meyers, J. L., Zhang, Y., Kudaravalli, R. & Ross, S. R. Murine retroviruses activate B cells via interaction with toll-like receptor 4. *Proc Natl Acad Sci U S A* **99**, 2281-6 (2002).
400. Kalmokoff, M. L. & Bradley, D. E. Contractile-tailed bacteriophages adsorb to Escherichia coli O128ab lipopolysaccharide that is altered by large plasmids to provide receptors and lipopolysaccharide heterogeneity within the serogroup. *Can J Microbiol* **41**, 163-9 (1995).
401. Tsai, C. M. & Frasch, C. E. A sensitive silver stain for detecting lipopolysaccharides in polyacrylamide gels. *Anal Biochem* **119**, 115-9 (1982).
402. Borck, K., Beggs, J. D., Brammar, W. J., Hopkins, A. S. & Murray, N. E. The construction in vitro of transducing derivatives of phage lambda. *Mol Gen Genet* **146**, 199-207 (1976).
403. Wood, W. B. Host specificity of DNA produced by Escherichia coli: bacterial mutations affecting the restriction and modification of DNA. *J Mol Biol* **16**, 118-33 (1966).
404. Murray, N. E., Brammar, W. J. & Murray, K. Lambdoid phages that simplify the recovery of in vitro recombinants. *Mol Gen Genet* **150**, 53-61 (1977).
405. Inagaki, M., Wakashima, H., Kato, M., Kaitani, K. & Nishikawa, S. Crucial role of the lipid part of lipopolysaccharide for conformational change of minor spike H protein of bacteriophage phiX174. *FEMS Microbiol Lett* **251**, 305-11 (2005).

406. Tamaki, S., Sato, T. & Matsuhashi, M. Role of lipopolysaccharides in antibiotic resistance and bacteriophage adsorption of Escherichia coli K-12. *J Bacteriol* **105**, 968-75 (1971).
407. Weidel, W. Bacterial viruses; with particular reference to adsorption/penetration. *Annu Rev Microbiol* **12**, 27-48 (1958).
408. Center for Drug Evaluation and Research (U.S.). *Guideline on validation of the Limulus Amebocyte Lysate test as an end-product endotoxin test for human and animal parenteral drugs, biological products, and medical devices* (U.S. Dept. of Health and Human Services, Public Health Service, Food and Drug Administration, Rockville, MD, 1987).
409. Yin, E. T. et al. Picogram-sensitive assay for endotoxin: gelation of Limulus polyphemus blood cell lysate induced by purified lipopolysaccharides and lipid A from Gram-negative bacteria. *Biochim Biophys Acta* **261**, 284-9 (1972).
410. Takayama, K. et al. Influence of fine structure of lipid A on Limulus amebocyte lysate clotting and toxic activities. *Infect Immun* **45**, 350-5 (1984).
411. Ashtekar, A. R. et al. TLR4-mediated activation of dendritic cells by the heat shock protein DnaK from Francisella tularensis. *J Leukoc Biol* **84**, 1434-46 (2008).
412. Levin, J. & Bang, F. B. The Role of Endotoxin in the Extracellular Coagulation of Limulus Blood. *Bull Johns Hopkins Hosp* **115**, 265-74 (1964).
413. Merril, C. R., Scholl, D. & Adhya, S. L. The prospect for bacteriophage therapy in Western medicine. *Nat Rev Drug Discov* **2**, 489-97 (2003).
414. Barondess, J. J. & Beckwith, J. bor gene of phage lambda, involved in serum resistance, encodes a widely conserved outer membrane lipoprotein. *J Bacteriol* **177**, 1247-53 (1995).
415. Lynne, A. M., Foley, S. L. & Nolan, L. K. Immune response to recombinant Escherichia coli Iss protein in poultry. *Avian Dis* **50**, 273-6 (2006).
416. Lynne, A. M., Skyberg, J. A., Logue, C. M. & Nolan, L. K. Detection of Iss and Bor on the surface of Escherichia coli. *J Appl Microbiol* **102**, 660-6 (2007).
417. Bagchi, A. et al. MyD88-dependent and MyD88-independent pathways in synergy, priming, and tolerance between TLR agonists. *J Immunol* **178**, 1164-71 (2007).
418. Hoshino, K., Kaisho, T., Iwabe, T., Takeuchi, O. & Akira, S. Differential involvement of IFN-beta in Toll-like receptor-stimulated dendritic cell activation. *Int Immunol* **14**, 1225-31 (2002).
419. Horng, T., Barton, G. M. & Medzhitov, R. TIRAP: an adapter molecule in the Toll signaling pathway. *Nat Immunol* **2**, 835-41 (2001).
420. Kaisho, T., Takeuchi, O., Kawai, T., Hoshino, K. & Akira, S. Endotoxin-induced maturation of MyD88-deficient dendritic cells. *J Immunol* **166**, 5688-94 (2001).
421. Kawai, T. et al. Lipopolysaccharide stimulates the MyD88-independent pathway and results in activation of IFN-regulatory factor 3 and the expression of a subset of lipopolysaccharide-inducible genes. *J Immunol* **167**, 5887-94 (2001).
422. Yamamoto, M. et al. Role of adaptor TRIF in the MyD88-independent toll-like receptor signaling pathway. *Science* **301**, 640-3 (2003).

423. Doyle, S. et al. IRF3 mediates a TLR3/TLR4-specific antiviral gene program. *Immunity* **17**, 251-63 (2002).
424. Hirsch, S., Austyn, J. M. & Gordon, S. Expression of the macrophage-specific antigen F4/80 during differentiation of mouse bone marrow cells in culture. *J Exp Med* **154**, 713-25 (1981).
425. Eske, K., Breitbach, K., Kohler, J., Wongprompitak, P. & Steinmetz, I. Generation of murine bone marrow derived macrophages in a standardised serum-free cell culture system. *J Immunol Methods* **342**, 13-9 (2009).
426. Tsan, M. F. & Baochong, G. Pathogen-associated molecular pattern contamination as putative endogenous ligands of Toll-like receptors. *J Endotoxin Res* **13**, 6-14 (2007).
427. Benko, S., Philpott, D. J. & Girardin, S. E. The microbial and danger signals that activate Nod-like receptors. *Cytokine* **43**, 368-73 (2008).
428. Alexopoulou, L., Holt, A. C., Medzhitov, R. & Flavell, R. A. Recognition of double-stranded RNA and activation of NF-kappaB by Toll-like receptor 3. *Nature* **413**, 732-8 (2001).
429. Hoebe, K. et al. Identification of Lps2 as a key transducer of MyD88-independent TIR signalling. *Nature* **424**, 743-8 (2003).
430. Palsson-McDermott, E. M. & O'Neill, L. A. Signal transduction by the lipopolysaccharide receptor, Toll-like receptor-4. *Immunology* **113**, 153-62 (2004).
431. Fitzgerald, K. A. et al. LPS-TLR4 signaling to IRF-3/7 and NF-kappaB involves the toll adapters TRAM and TRIF. *J Exp Med* **198**, 1043-55 (2003).
432. Selvarajoo, K. Discovering differential activation machinery of the Toll-like receptor 4 signaling pathways in MyD88 knockouts. *FEBS Lett* **580**, 1457-64 (2006).
433. Zughaier, S., Agrawal, S., Stephens, D. S. & Pulendran, B. Hexa-acylation and KDO(2)-glycosylation determine the specific immunostimulatory activity of Neisseria meningitidis lipid A for human monocyte derived dendritic cells. *Vaccine* **24**, 1291-7 (2006).
434. Petrovsky, N. & Aguilar, J. C. Vaccine adjuvants: current state and future trends. *Immunol Cell Biol* **82**, 488-96 (2004).
435. Mosca, F. et al. Molecular and cellular signatures of human vaccine adjuvants. *Proc Natl Acad Sci U S A* **105**, 10501-6 (2008).
436. Li, H., Nookala, S. & Re, F. Aluminum hydroxide adjuvants activate caspase-1 and induce IL-1beta and IL-18 release. *J Immunol* **178**, 5271-6 (2007).
437. Miyake, K. Innate recognition of lipopolysaccharide by Toll-like receptor 4-MD-2. *Trends Microbiol* **12**, 186-92 (2004).
438. Johnson, D. A. Synthetic TLR4-active glycolipids as vaccine adjuvants and stand-alone immunotherapeutics. *Curr Top Med Chem* **8**, 64-79 (2008).
439. Wheeler, R. D., Young, E. A., Rothwell, N. J., Hall, M. D. & Luheshi, G. N. Up-regulation of IL-18BP, but not IL-18 mRNA in rat liver by LPS. *Cytokine* **21**, 161-6 (2003).
440. Overbergh, L. et al. The use of real-time reverse transcriptase PCR for the quantification of cytokine gene expression. *J Biomol Tech* **14**, 33-43 (2003).

441. Mathers, A. R. & Cuff, C. F. Role of interleukin-4 (IL-4) and IL-10 in serum immunoglobulin G antibody responses following mucosal or systemic reovirus infection. *J Virol* **78**, 3352-60 (2004).
442. Strandberg, Y. et al. Lipopolysaccharide and lipoteichoic acid induce different innate immune responses in bovine mammary epithelial cells. *Cytokine* **31**, 72-86 (2005).
443. Rapisarda, A., Pastorino, S., Massazza, S., Varesio, L. & Bosco, M. C. Antagonistic effect of picolinic acid and interferon-gamma on macrophage inflammatory protein-1alpha/beta production. *Cell Immunol* **220**, 70-80 (2002).
444. Flesch, I. E. et al. Early interleukin 12 production by macrophages in response to mycobacterial infection depends on interferon gamma and tumor necrosis factor alpha. *J Exp Med* **181**, 1615-21 (1995).
445. Gu, Y., Hu, X., Liu, C., Qv, X. & Xu, C. Interleukin (IL)-17 promotes macrophages to produce IL-8, IL-6 and tumour necrosis factor-alpha in aplastic anaemia. *Br J Haematol* **142**, 109-14 (2008).
446. Yang, Y., Bao, M. & Yoon, J. W. Intrinsic defects in the T-cell lineage results in natural killer T-cell deficiency and the development of diabetes in the nonobese diabetic mouse. *Diabetes* **50**, 2691-9 (2001).
447. Oda, K. & Yamamoto, Y. Serum interferon-gamma, interleukin-4, and interleukin-6 in infants with adenovirus and respiratory syncytial virus infection. *Pediatr Int* **50**, 92-4 (2008).
448. Fischer, M. B. et al. The presence of MOMA-2+ macrophages in the outer B cell zone and protection of the splenic micro-architecture from LPS-induced destruction depend on secreted IgM. *Eur J Immunol* **37**, 2825-33 (2007).
449. Carroll, M. C. The complement system in regulation of adaptive immunity. *Nat Immunol* **5**, 981-6 (2004).
450. Fischer, M. B. et al. Regulation of the B cell response to T-dependent antigens by classical pathway complement. *J Immunol* **157**, 549-56 (1996).
451. Fischer, M. B., Ma, M., Hsu, N. C. & Carroll, M. C. Local synthesis of C3 within the splenic lymphoid compartment can reconstitute the impaired immune response in C3-deficient mice. *J Immunol* **160**, 2619-25 (1998).